



Centro Singular de investigación en Química Biológica y
Materiales Moleculares

**Rh(III)-catalyzed annulations based on C-H activation. Sustainable synthesis of carbon-
and heterocycles.**

Memoria que, para optar al grado de Doctor en Química por la
Universidad de Santiago de Compostela, presenta

Andrés Seoane Fernández

Santiago de Compostela, abril 2016



D. JOSÉ LUIS MASCAREÑAS CID, CATEDRÁTICO DEL DEPARTAMENTO DE QUÍMICA ORGÁNICA DE LA UNIVERSIDAD DE SANTIAGO DE COMPOSTELA Y D. MOISÉS GULÍAS COSTA, PROFESOR AYUDANTE DOCTOR DEL DEPARTAMENTO DE QUÍMICA ORGÁNICA DE LA UNIVERSIDAD DE SANTIAGO DE COMPOSTELA,

CERTIFICAN: Que la memoria adjunta, titulada *Rh(III)-catalyzed annulations based on C-H activation. Sustainable synthesis of carbo- and heterocycles*, que para optar al grado de Doctor en química presenta Don Andrés Seoane Fernández, ha sido realizada bajo nuestra dirección en los laboratorios del Centro Singular de Investigación en Química Biológica y Materiales Moleculares (CIQUS) de la Universidad de Santiago de Compostela.

Considerando que constituye trabajo de tesis, autorizamos su presentación en la Universidad de Santiago de Compostela.

Y para que así conste, se expide el presente certificado en Santiago de Compostela, a 28 de abril de 2016.



Fdo.: José Luis Mascareñas Cid

Fdo.: Moisés Gulías Costa



-We'll Never Survive.

*- Nonsense. You're only saying that because no
one ever has.*

William Goldman, The Princess Bride.



Acknowledgements.

En primer lugar me gustaría agradecer a mis directores de tesis, José Luis y el Moisés por haber confiado en mí dándome la oportunidad de dedicar casi 5 años a un proyecto apasionante dentro de un grupo increíble. Esta tesis ha llegado a buen puerto gracias a su apoyo y enseñanzas, que han permitido que el *mindundi* que entró, salga con más conocimiento, confianza y cariño por la química. Espero haber hecho justicia a la confianza depositada que depositaron en mí.

También me gustaría agradecer a mi familia el apoyo que me han dado. A mi madre por facilitarme la decisión sobre el camino que a seguir; a mi hermano, que, pese a ser más joven, es un gran ejemplo y que, además me ayudó enormemente a ejercitarse el cerebro mientras encontraba nuevas maneras de meterme con él y a mi padre que, ya desde pequeño, aguantaba mis incansables preguntas alentando mi curiosidad y encendiéndole en mí la chispa de la ciencia.

Agradezco también a Susana que aprovechó esa chispa y la avivó gracias a unas clases que siempre me maravillaron y también a Mar, que me consiguió que la química se convirtiese en mi primera opción y sin la cual no estaría escribiendo esto. Y, por supuesto, al grupo del Prof. Ricardo Alonso con el que me inicié en el mundo investigación.

Tampoco puedo dejar atrás a mis compañeros del grupo que consiguieron que el desarrollo de esta tesis, que a muchos les parece un camino interminable y lleno de obstáculos, se convirtiera en una experiencia excepcional que repetiría sin dudar. Primero, a los que me recibieron el primer año haciéndome sentir como en casa: A Helio, que estaba riéndose siempre de fondo; a Luci y su infinita paciencia; Isaac, bueno, una coma más; a Lara, por las frases lapidarias y a Cris, por ser de las pocas que recuerda lo tímidamente que puedo llegar a ser. Mateo, muchas gracias por poderme hacerme sentir orgulloso de la locura. Además quiero agradecer María Rey, que además de aligerarnos trabajo me mostró cómo disfruta a pesar de cada segundo de la vida sea un infierno y que las personas normales también leen cómics. No me puedo olvidar de Fernando, Paloma, Marisel, Sergio, Marta que fueron de gran ayuda durante, al menos, gran parte de estos años. Noe, muchísimas gracias, no sólo por los proyectos compartidos si no por ser un ejemplo y por lo mucho que me enseñaste, no sólo en sobre química si no sobre cómo se puede sobrevivir en este mundo con una sonrisa en la cara. En segundo lugar, a los que llegaron detrás: Ronald, siempre dispuesto a aportar un dato sobre lo que sea; Noelia 2, con la que he compartido proyecto en la mayor parte de ésta tesis y por lo que me siento enormemente agradecido. Muchas gracias también a Iván, porque el laboratorio sin él habría sido enormemente aburrido; David, que fue mi primer pupilo y con el que aprendí mucho; Jaime, que desgraciadamente para los demás, entiende el humor de una forma muy parecida a la mía. Agradecer también a Felipe, un gran Compañero y a Cagiao, que siempre tiene tiempo para apuntarse a un plan. No me puedo olvidar (aunque casi lo haya hecho) de Cesar y Xabi con los que compartí el último proyecto de la tesis. Aunque por falta de espacio no les puedo dedicar las palabras que se

merecen, también me gustaría agradecer a Jéssica, Natalia, Suso, Soraya, María Tomás, Rebeca, Paolo, Miguel, Tasneem, Jose, Jorge, Sandra y demás compañeros de edificio.

Esta tesis también habría sido imposible sin la estimable ayuda de Ramón y Mentxa y el resto de técnicos de la USC que han hecho una parte crucial del trabajo presentado aquí.

Me alegro también de poder haber completado esta etapa de mi vida manteniendo relación con algunos compañeros a los que conocí allá por primera vez de carrera. Iria... casi 10 años desde que empezamos y siempre un apoyo con el que contar y a Tito y María, descubrimiento tardío pero enormemente relevante en los años de doctorado.

Me gustaría agradecer también a la Fundación Barrié por darme la oportunidad de realizar una estancia predoctoral en el grupo del Prof. Rueping. I would also like to acknowledge Prof. Rueping for giving me the chance of doing a research stay in his group and to Ele, Laura, Thomas, Patricia, Aleksandra, Quentin, Anthony and Roman for treating me so well and making me miss Aachen.

A pesar de todo el apoyo recibido en el grupo, esta tesis habría sido más difícil sin todos aquellos que me permitieron desconectar al salir del laboratorio. Fundamentalmente el grupo Montoto/Ex San Agustinos: Viri, Ada, Pot, Wences, Colo, Judoka, Ildara, Javi, Soso, Kar y María que convirtieron la mayoría de los martes y muchos otros días en una experiencia digna de ser vivida y llena de zorcilla. A Colo le agradezco nuevamente por aguantarme como compañero de piso durante la mayor parte de estos años y por las eternas divagaciones sobre el mundo en general y la ciencia en particular.

También agradezco a todas las personas que no he podido nombrar, ya sea por falta de espacio o por un olvido imperdonable. Espero que perdonéis la omisión. Y por último a todo aquel que lea algo de esta memoria, aunque sea un párrafo, gracias por hacer que todo el trabajo que hay detrás no caiga en el olvido.

A mi familia y amigos.





Table of contents.

Abbreviations and acronyms.....	v
CHAPTER I: Introduction	1
1- Organic Synthesis: Applications and challenges.....	3
1.1 Introduction.	3
1.2. Requirements for modern Organic Chemistry.	4
2 - Organometallic Chemistry: The hammer in the reaction development toolbox.....	5
2.2. Transition metal-catalyzed cycloadditions.....	5
2.3. Cross coupling reactions.	7
3 - C-H functionalization, the “holy grail” of catalysis.	10
3.1 C-H functionalization, an overview.	10
3.2 Use of directing groups in C-H functionalization.	15
3.3 Mechanisms for C-H activation.....	16
3.3.1 Oxidative addition.	16
3.3.2 Sigma bond metathesis.....	17
3.3.3 Electrophilic substitution.	18
3.3.4 Concerted metallation-deprotonation (CMD).....	19
3.4. Rhodium (III)-catalyzed C-H functionalizations.	20
4 -Annulations based on C-H activation, an interesting match.	22
4.2. General overview.	22
4.2. General mechanistic aspects of oxidative annulations.	23
4.3. Some examples of oxidative annulations.....	24
4.3.1 (n+1) oxidative annulations.	24
4.3.2 (n+2) oxidative annulations.	25
4.3.3 (n+3) oxidative annulations.	27
4.3.4. (n+n+n) oxidative annulations	28
CHAPTER II: Intramolecular oxidative annulations of benzamides and acrylamides.....	31
1. – C-H functionalization of benzamides.....	33
1.1 C-H functionalization of benzamides.....	33
1.2 Oxidative annulation of benzamides.....	35
2. – Objectives	39
3. – Results and discussion.....	41

3.1 Optimization of the reaction conditions.....	41
3.2 Substrate scope.....	42
3.3 Mechanistic investigations.	45
3.3 Further studies on the intramolecular oxidative annulation of anilides.	48
3.4 Partially intramolecular oxidative annulation of benzhydroxamic derivatives.....	50
4. – Conclusions.	53
CHAPTER III: Assembly of benzoxepines and coumarins by oxidative annulations of <i>o</i>-vinylphenols.....	55
1. –Introduction.....	57
1.1 Relevance of the phenolic core: Benzoxepines and coumarins.....	57
1.2 C-H functionalization directed by phenols.....	58
2. –Objectives.....	67
3. –Results and discussion.....	69
3.1 Optimization of the reaction conditions.....	69
3.2 Substrate scope.....	70
3.3 (5+1) annulation towards coumarins.....	72
3.4 Mechanistic investigations.	72
4. – Conclusions.	77
CHAPTER IV: Dearomatizing (3+2) oxidative annulations of <i>o</i>-alkenylphenols and alkynes for the synthesis of spirocycles.....	79
1. –Precedents.....	81
1.1 Isolation of the spirocycle.....	81
1.2 Dearomatization of phenols.....	81
1.3 Hydroxyl-directed synthesis of spirocycles by oxidative annulation.....	84
1.3 Spirocycles as a synthetic goal.....	86
2. –Objectives.....	87
3. –Results and discussion.....	89
3.1 Optimization of the reaction conditions.....	89
3.2 Substrate scope.....	90
3.4 Mechanistic investigations.	92
3.5 Mechanistic proposal.	94
3.6 Formation of the azulenone.	95
4. – Conclusions.	97

CHAPTER V: Oxidative annulations of <i>o</i>-alkenylanilines	99
1. -Introduction	101
1.2 Reactivity of <i>o</i> -alkenylanilines.	101
2. Objectives	109
3. -Results and discussion.....	111
3.1 Initial studies on the N-substituent	111
3.3 Substrate scope.	115
3.4 Mechanistic hypothesis.	117
2. Conclusions	121
CHAPTER VI: Experimental part.....	123
1- General experimental procedures	125
2- CHAPTER II: Intramolecular oxidative annulations of benzamides and acrylamides.	127
2.1 Procedure for the synthesis of alkynylbenzamides (10-10p), exemplified for 10.	127
2.2 Procedure for the synthesis of alkynylbenzamides (14a-14d), exemplified for 14a.	132
2.3 Procedure for synthesis of hexynamides 18a and 18b, exemplified for 18b.	133
2.4 Procedure for catalytic reactions of alkynylbenzamides 11a-11q.....	134
2.5 Procedure for catalytic reactions of acrylamides 15a-15d.	139
2.6 Procedure for annulation of hexynamides 18a and 18b. exemplified for 18b.	140
2.7 Kinetic studies.....	140
2.8 DFT calculations	142
3- CHAPTER III: Assembly of benzoxepines and coumarins by oxidative annulations of <i>o</i> -vinylphenols.....	217
3.1 General considerations.	217
3.2 Procedure A for the synthesis of <i>o</i> -vinylphenols exemplified for 23a.....	217
3.3 Procedure B for the synthesis of <i>o</i> -vinylphenols exemplified for 25d.....	219
3.4 General procedure for the Rh-catalyzed reaction leading to oxepines 25.....	220
3.5 General procedure for the Rh-catalyzed synthesis of coumarines 28.....	226
3.6 Competition experiment between 23a and 23f.....	228
3.7 Procedure for comparing reaction rates.....	228
4- CHAPTER IV: Dearomatizing (3+2) oxidative annulations of <i>o</i> -alkenylphenols and alkynes for the synthesis of spirocycles.....	231
4.1 General considerations.	231
4.2 Procedure A for the synthesis of <i>o</i> -vinylphenols exemplified for 27a.....	231

4.3 Procedure B for the synthesis of <i>o</i> -vinylphenols exemplified for 27g.....	233
4.4 Procedure A for the Rh-catalyzed annulations.	234
4.5 Procedure B for the Rh-catalyzed annulations.....	241
4.6 Mechanistic experiments.....	243
4.7 Thermal rearrangement.....	247
5- CHAPTER V: Oxidative annulations of <i>o</i>-alkenylanilines	249
5.1 General considerations	249
5.2 Procedure for the synthesis of triflyl protected <i>o</i> -alkenylanilides (37a-37k) exemplified for 37a.....	249
5.3 General Procedure for the [4+2] C-H annulation leading to naphtylamides 39aa-39kd exemplified for 39aa.....	252
CHAPTER VII: Selected spectra	259
1. Selected spectra from chapter II.	261
2. Selected spectra from chapter III.	267
3. Selected spectra from chapter IV.....	270
4. Selected spectra from chapter V.	275

Abbreviations and acronyms.

BMIM	1-butyl-3-methylimidazolium	HRMS	High resolution	mass
Boc	<i>tert</i> -Butyloxycarbonyl		spectroscopy	
BQ	<i>p</i> -Benzoquinone	IPr	1,3-bis(2,6-di- <i>iso</i> -propylphenyl)imidazol-2-6ylidene	
CI	Chemical ionization			
CMD	Concerted Metallation-deprotonation	<i>J</i>	Coupling constant	
cod	1,5-cyclooctadiene	KIE	Kinetic isotopic effect	
Cp*	1,2,3,4,5-pentamethylcyclopentadienyl	LRMS	Low resolution	mass
Cp ^{iPr}	<i>iso</i> -propylcyclopentadienyl	<i>m</i>	Multiplet	
Cp ^{tBu}	1,3-di- <i>tert</i> -butylcyclopentadienyl	MBTE	Methyl <i>tert</i> -butyl ether	
Cy	Cyclohexyl	Mes	1,3,5-timethylbenzene	
<i>d</i>	Doublet	MOPS	3-(N-morpholino)propanesulfonic acid	
DABCO	1,4-diazabicyclo[2.2.2]octane			
dba	Dibenzylideneacetone	MS	Molecular sieves	
DBPO	Dibenzoylperoxide	MVK	Methylvinylketone	
DCC	<i>N,N</i> -dicyclohexylcarbodiimide	NMR	Nuclear magnetic resonance	
DCE	1,2-dichloroethane	NBS	<i>N</i> -bromosuccinimide	
DFT	Density functional theory	Ns	4-nitrobenzenesulfonyl	
DG	Directing group	nOe	Nuclear Overhauser effect	
DIAD	Diisopropylazadicarboxylate	r.t.	Room temperature	
DMAP	<i>N,N</i> -dimethylaminopyridine	Piv	2,2-dimethylpropionate	
DMF	<i>N,N</i> -dimethyl formamide	pin	Pinacolate	
DMS	Dimethyl sulfoxide	ppy	phenylpyridine	
dppb	1,4-bis(diphenylphosphino)butane	<i>q</i>	Quadruplet	
		<i>t</i>	Triplet	
<i>ee</i>	Enantiomeric excess	<i>t</i> -AmOH	2-methyl-2-butanol	
EI	Electron ionization	TBAF	Tetrabutylammonium fluoride	
ESI	Electrospray	TBS	<i>tert</i> -Butyldimethylsilyl	
equiv.	Equivalent	Tf	Trifluoromethylsulfonyl	

Abbreviations and acronyms.

TFA	Trifluoroacetic acid
TFAc	Trifluoroacetyl
THF	Tetrahydrofuran
TMEDA	<i>N,N,N',N'</i> -tetramethylethylenediamine
TMS	Trimethylsilyl
TS	Transition state
Ts	4-Methylbenzenesulfonyl



CHAPTER I: Introduction.





1- Organic Synthesis: Applications and challenges.

1.1 Introduction.

Defined as “The branch of science concerned with the substances of which matter is composed, the investigation of their properties and reactions, and the use of such reactions to form new substances”,¹ Chemistry is, arguably, one of the disciplines that have contributed the most to the well-being of mankind. Since the discovery of the fire until age of plastics, humans have modified molecules at their wish for their own benefit. By doing so, the art of creating and breaking chemical bonds has evolved, allowing us to advance as society to become what we currently are. This is the reason why the study of chemistry is of vital importance to pave the road towards a better world.

Among the many branches of chemistry, Organic Synthesis has gained its privileged place by its own merits. Its quest started on the beginning of the XIX century, when chemists found out that there was no need of any “vital force” in order to create naturally occurring molecules. The success of Organic Synthesis as main area of chemistry arises from the fact that, starting from a relatively small variety of “bricks” (fundamentally C, H, O, N, P, S and halogens) allows the obtention of a virtually infinite number of structures with varying properties. By using this tool we are able; not only to mimic nature, but to create our own molecules that, diverging from our environment, possess uses in medicine, biology, cosmetics, food industry and much more. In fact, from the moment we wake up to when we go to sleep, almost every object we lay our eyes on has been created or modified by using Organic Chemistry to make our existence easier.

One of the basic needs of the modern society and, specifically, chemical industry is the availability of relatively big amounts of diverse natural or synthetic molecules with divergent properties, which can be studied and used to solve problems encountered in our daily lives. To be able to obtain such quantities, it is mandatory to discover methods for the synthesis and isolation of these products. Moreover, organic compounds present high diversity and structural complexity, which leads to the necessity of highly selective transformations that can incorporate different motifs in the presence of various functional groups. During the past centuries, synthetic chemists have discovered and developed new methods that have been used to synthesize extremely complex molecules.²

¹ "Chemistry, n." *OED Online*. Oxford University Press, December 2015.

² (a) Nicoulaou, K. C.; Sorensen, E. J. *Classics in total synthesis: Targets, strategies, methods* Ed. Wiley-VCH, 1996. (b) Nicoulaou, K. C.; Sorensen, E. J. *Classics in total synthesis II: More targets, strategies, methods* Ed. Wiley-VCH, 2003. (c) Nicoulaou, K. C.; Chen, J. S. *Classics in total synthesis III: Further targets, strategies, methods* Ed. Wiley-VCH, 2011.

Introduction.

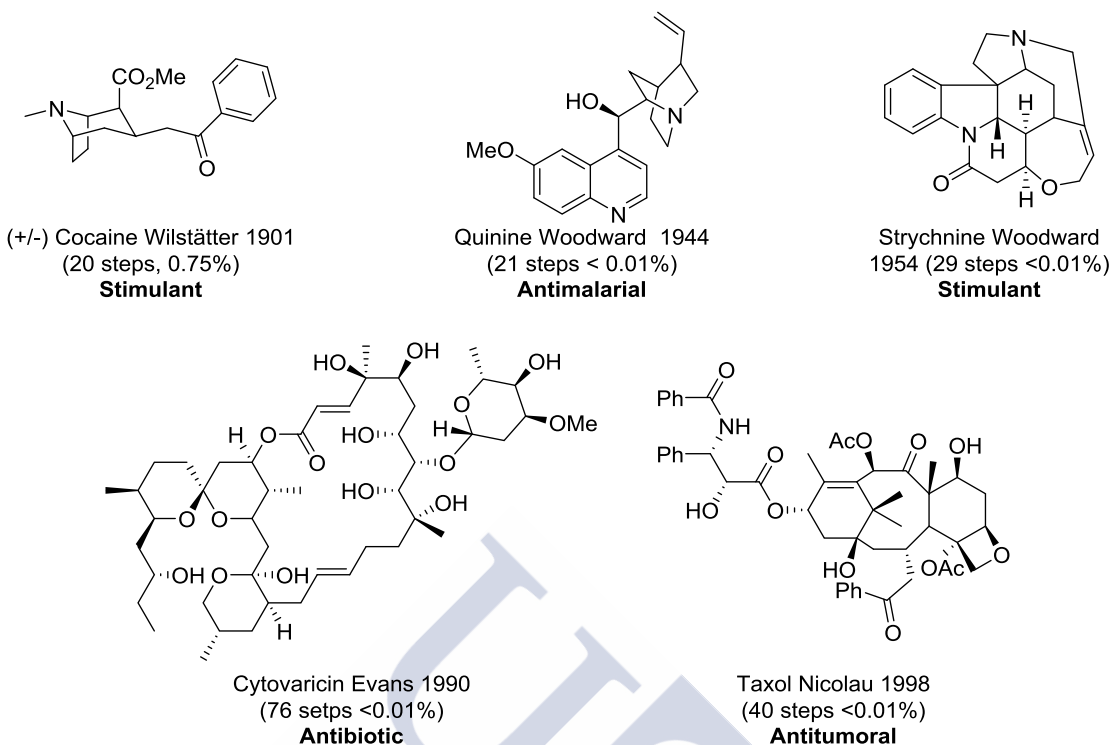


Fig 1. Example of classic total syntheses and their number of steps and total yield.

Despite these achievements are certainly impressive, they are somehow stained because, until not so long ago, chemists only purchased the synthesis of a complex molecule without stopping too much to evaluate the details of its obtention. Nowadays this vision has changed towards the quest for short and efficient synthesis.³

1.2. Requirements for modern Organic Chemistry.

As it has been mentioned before, Organic Synthesis has moved from the purchase of the synthesis of a given molecule to focus on the route needed for achieving that goal. This new vision has given rise to several new concepts:⁴ *Atom economy*, which is the efficiency of a chemical transformation in terms of the maximizing the incorporation of the atoms present in the reactants into the final product;⁵ *redox economy* meaning the use as few redox steps as possible in the synthetic conquest of a target compound;⁶ *step economy*, that refers to the minimization of transformations performed in an synthesis;⁷ *pot economy* meaning the use the minimum amount of workups and purification steps as possible⁸ and *green chemistry* which

³ Gaich, T.; Baran, P. S. *J. Org. Chem.* **2010**, *75*, 4657.

⁴ Newhouse, T.; Baran, P. S.; Hoffmann, R. W. *Chem. Soc. Rev.* **2009**, *38*, 3010.

⁵(a) Trost, B. M. *Science* **1991**, *254*, 1471. (b) Trost, B. M. *Angew. Chem. Int. Ed.* **1995**, *34*, 259. (c) Wender, P. A. *Tetrahedron* **2013**, *69*, 7529.

⁶ Burns, N. Z.; Baran, P. S.; Hoffmann, R. W. *Angew. Chemie - Int. Ed.* **2009**, *48*, 2854.

⁷(a) Wender, P. A.; Croatt, M. P.; Witulski, B. *Tetrahedron* **2006**, *62*, 7505. (b) Wender, P. A.; Verma, V. A.; Paxton, T. J.; Pillow, T. H. *Acc. Chem. Res.* **2008**, *41*, 40. (c) Wender, P. A.; Miller, B. L. *Nature* **2009**, *460*, 197.

⁸ Hayashi, Y. *Chem. Sci.* **2016**, *7*, 866.

includes, but is not limited to, minimization of waste and the use of toxic or hazardous chemicals⁹.

2- Organometallic Chemistry: The hammer in the reaction development toolbox.

One way of lowering the amount of steps needed for a total synthesis is the use of new reactions leading to different disconnections. In order to fulfill this goal, it is needed to find novel reactivities that do not suffer the limitations associated to carbon-based Organic Chemistry. This is why, from the late XIX century, chemists have been working with metals to expand the amount of transformations available. During the dawn of the so-called organometallic chemistry, the scientific community paid much of their attention into main group metals such as Li, Mg or B¹⁰. However, from the half of the XX century, the development of reactions catalyzed with metals such as Pd, Ni, Rh or Ru among other has given rise of a very productive era of transition metal-catalyzed chemistry, widening the scope of transformations available for the Synthetic Chemist. The main advantages of employing these reagents stem from their rich coordination chemistry and the possibility of changing their oxidation states, which result in mechanistic pathways with lower activation energies.¹¹

While organometallic stoichiometric reactions have been used from the very beginning of this chemistry, it was soon realized that translating it into synthetically useful contexts would require developing catalytic transformations.¹² In this way, with small amounts of organometallic precursor it is possible to transform large amounts of reactants.

2.2. Transition metal-catalyzed cycloadditions.

One of the fields in which transition metal catalysis has proven particularly useful is in the cycloaddition chemistry. According to the IUPAC gold book, cycloadditions are reactions in which two or more unsaturated molecules (or parts of the same molecule) are combined with the formation of a cyclic adduct in which there is a net reduction of the bond multiplicity.¹³ The most representative example of this kind of transformations is the Diels-Alder, a (4+2) reaction between a diene and a dienophile that generates cyclohexenes with a hundred percent atom economy.¹⁴

⁹ Anastas P.T.; Warner, J.C. *Green chemistry: Theory and practice*, Ed. Oxford university press, **1998**.

¹⁰ Astruc, D. *Organometallic chemistry and catalysis*, Springer-Verlag, **2007**.

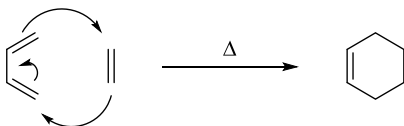
¹¹ (a) Hegedus, L.S. *Transition metals in the synthesis of complex organic molecules*, Ed. University Science of books, **1994**. (b) Crabtree, R.H. *The organometallic chemistry of transition metals*, Ed. Wiley, **2001**.

¹² Sabatier, P. *Catalysis in organic chemistry*, D. Van Nostrand Company, **1922**.

¹³ McNaught, A. D.; Wilkinson, A. *IUPAC compendium of chemical terminology 2nd Ed. (The "gold" book)*, Oxford, **1997**. XML on-line corrected version: <http://goldbook.iupac.org> (**2006-**) created by Nic, M.; Jirat, J.; Kosata, B. updates compiled by Jenkins, A.

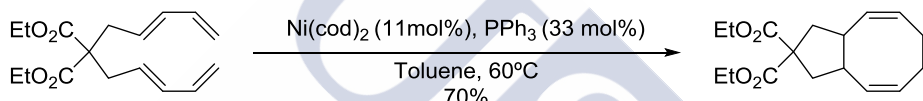
¹⁴ Diels, O.; Alder, K. *Justus Liebigs Ann. Chem.* **1928**, 460, 98.

Introduction.



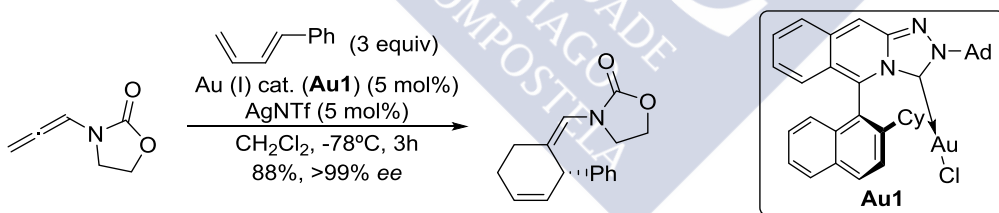
Scheme 1. Model of the Diels-Alder reaction.

These cycloadditions, work under the limitations of Woodward and Hoffmann rules, which result on the need of specific substitution so the frontier orbitals could overlap keeping orbital symmetry during the process.¹⁵ These structural requirements limit the scope of these reactions to specific substrates that are appropriately matched from the electronic point of view. One way of improving the scope of cycloadditions consists on the use of light or Lewis acids as promoters, although, they only work with substrates with strategically located substituents.¹⁶ Transition metals can be used to circumvent these limitations since they operate *via* different mechanisms, resulting in reactions that could not be obtained by any other means¹⁷ such as in this example by the group of Paul Wender, where they perform a Nickel-catalyzed (4+4) cycloaddition, otherwise forbidden under thermal conditions.¹⁸



Scheme 2. Paul Wender's Nickel-catalyzed (4+4) cycloaddition.

The use of transition metal complexes as promoters in this chemistry allows, not only to perform classically forbidden transformations, but also to do it under milder conditions and, in some cases, achieving highly enantioselective transformations such as demonstrated in our research group with allenamides and gold catalysis.¹⁹



Scheme 3. Enantioselective gold (I) catalyzed (4+2) cycloaddition.

¹⁵ (a) Woodward, R.; Hoffmann, R. J. Am. Chem. Soc. **1965**, *87*, 395. (b) Woodward, R.; Hoffmann, R. J. Am. Chem. Soc. **1965**, *87*, 2046. (c) Woodward, R.; Hoffmann, R. J. Am. Chem. Soc. **1965**, *87*, 2511.

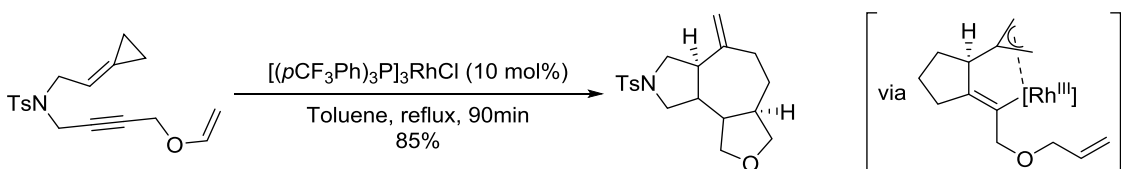
¹⁶ Carruthers, W. *Cycloaddition reactions in organic synthesis*, Pergamon press, **1990**. Kobayashi, S.; Jørgensen, K. A. *Cycloaddition reactions in organic synthesis*, Ed. Wiley-VCH, **2001**.

¹⁷ Lautens, M.; Klute, W.; Tam, W. *Chem. Rev.* **1996**, *96*, 49.

¹⁸ Wender, P. A.; Ihle, N. C. *J. Am. Chem. Soc.* **1986**, *8*, 4678.

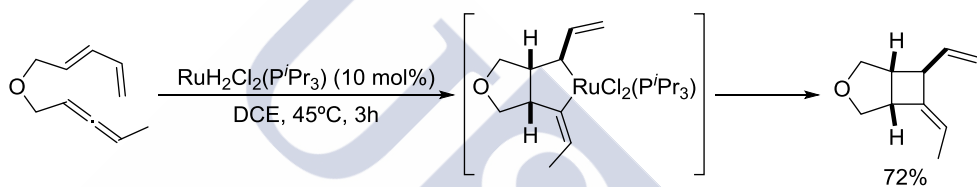
¹⁹ Francos, J.; Grande-Carmona, F.; Faustino, H.; Iglesias-Sigüenza, J.; Díez, E.; Alonso, I.; Fernández, R.; Lassaletta, J. M.; López, F.; Mascareñas, J. L. *J. Am. Chem. Soc.* **2012**, *134*, 14322.

Another advantage of the use of transition metals as catalysts, is that it is also possible to perform multicomponent annulations in a single step, as can be seen in a recent example from our research group.²⁰



Scheme 4. *Rh (I)-catalyzed (3+2+2) cycloaddition.*

Most of these transition metal catalyzed cycloadditions involve the generation of metallacycles resulting from the oxidation of the metal centre and a subsequent reductive elimination to regenerate the active catalyst as can be seen in this other example from our research group.²¹



Scheme 5. *(2+2) cycloaddition occurring via metallacycle.*

This type of metal-catalyzed annulations are extremely attractive and have led to many important discoveries in the last decades. However, since these reactions rely on the transformation of pi into sigma bonds, they require the presence of functionalized, unsaturated precursors and therefore, in many cases, the preparation of the precursors involve a relatively large number of steps.

2.3. Cross coupling reactions.

While metal-catalyzed cycloadditions like those shown above are extremely important reactions, transition metal catalysis has been also extensively used for many other transformations, prominently cross coupling reactions. The Mizoroki-Heck reaction is one elegant example of this approach²² which led Richard F. Heck to be awarded with the Nobel Prize in Chemistry in the year 2010.²³

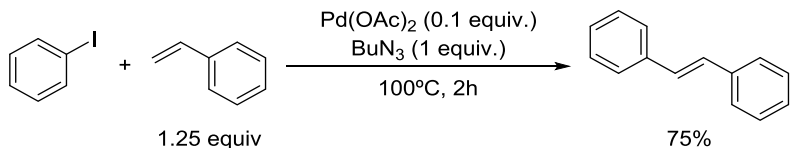
²⁰ Araya, M.; Gulías, M.; Fernández, I.; Bhargava, G.; Castedo, L.; Mascareñas, J. L.; López, F. *Chem. Eur. J.* **2014**, *20*, 10255.

²¹ Gulías, M.; Collado, A.; Trillo, B.; López, F.; Oñate, E.; Esteruelas, M. A.; Mascareñas, J. L. *J. Am. Chem. Soc.* **2011**, *133*, 7660.

²² (a) Mizoroki, T.; Mori, K.; Ozaki, A. *Bull. Chem. Soc. Jpn.* **1971**, *44*, 581 (b) Heck, R. F.; Nolley, J. P. *J. Org. Chem.* **1972**, *37*, 2320.

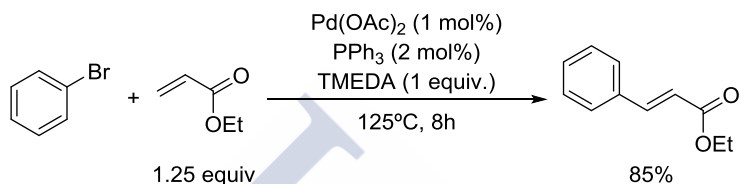
²³ http://www.nobelprize.org/nobel_prizes/chemistry/laureates/2010/

Introduction.



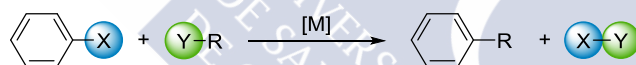
Scheme 6. The Heck reaction.

One of the advantages of the use of transition metals is the possibility to tune their reactivity by adding different ligands to improve the properties of the metallic centre.^{11a} For instance, Heck demonstrated that the range of reactive alkenes of his reaction could be expanded by adding phosphines to the reaction media.²⁴



Scheme 7. Use of phosphines as ligands to improve the Heck reaction.

From the second half of the XX century, cross coupling reactions have been gaining relevance for the construction of molecules, being nowadays widely used in industry.²⁵ Indeed, the well-known couplings developed by Suzuki and Negishi, which were also awarded with the Nobel Prize in chemistry in 2010, can be considered among the most relevant metal-catalyzed reactions discovered so far.



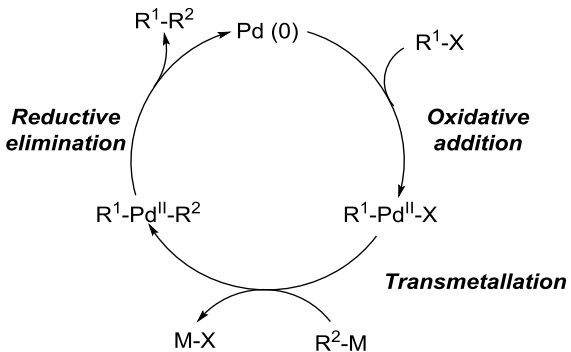
Scheme 8. Metal-catalyzed cross coupling reaction.

The mechanism of these reactions often starts with an oxidative addition of the metal to the C-X bond (being X a halogen or pseudohalogen) followed by the transmetalation with another metal-containing species (such as a borate in the case of the Suzuki coupling or zincate in the case of a Negishi coupling). A final reductive elimination joins the two hydrocarbons and regenerates the catalyst.²⁶

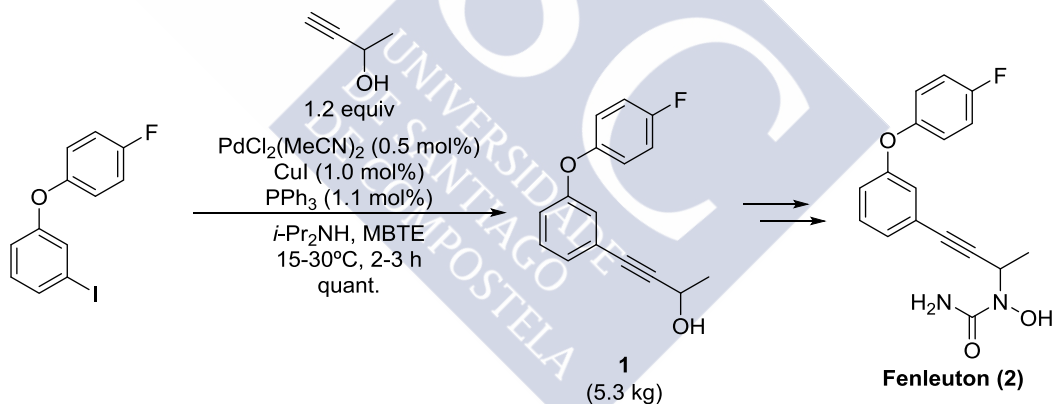
²⁴ Dieck, H. A.; Heck, R. F. *J. Am. Chem. Soc.* **1974**, 96, 1133.

²⁵ (a) Magano, J.; Dunetz, J. R. *Chem. Rev.* **2011**, *111*, 2177. (b) Busacca, C. A.; Fandrick, D. R.; Song, J. J.; Senanayake, C. H. *Transition metal catalysis in the pharmaceutical industry* Ed. John Wiley and sons, **2012**.

²⁶ (a) De Meijere, A.; Diederich, F. *Metal-catalyzed cross coupling reactions* Ed. Wiley-VCH, 2004.

**Scheme 9.** Classic mechanistic explanation of Pd catalyzed cross-couplings.

After the initial discovery of such processes, the scientific community demonstrated that the coupling reactions could be carried out using other organometallic compounds (such as magnesium in the Kumada coupling,²⁷ tin in the Stille coupling²⁸ or silicon in the Hiyama coupling²⁹) and remarkably reducing the catalyst loadings; therefore, turning them into a tool which has been used in uncountable synthetic applications.³⁰ In addition to the above reactions, the Sonogashira coupling provides an excellent way of attaching alkynes to different substrates. For instance, Thomas and co-workers at Abbot demonstrated the utility of this transformation in the kilogram-scale synthesis of **1**, an intermediate of Fenleuton a 5-lipoxygenase inhibitor.³¹

**Scheme 10.** Kilogram synthesis of Fenleuton intermediate **1**.

While the above reactions were designed for the construction of carbon-carbon bonds, it is also possible to make carbon-nitrogen bonds using the well-known Buchwald-Hartwig amination,³² or introduce other heteroatoms such as sulfur or oxygen³³ starting from

²⁷ (a) Corriu, R. J. P.; Masse, J. P. *J. Chem. Soc. Chem. Commun.* **1972**, No. 3, 144a. (b) Tamao, K.; Sumitani, K.; Kumada, M. *J. Am. Chem. Soc.* **1972**, 94, 4374.

²⁸ Milstein, D.; Stille, J. K. *J. Am. Chem. Soc.* **1978**, 100, 3636.

²⁹ Hatanaka, Y.; Hiyama, T. *J. Org. Chem.* **1988**, 53, 918.

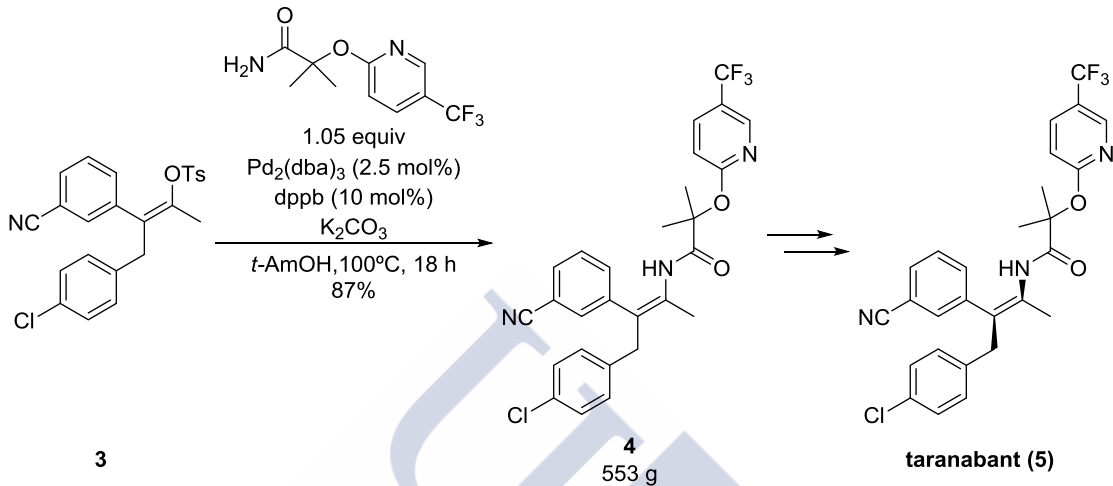
³⁰ Nicolaou, K. C.; Bulger, P. G.; Sarlah, D. *Angew. Chemie. Int. Ed.* **2005**, 44, 4442.

³¹ Thomas, A. V.; Patel, H. H.; Reif, L. A.; Chemburkar, S. R.; Sawick, D. P.; Shelat, B.; Balmer, M. K.; Patel, R. R. *Org. Process Res. Dev.* **1997**, 1, 294.

³² Yang, B. H.; Buchwald, S. L. *J. Organomet. Chem.* **1999**, 576, 125.

Introduction.

(pseudo)halides. As in the case of cross-coupling carbon-carbon reactions, these hetero-coupling processes have represented a breakthrough in our way of thinking of possible disconnections, also finding their place in industry. For instance, the synthesis of Taranabant (**5**), a cannabinoid-1 receptor inverse agonist for the treatment of obesity developed at Merck by Wallace and co-workers, makes use of a Pd-catalyzed amination as key synthetic step.³⁴



Scheme 11. Multigram synthesis of Taranabant intermediate 4.

Despite their proven effectiveness, cross coupling reactions are still far from perfect since they still present several limitations. Perhaps, the most important of those is the requirement of specific functionalized reaction partners, which, often, results in the necessity of additional steps to synthesize the corresponding precursors. They also generate stoichiometric amounts of byproducts since the (pseudo)halide and the metal are not incorporated in the final molecule.³⁵

3- C-H functionalization, the “holy grail” of catalysis.³⁶

3.1 C-H functionalization, an overview.³⁷

Although the above mentioned cross-coupling reactions represented invaluable milestones for Organic Synthesis, there is yet much room to progress in terms of achieving fully atom economical catalytic transformations. To fulfill this goal, it is critical to reduce the amount of functional groups that are lost during the reaction course. An ideal solution for this challenge is being able to generate transition metal organometallic species directly from hydrocarbons

³³ Hartwig, J. F. *Nature* **2008**, *455*, 314.

³⁴ Wallace, D. J.; Campos, K. R.; Schultz, C. S.; Klapars, A.; Zewge, D.; Crump, B. R.; Phenix, B. D.; McWilliams, J. C.; Krska, S.; Sun, Y.; Chen, C.-y.; Spindler, F. *Org. Process Res. Dev.* **2009**, *13*, 84.

³⁵ Yu, J-Q.; Shi, Z. C-H activation, Ed. Springer-Verlag, 2010.

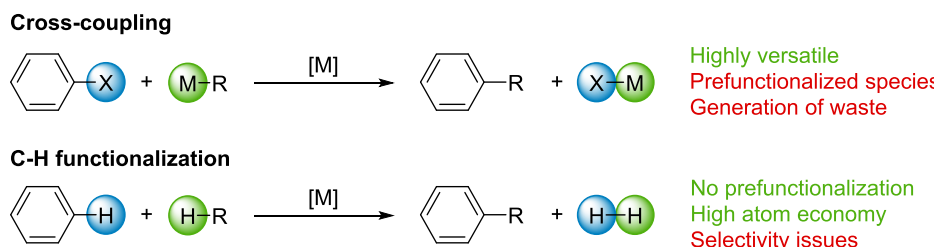
³⁶ Arndtsen, B. A.; Bergman, R. G.; Mobley, T. A.; Peterson, T. H. *Acc. Chem. Res.* **1995**, 28, 154.

³⁷ For selected reviews on C-H activation see: (a) Shilov, A. E.; Shul, G. B. *Chem. Rev.* **1997**, 97, 2879. (b)

Jia, C.; Kitamura, T.; Fujiwara, Y. *Acc. Chem. Res.* **2001**, *34*, 633. (d) Bergman, R. G. *Nature* **2007**, *446*,

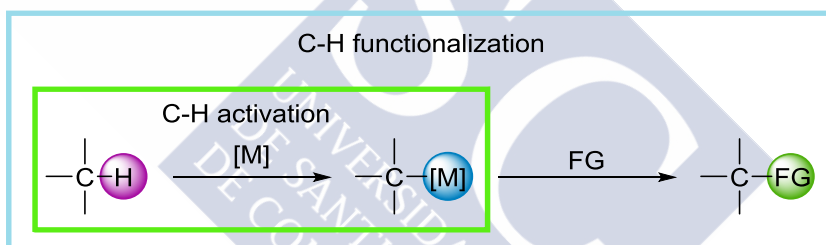
391. (e) Li, B.-J.; Shi, Z.-J. *Chem. Soc. Rev.* **2012**, *41*, 5588. (f) Hartwig, J. F. *J. Am. Chem. Soc.* **2015**, *138*, 2.

by replacing one hydrogen atom for a metal centre. This approach, known as C-H activation, has been receiving increasing attention during the past decades. One of its main advantages is that, since C-H bonds are ubiquitous in organic molecules almost any organic molecule can participate in these transformations and therefore, it opens a wide range of opportunities for developing unconventional coupling reactions.



Scheme 12. Cross coupling vs. C-H functionalization.

To avoid confusions, it is important to define well the concepts of C-H activation and functionalization. This task can be done using the organometallic point of view which states that C-H functionalization reaction converts a C-H bond into a C-X bond ($X \neq H$) via the formation of an organometallic intermediate.³⁸ This intermediate is formed through the metallation of the parent hydrocarbon, formally a C-H activation.³⁹



Scheme 13. Definitions of C-H activation and C-H functionalization.

C-H functionalizations, although very attractive, face several fundamental challenges. On one hand, the nature of the C-H bond, strong and poorly polarized makes the metallation step harder than for the case of halides (the bond strength of an aromatic C-H is around 110 kcal/mol while the corresponding for a C-I bond is only 65 kcal/mol). On the other hand, the aforementioned ubiquity of C-H bonds requires regioselective metallations at the desired position of the molecule. A general approach to face these problems consists on the use of directing groups capable of approximating the metal to the desired C-H bond.⁴⁰

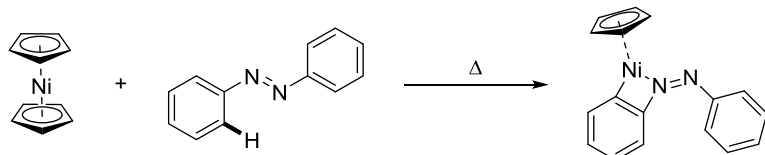
³⁸ Godula, K.; Sames, D. *Science*. **2006**, 312, 67.

³⁹ Hashiguchi, B. G.; Bischof, S. M.; Konnick, M. M.; Periana, R. A. *Acc. Chem. Res.* **2012**, 45, 885.

⁴⁰ For an exhaustive and comprehensive review on the use of directing groups in C-H functionalization see: Chen, Z.; Wang, B.; Zhang, J.; Yu, W.; Liu, Z.; Zhang, Y. *Org. Chem. Front.* **2015**, 2, 1107.

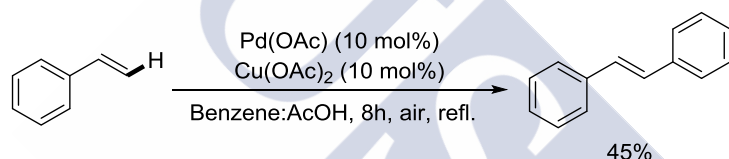
Introduction.

In fact, the beginning of the metal-promoted C-H activation field can be traced back to the seminal work of Kleiman and Dubeck describing the metallation of diazobenzene with a Ni (0) complex by using a nitrogen-based directing group.⁴¹



Scheme 14. First example of stoichiometric C-H activation, achieved by the use of a directing group.

In the late 60's Fujiwara demonstrated that organometallic species generated by C-H activation could engage in standard organometallic steps such as in migratory insertion of alkenes, which could lead to functional group-free cross coupling reactions.⁴² These processes could also be performed catalytically by using oxidants to regenerate the catalyst. This seminal Heck-type addition across double bonds took place with low yields and required the use of one of the substrates as solvent.⁴³



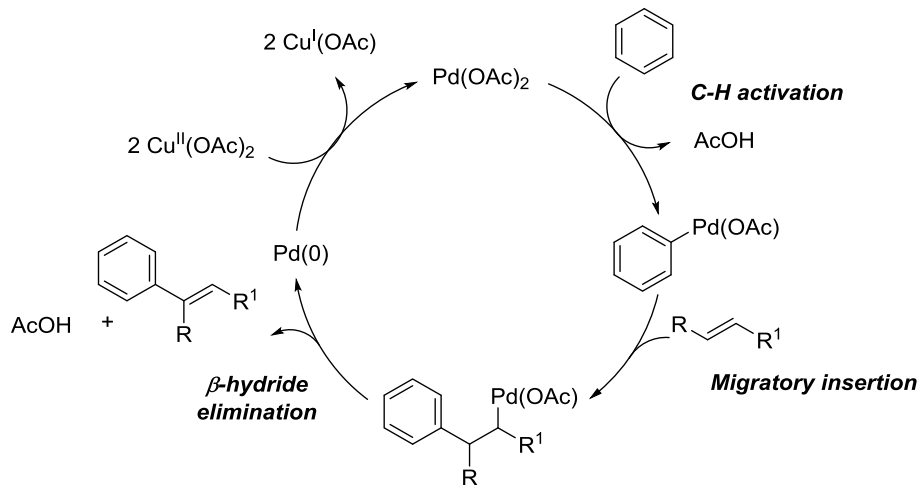
Scheme 15. Fujiwara-Moritani reaction.

The mechanism proposed for this reaction involves an initial metallation of the arene, insertion into the olefin and β -hydride elimination to release the stilbene and regenerate the catalyst.

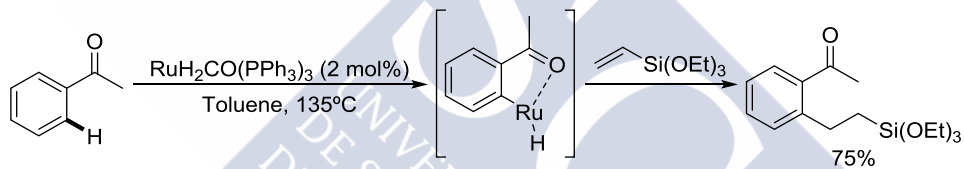
⁴¹ Kleiman, J. P.; Dubeck, M. *J. Am. Chem. Soc.* **1963**, *85*, 1544.

⁴² (a) Moritani, I.; Fujiwara, Y. *Tetrahedron Lett.* **1967**, *8*, 1119. (a) Moritani, I.; Fujiwara, Y. *Tetrahedron Lett.* **1968**, *9*, 4819.

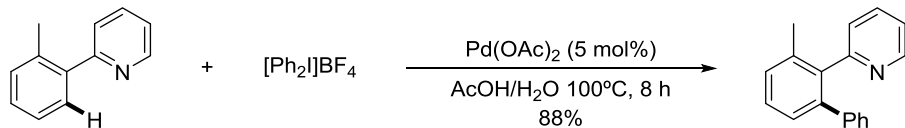
⁴³ Fujiwara, Y.; Moritani, I.; Danno, S.; Asano, R.; Teranishi, S. *J. Am. Chem. Soc.* **1969**, *91*, 7166.

**Scheme 16.** Mechanism of the Fujiwara-Moritani reaction.

Despite being a very promising approach, the interest for C-H functionalization dropped due to the lack of efficient catalytic processes. It was not until Murai published his revolutionizing work on Ruthenium catalyzed selective *ortho*-directed C-H functionalization of aryl ketones⁴⁴ that catalytic C-H activation was seriously considered as a plausible alternative to traditional cross couplings chemistry.

**Scheme 17.** Murai's pioneering work on C-H functionalization.

This milestone in the field of C-H functionalization ignited further work in the field and many other coupling processes, mainly involving palladium, have been described. Therefore, currently, the carbon-hydrogen bond can be, in some way, thought as a functional group that can be modified.⁴⁵ For instance, by using palladium catalysis, Sanford *et al.* were able to achieve the arylation of phenylpyridines with iodonium salts as shown below.⁴⁶

**Scheme 18.** C-H arylation of 2-phenylpyridinines with iodonium salts.

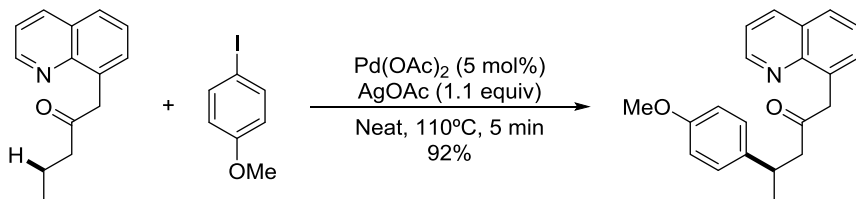
⁴⁴ Shinji Murai, Fumitoshi Kakiuchi, Shinya Sekine, Yasuo Tanaka, Asayuki Kamatani, Motohito Sonoda, N. C. *Nature* **1993**, *366*, 529.

⁴⁵ Chen, X.; Engle, K. M.; Wang, D. H.; Jin-Quan, Y. *Angew. Chemie. Int. Ed.* **2009**, *48*, 5094.

⁴⁶ Kalyani, D.; Deprez, N. R.; Desai, L. V.; Sanford, M. S. *J. Am. Chem. Soc.* **2005**, *127*, 7330.

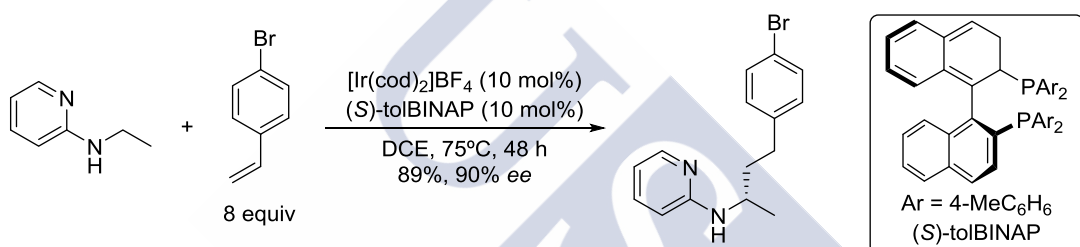
Introduction.

Although this kind of chemistry has been mainly applied for C(sp²)-H bonds, it is also possible to functionalize C(sp³)-H bonds, such as demonstrated by the group of Daugulis which was even able to discriminate between different C(sp³)-H bonds.⁴⁷



Scheme 19. Arylation of C(sp³)-H bond with aryl iodides.

Moreover, and albeit yet underdeveloped, there is the possibility of carrying out enantioselective C-H functionalizations by making use of appropriate chiral ligands as can be seen in the following example described by Shibata and co-workers.⁴⁸



Scheme 20. Asymmetric alkylation of C(sp³)-H bond with styrenes.

Nowadays metal-promoted C-H functionalization reactions are widely employed by chemists in such a way that these transformations are now included in their portfolios significantly shortening total syntheses.⁴⁹ One of the many examples of applications of synthetic shortcuts can be seen in this example by Du Bois where the enantioselective synthesis of Tetrodotoxin can be reduced in 35 steps by employing two different C-H functionalization steps including as a key step Rh-catalyzed nitrene insertion into a carbon-hydrogen bond.⁵⁰

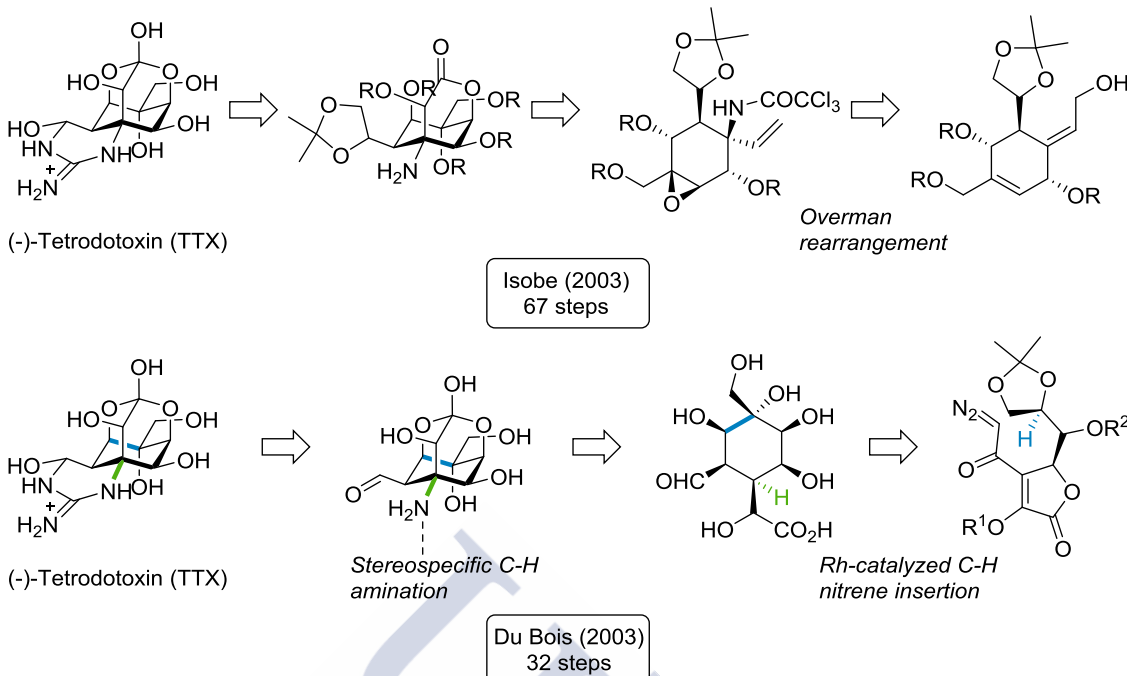
⁴⁷ Zaitsev, V. G.; Shabashov, D.; Daugulis, O. *J. Am. Chem. Soc.* **2005**, *127*, 13154.

⁴⁸ Pan, S.; Endo, K.; Shibata, T. *Org. Lett.* **2011**, *13*, 4692.

⁴⁹ (a) Gutekunst, W. R.; Baran, P. S. *Chem. Soc. Rev.* **2011**, *40* (4), 1976. (b) Yamaguchi, J.; Yamaguchi, A. D.; Itami, K. *Angew. Chemie. Int. Ed.* **2012**, *51*, 8960.

⁵⁰ (a) Ohyabu, N.; Nishikawa, T.; Isobe, M. *J. Am. Chem. Soc.* **2003**, *125*, 8796. (b) Hinman, A.; Du Bois, J. *J. Am. Chem. Soc.* **2003**, *125*, 11510.

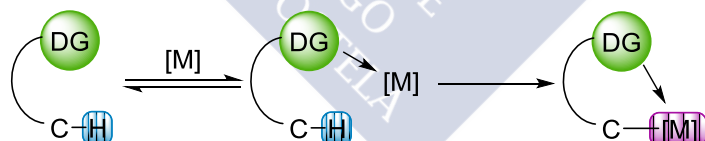
⁴⁰ Chen, Z.; Wang, B.; Zhang, J.; Yu, W.; Liu, Z.; Zhang, Y. *Org. Chem. Front.* **2015**, *2*, 1107.



Scheme 21. Step shortening in the synthesis of (-)-TTX by using C-H activation.

3.2 Use of directing groups in C-H functionalization.

As it has been mentioned before, the most widespread method to achieve selectivity in C-H activation transformations, is the employment of directing groups capable of placing the metal in a position close to the reactive centre. This approach, not only enhances selectivity, but also lowers the entropic cost of the C-H activation thus facilitating the process. Also, the possibility of tuning the electronic characteristics of the directing group further allows the modulation of the reactivity of the metal centre, in the same way as ligands can do.



Scheme 22. Site selectivity controlled by the use of DG.

A great variety heteroatom-containing directing groups have been used for this end. These directing groups differ on properties such as their coordinating strength or denticity, as seen in the following examples.⁵¹

⁵¹ (a) Vogler, T.; Studer, A. *Org. Lett.*, **2008**, *10*, 129. (b) N. M. Neisius and B. Plietker, *Angew. Chem., Int. Ed.*, **2009**, *48*, 5752 (b) Sonoda, M.; Kakiuchi, F.; Kamatani, A.; Chatani, N.; Murai, S. *Chem. Lett.*, **1996**, *25*, 109 (c) Boebel, T. A.; Hartwig, J. F. *J. Am. Chem. Soc.*, **2008**, *130*, 7534. (d) Yamada, S.; Obora, Y.; Sakaguchi S.; Ishii, Y. *Bull. Chem. Soc. Jpn.*, **2007**, *80*, 1194. (e) Nishino, M.; Hirano, K.; Satoh, T.; Miura, M. *Angew. Chem., Int. Ed.*, **2013**, *52*, 4457

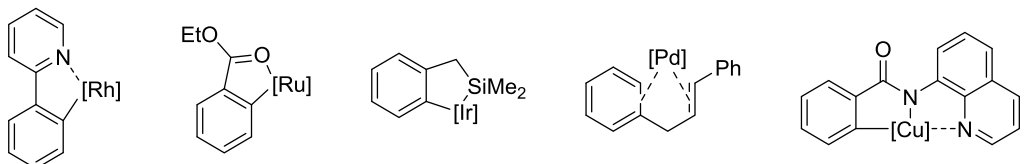


Fig 2. Diversity of directing groups.

While in most cases the directing groups have been used for functionalizing aryl C-H bonds in *ortho* positions, there have been also elegant approaches that allow *meta*⁵² or even *para*⁵³ functionalizations.

3.3 Mechanisms for C-H activation.⁵⁴

C-H functionalization reactions may operate under different activation modes that are strongly dependant on the choice of the metal catalyst and the different additives employed. The different reaction pathways can be summarized into the following categories:

3.3.1 Oxidative addition.

Oxidative addition reactions usually occur with low-valent, electron-rich transition metals and they are facilitated when they are coordinatively unsaturated. In this mechanism, the metal “inserts” into the C-H bond, raising its oxidation state by two units.^{37d}



Scheme 23. Mechanism of an oxidative addition into a C-H bond.

This mechanism of activation is the one proposed in this work by Hartwig where they achieve the *meta*-selective borylation of anilines.⁵⁵

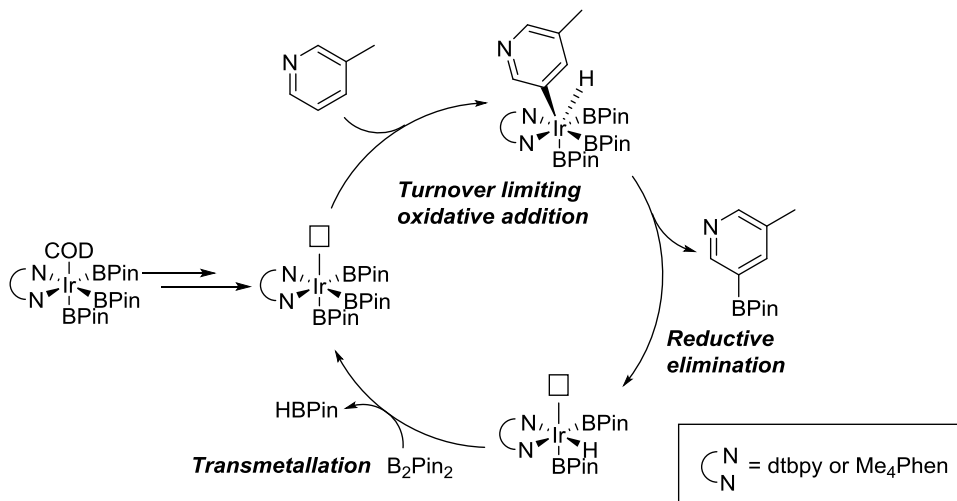
⁵² Phipps, R. J.; Gaunt, M. J. *Science*, **2009**, 323, 1953.

⁵³ Bag, S.; Patra, T.; Modak, A.; Deb, A.; Maity, S.; Dutta, U.; Dey, A.; Kancherla, R.; Maji, A.; Hazra, A.; Bera, M.; Maiti, D. *J. Am. Chem. Soc.* **2015**, 137, 11888.

⁵⁴ For reviews on the different modes of C-H activation see: (a) Labinger, J. a; Bercaw, J. E. *Nature* **2002**, 417, 507. (b) Lapointe, D.; Fagnou, K. *Chem. Lett.* **2010**, 39, 1118. (c) Balcells, D.; Clot, E.; Eisenstein, O. *Chem. Rev.* **2010**, 110, 749. (d) Editor, G.; McGrady, J.; Boutadla, Y.; Davies, D. L.; Macgregor, S. A.; Poblador-bahamonde, A. I.; Balcells, D.; Moles, P.; Blakemore, J. D.; Raynaud, C.; Brudvig, G. W.; Crabtree, R. H.; Eisenstein, O.; Trans, D. *Dalt. Trans.* **2009**, 5820.

^{37d} Bergman, R. G. *Nature* **2007**, 446, 391.

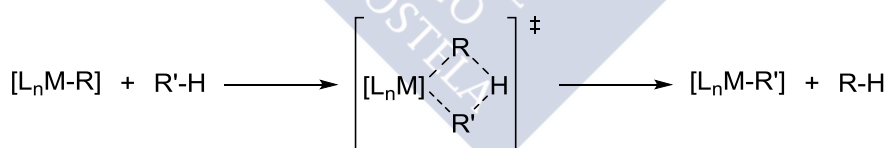
⁵⁵ Larsen, M. A.; Hartwig, J. F. *J. Am. Chem. Soc.* **2014**, 136, 4287.

**Scheme 24.** Example of C-H activation via oxidative addition.

In this reaction an initial dissociation of cyclooctadiene ligand from the Ir (I) complex unsaturates the metal centre, which allows the oxidative addition into the C-H bond to generate an Ir (III) intermediate. This species evolves upon reductive elimination leading to the borylated picoline and the reduced catalyst, which undergoes transmetallation to reenter the cycle.

3.3.2 Sigma bond metathesis.

A different way of achieving metallation of C-H bonds, mainly promoted by early transition metals with d^0 configuration like scandium, lanthanides or actinides and, in some cases, other metals such as Ru,⁵⁶ relies on a concerted exchange of a metal-ligand sigma bond with one carbon-hydrogen bond of an incoming substrate in a formal $[2\sigma + 2\sigma]$ transition state structure.⁵⁷

**Scheme 25.** Mechanism of the σ bond metathesis.

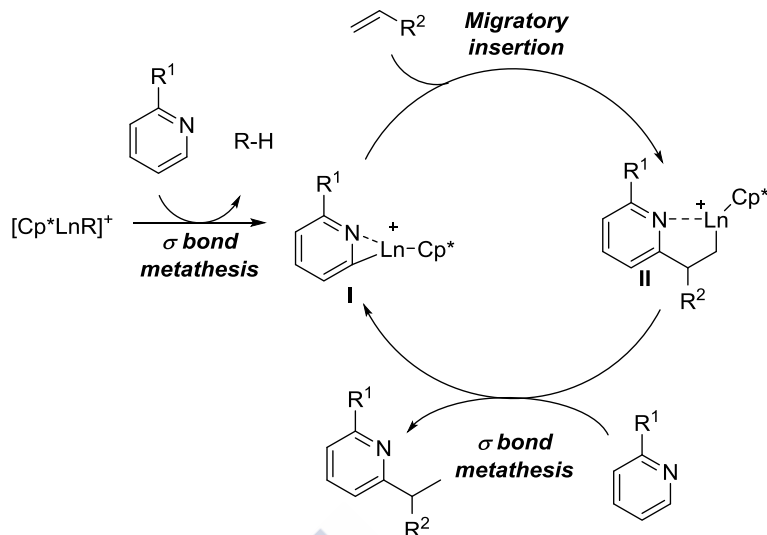
The group of Hou reported a rare earth-based C-H addition of pyridines to olefins that proceeded *via* sigma bond metathesis. The mechanism starts with an initial C-H activation followed migratory insertion generating a metallacyclic intermediate **II** which reacts with another molecule of pyridine by a second metathesis that regenerates the catalyst and delivers the proton to the C-M bond.⁵⁸

⁵⁶ Hartwig, J. F.; Bhandari, S.; Rablen, P. R. *J. Am. Chem. Soc.* **1994**, *116*, 1839.

⁵⁷ Waterman, R. *Organometallics* **2013**, *32*, 7249.

^{55a} Labinger, J. a; Bercaw, J. E. *Nature* **2002**, *417*, 507.

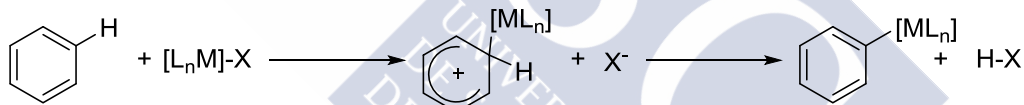
⁵⁸ Guan, B. T.; Hou, Z. *J. Am. Chem. Soc.* **2011**, *133*, 18086.



Scheme 26. Example of C-H activation via σ bond metathesis.

3.3.3 Electrophilic substitution.

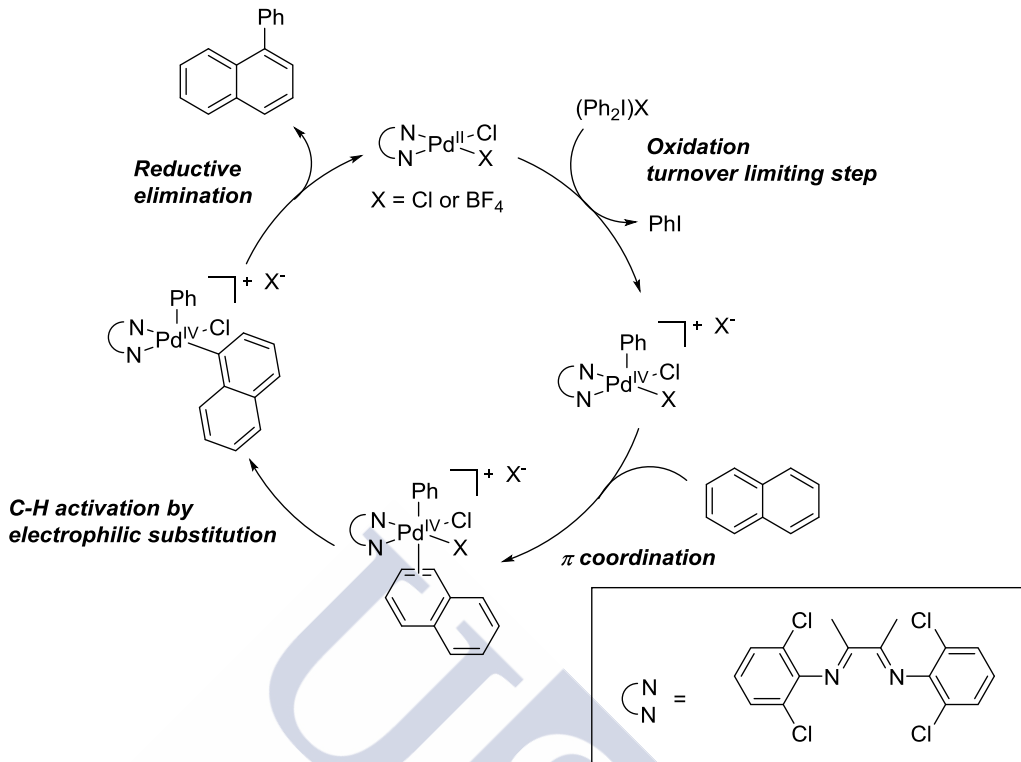
When the metal is in a higher oxidation state and the substrate is relatively electron-rich, another metallation mode can take place. In this case, the nucleophilic hydrocarbon attacks the metal generating a delocalized cationic species (Wheland intermediate, in the case of an aromatic system) that now loses the acidic proton generating the metallated intermediate.^{55a}



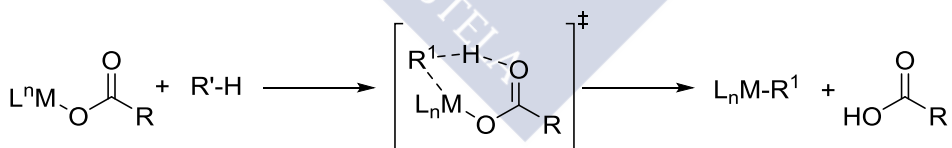
Scheme 27. Mechanism of the electrophilic metallation.

This mechanism is invoked in the arylation of naphthalene performed by the group of Melanie Sanford.⁵⁹ The observation of a KIE value of 1.0 ± 0.1 was interpreted in terms of the cleavage of the carbon-hydrogen bond not being involved in the turnover-limiting step. This result is consistent with an electrophilic palladation followed by a fast cleavage of the acidic C-H bond from the Wheland intermediate.

⁵⁹ Hickman, A. J.; Sanford, M. S. *ACS Catal.* **2011**, 1, 170.

**Scheme 28.** *Pd-catalyzed arylation of naphthalene.***3.3.4 Concerted metallation-deprotonation (CMD).**

Closely related to the electrophilic substitution mechanism is the CMD process. Both mechanisms have been often mistaken and, in fact, CMD was proposed in order to justify some experimental data that electrophilic substitution could not fully explain. In the latter, the metal centre weakens the C-H bond while a base, generally coordinated to the metal, abstracts the proton in a concerted manifold.^{55b,60}

**Scheme 29.** *Mechanism of the CMD.*

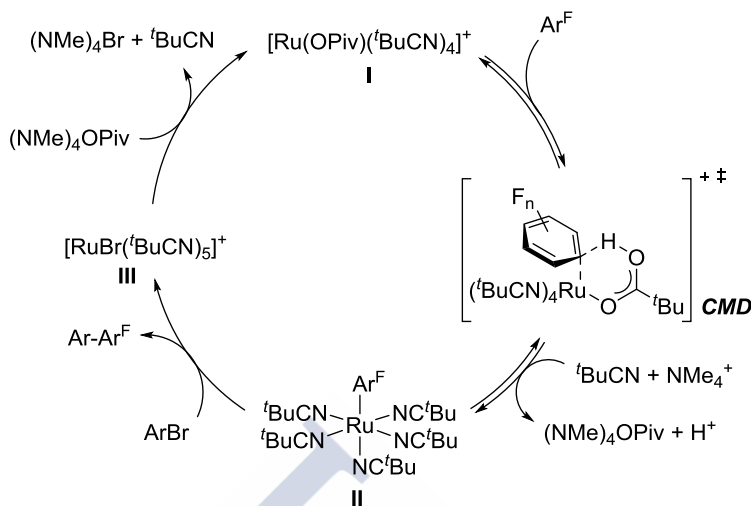
Recently, the group of Larrosa, described this mode of activation in his Ru (II)- catalyzed arylation of fluoroarenes with aryl halides. In their publication they also study this pathway by DFT calculations, which helped them to propose a mechanism. Their hypothesis starts with the *in situ* formation of the cationic species **I** which undergoes the CMD into the fluoroarene leading to complex **II**. This intermediate arylruthenium species undergoes a

^{55b} Lapointe, D.; Fagnou, K. *Chem. Lett.* **2010**, 39, 1118

⁶⁰ Ackermann, L. *Chem. Rev.* **2011**, 111, 1315.

Introduction.

formal oxidative addition/reductive elimination step with the aryl halide and complex **III**, which, after halide abstraction regenerates **I** closing the cycle.⁶¹



Scheme 30. *Ru-catalyzed arylation of fluoroarenes.*

3.4. Rhodium (III)-catalyzed C-H functionalizations.

In comparison to the widely used nickel, platinum and palladium catalysts; Rhodium presents exciting divergent properties for catalytic processes involving C-H activations.⁶² In particular, Rhodium has the ability to switch easily between oxidation states such as Rh (III) and Rh (IV) or even Rh (V) which opens a window for new reactivities. It also allows different coordination geometries, providing versatility in terms of ligand variability.⁶³ A pioneering example on the use of Rh (III) to activate C-H bonds was demonstrated by Maitlis in 1987, presumably operating *via* σ bond metathesis,⁶⁴ and, later by Davies employing a pentamethylcyclopentadienyl Rhodium dimer.⁶⁵

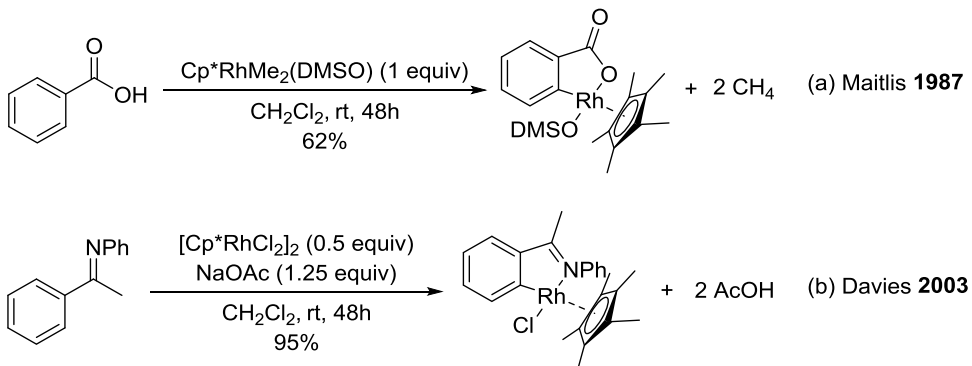
⁶¹ Simonetti, M.; Perry, G. J. P.; Cambeiro, X. C.; Juliá, F.; Arokianathar, J. N.; Larrosa, I. *J. Am. Chem. Soc.* **2016**, *138*, 3596.

⁶² Evans, A. *Modern Rhodium-catalyzed organic reactions*, Ed. Wiley-VCH, **2005**.

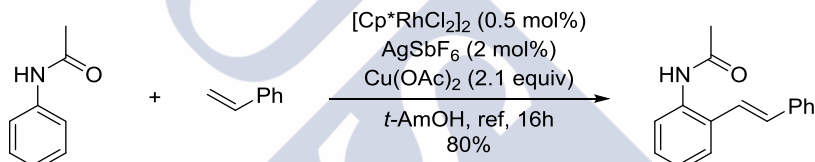
⁶³ Housecroft, C. E.; Sharpe, A. G. *Inorganic chemistry 2^o Ed.* Ed. Pearson Prentice Hall, **2006**.

⁶⁴ Kisenyi, J. M.; Sunley, G. J.; Cabeza, J. A.; Smith, A. J.; Adams, H.; Salt, N. J.; Maitlis, P. M. *J. Chem. Soc., Dalton Trans.*, **1987**, 2459.

⁶⁵ Davies, D. L.; Al-Duaij, O.; Fawcett, J.; Giardiello, M.; Hilton, S. T.; Russell, D. R. *Dalt. Trans.* **2003**, *2*, 4132.

**Scheme 31.** First example of C-H activation by $[Cp^*\text{RhCl}_2]_2$.

Following the pioneering work of Miura, which demonstrated that a $Cp^*\text{Rh}$ complex could be an efficient catalyst for C-H functionalization,⁶⁶ many other examples have been reported in the literature.⁶⁷ For instance, the group of Glorius developed an olefination of acetilanilides using styrenes and a silver salt to activate the Rhodium (III) catalyst by abstracting a chlorine atom from the active catalytic complex.⁶⁸

**Scheme 32.** $Rh\text{ (III)}$ -catalyzed C-H olefination.

The most widely employed precatalyst in this chemistry is $[Cp^*\text{RhCl}_2]_2$ which dissociates in presence of external ligands or additives to form the active monomers that perform the C-H activation step. The presence of the Cp^* ligand appears to be crucial for the reactivity which can be explained in terms of the stabilization of the high oxidation states of the rhodium.⁶⁹ After the metallation of the organic substrate, the complex adopts a characteristic piano stool configuration as shown in Figure 3 where phenylpyridine is activated and one of the chlorine atoms has been replaced by iodine to facilitate crystallization.⁷⁰

⁶⁶ Ueura, K.; Satoh, T.; Miura, M. *Org. Lett.* **2007**, *9*, 1407.

⁶⁷ (a) Satoh, T.; Miura, M. *Chem. Eur. J.* **2010**, *16*, 11212. (b) Song, G.; Wang, F.; Li, X. *Chem. Soc. Rev.* **2012**, *41*, 3651.

⁶⁸ Patureau, F. W.; Glorius, F. *J. Am. Chem. Soc.* **2010**, *132*, 9982.

⁶⁹ Maitlis, P. M. *Acc. Chem. Res.* **1978**, *11*, 301.

⁷⁰ Luo, C. Z.; Gandeepan, P.; Jayakumar, J.; Parthasarathy, K.; Chang, Y. W.; Cheng, C. H. *Chem. Eur. J.* **2013**, *19*, 14181.

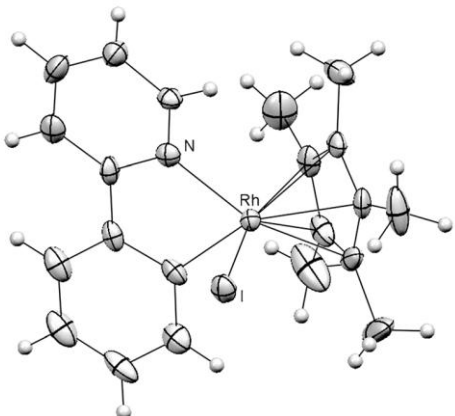


Fig 3. Crystal structure of the $Cp^*\text{Rh}(\text{ppy})\text{I}$ complex.

The mode of C-H bond activation by $Cp^*\text{Rh}$ (III) complexes, particularly for arenes, has been mainly described as concerted metallation-deprotonation.⁷¹

4-Annulations based on C-H activation, an interesting match.

4.2. General overview.

As it has been explained before, one of the most prominent ways of performing successful C-H functionalizations consists on the employment of directing groups.⁴⁰ However, despite the considerable advantages of using such groups for achieving selectivity, there is still one major drawback, which is that, in most of the cases, the directing group is only used as coordinating motif and it is not needed in the final structure. This means that additional steps are needed for the inclusion of such moiety in the backbone and for its subsequent elimination after the reaction. The use of transient directing groups avoids the extra steps needed for their elimination⁷² but they still generate waste and present low atom economy.

However, given the fact that some directing groups can form metallacyclic species after the C-H activation, it is possible to envision the use of such intermediates for similar transformations than those arising from already formed metallacycles, as the cycloadditions seen before. In this way, at least some atoms of the directing group will become part of the final cycle and therefore, it is not wasted. In addition, this approach provides a very appealing way of making reactive metallacycles that does not require the presence of unsaturations in the parent substrate. These reactions would imply an important increase in the molecular complexity and could become a very interesting and atom economical alternative to build cyclic molecules.

This methodology would also open a door for a straightforward access to a wide range of heterocycles, which are very common skeletons present in countless naturally occurring

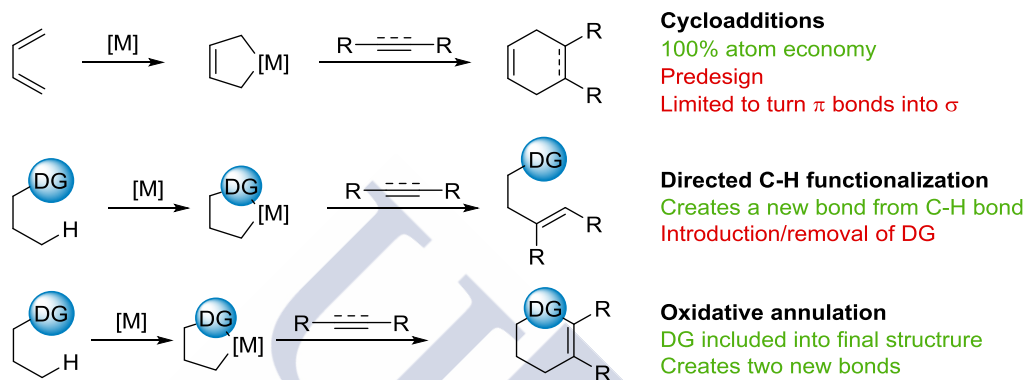
⁴⁰ Chen, Z.; Wang, B.; Zhang, J.; Yu, W.; Liu, Z.; Zhang, Y. *Org. Chem. Front.* **2015**, 2, 1107.

⁷¹ Li, L.; Brennessel, W. W.; Jones, W. D. *Organometallics* **2009**, 28, 3492.

⁷² Wang, X.-C.; Gong, W.; Fang, L.-Z.; Zhu, R.-Y.; Li, S.; Engle, K. M.; Yu, J.-Q. *Nature* **2015**, 519, 334.

and/or biologically active products⁷³, as well as molecules relevant for materials science such as OLEDs.⁷⁴

While one could be tempted to include this approach to cyclic skeletons among the category of formal cycloadditions, the name oxidative annulation might be more suitable, owing to the oxidation state of the final product in comparison with the starting materials and the IUPAC gold book definition of annulation: "A transformation involving fusion of a new ring to a molecule *via* two new bonds".¹³



Scheme 33. Oxidative annulations in contrast with cycloaddition and directed C-H functionalization.

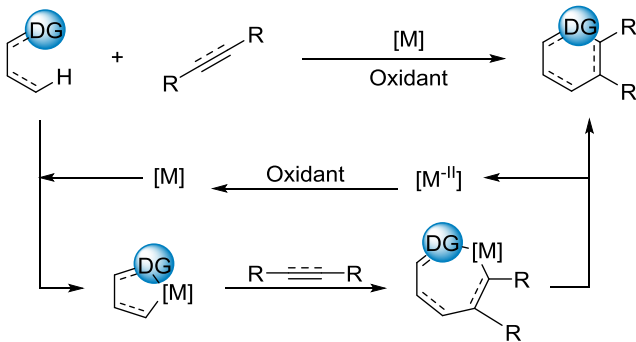
4.2. General mechanistic aspects of oxidative annulations.

The most common mechanism of these transformations involves the formation of the metallacyclic species which, after migratory insertion into an unsaturated partner generates a new metallacycle that, upon reductive elimination leads to the final molecule. The metal complex (usually from Pd, Rh, Ru or Ir) normally needs an additional reoxidation step in order to complete the catalytic cycle.

¹³ McNaught, A. D.; Wilkinson, A. *IUPAC compendium of chemical terminology 2nd Ed. (The "gold" book)*, Oxford, 1997. XML on-line corrected version: <http://goldbook.iupac.org> (2006-) created by Nic, M.; Jirat, J.; Kosata, B. updates compiled by Jenkins, A.

⁷³ (a) Majumdar, K. C.; Chattopadyay, S. K. *Heterocycles in natural product synthesis* Ed. Wiley-VCH, 2011. (b) Lamberth, C.; Dinges, J. *Bioactive heterocyclic compound classes: Pharmaceuticals* Ed. Wiley-VCH, 2012.

⁷⁴ Chen, D.; Su, S.-J.; Cao, Y. *J. Mater. Chem. C* **2014**, 2, 9565.



Scheme 34. General mechanism of oxidative annulations.

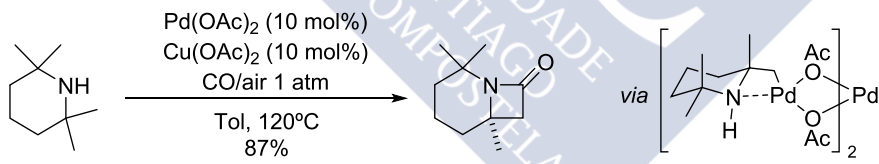
There is also the possibility that the directing group is not included in the final cycle if two consecutive C-H activations occur however in this latter case, the utility of the directing group would be just as auxiliary.

4.3. Some examples of oxidative annulations.

Oxidative annulations can be sorted according to different criteria. Herein we have chosen a classification based on the number of atoms provided by the unsaturated reaction partner. We have selected only a few representative examples among the vast number of reactions that have been described in recent years.⁷⁵

4.3.1 (n+1) oxidative annulations.

In these reactions, the coupling partner acts as a one-carbon surrogate. The most common reagent for this purpose is carbon monoxide. An example of the use of this gas is shown in scheme 35.⁷⁶



Scheme 35. (3+1) Oxidative annulations of aliphatic amines with CO.

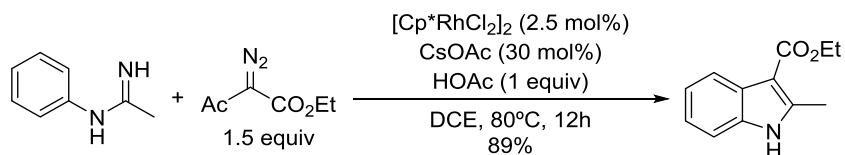
A key element for the success of this reaction is the use of highly hindered amines unable to form inactive palladium diamine species. In the same communication the authors describe the isolation of a trimeric palladium complex formed prior to the carbonylation, after the C-H activation.

It is also possible to use other molecules to act as one-atom donors such as diazo compounds, since they can generate carbenes by the loss of a nitrogen molecule such as can be seen in the

⁷⁵ Guliás, M.; Mascareñas, J. L. *Angew. Chem. Int. Ed.* **2016**, *in Press*.

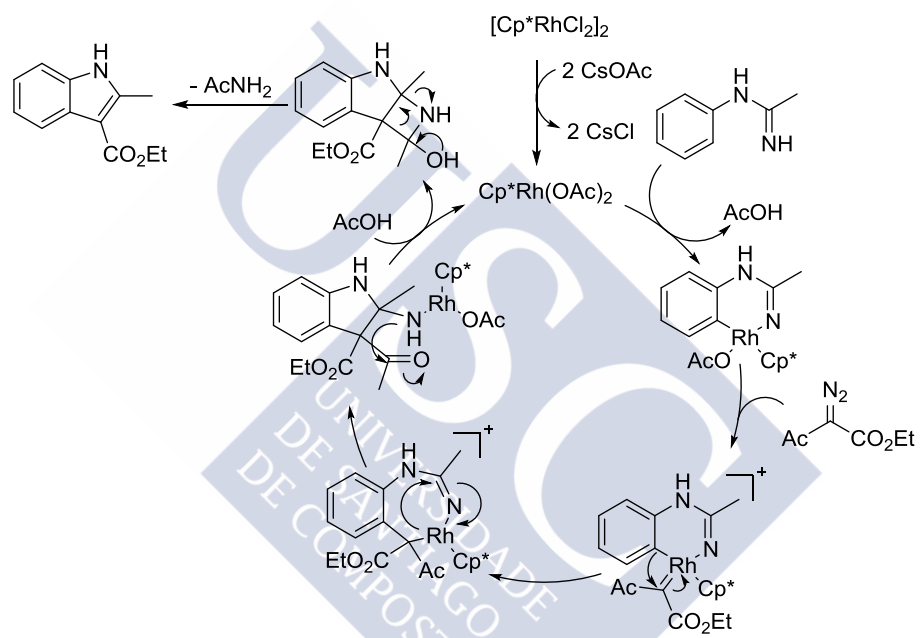
⁷⁶ McNally, A.; Haffemayer, B.; Collins, B. S. L.; Gaunt, M. J. *Nature* **2014**, *510*, 129.

following example involving a Rh (III)-catalyzed reaction between imidamides and diazocompounds for the synthesis of indoles.⁷⁷



Scheme 36. Oxidative annulations of imidamides to diazocompounds.

In this case, the last step of the reaction involves a migratory insertion instead of the more standard reductive elimination so the reaction can be carried out in the absence of external oxidants.



Scheme 37. (4+1) Oxidative annulations of imidamides with diazocompounds.

4.3.2 (n+2) oxidative annulations.

In these transformations, the reaction partners are usually compounds featuring double or triple carbon-carbon bonds. Frequently, these transformations present a higher catalytic turnover when using rhodium (III) instead of palladium, probably due to the easier insertion of alkynes.^{68a} The seminal work of Miura in oxidative annulations of benzoic⁶⁷ acids opened the door for these reactions usually performed with the standard Rh (III) complexes although it has been later shown that it is possible to use other transition metals such as Ru⁷⁸ or Co.⁷⁹

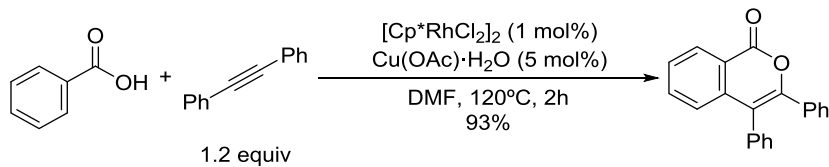
⁷⁷ Qi, Z.; Yu, S.; Li, X. *Org. Lett.* **2016**, *18*, 700.

^{68a} Satoh, T.; Miura, M. *Chem. Eur. J.* **2010**, *16*, 11212.

⁶⁷ Ueura, K.; Satoh, T.; Miura, M. *Org. Lett.* **2007**, *9*, 1407.

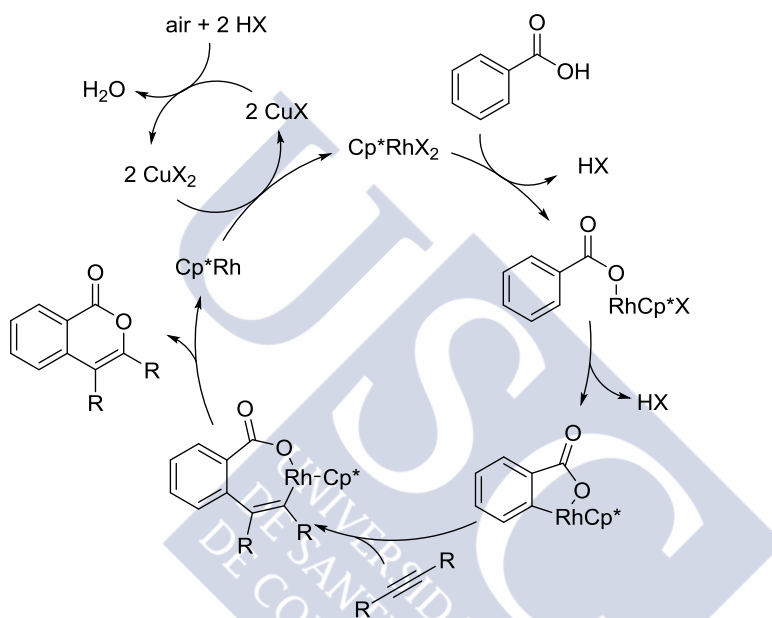
⁷⁸ (a) Ackermann, L.; Wang, L.; Lygin, A. V. *Chem. Sci.* **2012**, *3*, 177. (b) Deponti, M.; Kozhushkov, S. I.; Yufit, D. S.; Ackermann, L. *Org. Biomol. Chem.* **2013**, *14*, 2.

Introduction.



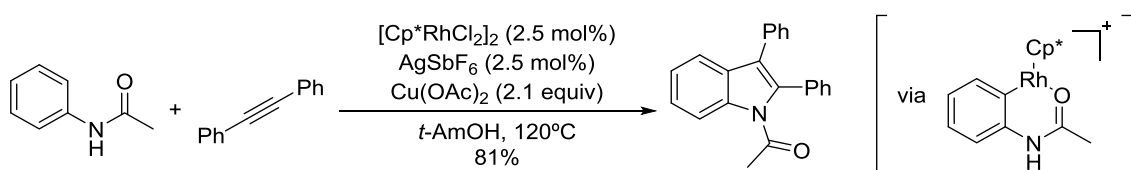
Scheme 38. Miura's oxidative annulation of benzoic acids and alkynes.

In this pioneering example, the carboxylic acid acts as the directing group and the annulation involves the cleavage of an O-H and a C-H bond.



Scheme 39. (4+2) oxidative annulations of benzoic acids to alkynes.

The group of Fagnou, reported an extremely relevant methodology to generate indoles by a formal (3+2) annulation between anilides and alkynes. To obtain high yields a silver salt must be added in order to generate a much more reactive cationic catalyst.⁸⁰



Scheme 40. Synthesis of indoles pioneered by Fagnou and co-workers.

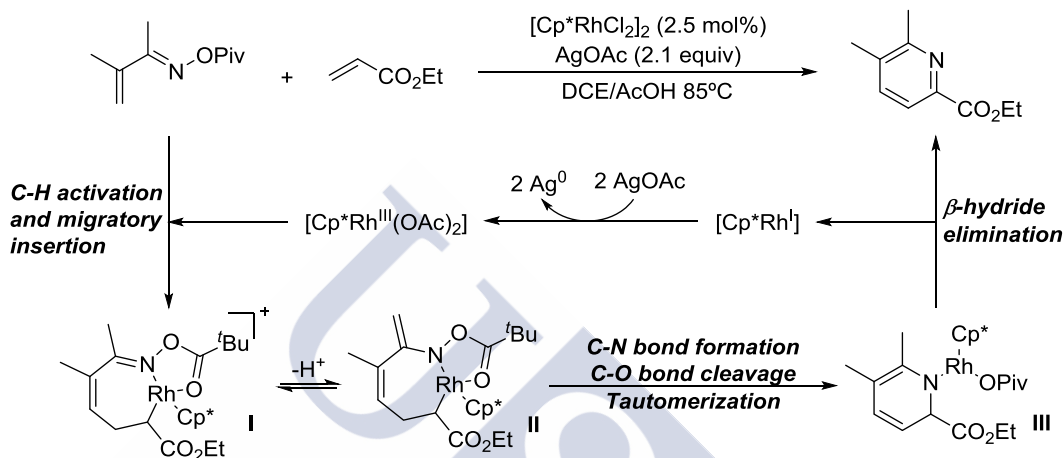
It is also possible to use alkenes as coupling partners in this type of annulations although the number of reports is lower than with alkynes, probably due olefins having poorer

⁷⁹ Sen, M.; Kalsi, D.; Sundararaju, B. *Chem. Eur. J.* **2015**, 21, 15529.

⁸⁰ (a) Stuart, D. R.; Bertrand-Laperle, M.; Burgess, K. M. N.; Fagnou, K. *J. Am. Chem. Soc.* **2008**, 130, 16474. (b) Stuart, D. R.; Alsabeh, P.; Kuhn, M.; Fagnou, K. *J. Am. Chem. Soc.* **2010**, 132, 18326.

coordinating abilities. Despite this drawback, they can still be found in some cases like this illustrative example by Prof Rovis and co-workers that relies on the use of oximes as directing group.⁸¹

A crucial step of this reaction is related to the increase in acidity of the β -hydrogen of the imine in intermediate I owing to the coordination to the Rhodium. It is also noteworthy that the β -hydrogen elimination in intermediate I is prevented, presumably due to the saturation of the Rhodium coordination sphere by the oxygen of the pivalate.



Scheme 41. Synthesis of pyridines by oxidative annulation.

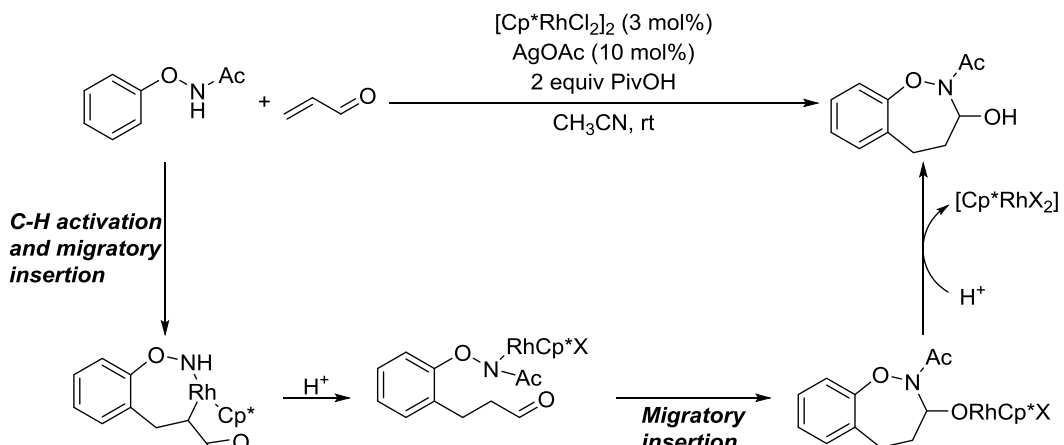
4.3.3 (n+3) oxidative annulations.

Although less common, there are also examples of annulations in which the reaction partner participates in the final cycle with more than two atoms.. One example of this idea is the synthesis of oxazepines by a (4+3) annulation. The reaction proceeds through two consecutive migratory insertions of an alkene and a carbonyl. The final seven-membered cycle is then released through a protodemetallation.⁸²

⁸¹ Esters, O.; Neely, J. M.; Rovis, T. *J. Am. Chem. Soc.* **2013**, 135, 66.

⁸² Duan, P.; Lan, X.; Chen, Y.; Qian, S.-S.; Li, J. J.; Lu, L.; Lu, Y.; Chen, B.; Hong, M.; Zhao, J. *Chem. Comm.* **2014**, 50, 12135.

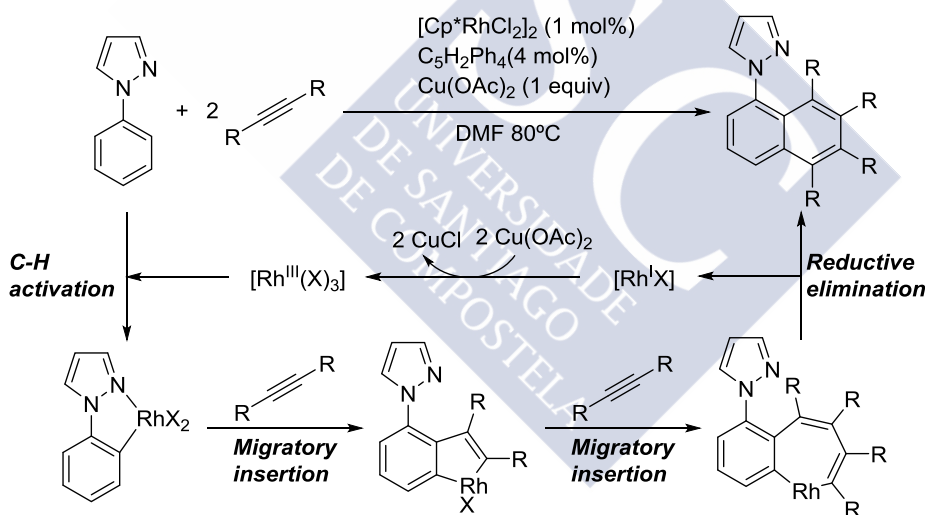
Introduction.



Scheme 42. (4+3) oxidative annulation for the synthesis of benzoxazepines.

4.3.4. ($n+n+n$) oxidative annulations.

Several examples of multicomponent annihilations have also been described. Miura and Satoh reported in 2008 a trimerization of a phenylazol containing arene and two alkynes by using the standard Cp^* rhodium catalyst in presence of an additional tetraphenylcyclopentadiene ligand.⁸³

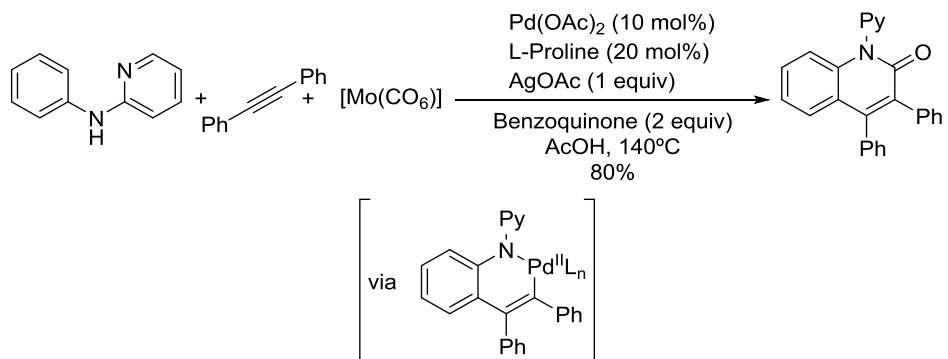


Scheme 43. Synthesis of naphthalenes by (2+2+2) annulation.

Introducing in the system an additional coupling partner such as carbon monoxide allows carrying out ($n+2+1$) annihilations such as demonstrated by Wu and co-workers in the following example.⁸⁴

⁸³ Umeda, N.; Tsurugi, H.; Satoh, T.; Miura, M. *Angew. Chemie. Int. Ed.* **2008**, *47*, 4019.

⁸⁴ Chen, J.; Natte, K.; Spannenberg, A.; Neumann, H.; Beller, M.; Wu, X. F. *Chem. Eur. J.* **2014**, *20*, 14189.

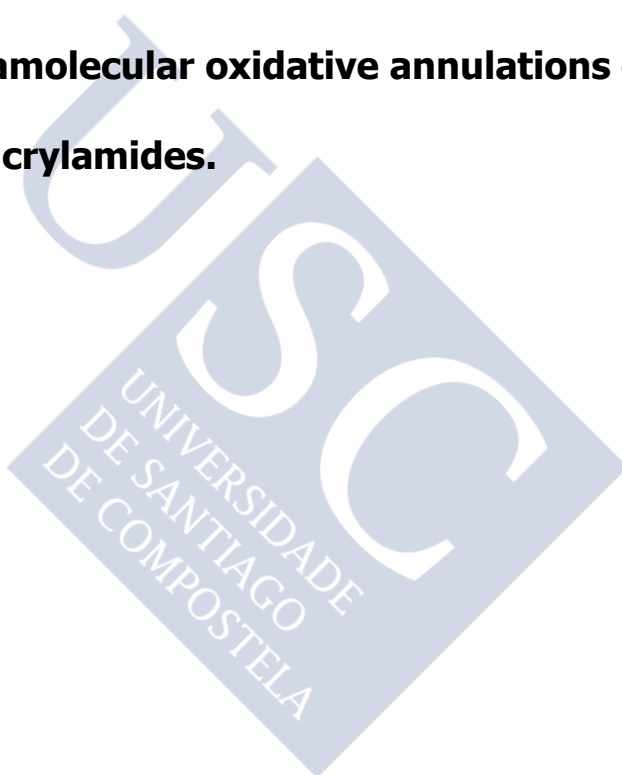


Scheme 44. *Synthesis of 2-quinolinones by a (3+2+1) oxidative annulation.*

In addition to the above oxidative annulations, in recent years there have been many other reports on related reactions so that, these once considered anomalous reactions can now be added to the toolbox of metal-catalyzed cycloadditions.



**CHAPTER II: Intramolecular oxidative annulations of
benzamides and acrylamides.**



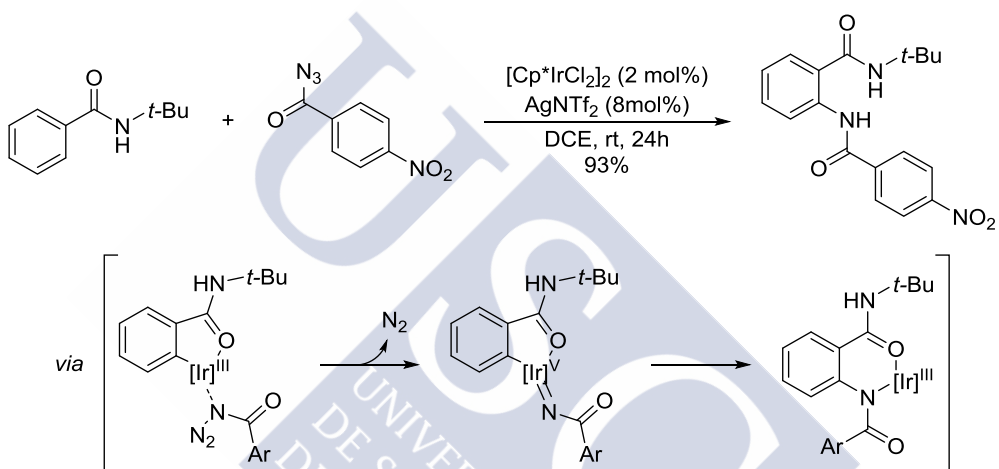


1- C-H functionalization of benzamides.

1.1 C-H functionalization of benzamides.

Benzamides, owing to the presence of an amide directing group, are able to participate in a wide range of C-H functionalization reactions. In fact, a great variety of transformations has been described using different metal complexes to introduce diverse functional groups.⁴⁰

For instance, Sukbok Chang and co-workers developed an iridium-catalyzed *ortho*-amination of benzamides. In their communication, they report the formation of a 5-membered metallacycle coordinated to the azide which would form a nitrene intermediate that, upon reductive elimination, generates the amidated product.⁸⁵



Scheme 45. *Ir (III)-catalyzed C-H amidation of benzamides.*

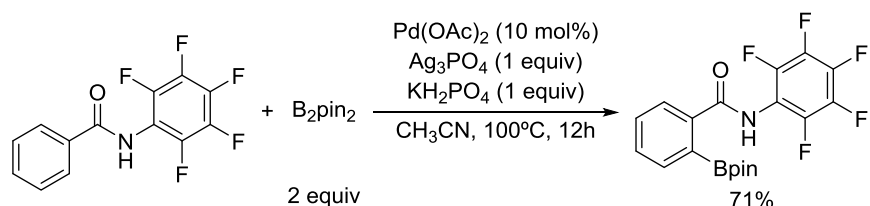
Also, the group of Prof. Jin-Quan Yu has demonstrated the importance of an appropriate choice of the directing group by using an electronically tuned pentafluorophenyl benzamide to carry out several Palladium catalyzed reactions.⁸⁶ One example of this directing group is the palladium-catalyzed borylation of arenes.⁸⁷

⁴⁰ Chen, Z.; Wang, B.; Zhang, J.; Yu, W.; Liu, Z.; Zhang, Y. *Org. Chem. Front.* **2015**, 2, 1107.

⁸⁵ Ryu, J.; Kwak, J.; Shin, K.; Lee, D.; Chang, S. *J. Am. Chem. Soc.* **2013**, 135, 12861.

⁸⁶ (a) Wasa, M.; Engle, K. M.; Yu, J.-Q. *J. Am. Chem. Soc.* **2010**, 132, 3680. (b) Yoo, E. J.; Ma, S.; Mei, T.; Chan, K. S. L.; Yu, J. *J. Am. Chem. Soc.* **2011**, 133, 7652. (c) He, J.; Shigenari, T.; Yu, J.-Q. *Angew. Chemie Int. Ed.* **2015**, 54, 6545.

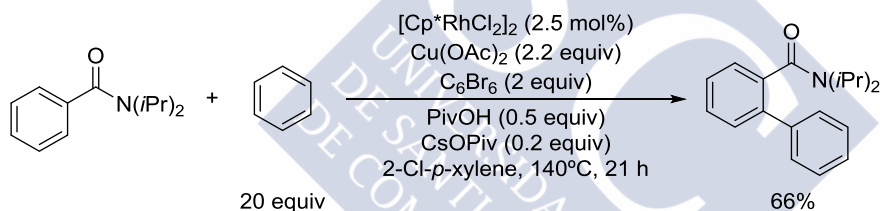
⁸⁷ Dai, H.-X.; Yu, J.-Q. *J. Am. Chem. Soc.* **2012**, 134, 134.



Scheme 46. C-H borylation of pentafluorophenyl benzamides.

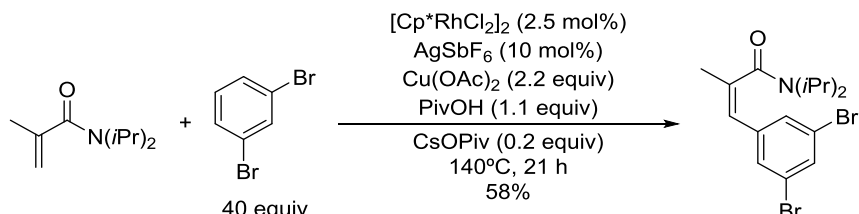
For these reactions they report the use of the very electron poor pentafluorophenyl benzamide as critical for the success of the reactions. Probably due to the delocalization of the negative charge which makes it behave more as an L ligand while still keeping its coordinating abilities.⁸⁸

Rhodium catalysis has been predominantly used with this motif. An elegant example reported by Glorius and coworkers describe the Rhodium-catalyzed cross dehydrogenative coupling of benzamides and simple arenes with hexabromobenzene as additive.⁸⁹ Although crucial for the success of the reaction, the role of the additive is still unclear. However, it was suggested that it acts as an oxidant. This is due to the fact that pentafluorobenzene was isolated from the reaction mixture, probably arising from an oxidative addition of the reduced Rh (I) catalyst to the Ar-Br bond followed by protodemetallation. It is also supposed to be somehow favoring the undirected C-H activation of the simple arene.



Scheme 47. Rh (III)-catalyzed C-H cross dehydrogenative coupling of benzamides with arenes.

Amide-directed C-H functionalizations can be also applied to vinylic substrates. For instance, the group of Glorius was also able to carry out a similar arylation to the above one, but using acrylamides instead of benzamides.⁹⁰



Scheme 48. Rh (III)-catalyzed C-H cross dehydrogenative coupling of acrylamides with arenes.

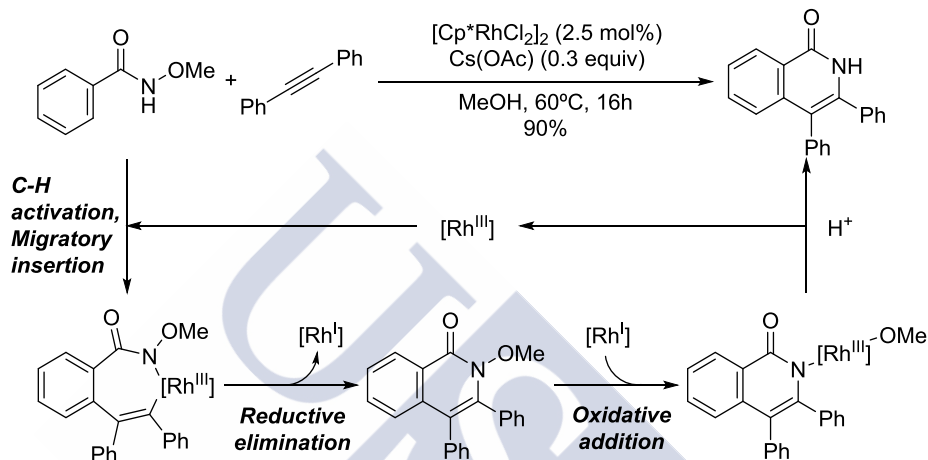
⁸⁸ Chan, K. S. L.; Wasa, M.; Wang, X.; Yu, J. Q. *Angew. Chemie. Int. Ed.* **2011**, *50*, 9081.

⁸⁹ Wencel-Delord, J.; Nimphius, C.; Wang, H.; Glorius, F. *Angew. Chemie - Int. Ed.* **2012**, *51*, 13001.

⁹⁰ Wencel-Delord, J.; Nimphius, C.; Patureau, F. W.; Glorius, F. *Chem. Asian J.* **2012**, *7*, 1208.

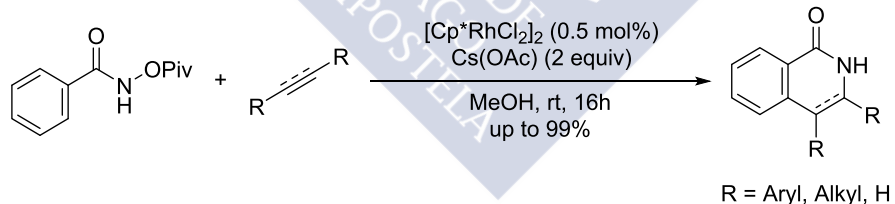
1.2 Oxidative annulation of benzamides.

The first report of the use of benzamides in Rh(III) catalyzed C-H functionalizations was, in fact an oxidative annulation. It was reported by the group of Fagnou as an extension for their work on the synthesis of indoles.⁹¹ Inspired by Yu's work,⁹² they used benzhydroxamic acid derivatives and, interestingly, they found out that the N-O bond was cleaved after the reaction, presumably by oxidative addition of the reduced Rh (I) into the N-O bond followed by ligand exchange. This side reaction allowed them to get rid of the copper oxidant needed to recover the catalyst.



Scheme 49. *Rh (III)-catalyzed oxidative annulation of benzhydroxamic acid derivatives.*

They further developed their work by establishing calculations on the mechanism, tuning the internal oxidant and significantly expanding the scope including terminal alkynes and olefins as coupling partners.⁹³



Scheme 50. *Rh (III)-catalyzed oxidative annulation of pivaloyl substituted benzhydroxamic acids.*

The inclusion of an internal oxidant has been widely used since this work, not only cleaving the N-O bond as in this case, but also switching the connection to release the R-NH ⁹⁴ or using N-N bonds.⁹⁵

⁹¹ Guimond, N.; Gouliaras, C.; Fagnou, K. *J. Am. Chem. Soc.* **2010**, *132*, 6908.

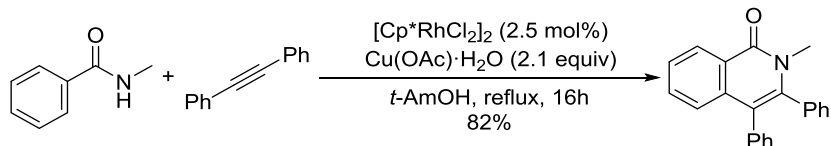
⁹² Wasa, M.; Yu, J.-Q. *J. Am. Chem. Soc.* **2008**, *130*, 14058.

⁹³ Guimond, N.; Gorelsky, S. I.; Fagnou, K. *J. Am. Chem. Soc.* **2011**, *133*, 6449.

⁹⁴ Zhang, Z.; Jiang, H.; Huang, Y. *ACS Catal.* **2015**, 6999.

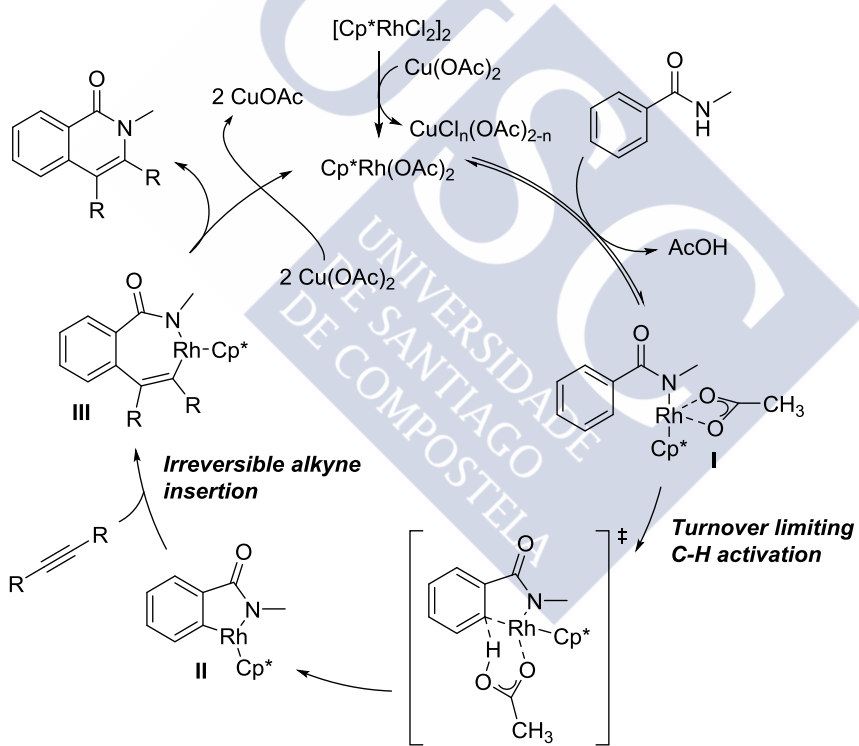
⁹⁵ Liu, B.; Song, C.; Sun, C.; Zhou, S.; Zhu, J. *J. Am. Chem. Soc.* **2013**, *135*, 16625.

Shortly after, the group of Miura⁹⁶ and the group of Hyster and Rovis published an extension of this work where they managed to carry out the reaction without the need of the N-O bond.⁹⁷



Scheme 51. Rovis' Rh (III)-catalyzed oxidative annulation of benzamides with alkynes.

After extensive mechanistic studies, they established a mechanistic hypothesis. Their proposal involves the formation of the active catalytic species⁹⁸ by ligand exchange of the chlorides with the acetates and a subsequent N-H cleavage leading to intermediate I. A CMD step would deliver the metallacycle II that can undergo migratory insertion into the alkyne followed by reductive elimination yielding the isoquinoline. The reduced catalyst is then reoxidized by the copper acetate.



Scheme 52. (4+2) oxidative annulations of benzamides with alkynes.

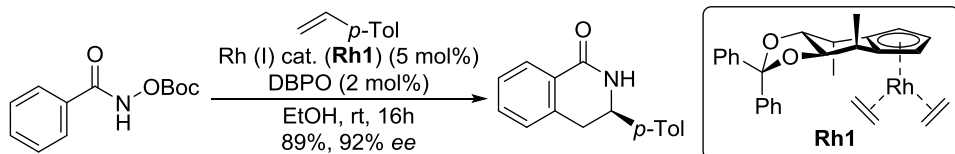
Inspired on Fagnou's work on the annulation of benzamides and alkenes, the group of Cramer sought for an enantioselective version of such coupling. Since the Cp^* is essential for

⁹⁶ Mochida, S.; Umeda, N.; Hirano, K.; Satoh, T.; Miura, M. *Chem. Lett.* **2010**, 39, 744.

⁹⁷ Hyster, T. K.; Rovis, T. *J. Am. Chem. Soc.* **2010**, 132, 10565.

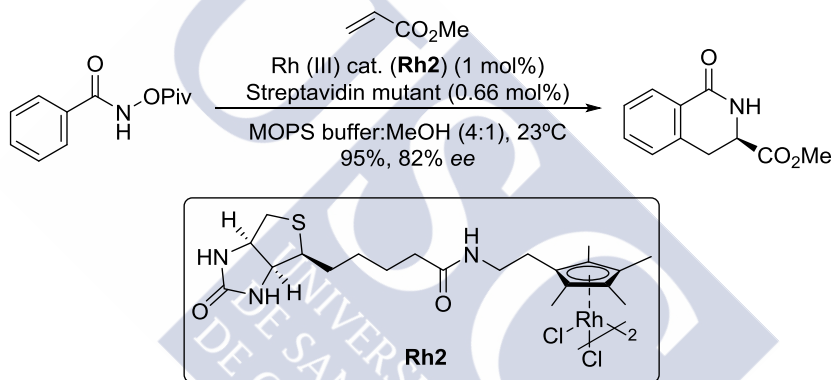
⁹⁸ The ligand exchange between chlorines and acetates is detected by UV/Vis in: Li, L.; Brennessel, W. W.; Jones, W. D. *Organometallics* **2009**, 28, 3492.

the reactivity and the other three positions have to be available for different mechanistic steps, there is no possibility of adding any chiral ligand to obtain enantioselectivity. To solve this problem they introduced the use of chiral cyclopentadienes that shield one face of the benzamide favoring one orientation of the alkene.⁹⁹



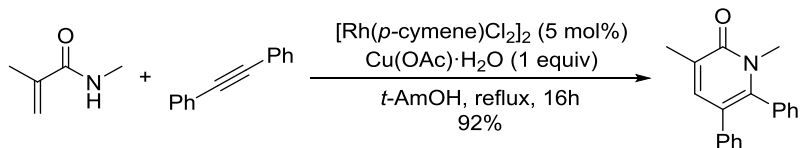
Scheme 53. *Rh (III)-catalyzed enantioselective oxidative annulation of benzhydrazamic derivatives.*

At the same time, the groups of Rovis and Ward published an alternative version for achieving enantioselective annulations by engineering an artificial metallozyme based on biotin-streptavidin interactions leading to yields up to 95% and enantiomeric excesses up to 86%.¹⁰⁰



Scheme 54. *Streptavidin/Rh (III)-catalyzed enantioselective oxidative annulation of benzhydrazamic acid derivatives.*

Acrylamides also undergo oxidative annulations under transition-metal catalysis. For instance, Ackermann and co-workers described an oxidative annulation of acrylamides for the synthesis of 2-pyridones using a ruthenium complex.¹⁰¹



Scheme 55. *Rh (III)-catalyzed oxidative annulation of benzamides with alkynes.*

⁹⁹ Ye, B.; Cramer, N. *Science*. **2012**, *338*, 504.

¹⁰⁰ Hyster, T. K.; Ward, T. R.; Rovis, T. *Science*. **2012**, *338*, 501.

¹⁰¹ Ackermann, L.; Lygin, A. V; Hofmann, N. *Org. Lett.* **2011**, *13*, 3278.

These annulations of benzamides and acrylamides were further studied by the groups of Fagnou, Miura and Rovis as well as others. becoming a powerful and robust transformation.¹⁰²

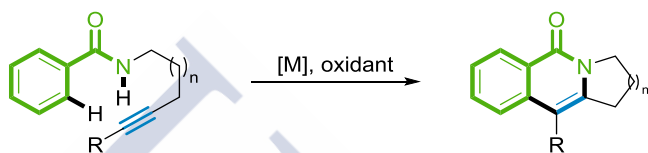


¹⁰² For more reports on the oxidative annulation of benzamides see: (a) Ya Du, T. K. H.; Rovis, T. *Chem. Commun.* **2011**, 47, 12074. (b) Cui, S.; Zhang, Y.; Wu, Q. *Chem. Sci.*, **2013**, 4, 3421. (c) Cui, S.; Zhang, Y.; Wu, Q. *Chem. Sci.*, **2013**, 4, 3912. (d) Hyster, T. K.; Ruhl, K. E.; Rovis, T. *J. Am. Chem. Soc.* **2013**, 135, 5364. (e) Huckins, J. R.; Bercot, E. A.; Thiel, O. R.; Hwang, T.; Bio, M. M. *J. Am. Chem. Soc.* **2013**, 135, 14492. (f) Shi, Z.; Grohmann, C.; Glorius, F. *Angew. Chemie. Int. Ed.* **2013**, 52, 5393. (g) Yu, D.; Azambuja, F. De; Glorius, F. *Angew. Chemie. Int. Ed.* **2014**, 53, 2754. (h) Yu, D.-G.; de Azambuja, F.; Gensch, T.; Daniliuc, C. G.; Glorius, F. *Angew. Chemie Int. Ed.* **2014**, 53, 1. (i) Peng, X.; Wang, W.; Jiang, C.; Sun, D.; Xu, Z.; Tung, C.-H. *Org. Lett.* **2014**, 16, 5354.

2- Objectives

When we started our work in this research area, the reports in the oxidative annulations of benzamides were scarce and limited to the initial reports of Rovis, Miura and Fagnou. Therefore we considered that there were many aspects in this chemistry that would deserve further attention.

Among others, we considered the possibility of achieving intramolecular annulations, given that this would provide a nice way to obtain relatively complex polycycles from very simple starting materials in an atom economical manner. Following these thoughts we considered the development of a fully intramolecular oxidative annulation leading to tricyclic isoquinolines.



Scheme 56. General objective.

This type of tricyclic cores is present in a wide range of biologically relevant products, such as the ones shown in the figure and therefore, a practical access to these structures was considered worthy.

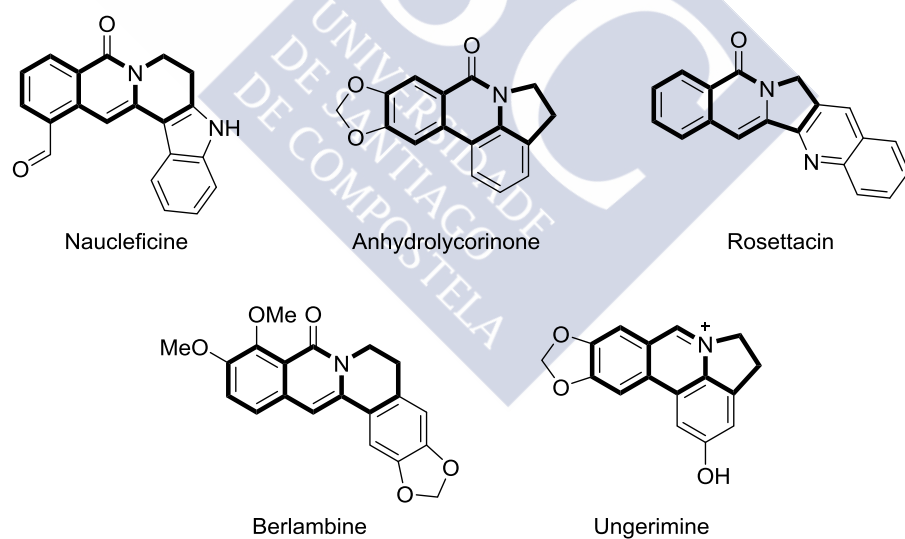
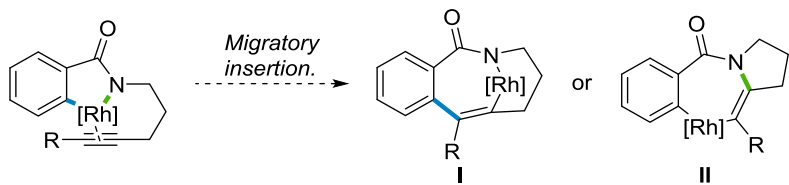


Fig 4. Natural products presenting a tricyclic isoquinoline core.

Although, this adaptation from inter to intramolecular reactions might seem obvious, a more careful analysis on the basis of the proposed mechanism revealed that it could be not so trivial. According to the hypothetical mechanism, consisting of a migratory insertion of the alkyne into the C-Rh bond of the resulting species from the C-H activation, this step would generate a bridged bicyclic intermediate such as **I**, that seems to be quite strained and, hence,

might not be formed. Alternatively, the reaction could take place by migratory insertion into the Rh-H bond, which would produce a much more comfortable species **II**.¹⁰³



Scheme 57. Possible intermediates after the migratory insertion.

On these bases there were a number of interesting challenges to be pursued:

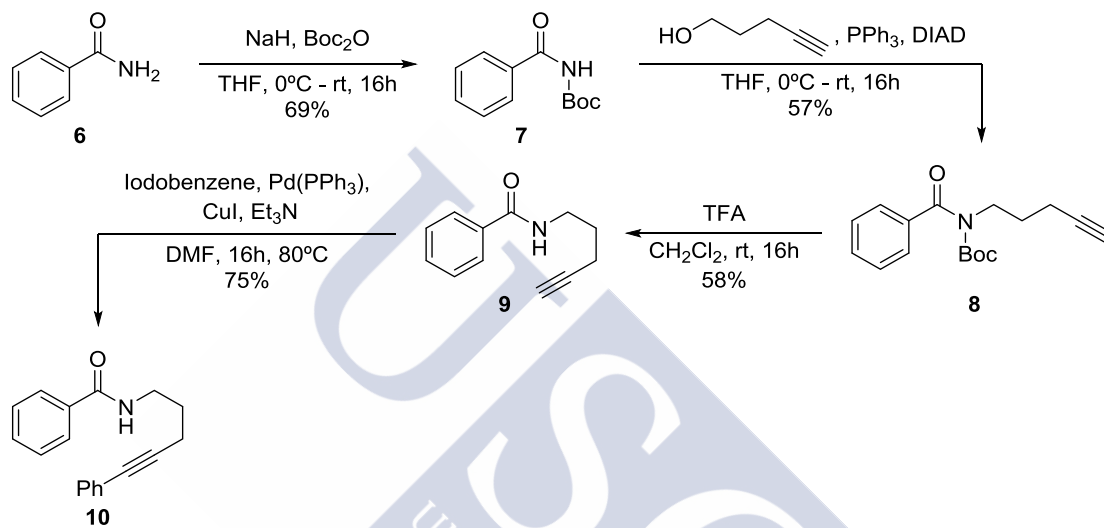
- Study the effect of the intramolecularity, including changes on the reactivity and regioselectivity.
- Easily access to biologically relevant tricyclic isoquinolines
- Study the mechanistic pathway through experimental and computational calculations.

¹⁰³ These two possibilities are described in: Li, B.; Feng, H.; Xu, S.; Wang, B. *Chem. Eur. J.* **2011**, *17*, 12573.

3- Results and discussion.

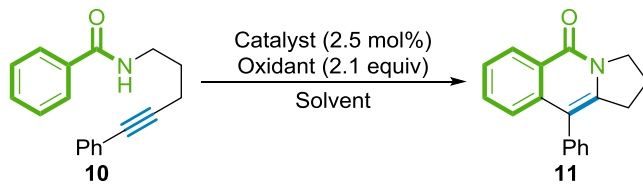
3.1 Optimization of the reaction conditions.

To study the viability of the reaction we synthesized the model substrate **10**. The preparation of this alkyne-tethered benzamide was achieved by an initial Boc protection of benzamide followed by a Mitsunobu type reaction with pentynol and deprotection. This sequence led to the terminal alkyne-tethered benzamide **9**. A final Sonogashira coupling with iodobenzene provided **10** in a 17% overall yield without major optimization.



Scheme 58. Synthesis of model substrate **10**.

With the model substrate in hand we screened several reaction conditions, varying the solvent and the catalytic system. The results of these experiments are summarized in Table 1.

Table 1 Screening of reaction conditions.

Entry	Catalyst	Oxidant	Solvent	Yield (%) ^b
1	[Cp*RhCl ₂] ₂	Cu(OAc) ₂	Toluene	57
2	[Cp*RhCl ₂] ₂	Cu(OAc) ₂	t-AmOH	98
3	[Cp*RhCl ₂] ₂	Cu(OAc) ₂	Acetone	35
4	[Cp*RhCl ₂] ₂	Cu(OAc) ₂	DMF	58
5	[Cp*Rh(CH ₃ CN) ₂](AgSbF ₆) ₂	Cu(OAc) ₂	t-AmOH	- ^c
6	[Cp*RhCl ₂] ₂ / AgSbF ₆	Cu(OAc) ₂	t-AmOH	- ^c
7	[Ru(p-cymene)Cl ₂] ₂	Cu(OAc) ₂	t-AmOH	50
8	[Cp*IrCl ₂] ₂	Cu(OAc) ₂	t-AmOH	23
9	Pd(OAc) ₂	Benzoquinone ^d	t-AmOH	- ^e

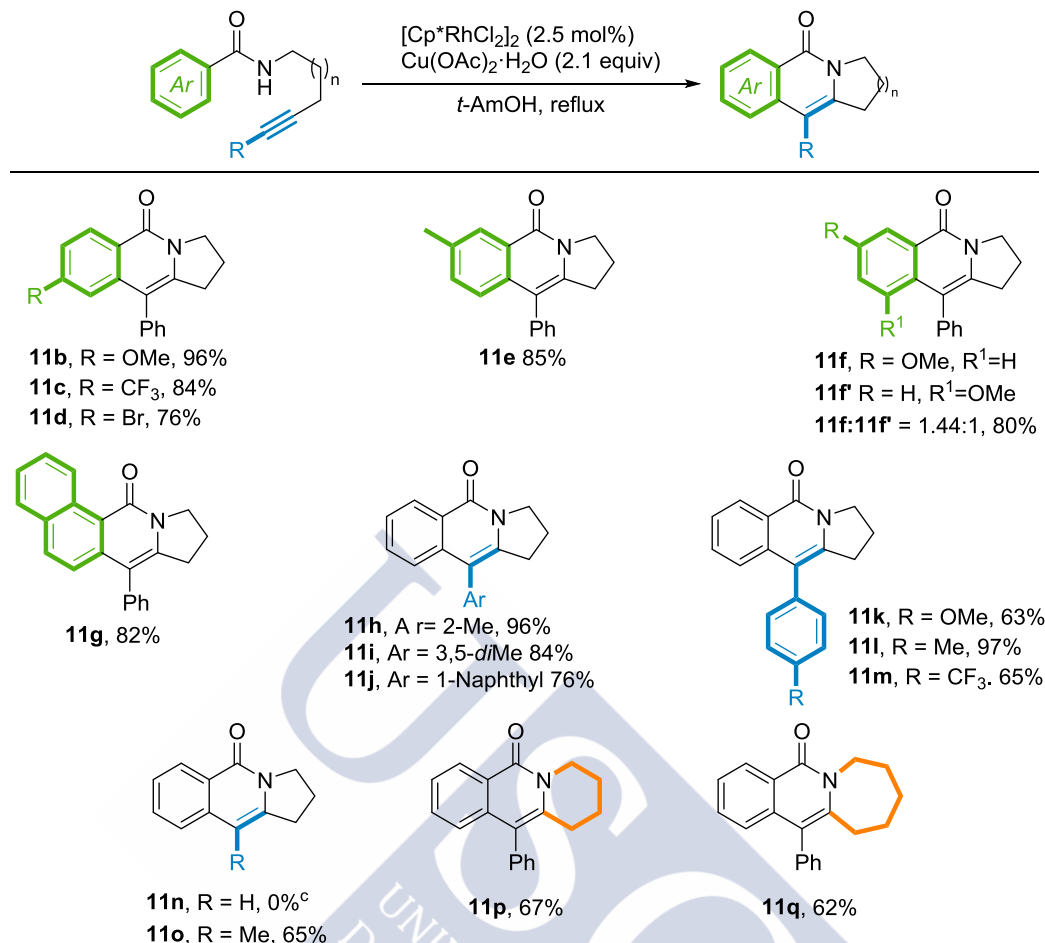
^a Reaction conditions: **10** (0.25 mmol), catalyst (2.5 mol %), oxidant (2.1 equiv), solvent (2 mL), 110 °C, 12 h. ^b Isolated yield. ^c Complex mixture of products. ^d 0.5 equiv of *p*-TsOH were added. ^e Recovery of the starting material.

As shown in table 1, the reaction proved to be more efficient in *t*-AmOH than in any other solvent tested, affording the tricyclic product in an excellent yield of 98% (entry 2). Interestingly, cationic Rhodium complexes, which have been reported to work in intermolecular cases,¹⁰⁴ led to a complex mixture of products (entries 5 and 6). We also checked other metal catalysts to carry out the transformation, however, they both showed much poorer performance. [Ru(*p*-cymene)Cl₂]₂ yielded the isoquinoline albeit in lower yield and with poor conversion (entry 7). Even lower conversion was achieved with the [Cp*IrCl₂]₂ catalyst, which yielded the isoquinoline in a 23% (entry 8). Palladium acetate failed to promote any transformation of the substrates, recovering most of the starting material after 12h at a 110°C (entry 9).

3.2 Substrate scope.

With the optimized conditions in hand, we proceeded to study the scope of the transformation. For this purpose we synthesized and tried a variety of substrates featuring different electronic and steric properties. These results are summarized in Scheme 59.

¹⁰⁴ Hyster T. K.; Rovis, T. *Chem. Sci.*, **2011**, 2, 1606.



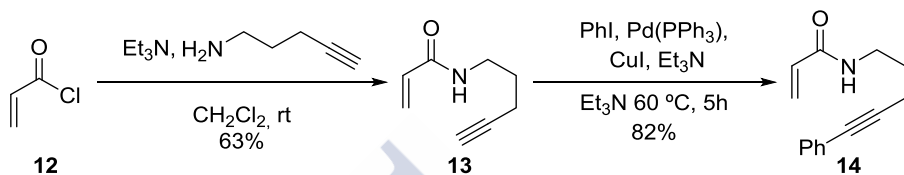
^a Reaction conditions: Benzamide (0.25 mmol), $[\text{Cp}^*\text{RhCl}_2]_2$ (2.5 mol%), $\text{Cu}(\text{OAc})_2 \cdot \text{H}_2\text{O}$ (2.1 equiv), *t*-AmOH (2 mL), 110 °C, 12 h. ^b Isolated yields. ^c The starting material was mostly recovered.

Scheme 59. Scope of the intramolecular oxidative annulation of benzamides and alkynes.

As it can be deduced from the data included in scheme above, the reaction is quite robust and tolerates a wide range of substituents in the benzamide, including electron donating groups like OMe (**11b**) and electron functionalities such as CF₃ (**11c**). It is also noteworthy that the annulation is compatible with the presence of aromatic C-Br bonds which is relevant because they could be engaged in further modifications. When a methyl group is placed at the *meta* position of the benzamide, the activation takes place regioselectively at the less hindered C-H bond (**11e**). However, with the methoxy derivative, we observed the formation of a 1.44:1 mixture of regioisomers (**11f**). This is probably due to the minor steric differentiation or a competitive coordination of the oxygen to the metal centre. Naphthaleneamides also participate in the annulation providing the regioselective functionalization at the 2-position of the naphthalene. Different arene substituents with varying steric properties can be added at the terminal position of the alkyne without considerably affecting the yield (**11h - 11j**). Electronic variations of the aryl substituent of the alkyne are also permitted, albeit in lower yields when those effects are drastic such as when methoxy or trifluoromethyl moieties are included (**11k - 11m**). The reaction also proceeds

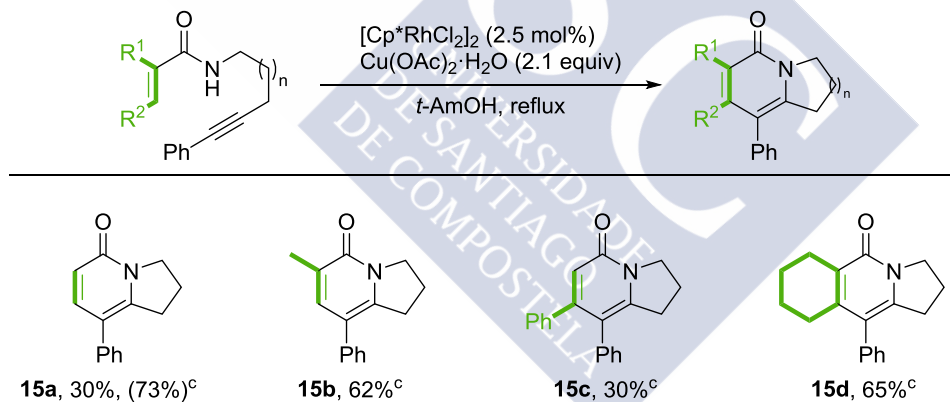
with longer tethers (**11p**, **11q**) and is not limited to aryl substituted alkynes, as alkyl substituted alkyne **11o** do also undergo the reaction. Nonetheless, terminal alkynes failed to react, leading to the recovery of the starting materials.

Given the good reactivity obtained observed in the above annulation with benzamides, we also thought of expanding the scope to acrylamides.¹⁰⁵ These starting materials were synthesized, as exemplified in the following scheme, by reaction of the corresponding acryloyl chloride with 4-pentynamine followed by a Sonogashira coupling to introduce the aryl moiety.



Scheme 60. *Synthesis of acrylamide **14**.*

As shown in Scheme 61, the reaction takes place in the above standard conditions albeit in lower yields. However it is possible to improve the yields by adding 1.2 equiv of cesium acetate. Although the role of this additive has not been extensively studied, it is possible that its addition facilitates the carboxylate-assisted C-H activation.^{55b, 61}



^a *Reaction conditions:* Acrylamide (0.25 mmol), $[\text{Cp}^*\text{RhCl}_2]_2$ (2.5 mol%), $\text{CuOAc}_2 \cdot \text{H}_2\text{O}$ (2.1 equiv), *t*-AmOH (2 mL), 110 °C, 12 h. ^b Isolated yields. ^c 1.2 equiv of CsOAc were added.

Scheme 61. *Scope of the intramolecular oxidative annulation of acrylamides.*

The reaction tolerates substitution at both positions of the double bond to give the expected products in yields around 60-70% (**15a**, **15b**, **15d**). However, when the β -hydrogen is replaced by a phenyl group, the yield drops to a 30% (**15c**).

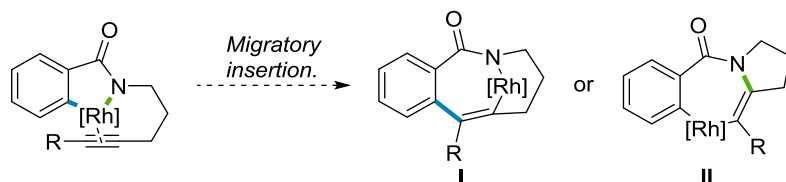
^{55b} Lapointe, D.; Fagnou, K. *Chem. Lett.* **2010**, 39, 1118.

⁶¹ Ackermann, L. *Chem. Rev.* **2011**, 111, 1315.

¹⁰⁵ For related annulation with acrylamides see: (a) Su, Y.; Zhao, M.; Han, K.; Song, G.; Li, X. *Org. Lett.* **2010**, 12, 5462. (b) Hyster, T. K.; Rovis, T. *Chem Sci* **2011**, 2, 1606.

3.3 Mechanistic investigations.

Despite the success of the reaction suggests that the migratory insertion step is probably involving a N-metallation instead of a C-metallation, we carried out several studies to shed a light into this question. Our co-worker, Dr. Rebeca García Fandiño, performed DFT calculations to compare the potential energy surface of the mechanisms involving the formation of either intermediate **I** or **II**.¹⁰⁶¹⁰⁷



Scheme 62. Possible intermediates after the migratory insertion.

For these calculations, carried out with the model substrate **10** in methanol, coordinatively unsaturated $\text{Cp}^*\text{Rh}(\text{OAc})_2$ was considered as the active catalytic species. This species would arise from the dissociation of the $[\text{Cp}^*\text{RhCl}_2]_2$ complex and a posterior ligand exchange with the acetates present in the media as has been described in previous studies.¹⁰⁸

As expected, the catalytic cycle starts with the coordination of the active Rhodium complex to the benzamide with concomitant loss of acetic acid. Next, the C-H activation step occurs via a concerted metallation-deprotonation transition state (**TS1**) leading to intermediate **B**, in which the acetic acid is still bound to the metal.¹⁰⁹ **TS1** exhibits a relative free Gibbs energy of 35.6 kcal mol⁻¹ and structural features similar to the ones described in intermolecular reactions (C-H and O-H distances for the proton transfer are 1.33 and 1.31 Å respectively and the Rh-C distance is 2.3 Å).¹⁰³ⁱ

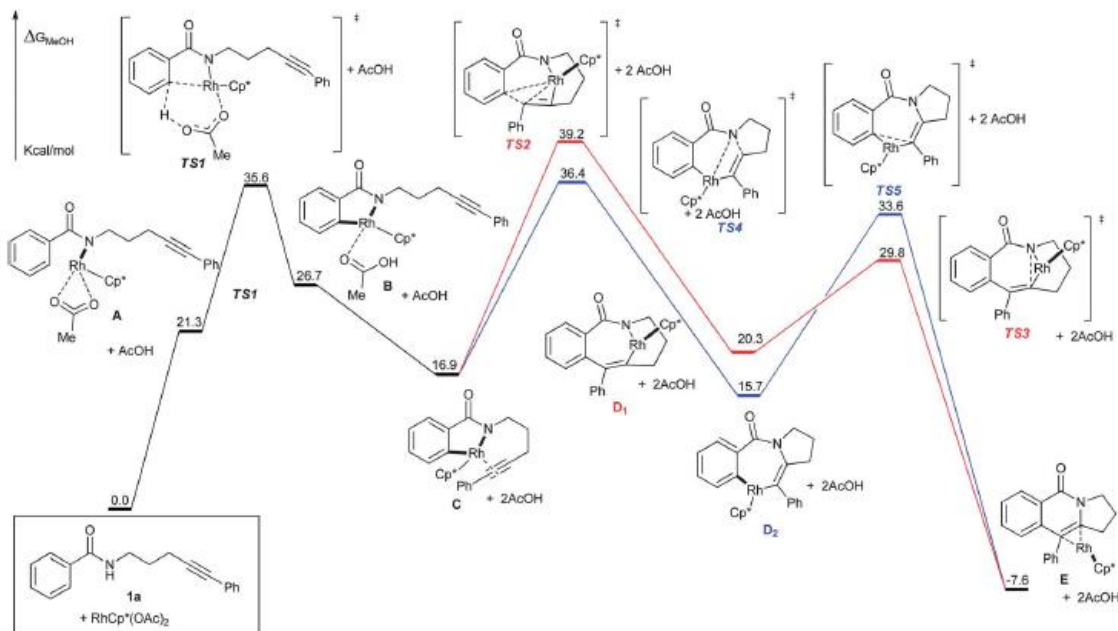
¹⁰⁶ Gas phase calculations were performed with Gaussian03 and Gaussian09 at DFT level. The geometries of all complexes here reported were optimized using the B3LYP hybrid functional. Optimizations were carried out using the standard 6-31G (d) basis set for C, H, O, and N. PCM calculations (MeOH for stationary points were performed using the 6-311+G-(2df,2p) basis set for C, H, O, and N, and SDD for Rh. Electronic energy values calculated with the smaller basis set have been corrected using the residual energy at the zero point vibrational energy (ZPE).

¹⁰⁷ For more DFT calculations in benzamide oxidative annulations see (a) Xing, Z.; Huang, F.; Sun, C.; Zhao, X.; Liu, J.; Chen, D. *Inorg. Chem.* **2015**, *54*, 3958. (b) Guo, W.; Zhou, T.; Xia, Y. *Organometallics* **2015**, *34*, 3012. (c) Zhou, T.; Guo, W.; Xia, Y. *Chem. Eur. J.* **2015**, *21*, 9209. ^{55b} D.; Fagrou, K. *Chem. Lett.* **2010**, *39*, 1118.

¹⁰⁸ Xu, L.; Zhu, Q.; Huang, G.; Cheng B.; Xia, Y. *J. Org. Chem.*, **2011**, *77*, 3017.

¹⁰⁹ Preliminary calculations were also conducted for the CMD step with the alkyne coordinated to Rh(III) and the acetate monocoordinated. The energy found was very high and consequently this pathway was ruled out.

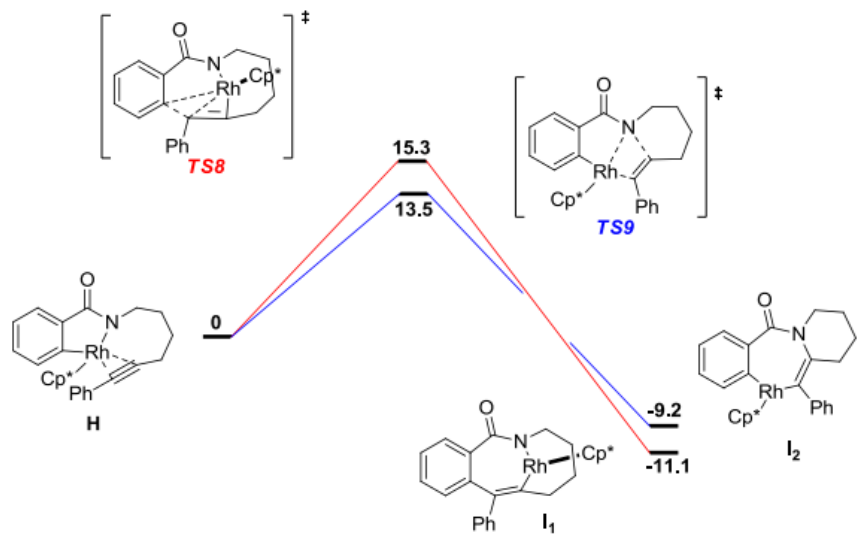
¹⁰³ⁱ Peng, X.; Wang, W.; Jiang, C.; Sun, D.; Xu, Z.; Tung, C.-H. *Org. Lett.* **2014**, *16*, 5354.



Scheme 63. DFT calculations for the mechanism of the intramolecular oxidative annulation.

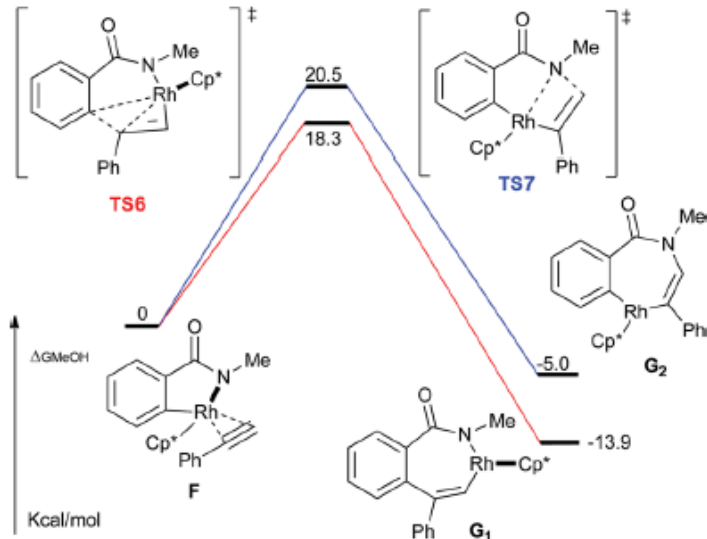
From this point, release of the acetic acid and its substitution by the alkyne in the coordination sphere leads to intermediate C. At this stage, two possibilities are opened, either a carbometallation or aminometallation steps can happen. The first case, usually invoked in intermolecular reactions, involves the insertion of the alkyne in the Rh-C bond leading to intermediate D₁ *via* TS2 (red line, $\Delta G = 22.3 \text{ kcal mol}^{-1}$). D₁ would undergo a reductive elimination *via* TS3 ($\Delta G = 9.5 \text{ kcal mol}^{-1}$) releases the product and the reduced Rh(I) complex which is further reoxidized to Rh (III) by the copper (II) acetate. It is remarkable that the C-Rh-N angle in D₁ (76.5°) is similar to the one in intermediate C (79.3°) and in TS2 (74.2°) which suggests that the formation of a bridged system does not lead to a high structural and angular distortion. The remaining tension could, on the other hand be responsible to the lower barrier for the reductive elimination. In the second case (blue line), the nitrometallation towards intermediate D₁ *via* TS2 has a 2.8 kcal mol⁻¹ smaller barrier than the above route. The distances of the bonds being broken and formed are relatively large (Rh-N 2.148 Å and alkyne-N 2.127 Å respectively) suggesting an early transition state. As in the previous case, reductive elimination, which may occur *via* TS4 or TS5, yields the annulated product and the Rh(I) complex reoxidized by Copper acetate to recover the active catalyst. These results suggest that the formation of the bridged Rhodium intermediate is slightly disfavored, as might be expected.

When the same calculations are performed with a substrate presenting a longer tether, namely one more methylene in the connecting chain, analogous results were obtained although, in this case the differences in energy were of only 1.8 kcal mol⁻¹.



Scheme 64. DFT calculations for the mechanism of the elongated intramolecular annulation.¹¹⁰

With those results in hand we were curious to know whether the insertion into the Rh-N bond could also be considered in intermolecular cases. For that purpose we carried out similar calculations omitting the alkyl tether. The results indicate that the carbometallation is slightly favorable by $2.2 \text{ kcal mol}^{-1}$ which is consistent with the proposed mechanisms although it does not completely rule out the possibility of a Rh-N bond insertion in some cases.

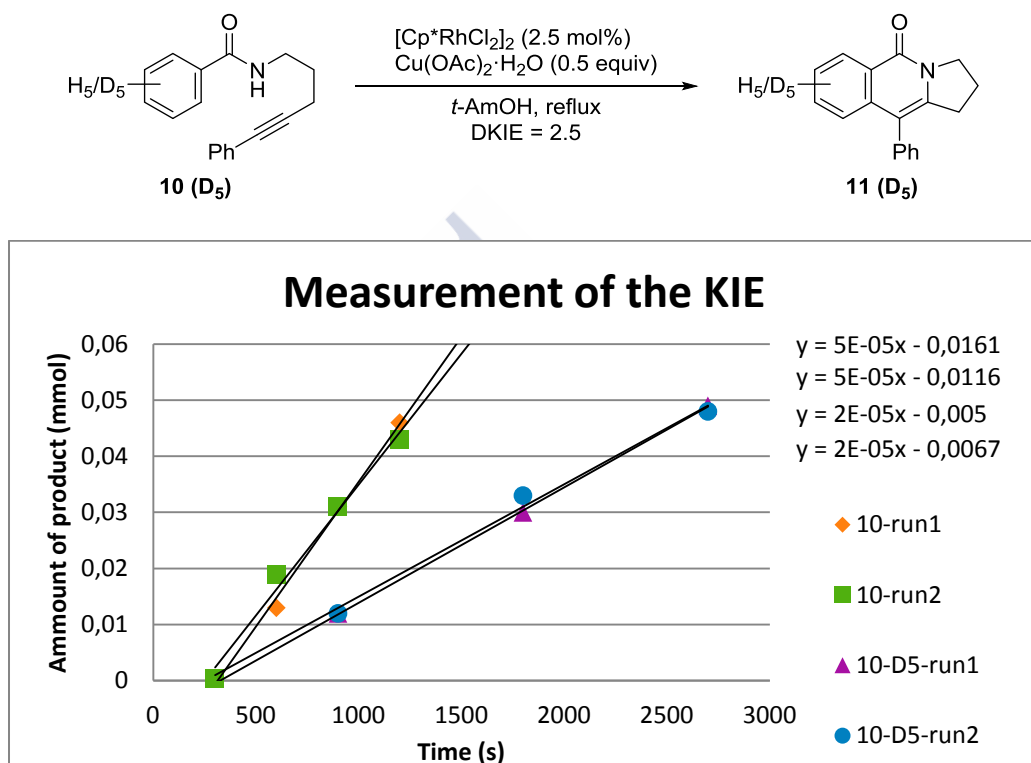


Scheme 65. DFT calculations for the C-Rh and Rh-N insertion in the intermolecular annulation.

To complement these computational studies, we performed a series of experimental assays. At first, we performed a study of the kinetic isotopic effect in a competition experiment to find out whether the C-H activation step is influencing the reaction rate. Towards that end,

¹¹⁰ A conventional energy of 0 kcal mol^{-1} was assigned to intermediate **H**.

we synthesized the benzamide **10-D₅** as described in scheme 58. We then run the reactions in separate vessels under the optimized conditions taking aliquots every 5 minutes which were quenched by diluting with dichloromethane and filtered through a florisil pad. NMR analysis of the amount of isoquinoline present at each aliquot allowed calculating a KIE value of 2.5. This is consistent with a moderate influence of the C-H cleavage in the reaction rate, which is in agreement with the energetic profile resulting from the computational studies.

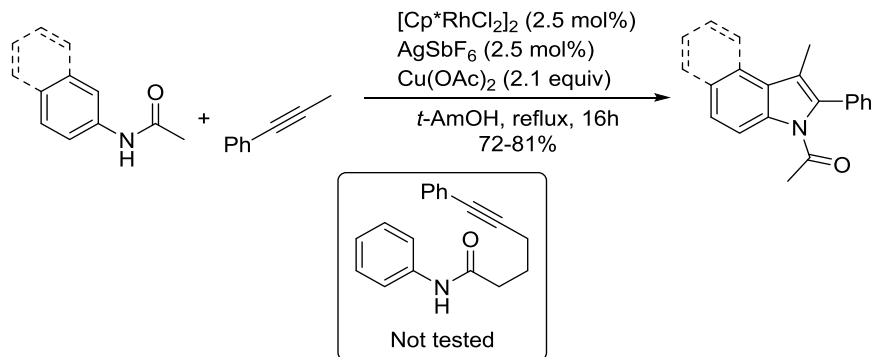


Scheme 66. Study of the KIE

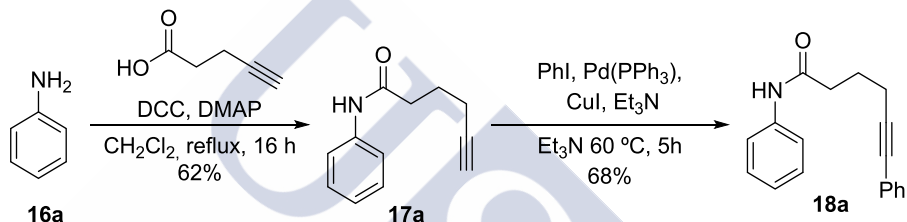
3.3 Further studies on the intramolecular oxidative annulation of anilides.

At this point of the research, we were curious about the possibility of extending the intramolecularity in oxidative annulations to other precursors like anilides, as this would lead to interesting polycyclic indoles. As commented in the introduction, Fagnou and co-workers had previously developed a brilliant method for the obtention of indoles by a rhodium-catalyzed intramolecular oxidative annulation between acetamides and alkynes (scheme 40). ⁸¹ However, intramolecular versions had not been studied and, hence, we decided to make the precursors **38** (scheme 68) to check their reactivity.

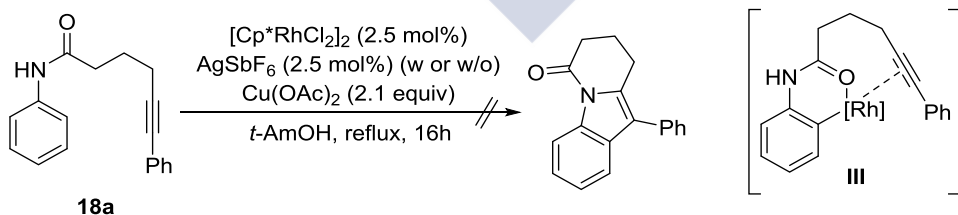
⁸¹ (a) Stuart, D. R.; Bertrand-Laperle, M.; Burgess, K. M. N.; Fagnou, K. *J. Am. Chem. Soc.* **2008**, 130, 16474. (b) Stuart, D. R.; Alsabeh, P.; Kuhn, M.; Fagnou, K. *J. Am. Chem. Soc.* **2010**, 132, 18326.

**Scheme 67.** *Synthesis of indoles by oxidative annulation.*

The synthesis of the alkyne tethered anilide **18a** was done by the condensation of aniline with 5-pentynoic acid followed by a Sonogashira coupling to yield the internal alkyne.

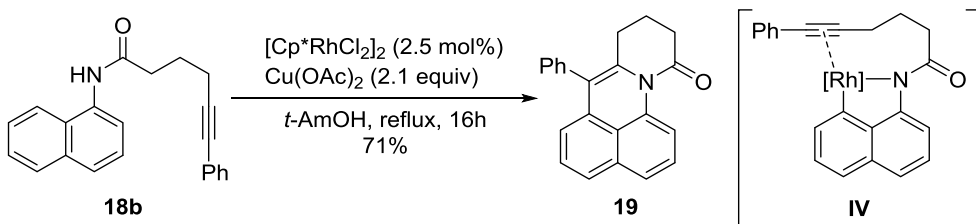
**Scheme 68.** *Synthesis of anilide 18a.*

Treatment of the anilide **18a** under the same conditions described by Fagnou for the intermolecular cases failed on yielding even traces of the tricyclic indole, either with or without the silver salt and the a complex mixture or starting material was recovered respectively. Although at the beginning we were a little surprised by this result, a close look into the hypothetical intermediate resulting from the C-H activation (**III**), allows inferring that it would not be easy for the alkyne to come close to the C-Rh bond and, thereby, undergo the required migratory insertion step. So species **III** is likely a death intermediate unable to further evolve which hampers the catalytic cycle.

**Scheme 69.** *Failed intramolecular version of the annulation of anilide 28a.*

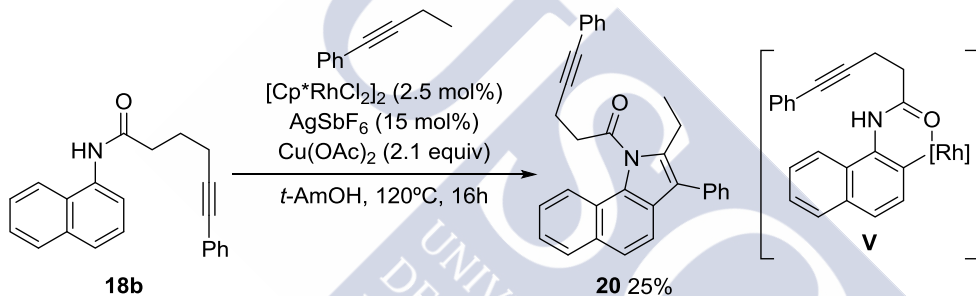
We also synthesized and tested the naphthaleneacetamide **18b**, which was easily assembled by an analogous procedure as stated before. Remarkably, in this case we did observe reactivity but, instead of forming the indole resulting from a (3+2) annulation, we observed the (4+2) adduct **19** in the absence of the chlorine scavenger while with the addition of the silver salt, decomposition of the starting material was observed. The formation of tetracycle

19 can be rationalized assuming that the 5-membered rhodacycle **IV** resulting from the activation of the C8-H bond, can evolve to the product by N-metallation and reductive elimination.



Scheme 70. Intramolecular (4+2) oxidative annulation of naphthaleneacetamide **18b**.

Interestingly, a competition experiment between naphthaleneacetamide **18b** and an external alkyne in presence of a silver salt, led to the preferential formation of the indole **20** in a 25% yield. This result confirms the viability of activating the C-H bond at the position 8 of the naphthalene, most probably in a reversible manner.



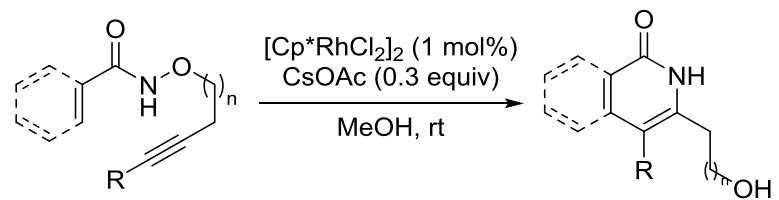
Scheme 71. Competition between inter- and intramolecular annihilations of naphthaleneacetamide **18b**.

Overall, the above results confirm that a direct translation of intramolecular oxidative annihilations to intramolecular settings is not obvious and different factors can significantly affect the reaction outcome.

3.4 Partially intramolecular oxidative annulation of benzhydroxamic derivatives.

During our investigations, and just before we submitted our work for publication, the group of Park described an interesting strategy to control the regioselectivity of the annulation. Their idea was based on connecting the alkyne tether to the benzamide using a cleavable N-O bond. Although the reaction mechanism could be considered intramolecular, the required cleavage of the N-O bond to regenerate the catalyst leads to products similar to those obtained in intermolecular annihilations.¹¹¹

¹¹¹ Xu, X.; Liu, Y.; Park, C. *Angew. Chem. Int. Ed.* **2012**, *51*, 9372.



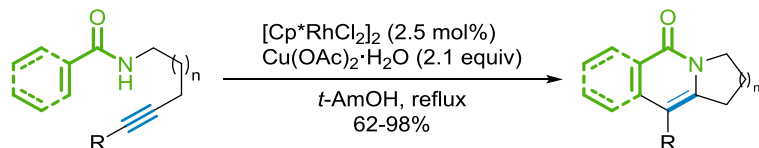
Scheme 72. *Rh (III)-catalyzed semi-intramolecular oxidative annulation of benzhydroxamic acid derivatives.*





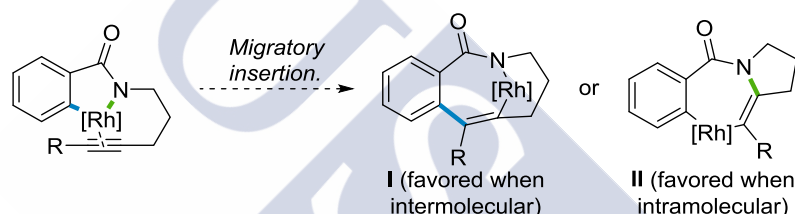
4- Conclusions.

In conclusion we have developed a fully intramolecular version of the oxidative annulation of benzamides and alkynes and demonstrated that it presents a wide scope to make a great variety of tricycles and that, this chemistry can be extended to more challenging acrylamides.



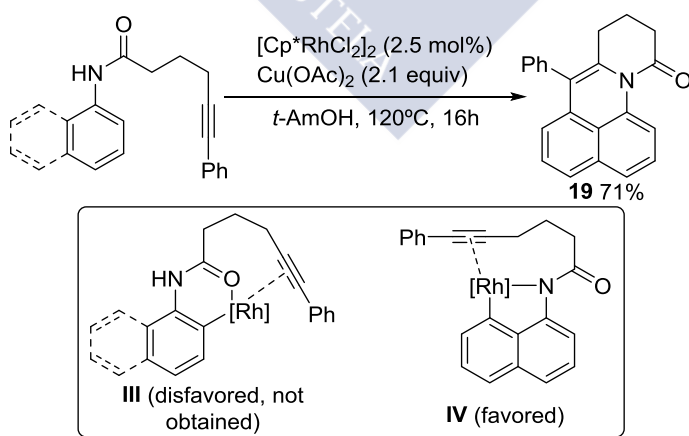
Scheme 73. Oxidative annulation of acryl and benzamides.

Our mechanistic studies provide evidences pointing that the migratory insertion into the Rh-N bond is more favorable than the insertion into the Rh-C bond, most probably because of geometric reasons. Similar intermolecular processes prefer to proceed through carbometallation instead of aminometallations.



Scheme 74. *Rh-C* vs. *Rh-N* insertion.

We have also demonstrated how, in the case of anilides, tethering the two reactive moieties can shut down the reactivity, while in naphthaleneacetamides that have other available C-H bonds to be activated, the intramolecular annulation is possible, in this case leading to products which arise from formal (4+2) annulations.¹¹²

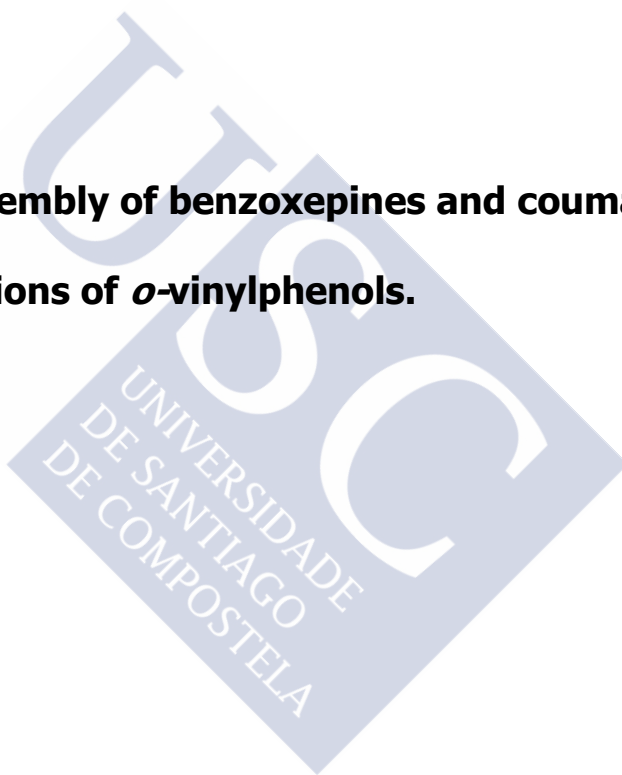


Scheme 75. Oxidative annulation of naphthaleneacetamides.

¹¹² This work was done in collaboration with Dr. Noelia Quiñones and published in: Quiñones, N.; Seoane, A.; García-Fandiño, R.; Mascareñas, J. L.; Gulías, M. *Chem. Sci.* **2013**, *4*, 2874.



**CHAPTER III: Assembly of benzoxepines and coumarins by
oxidative annulations of *o*-vinylphenols.**

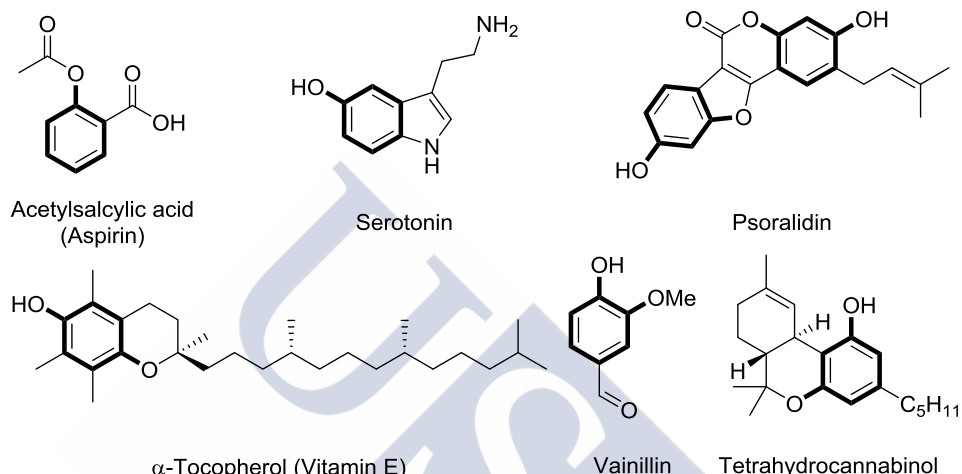




1- Introduction.

1.1 Relevance of the phenolic core: Benzoepines and coumarins.

The phenolic skeleton is widely spread in a huge variety of natural products and derivatives, either in its free form or protected as cyclic or acyclic ethers or esters. Many phenol-containing products show highly relevant biological properties¹¹³ and therefore, the development of synthetic access to these derivatives is a very appealing goal.¹¹⁴



Scheme 76. *Naturally occurring phenols.*

Among all the products with phenolic frameworks, benzoepines and coumarins stand out for their interesting properties. The former, have proven to have antiplasmodial, antimycobacterium and anticancer activities as well as other others.¹¹⁵ On the other hand, coumarins are a versatile scaffold for organic synthesis and present a wide range of interesting properties, which result in their use in very different fields with varying purpose such as fluorescence probes or anticancer and anticoagulant drugs.¹¹⁶ These properties make benzoepines and coumarins quite interesting synthetic targets.¹¹⁷

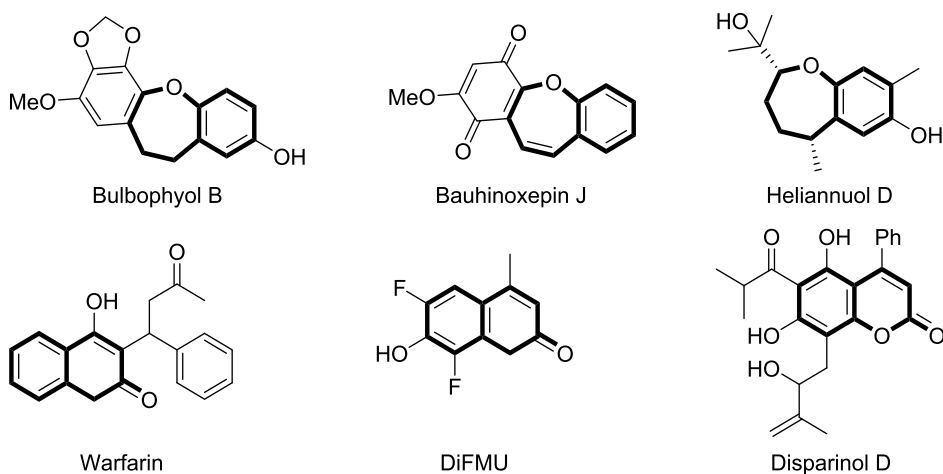
¹¹³ Gomes, C. A.; Girão Da Cruz, T. G.; Andrade, J. L.; Milhazes, N.; Borges, F.; Marques, M. P. M. *J. Med. Chem.* **2003**, *46*, 5395.

¹¹⁴ (a) Tyman, J. H. P *Synthetic and natural phenols*. Ed. Elsevier, **1996**. (b) Rappaport, Z. *The chemistry of phenols*. Ed. Wiley Interscience, **2003**.

¹¹⁵(a) Sprogøe, K.; Manniche, S.; Larsen, O.; Christophersen, C. *Tetrahedron* **2005**, *61*, 8718. (b) Narita, K.; Nakamura, K.; Abe, Y.; Katoh, T. *Eur. J. Org. Chem.* **2011**, 4985.

¹¹⁶ For the synthesis and biological properties of coumarins see: (a) Borges, F.; Roleira, F.; Milhazes, N.; Santana, L.; Uriarte, E. *Curr. Med. Chem.* **2005**, *12*, 887. (b) Musa, M. A.; Cooperwood, J. S.; Khan, M. O. F. *Curr. Med. Chem.* **2008**, *15*, 2664. Wagner, B. D. *Molecules* **2009**, *14*, 210.

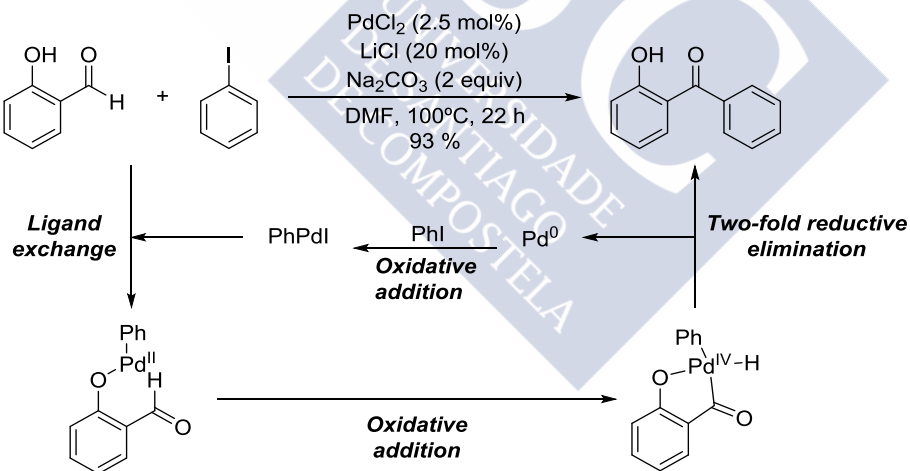
¹¹⁷ For the synthesis of oxepines see: Snyder, N. L.; Haines, H. M.; Peczu, M. W. *Tetrahedron* **2006**, *62*, 9301.



Scheme 77. Benzoxepines and coumarins.

1.2 C-H functionalization directed by phenols.

The hydroxyl moiety of phenols has been used as a directing group for a number of C-H functionalizations. For instance, Miura and co-workers developed a Palladium- catalyzed arylation of salicylaldehydes that involves an initial complexation between the Pd (II) (generated from the oxidative addition of the *in situ* generated Pd (0) species into the iodobenzene) and the OH group, followed by the activation of the C-H bond from the aldehyde by another oxidative addition.¹¹⁸

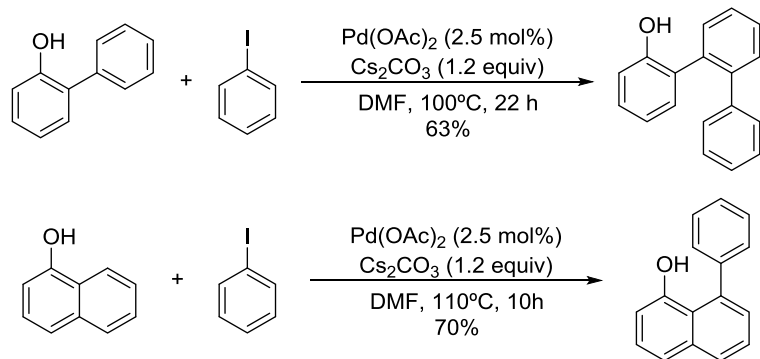


Scheme 78. C-H arylation of salicylaldehydes.

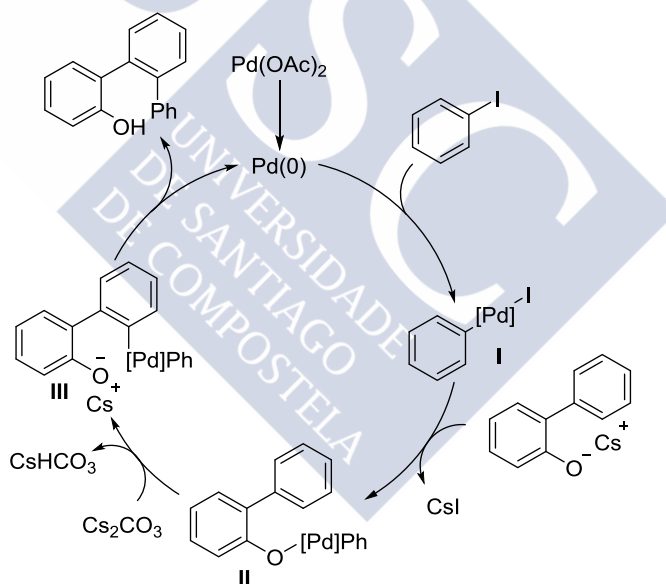
They later extended this kind of functionalizations to *ortho*-arylphenols and naphthols which could be arylated regioselectively with iodoarenes.¹¹⁹

¹¹⁸ Satoh, T.; Itaya, T.; Miura, M.; Nomura, M. *Chem. Lett.* **1996**, 9, 823.

¹¹⁹ (a) Satoh, T.; Kawamura, Y.; Miura, M.; Nomura, M. *Angew. Chem. Int. Ed.* **1997**, 36, 1740. (b) Satoh, T.; Inoh, J.; Kawamura, Y.; Miura, M.; Nomura, M. *Bull. Chem. Soc. Jpn.* **1998**, 71, 2239.

**Scheme 79.** *C-H arylation of phenols and naphthols.*

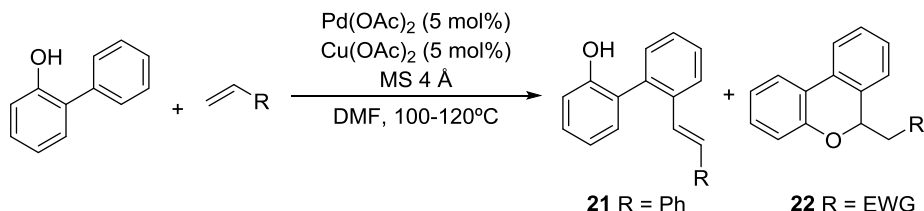
In their report, they demonstrate that the use of carbonate as base is essential for the transformation, probably because the deprotonation of the phenol leading to the phenoxide favors the reaction with the arylpalladium iodide intermediate species (**I**). The proposed mechanism starts with the formation of a Pd (0) species, which oxidatively adds onto the aryl halide generating the aforementioned arylpalladium intermediate **I**. This is followed by the C-H activation leading to diarylpalladium complex **III** which, upon reductive elimination, regenerates the catalyst and releases the product.

**Scheme 80.** *Proposed mechanism of the arylation.*

In their continuous efforts on pushing this chemistry forward, the same authors also described an olefination of *ortho*-phenylphenols by means of Cu and Pd catalysis under air (scheme 81). When using electron poor alkenes, there is a subsequent oxamichael reaction that produces the cyclized benzochromene derivatives (**21**).¹²⁰ The last cyclization reaction can be avoided by using acetic acid as solvent such published in a recent report by the group

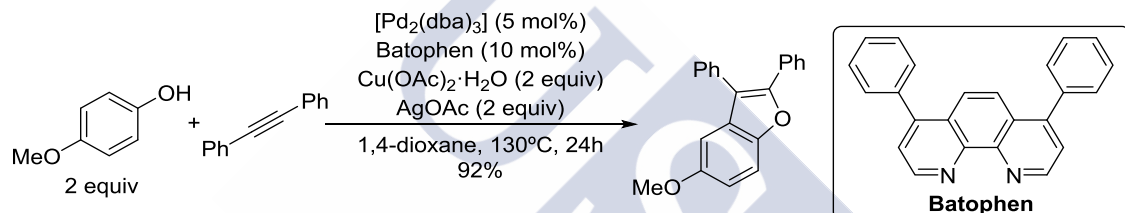
¹²⁰ Miura, M.; Tsuda, T.; Satoh, T.; Nomura, M. *Chem. Lett.* **1997**, 11, 1103.

of Sun.¹²¹ The proposed mechanism starts by the coordination of the phenolic oxygen to the Pd (II) species followed by C-H activation to produce a six-membered palladacyclic intermediate. Migratory insertion of the olefin followed by β -hydride elimination release the alkenylated product and a Pd (0) species that is reoxidized by Cu (II).¹²²



Scheme 81. *C-H olefination of phenols and naphthols.*

Sahoo and co-workers demonstrated the possibility of carrying out oxidative annulations of phenols with alkynes under palladium catalysis to obtain benzofuran derivatives.¹²³



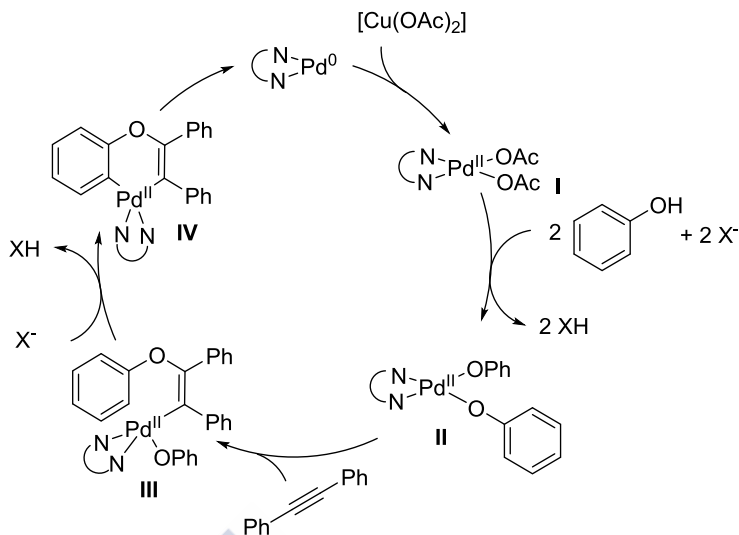
Scheme 82. *Synthesis of furans by Pd-catalyzed oxidative annulation.*

In this communication they hypothesize two different mechanistic possibilities, describing as more likely the one that starts with the formation of the active Pd (II) catalyst I by coordination of the ligand to the Pd (0) precatalyst and subsequent oxidation by the copper (II) salt. This complex can be attacked by the phenol forming the phenoxide species II liberating acetic acid. A phenoxy palladation of the alkyne affords III which, upon base-assisted intramolecular C-H activation, leads to metallacycle IV. Finally, reductive elimination delivers the benzofuran and regenerates the Pd (0) species that reenters the cycle.

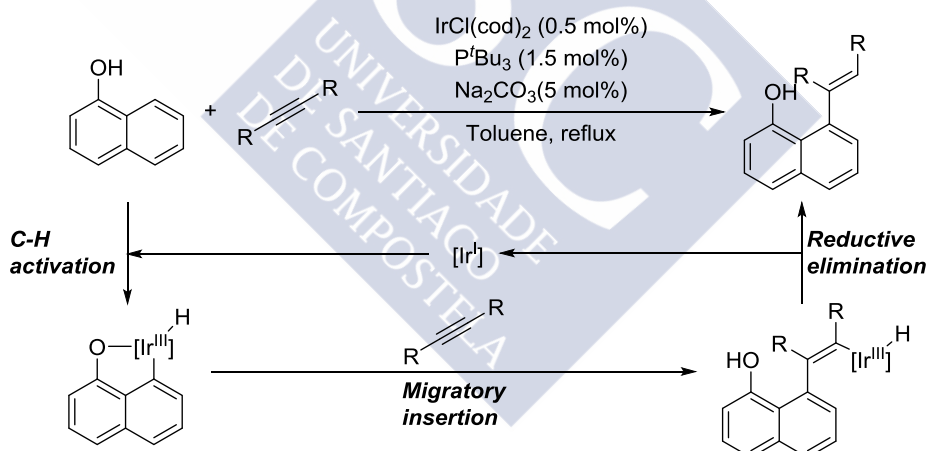
¹²¹ Zhang, C.; Ji, J.; Sun, P. *J. Org. Chem.* **2014**, *79*, 3200.

¹²² It is possible an alternative mechanism in which the palladium remains in the formal oxidation state of Pd (II) such as Hosokawa, T.; Murahashi, S. I. *Acc. Chem. Res.* **1990**, *23*, 49.

¹²³ Kuram, M. R.; Bhanuchandra, M.; Sahoo, A. K. *Angew. Chemie. Int. Ed.* **2013**, *52*, 4607.

**Scheme 83.** Mechanistic hypothesis.

The group of Miura also demonstrated the possibility of using Iridium (I) catalysis to promote the olefination of naphthols in a redox-neutral manner. After coordinating to the hydroxyl, the Ir (I) activates the carbon-hydrogen bond by oxidative addition, which generates an iridium-hydride complex. Migratory insertion of the alkyne and reductive elimination affords the product and regenerates the catalyst.¹²⁴

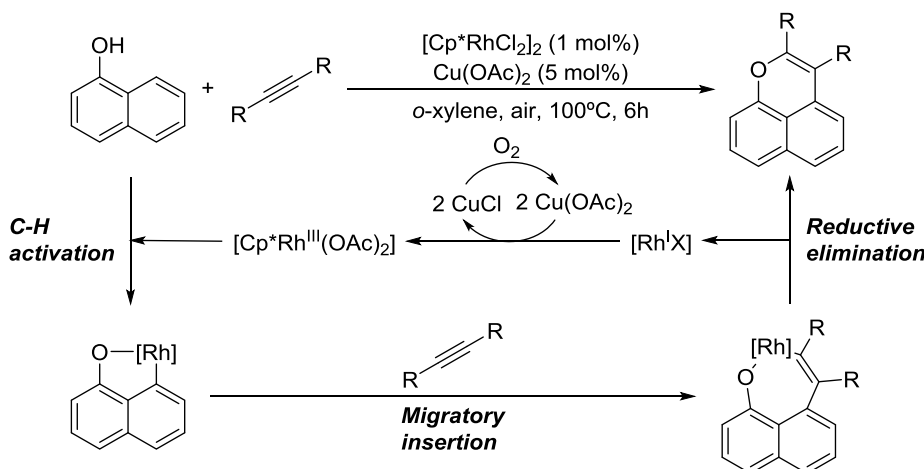
**Scheme 84.** Regioselective addition of naphthols to alkynes.

Miura and co-workers also reported that, using a higher-oxidation state Rh (III)¹²⁵ or Ru (II)¹²⁶ precatalyst, under oxidative conditions allows a formal (4+2) annulation of naphthols and alkynes to take place leading to naphthopyrans.

¹²⁴ Satoh, T.; Nishinaka, Y.; Miura, M.; Nomura, M. *Chem. Lett.* **1999**, 7, 615.

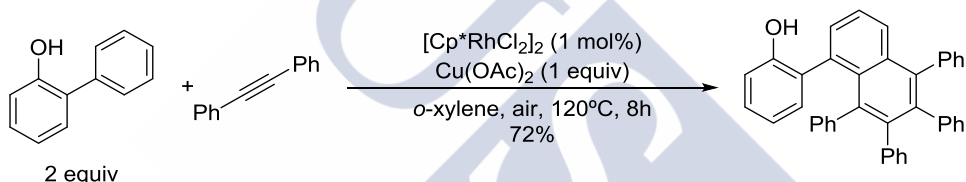
¹²⁵ Mochida, S.; Shimizu, M.; Hirano, K.; Satoh, T.; Miura, M. *Chem. Asian J.* **2010**, 5, 847.

¹²⁶ Ackermann, L.; Pospech, J.; Potukuchi, H. K. *Org. Lett.* **2012**, 14, 2146.



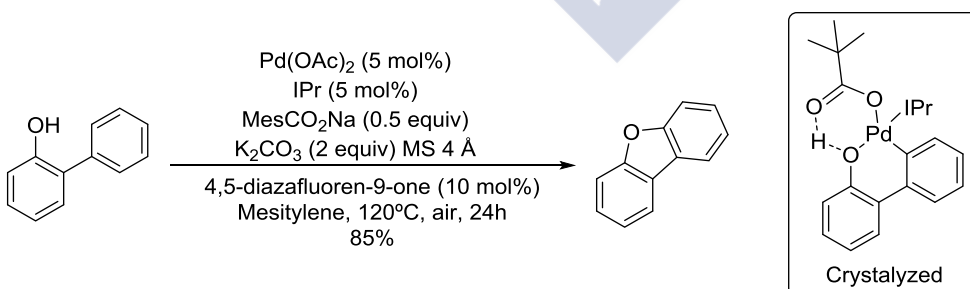
Scheme 85. Oxidative annulation of naphthols and alkynes

Curiously, in the same report, the authors also showed that, when using *ortho*-phenylphenols and diarylalkynes, a multicomponent formal (2+2+2) cycloaddition occurs.



Scheme 86. (2+2+2) Oxidative annulation of biphenols and alkynes.

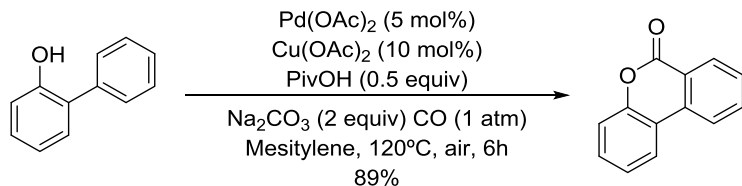
The group of Liu has recently shown that using Pd (II) catalysts and specific ligands and additives, 2-arylphenols are efficiently converted into dibenzofurans.¹²⁷ They were also able to crystallize the palladacyclic intermediate when sodium pivalate was used as base. This species evolves to the product by reductive elimination. The reduced catalyst is reoxidized by air with mediation of the fluorenone. Copper is also able to promote this transformation, but only when strongly electron withdrawing groups are attached on the phenol ring.



Scheme 87. Pd-catalyzed synthesis of benzofurans by C-H activation/cyclization.

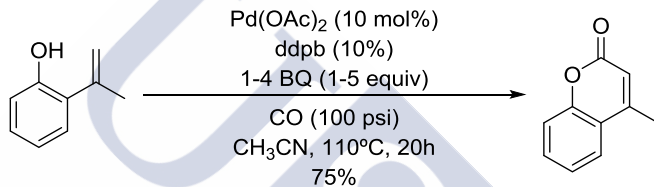
¹²⁷ Xiao, B.; Gong, T.; Liu, Z.; Liu, J.; Luo, D.; Xu, J.; Liu, L. *J. Am. Chem. Soc.* **2011**, 133, 9250.

Carrying out a similar transformation in the presence of carbon monoxide yields highly valuable dibenzopyranones in a formal (5+1) C-H process.¹²⁸ This transformation can be also carried out under ruthenium catalysis.¹²⁹



Scheme 88. *Pd-catalyzed cyclocarbonylation of biphenols.*

The group of Howard Alper has recently reported a related carbonylation using alkenyl- instead of arylphenols, albeit the process requires the use of a high pressure of carbon monoxide pressure (up to 100 psi) in order to obtain good conversions.¹³⁰



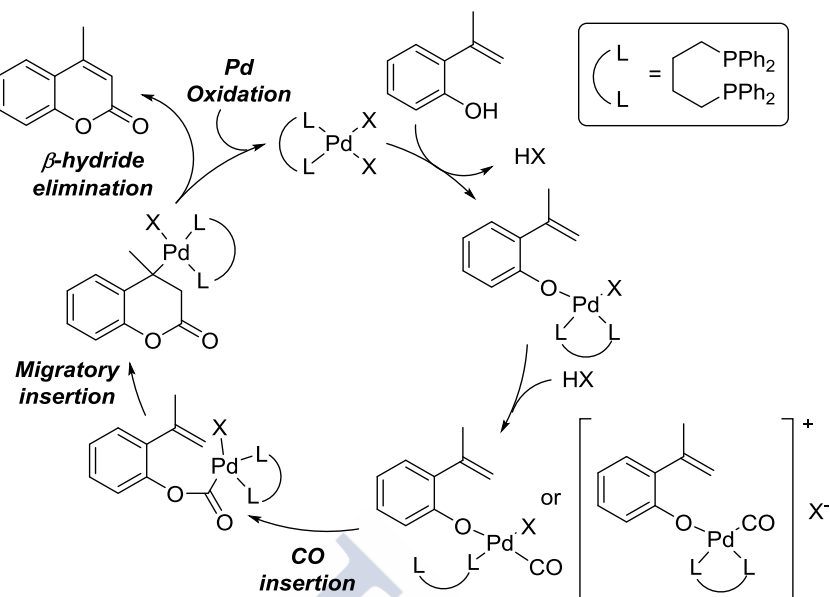
Scheme 89. *Pd-catalyzed cyclocarbonylation of *o*-vinylphenols.*

The proposed mechanism starts with the complexation of the palladium with the phenol followed by the coordination of the carbon monoxide. Insertion of the carbonyl ligand into the Pd-O bond and migratory insertion into the alkene leads to the cyclized product, which undergoes β -hydride elimination to release the product and the reduced form of the catalyst that is further reoxidized by the benzophenone.

¹²⁸ Luo, S.; Luo, F.; Zhang, X.; Shi, Z. *Angew. Chem. Int. Ed.* **2013**, *52*, 10598.

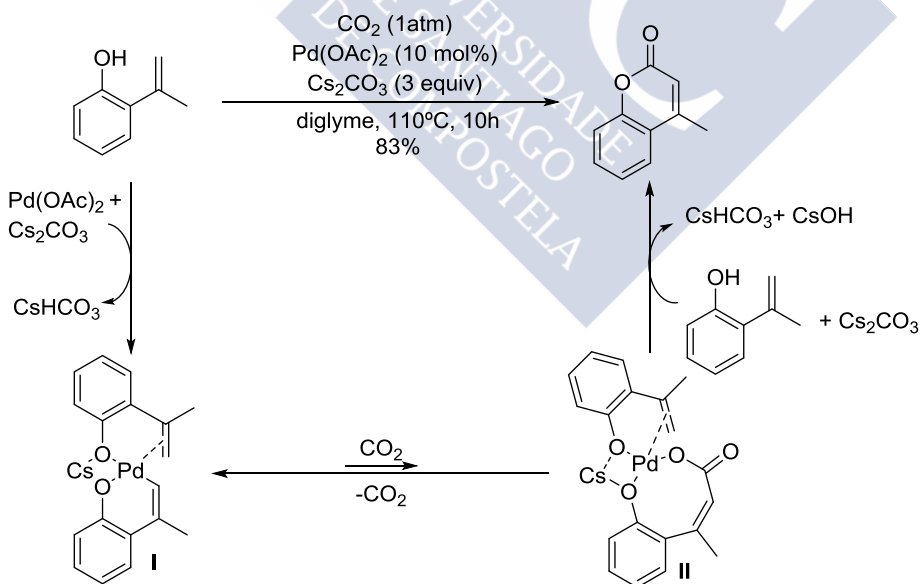
¹²⁹ Inamoto, K.; Kadokawa, J.; Kondo, Y. *Org. Lett.* **2013**, *15*, 3922.

¹³⁰ Ferguson, J.; Zeng, F.; Alper, H. *Org. Lett.* **2012**, *14*, 5602.



Scheme 90. Oxidative carbonylation of *o*-vinylphenols.

In 2013, Iwasawa reported a related carbonylation using CO_2 instead of CO , while being able to lower the gas pressure to 1 atm. In this work they describe the Palladium-catalyzed C-H activation of the olefin one unit of vinylphenol followed by coordination by a second molecule of vinylphenol. The reversible nucleophilic carboxylation of the metallacycle leads to palladacycle II which reacts with another molecule of vinylphenol and base to afford the coumarin with the regeneration of the cyclometallated intermediate I.¹³¹



Scheme 91. Oxidative carbonylation of *o*-vinylphenols.

¹³¹ Sasano, K.; Takaya, J.; Iwasawa, N. *J. Am. Chem. Soc.* **2013**, *135*, 10954.

From the above discussion it seems clear that, readily available phenols and derivatives can be transformed into a variety of products, including several oxacycles, using catalytic processes involving C-H activations, generally directed by the phenolic OH group. However, the number of transformations is still limited, and many challenges related with synthetic and mechanistic aspects of these transformations remain to be approached.

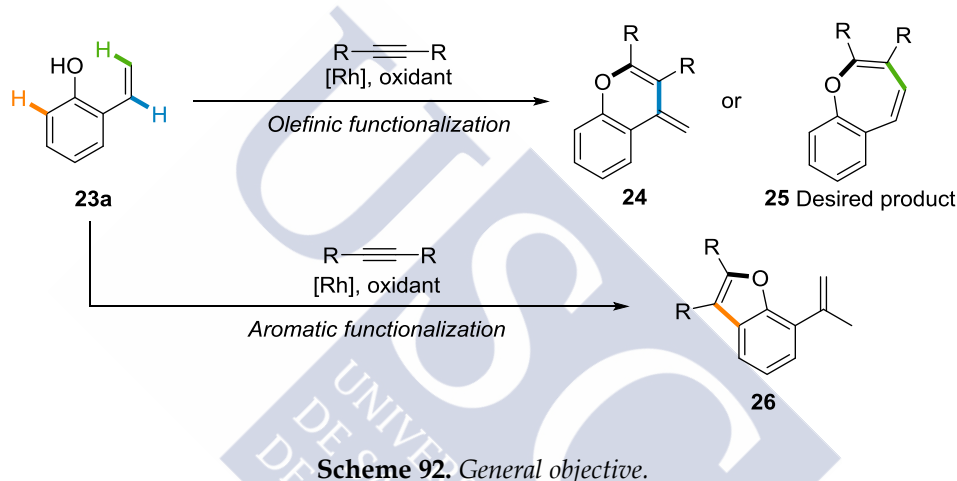




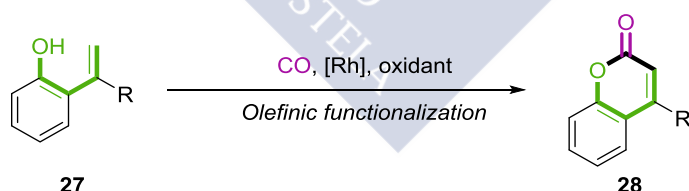
2- Objectives.

Considering the precedents on the C-H functionalization of phenols, it was uncertain for us which would be the reactivity of *o*-vinylphenols in the presence of an alkyne when treated under conditions that promote C-H activations. As indicated in scheme 92, vinylphenols contain several potentially cleavable carbon-hydrogen bonds and depending on the process, different possible annulation products could be formed.^{120,123,132} In particular, and taking into account the precedent of carbonylation reactions, we were particularly attracted by the possibility of activating the terminal C-H bonds and in this way, gaining access to benzoxepines, which had not been obtained using this chemistry.

In principle we envisioned to investigate the performance of these substrates in presence of Rh (III) catalysts since they had proven their utility in other annulations with alkynes.



Alternatively, the use of carbon monoxide as reaction partner might provide an attractive, atom economical and mild entry to coumarins.



Scheme 93. Synthesis of coumarins.

¹²⁰ Miura, M.; Tsuda, T.; Satoh, T.; Nomura, M. *Chem. Lett.* **1997**, 11, 1103.

¹²³ Kuram, M. R.; Bhanuchandra, M.; Sahoo, A. K. *Angew. Chemie. Int. Ed.* **2013**, 52, 4607.

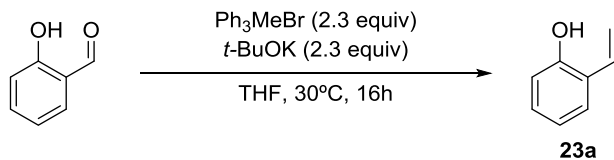
¹³² Hu, J.; Hirao, H.; Li, Y.; Zhou, J. *Angew. Chemie. Int. Ed.* **2013**, 52, 8676.



3- Results and discussion.

3.1 Optimization of the reaction conditions.

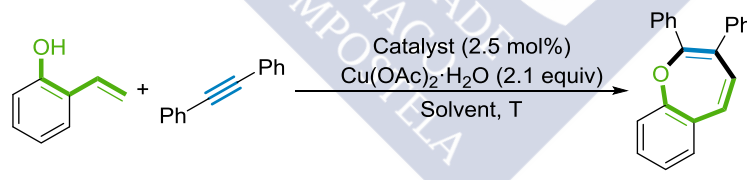
To study the viability of the reaction, we synthesized model the substrate **23a** by a Wittig reaction from commercially available salicylaldehyde in 96% yield.



Scheme 94. *Synthesis of model substrate 23a.*

With the model substrate in hand we started to explore its performance under different conditions with diphenylacetylene as reaction partner. As shown in table 2, using Rh catalysis we observed the formation of the benzoxepin product. The reaction works in a variety of solvents (entries 1,4, 5) being acetonitrile the one that gives better yield rising from 51 to 91% even reducing the amount of copper (entry 6). It is also possible to reduce the equivalents of alkyne oxidant to 1.5, which even allowed to slightly increase the yield to an excellent 96% (entry 7). Decreasing the amount of Copper acetate to 10 mol% the reaction is slower and the yield drops to an 87% (entry 8). Other metals failed to yield the oxepin, either due to lack of conversion with an iridium Cp* complex (entry 2) or decomposition of the vinylphenol with a Ru catalyst (entry 3). We also confirmed that the rhodium is crucial for the reaction since its omission leads to no conversion of the starting materials.

Table 2. Screening of the reaction conditions

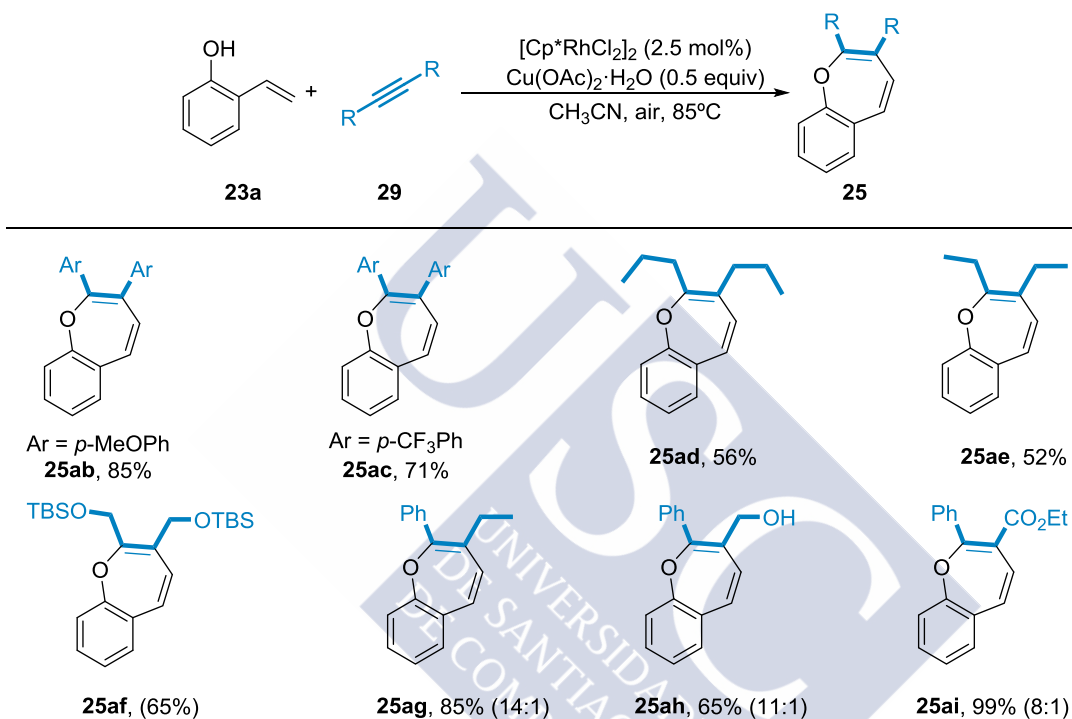


Entry	Catalyst	38a (equiv)	Solvent	T (°C)	Yield (%) ^b
1	[Cp*RhCl ₂] ₂	2	Toluene	100	52
2	[Cp*IrCl ₂] ₂	2	Toluene	100	0 ^c
3	[Ru(p-cymene)Cl ₂] ₂	2	Toluene	100	Traces ^d
4	[Cp*RhCl ₂] ₂	2	DMF	100	72
5	[Cp*RhCl ₂] ₂	2	t-AmOH	100	83
6	[Cp*RhCl ₂] ₂	2	CH ₃ CN	85	91 ^e
7	[Cp*RhCl ₂] ₂	1.5	CH ₃ CN	85	97 ^e
8	[Cp*RhCl ₂] ₂	1.5	CH ₃ CN	85	87 ^f
9	none	1.5	CH ₃ CN	85	0 ^c

^a Reaction conditions: **32a** (0.33 mmol), catalyst (2.5 mol %), Cu(OAc)₂ H₂O (2.1 equiv), solvent (2 mL). ^b Isolated yield. ^c Recovery of the starting materials. ^d Complex mixture. ^e 0.5 equiv of Cu(OAc)₂ H₂O/air balloon were used. ^f 0.1 equiv of Cu(OAc)₂ H₂O/air balloon were used, 16h.

3.2 Substrate scope.

With the optimized conditions in hand, we proceeded to study the scope of the reaction with regard to the alkyne. Symmetrical alkynes bearing electron-rich or electron-poor substituents efficiently participate in the reaction leading to the desired oxepines in good yields (**25ab** and **25ac**), alkynes bearing aliphatic substituents can also be used, although the yield drops to about 50% (**25ad** and **25ae**). It is also possible to use alkynes with silyloxy substituents as well with esters or free hydroxyl groups (**25af**, **25ah** and **25ai**). Interestingly unsymmetrical alkynes afford the corresponding products with selectivities up to 14:1 (**25ag**).



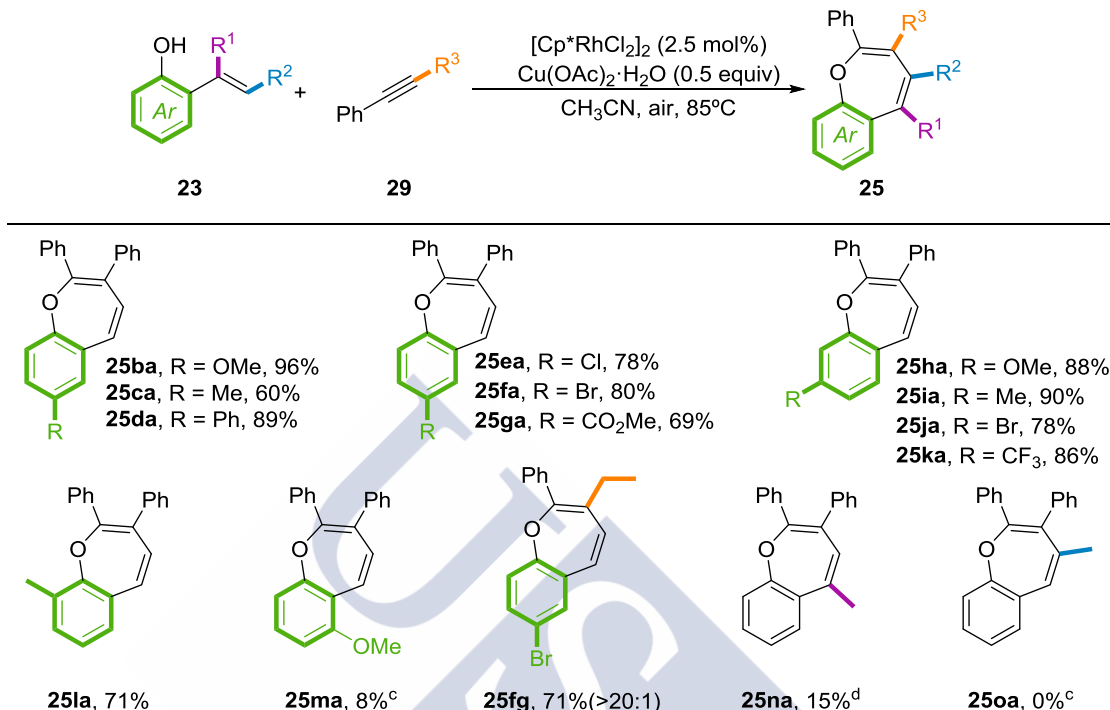
^a Reaction conditions: **23** (0.33 mmol), **29** (1.5 equiv), $[\text{Cp}^*\text{RhCl}_2]_2$ (2.5 mol%), $\text{Cu(OAc)}_2 \cdot \text{H}_2\text{O}$ (0.5 equiv), CH_3CN (2 mL), 85°C . ^b Isolated yields based on **29**.

Scheme 95. Scope of the alkynes.

To examine the scope with respect to the phenols, we synthesized several hydroxystyrenes using the same procedure shown in scheme 94.¹³³ As disclosed above, reaction tolerates different electronically biased aromatic rings with substitution at different positions. When electron-donating groups are placed at the *para* position of the hydroxyl, the expected oxepines are obtained in good to excellent yields (**25ba**–**25da**). The same scenario happens for electron-withdrawing substituents (**25ea**–**25ga**). The *ortho* position of the phenol can also be substituted with no changes in the reactivity. Moreover, the reaction is also unaffected by substitution at the *para* position of the double bond leading to products (**25ha**–**25ka**) in good to excellent yields. However, when the internal position of the alkene is substituted with a methyl group the oxepin is obtained in low yields in favor of two different byproducts

¹³³ In collaboration with Noelia Casanova

(25na). Interestingly the reaction is not efficient when there is substitution at the *ortho* position of the olefin or at the double bond leading to an 8% yield and a complex mixture of products respectively (25ma, 25oa).



^a Reaction conditions: 23 (0.33 mmol), 29 (1.5 equiv), [Cp*RhCl₂]₂ (2.5 mol%), Cu(OAc)₂·H₂O (0.5 equiv), CH₃CN (2 mL), 85°C. ^b Isolated yields based on 29. ^c Complex mixture. ^d Isolated with two different byproducts.

Scheme 96. Scope of the *o*-vinylphenols.

The structure of the products was unambiguously confirmed by X-Ray diffraction of oxepine 25aa as seen below.

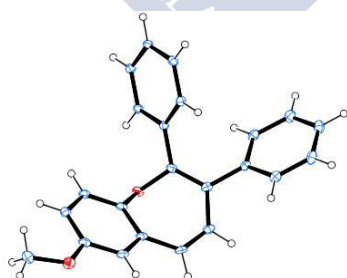


Fig 5. Structure of 25aa obtained by X-Ray diffractometry.

To elucidate the regiochemistry of the products arisen from when unsymmetrical alkynes where used, we carried out nOe experiments between the aliphatic side chain of the alkyne and the hydrogen at C4, as exemplified below.

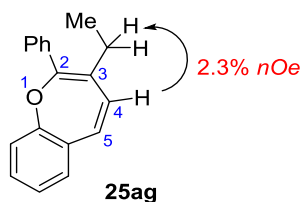
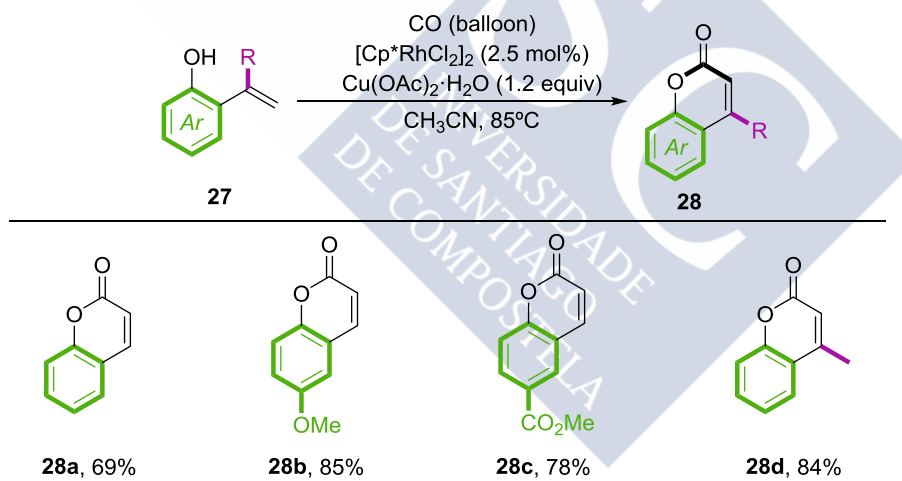


Fig 6. Determination of the regiochemistry of 25ag by *n*Oe.

In summary, we have described a new and attractive method of making a variety of benzoxepines from trivial starting material.

3.3 (5+1) annulation towards coumarins.

After the good results of the (5+2) annulation, we wondered whether it was possible to use carbon monoxide as coupling partner in order to obtain coumarins. Gratifyingly, when *o*-vinylphenol was treated under the reaction conditions in an atmosphere of carbon monoxide and 1.2 equivalents of copper acetate, the corresponding coumarin was obtained (**28a**). The reaction also works efficiently with electron-poor or electron-rich substituents (**28b** and **28c**). Interestingly, in contrast to the annulations to alkynes, the carbonylation tolerates substitution at the internal position and therefore, coumarin **28d** can be isolated in an 84% yield.

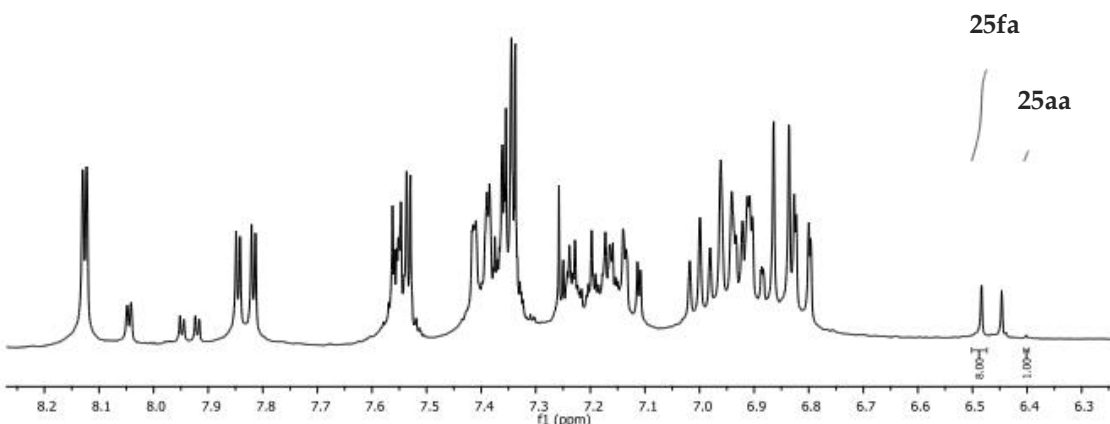
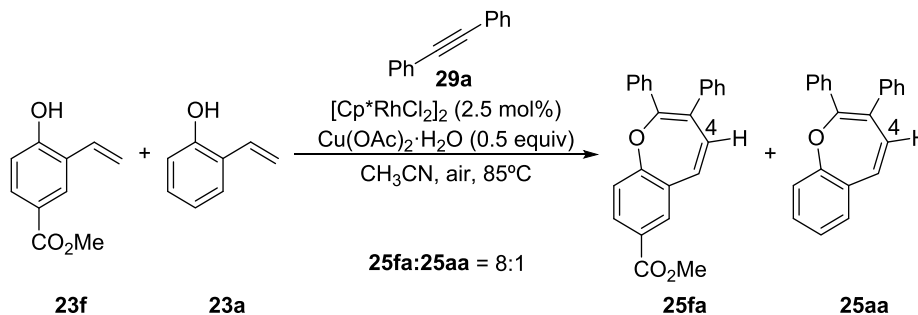


^a Reaction conditions: 27 (0.5 mmol), [Cp^{*}RhCl₂]₂ (2.5 mol%), Cu(OAc)₂·H₂O (1.2 equiv), CH₃CN (2 mL), 85°C. overnight.

Fig 7. Scope of the carbonylation.

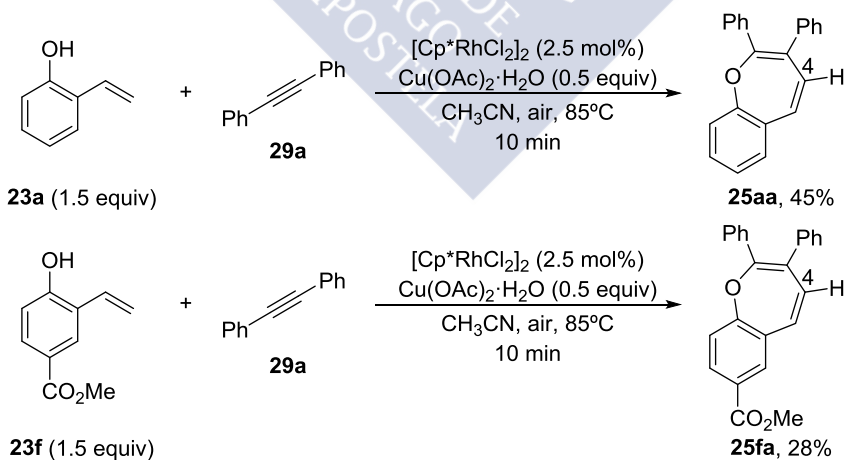
3.4 Mechanistic investigations.

In an effort to obtain mechanistic information about this transformation, we carried out several experiments. First of all we performed a competition between phenols **23a** and **23f**. When both are mixed together, the electron poor **23f** reacts preferentially leading to an 8:1 mixture of both oxepines.



Scheme 97. Competition between **25aa** and **25fa**.

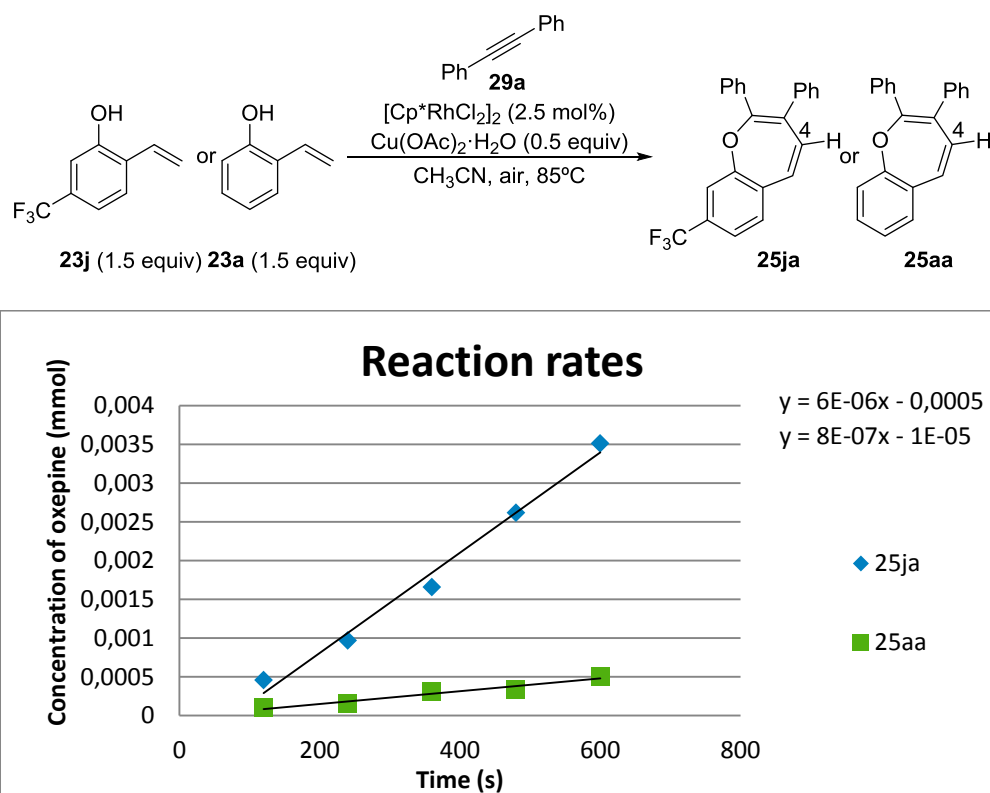
However, when the reactions are carried out in separate vessels the formation of **25aa** is faster. This divergence can be explained in terms of an irreversible formation of a phenoxide-Rh complex that should be easier for more acidic protons while, further steps could be favorable for more electron-rich substrates.



Scheme 98. Reaction yields after 10 min of reaction of **25aa** and **25fa**.

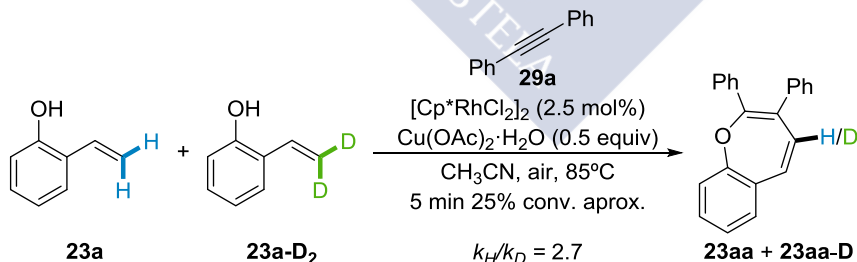
We also measured the relative reaction rates between standard vinylphenol and an electron-poor counterpart, with a trifluoromethyl substituent *para* to the olefin. Like in the previous

case, the electron rich substituent reacts preferentially, being over 7.5 times faster than the other.



Scheme 99. Reaction rates of 25ja and 25aa.

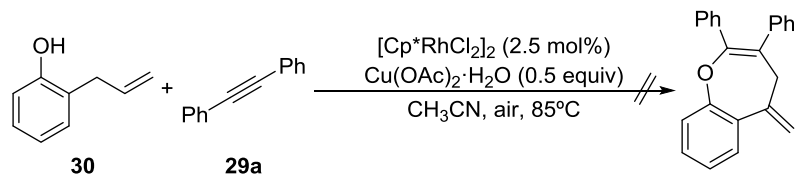
KIE measurements using a competition experiment between **23aa** and **23aa-D₂** gave a value of 2.7 suggesting that the C-H bond cleavage is somehow influencing the reaction rate, but not necessarily meaning that it is the turnover-determining step.¹³⁴



Scheme 100. Measurement of the KIE.

To explore the importance of the conjugation of the olefin with the aromatic ring, we carried out the reaction using *o*-allylphenol **30** instead of *o*-vinylphenol. When **30** is treated with diphenylacetylene under the usual conditions we observed almost no conversion, with recovery of the majority of the starting phenol, suggesting that the conjugation of the vinyl motif is crucial for a successful outcome.

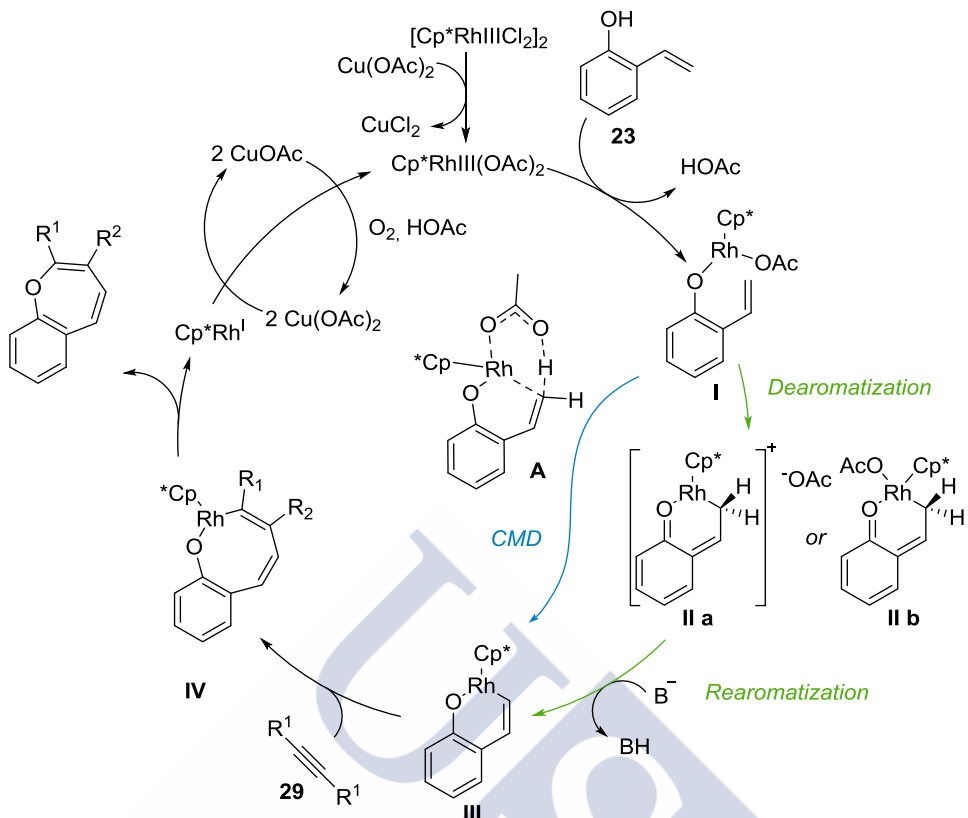
¹³⁴ Simmons, E. M.; Hartwig, J. F. *Angew. Chemie. Int. Ed.* **2012**, *51*, 3066.

**Scheme 101.** Reaction of allylphenol.

Considering all the data presented above, a plausible mechanistic hypothesis is presented in scheme 102. The process could be initiated by the dissociation of the Cp^*Rh dimer to generate a rhodium-acetate complex, most probably the active catalytic species. A first O-H cleavage of the phenol and coordination to the metal would give rise to the intermediate **I** which can dearomatize to the quinone-type metallacycle **II**¹³⁵. A base-assisted deprotonation recovers the aromaticity leading to rhodacycle **III** which, by migratory insertion, affords intermediate **IV**. This rhodacycle can now evolve by reductive elimination releasing the oxepin and the reduced catalyst that is reoxidized by the copper acetate with air as the final oxidant. The carbonylation leading to coumarins would follow a similar pathway *via* insertion of the carbon monoxide in intermediate **III** followed by reductive elimination as in the (5+2) mechanism. An alternative mechanism involving a concerted metallation-deprotonation (CMD) C-H activation *via* transition state **A** is less consistent with the experimental data^{55b} but cannot be fully discarded.

^{55b} Lapointe, D.; Fagnou, K. *Chem. Lett.* **2010**, 39, 1118.

¹³⁵ This kind of mechanism has been proposed for amines with Ir in Ye, K.-Y.; He, H.; Liu, W.-B.; Dai, L.-X.; Helmchen, G.; You, S.-L. *J. Am. Chem. Soc.* **2011**, 133, 19006.

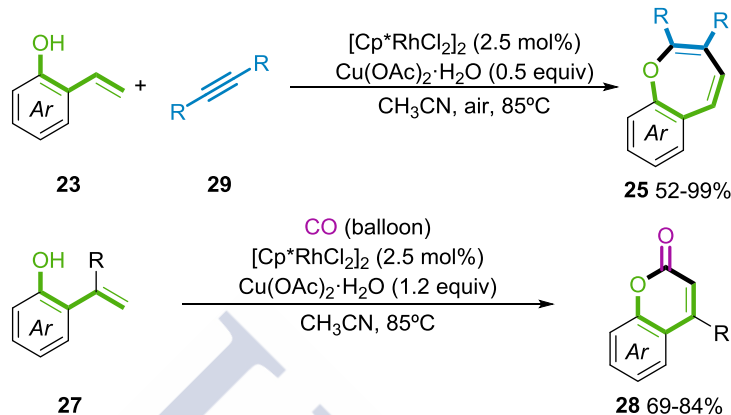


Scheme 102. Mechanistic hypothesis.

UNIVERSIDADE
DE SANTIAGO
DE COMPOSTELA

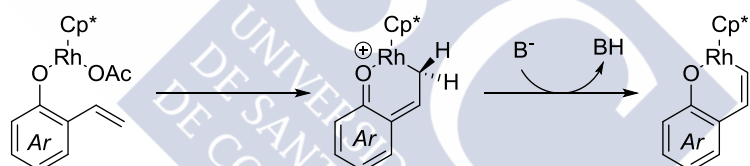
4- Conclusions.

In conclusion, we have developed a robust methodology to build benzoxepines and coumarins from readily available *o*-vinylphenols by formal (5+1) and (5+2) annulations either with alkynes or carbon monoxide.



Scheme 103. (5+2) and (5+1) oxidative annulation of *o*-vinylphenols.

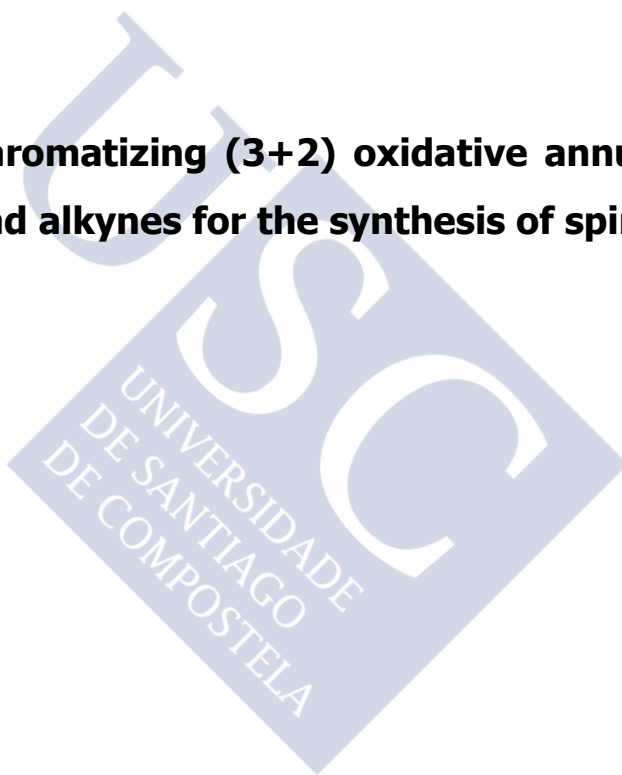
Experimental data are consistent with a mechanism in which the C-H activation involves a non concerted dearomatization/rearomatization process instead of the more common CMD.¹³⁶



¹³⁶ These results were published in Seoane, A.; Casanova, N.; Quiñones, N.; Mascareñas, J. L.; Gulías, M. *J. Am. Chem. Soc.* **2014**, *136*, 834.



CHAPTER IV: Dearomatizing (3+2) oxidative annulations of *o*-alkenylphenols and alkynes for the synthesis of spirocycles

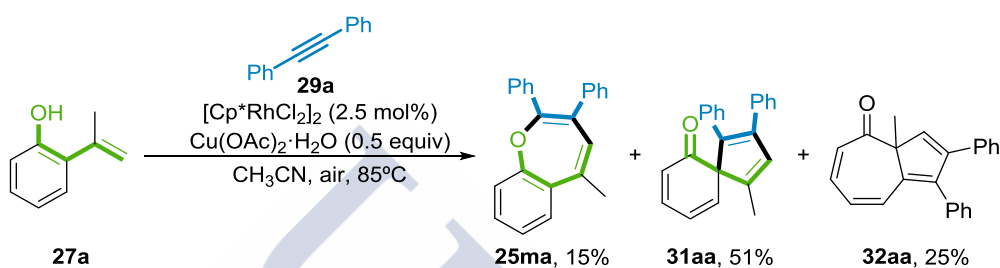




1- Precedents.

1.1 Isolation of the spirocycle.

As commented before, while working on the annulation of *o*-vinylphenols and alkynes, we observed that, when a methyl substituent was located at the internal position of the double bond only a 15% of the benzoxepin was observed in favor of two different byproducts. Isolation of those products allowed us to characterize them as the dearomatized spirocycle **31aa** and the azulenone **32aa**.

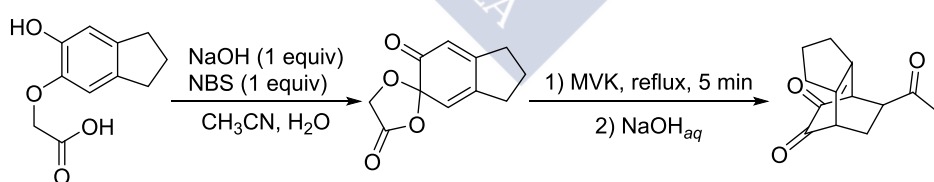


Scheme 105. Different products arising from the oxidative annulation of alkenylphenols with alkynes.

This unexpected and intriguing reactivity prompted us to further investigate this transformation to further optimize it and understand the mechanism.

1.2 Dearomatization of phenols.

Although energetically unfavorable, the dearomatization of aromatic rings is a powerful way of obtaining new structures with increased molecular complexity from simple planar structures.¹³⁷ In particular, phenols are common substrates for these transformations since the lone pair of the heteroatom allows for an easier breaking of the aromaticity.¹³⁸ An example of this approach is the synthesis of the core of Ryanodine by Deslongchamps in 1969.¹³⁹



Scheme 106. Synthetic approach towards Ryanodine.

Among the many ways of inducing the dearomatization of phenols, the oxidation to quinones¹⁴⁰ and the generation of quinone methides¹⁴¹ stand out for their versatility and

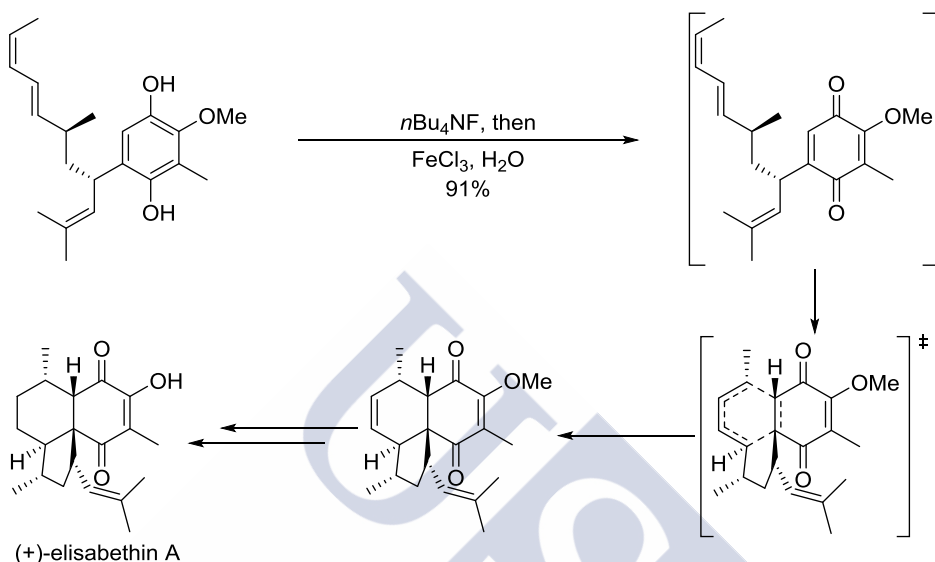
¹³⁷(a) Mander, L. N. *Synlett* **1991**, 134. (b) Roche, S. P.; Porco, J. A. *Angew. Chemie. Int. Ed.* **2011**, *50*, 4068.

¹³⁸ Quideau, S.; Pouységú, L.; Deffieux, D. *Synlett* **2008**, No. 4, 467.

¹³⁹ Berney, D.; Deslongchamps, P. *Can. J. Chem.* **1969**, *47*, 515.

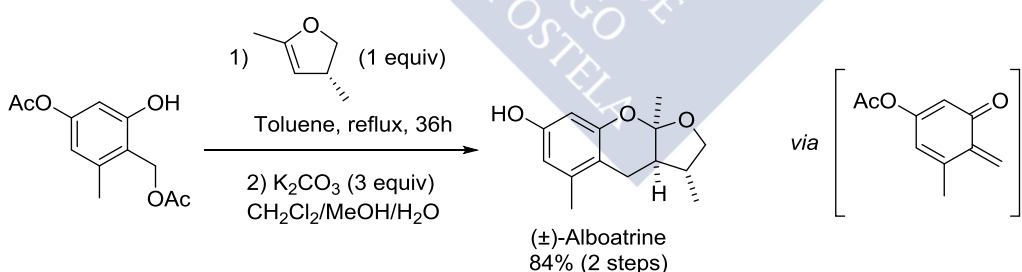
¹⁴⁰ Magdziak, D.; Meek, S. J.; Pettus, T. R. R. *Chem. Rev.* **2004**, *104*, 1383.

numerous products have been synthesized by using these methodologies. An example can be seen in the total synthesis of Elisabethin A by the group of Mulzer in 2003.¹⁴² Their procedure involves the generation of a highly reactive dearomatized quinone that undergoes a fast intramolecular Diels-Alder cycloaddition to produce the core of the natural product.



Scheme 107. Key step in the total synthesis of Elisabethin A.

The use of *ortho* quinone methides is exemplified in the total synthesis of (\pm)-Alboatrin by Baldwin and co-workers which also involves a Diels-Alder cyclization although in this case, the quinone is the diene instead of the dienophile.¹⁴³ Other methods for the dearomatization of phenols rely on photoisomerizations, oxidations or acid or base-mediated elimination.¹³⁸



Scheme 108. Key step in the total synthesis of (\pm)-Alboatrin.

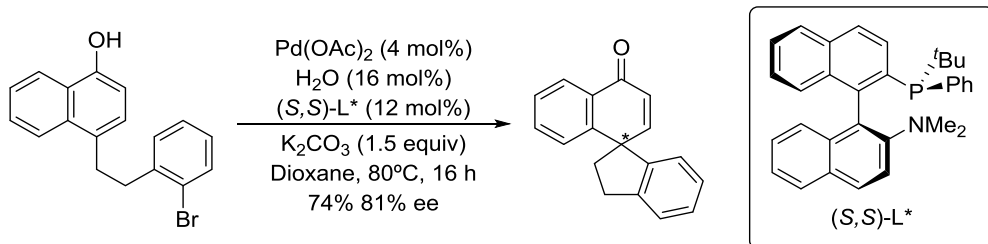
¹⁴¹ Van de Water, R. W.; Pettus, T. R. R. *Tetrahedron* **2002**, *58*, 5367. Toteva, M. M.; Richard, J. P. *Adv. Phys. Org. Chem.* **2011**, *45*, 39

¹³⁸ (a) Mander, L. N. *Synlett* **1991**, 134. (b) Roche, S. P.; Porco, J. A. *Angew. Chemie. Int. Ed.* **2011**, *50*, 4068.

¹⁴² Heckrodt, T. J.; Mulzer, J. *J. Am. Chem. Soc.* **2003**, *125*, 4680.

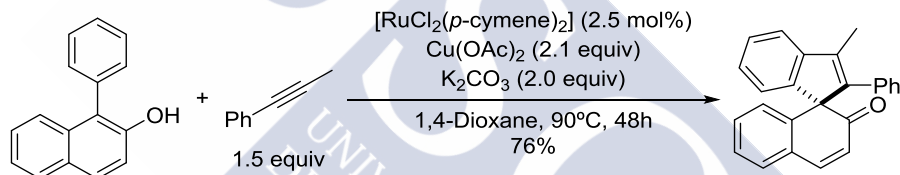
¹⁴³ Rodriguez, R.; Adlington, R. M.; Moses, J. E.; Cowley, A.; Baldwin, J. E. *Org. Lett.* **2004**, *6*, 3617.

In addition to the aforementioned methods, transition metals can also promote reactions that involve the dearomatization of phenolic derivatives.¹⁴⁴ In 2011, Buchwald and co-workers developed an arylative dearomatization catalyzed by Pd (0). They also demonstrated that the reaction could be performed in an enantioselective manner by using chiral phosphines.¹⁴⁵



Scheme 109. *Pd(0)-catalyzed dearomatizing arylation of phenols.*

Later, while we were working in the synthesis of the oxepines and coumarins, Luan and co-workers published a Ru(II)-catalyzed dearomatizing oxidative annulation of naphthols with alkynes. Although no explanation is given, in the same communication they report that, when phenols are used instead of naphthols, the reaction delivers less than a 5% of the spirocyle¹⁴⁶



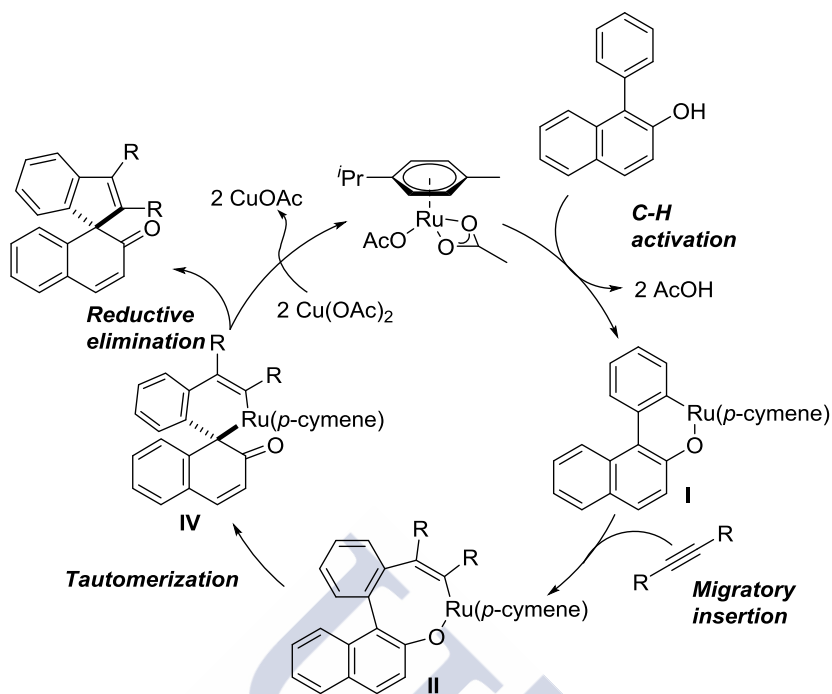
Scheme 110. *Ru(II)-catalyzed dearomatizing annulation of naphthols.*

Their mechanistic hypothesis starts with the formation of the active catalytic species followed by a hydroxyl directed C-H activation. A migratory insertion of the alkyne leads to the eight-membered metallacycle **II** which, to release the strain, evolves through keto tautomerization towards the ruthenacycle **III**. A final reductive elimination yields the spirocyle and the reduced catalyst which is further reoxidized by the copper acetate.

¹⁴⁴ For selected examples see (a) Wiegand, S.; Schafer, H. J. *Tetrahedron* **1995**, *51*, 5341. (b) Nemoto, T.; Ishige, Y.; Yoshida, M.; Kohno, Y.; Kanematsu, M.; Hamada, Y. *Org. Lett.* **2010**, *12*, 5020. (c) Wu, Q.; Liu, W.; Zhuo, C.; Rong, Z.; Ye, K.; You, S. *Angew. Chem. Int. Ed.* **2011**, *50*, 4455.

¹⁴⁵ Rousseaux, S.; García-Fortanet, J.; Del Agua Sanchez, M. A.; Buchwald, S. L. *J. Am. Chem. Soc.* **2011**, *133*, 9282.

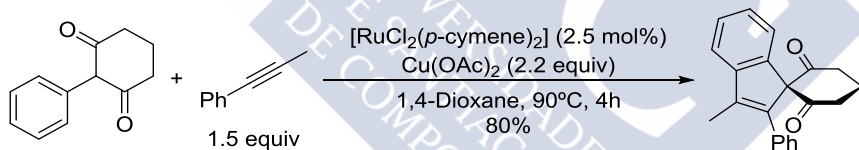
¹⁴⁶ Nan, J.; Zuo, Z.; Luo, L.; Bai, L.; Zheng, H.; Yuan, Y.; Liu, J.; Luan, X.; Wang, Y. *J. Am. Chem. Soc.* **2013**, *135*, 17306.



Scheme 111. Mechanistic hypothesis.

1.3 Hydroxyl-directed synthesis of spirocycles by oxidative annulation.

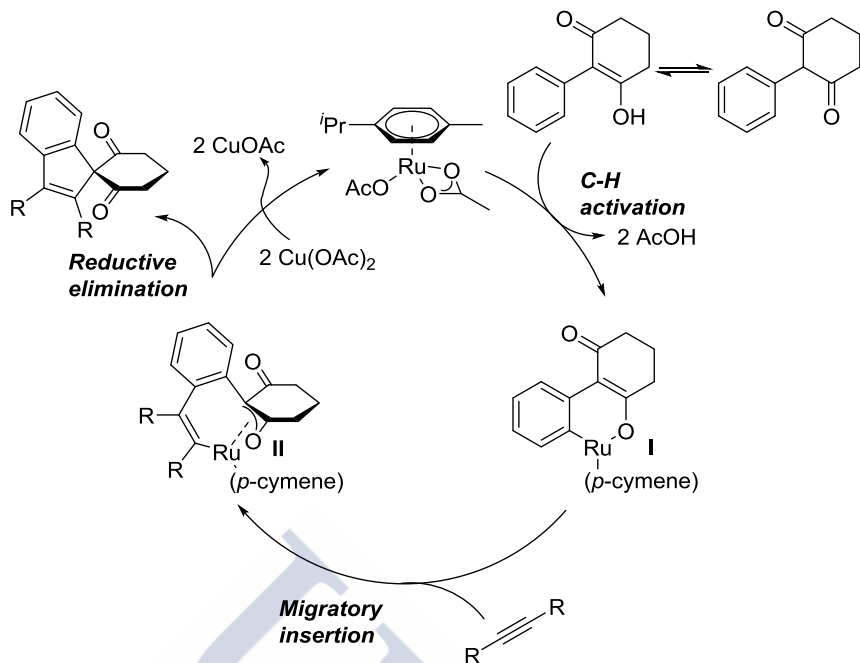
A related example was developed at the group of Lam by using ruthenium catalysis and 1,3 diketones that act as masked enols.¹⁴⁷



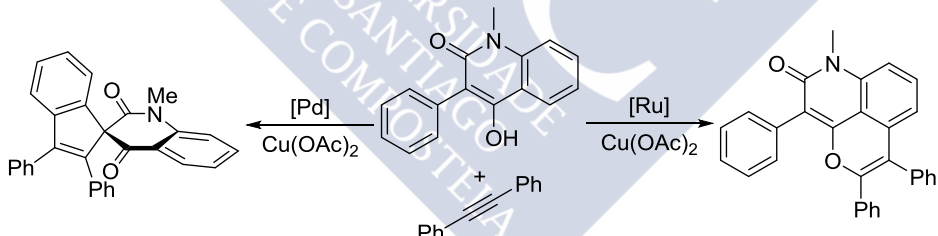
Scheme 112. $\text{Ru}(\text{II})$ -catalyzed dearomatizing annulation of designed diketones.

The proposed mechanism starts with a keto-enol tautomerization and hydroxyl-directed C-H activation to give intermediate I. This ruthenacycle evolves via migratory insertion leading to the oxa- π -allylruthenium, which can also be depicted as the C- or O- bound forms. Finally a C-C reductive elimination affords the spirodiketone and the reduced Ruthenium catalyst. Copper acetate may oxidize the Ru (0) to Ru (II) which is reincorporated into the catalytic cycle.

¹⁴⁷ Chidipudi, S. R.; Khan, I.; Lam, H. W. *Angew. Chem. Int. Ed.* **2012**, *51*, 12115.

**Scheme 113.** Mechanistic hypothesis.

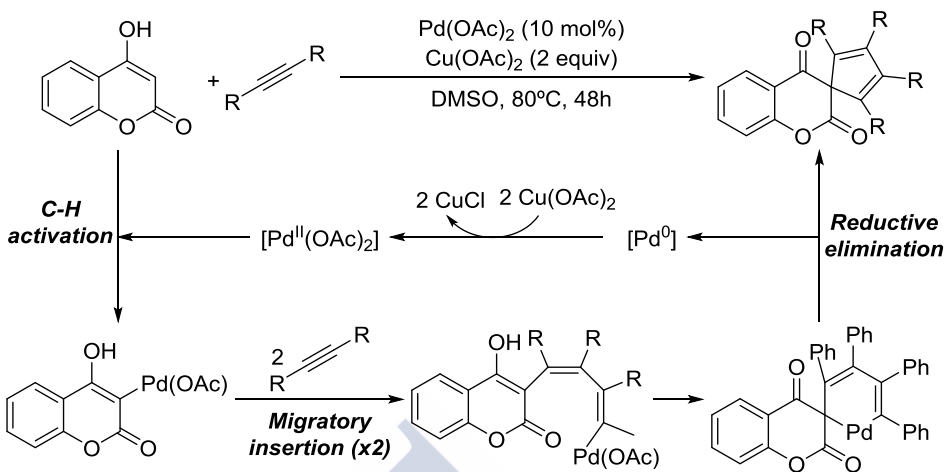
The same group reported an interesting catalyst-dependant divergent reactivity. Using slightly different substrates, they were able to assemble tricyclic chromenes with ruthenium while a palladium-carbene based catalyst afforded the previously described spirocycles. In their communication, the authors were unable to clarify the reason behind this catalyst-dependant divergence.¹⁴⁸

**Scheme 114.** Divergent oxidative annulation of specific diketones.

The group of Wang also reported a palladium-catalyzed (2+2+1) annulation between hydroxycoumarins and alkynes leading to spirocyclopentadienechroman-2,4-diones. In their report they explain the reaction in terms of the activation of the olefinic C-H bond of the coumarin followed by two consecutive migratory insertions leading to intermediate I which, after a cyclopalladation driven by the conversion of the enol into a ketone, yields the six-membered intermediate III. This intermediate undergoes reductive elimination releasing the

¹⁴⁸ Dooley, J. D.; Reddy Chidipudi, S.; Lam, H. W. *J. Am. Chem. Soc.* **2013**, 135, 10829.

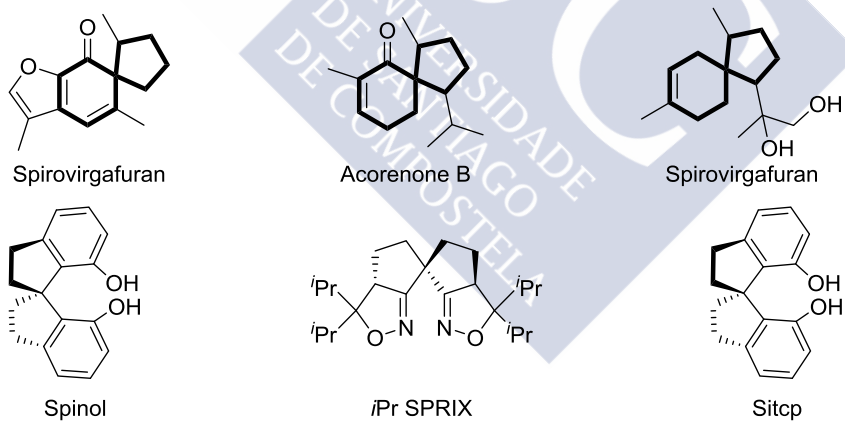
spirocycle and reoxidation of the catalyst to reinitiate the cycle.¹⁴⁹ This methodology was later applied by Luan using naphthols as the one-atom component.¹⁵⁰



Scheme 115. (2+2+1) oxidative annulation for the synthesis of spirocycles.

1.3 Spirocycles as a synthetic goal.

Spirocyclic compounds are relevant,¹⁵¹ not only due to their unique structural properties which have been used in order to build chiral ligands,¹⁵² but also because of their presence in several natural products.¹⁵³ In particular, spiro[5.4]nonane systems are quite common in many terpenes of natural origin. This is why methods leading to them are of high interest.¹⁵⁴



Scheme 116. Naturally occurring products and chiral ligand containing spirocycles.

¹⁴⁹ Peng, S.; Gao, T.; Sun, S.; Peng, Y.; Wu, M. *Adv. Synth. Catal.* **2014**, 356, 319.

¹⁵⁰ Gu, S.; Luo, L.; Liu, J.; Bai, L.; Zheng, H. *Org. Lett.* **2014**, No. Ii, 10.

¹⁵¹ (a) Krapcho, P. A. *Synthesis* **1974**, 383. (b) Sannigrahi, M. *Tetrahedron* **1999**, 55, 9907.

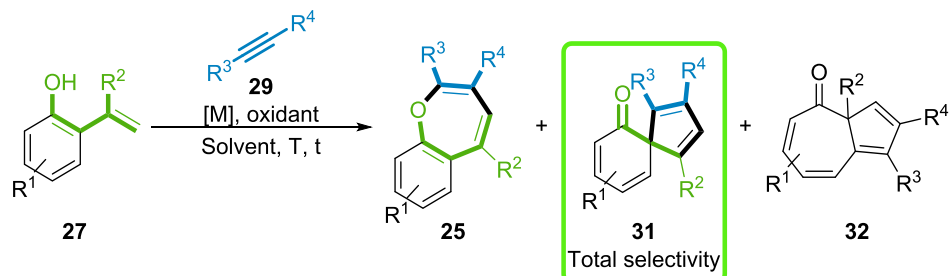
¹⁵² Ding, K.; Han, Z.; Wang, Z. *Chem. Asian. J.* **2009**, 4, 32.

¹⁵³ Rios, R. *Chem. Soc. Rev.* **2012**, 41, 1060.

¹⁵⁴ Quasdorff, K. W.; Overman, L. E. *Nature* **2014**, 516, 181.

2- Objectives.

Considering the precedents shown above, we aimed to further study dearomatizing (3+2) oxidative annulation of *o*-alkenylphenols with alkynes, trying to enhance the selectivity of the process towards the formation of the spirocycle.



Scheme 117. Objective.

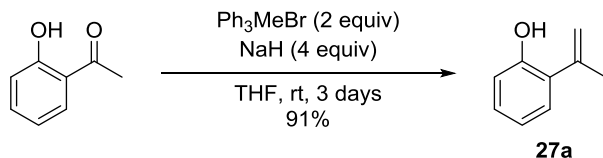
We also wanted to investigate the mechanistic pathway and the reason why the substituent of the olefin changes the reactivity towards the spirocycle. Finally, we also need to provide an explanation for the formation of the azulenone **32aa**.



3- Results and discussion.

3.1 Optimization of the reaction conditions.

To accomplish our goals we started with the synthesis of alkenylphenol **27a** as described earlier.



Scheme 118. Synthesis of model substrate **47a**.

With the model substrate in hand, we explored its reactivity against diphenylacetylene under different conditions in order to improve the selectivity of the transformation. The results of this screening are summarized in the table below.

Table 3. Screening of the reaction conditions.

Entry	Catalyst	Solvent	T (°C)	Yield (%) ^b		
				50	53aa	54aa
1	[Cp*RhCl ₂] ₂	CH ₃ CN	85	15	51	25
2	[Cp*RhCl ₂] ₂	t-AmOH	100	12	18	15
3	[Cp*RhCl ₂] ₂₂	Toluene	100	8	19	17
4	[Cp*RhCl ₂] ₂	CH ₃ CN	rt		44	4
5	[Cp*RhCl ₂] ₂	CH ₃ CN	40		97 ^c	Traces
6	[Cp*RhCl ₂] ₂	CH ₃ CN	40		91 ^d	8
7	[Ru(p-cymene)Cl ₂] ₂	CH ₃ CN	40		15	5 ^e
8	Pd(OAc) ₂	CH ₃ CN	40		<10	- ^e
9	none	CH ₃ CN	85	-	-	- ^f

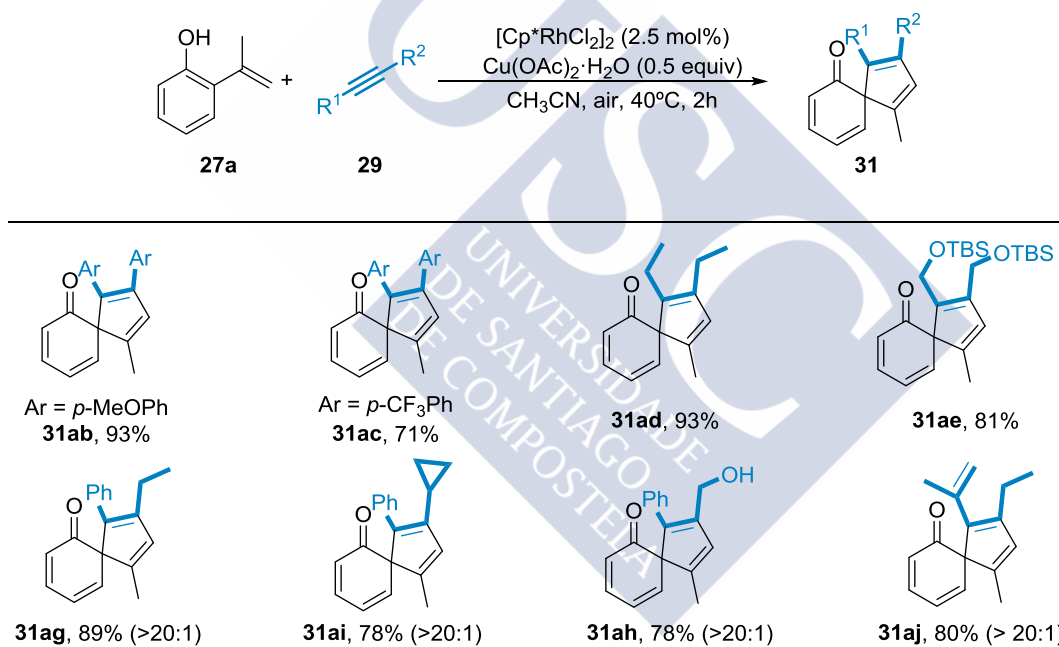
^aReaction conditions: **27a** (0.33 mmol), catalyst (2.5 mol %), alkyne (1.5 equiv), Cu(OAc)₂ H₂O (0.5 equiv), solvent (2 mL), air balloon. ^b Isolated yield. ^c In 2h. ^d 0.1 equiv of Cu(OAc)₂ H₂O/air balloon were used, 16h. ^e Decomposition of the alkenylphenol. ^f Starting materials were recovered.

As seen above, the reaction works productively in acetonitrile, and leads to lower overall yields when other solvents are used (entries 1-3). The reaction also works at room temperature although the yield drops to a 44% but, in this case, no benzoxepin is formed (entry 4). When the reaction is carried out at 40 °C and stopped after two hours, only the spirocycle **53aa** is formed with traces of the azulenone **54aa** (entry 5). It is even possible to lower the amount of copper oxidant to 10 mol % by increasing the reaction time without diminishing the overall yield, although a slightly higher proportion of the azulenone is

formed (entry 6). Other metal catalysts do not participate efficiently in the reaction, being ruthenium cymene complex slightly better than palladium (entries 7, 8). Finally, we confirmed the necessity of the catalyst since in the absence of the rhodium complex, the starting material is recovered (entry 9).

3.2 Substrate scope.

With the optimized conditions in hand, we proceeded to study the scope of the reaction with regard to the alkyne. Symmetrical alkynes bearing electron-rich or electron-poor substituents participate in the reaction leading selectively to the spirocyclics in good yields (**31ab** and **31ac**), aliphatic alkynes can also be used (**31ad**). Silylprotected hydroxyls are tolerated without their deprotection (**31ae**). Interestingly, unsymmetrical alkynes afford the corresponding products with higher selectivities than for the oxepines with selectivities above 20:1 (**31ag**–**31aj**). The alkyne can be substituted with free alcohols (**31ah**) without affecting the yield or regioselectivity. Enynes also undergo the annulation with in good yield and nearly perfect regioselectivity (**31aj**).

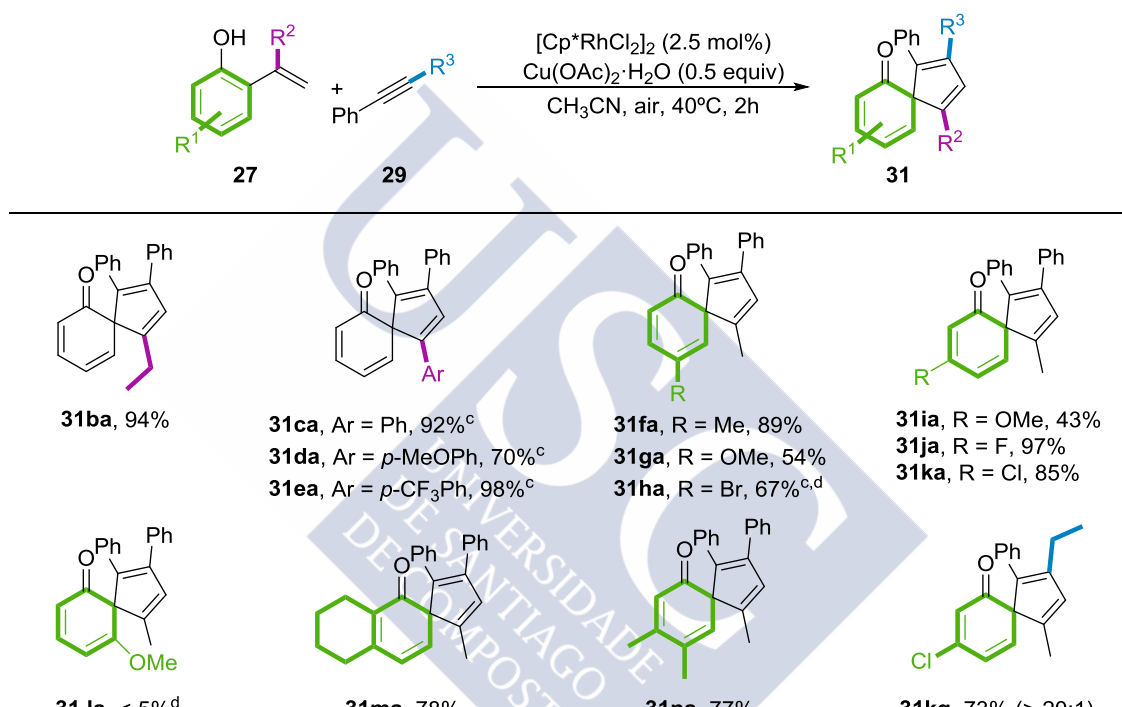


Reaction conditions: **27a** (0.33 mmol), $[\text{Cp}^*\text{RhCl}_2]_2$ (2.5 mol %), $\text{Cu}(\text{OAc})_2 \cdot \text{H}_2\text{O}$ (0.5 equiv), CH_3CN (2 mL), 40°C air balloon, 2h.

Scheme 119. Scope of the alkynes.

Next, we moved to investigate the effect of the substitution on the alkenylphenols by synthesizing a variety of substrates with different substituents at the internal position of the alkene, prepared also by a Wittig reaction from the 2'-hydroxyacetophenones. As shown below, it is possible to include different substitution patterns at the inner position of the double bond such as an ethyl group (**31ba**) or aromatic rings with diverse electronic properties although in these latter cases, heating to 60°C is needed in order to reach full conversion and obtain good yields (**31ca**–**31ea**). Substituents in *para* to the hydroxyl are well

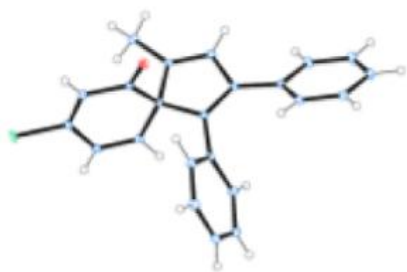
tolerated (**31fa**-**31ha**). However, for the reactions with the alkenylphenols bearing a bromine atom, we needed to raise the temperature to 60 °C to obtain decent yields which resulted in the formation of an 18% of the azulenone **32ha** (**31ha**) Substitution in *para* to the double bond is allowed (**31ia**-**31ka**) despite the lower yield of 43% of the methoxy derivative (**31ia**) due to stability issues. The presence of substituents at the *ortho* position of the hydroxyl does not affect the reactivity (**31na**) unlike the substitution at the *ortho* position of the alkenyl substituent which, shuts down the reactivity (**31la**) most probably due to the steric interactions. Double substituted substrates can also be used (**31ma**, **31na**) and, the reaction can be also achieved when unsymmetrical alkynes are employed without loss of the excellent regioselectivity as exemplified by **3kg**.¹⁵⁵



Scheme 120. Scope of the alkenylphenols.

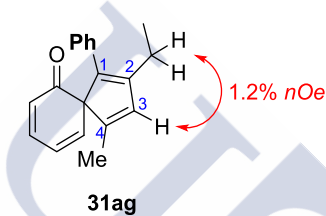
The structure of the spirocycles was unambiguously confirmed by X-Ray crystallography, resolving the structure of product **31la**.

¹⁵⁵ In collaboration with Noelia Casanova.



Scheme 121. Structure of **31la** obtained by X-Ray diffractometry.

To determine the regiochemistry when unsymmetrical alkynes were used, we carried out nOe experiments. We observed nOe between the aliphatic side chain of the alkyne and the hydrogen at C4, as exemplified below.



Scheme 122. Determination of the regiochemistry of **31ag** by nOe.

3.4 Mechanistic investigations.

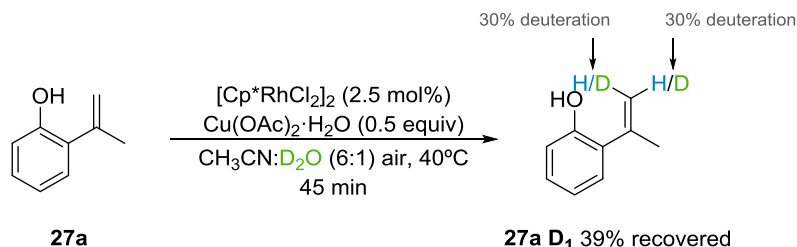
To shed light into the mechanism, we first synthesized the dideuterated alkenylphenols **27c-D₂** by using the trideuterated phosphonium iodide instead of the normal ylide. With the substrate in hand, we carried out a competition experiment to elucidate if, under the new conditions, there was an influence of the C-H activation in the reaction rate. Indeed, we observed value of the kinetic isotopic effect of $k_H/K_D \approx 2.3$ which, although relatively weak indicates that the cleavage of the carbon-hydrogen might be influencing the reaction rate.



Scheme 123. Measurement of the KIE.

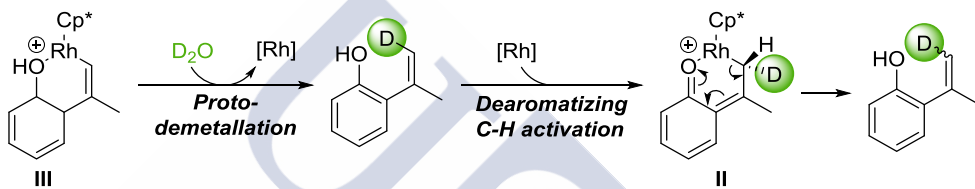
Interestingly, treatment of substrate **27a** under the standard conditions with deuterated water in the absence of alkyne, led to the deuteration of both terminal positions of the double bond. This result seems to be consistent with the non-concerted dearomatization-rearomatization mode of the C-H activation since, in this pathway, there is an intermediate in which both protons are undistinguishable.

¹³⁴ Simmons, E. M.; Hartwig, J. F. *Angew. Chemie. Int. Ed.* **2012**, *51*, 3066.



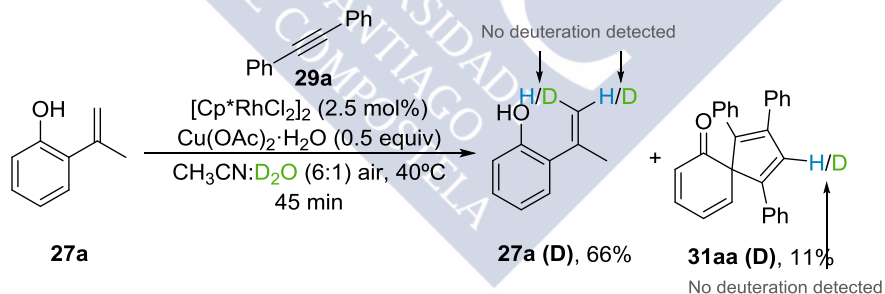
Scheme 124. Deuteration experiments.

The mechanistic rationale behind this result relies on the formation of the Z-deuterated alkenylphenols by protodemettalation of the six-membered rhodacycle III. This monodeuterated species reenters in the cycle leading to the formation of both isomers.¹⁵⁶



Scheme 125. Mechanistic rationale for the E/Z deuteration.

Carrying out the same reaction in presence of the alkyne affords the starting material and the product without deuterium suggesting that, in the presence of the alkyne, the rhodacycle is prone to undergo the migratory insertion instead of the protodemettalation.

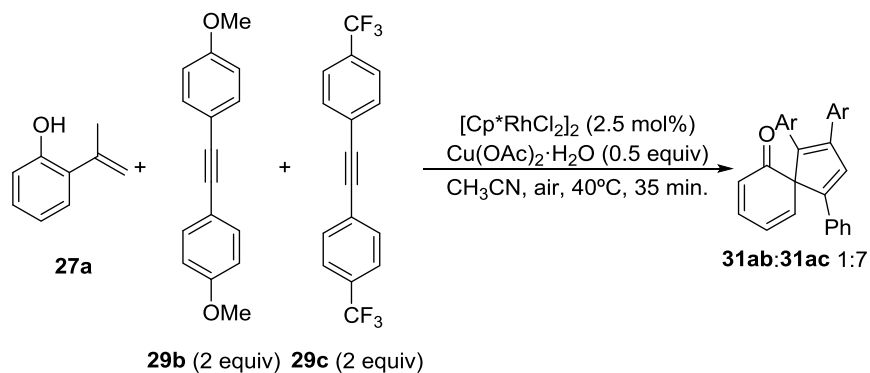


Scheme 126. Reversibility experiment in presence of the alkyne.

A competition experiment between electron-deficient **29c** and electron rich **29b** alkynes showed a preference for the formation of **29c** which can be explained in terms of a preferential coordination and subsequent reaction of the electron-poor acetylene.¹⁵⁷

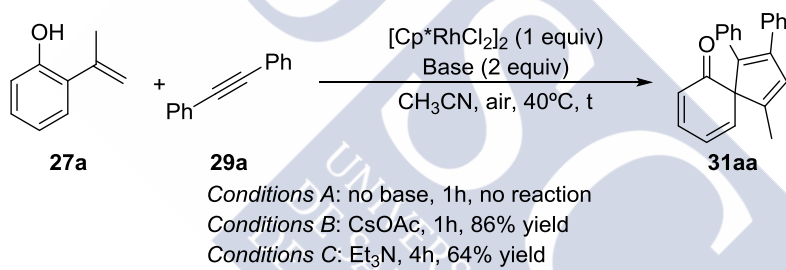
¹⁵⁶ Control experiments indicate that the presence of $[\text{Cp}^*\text{RhCl}_2]_2$, $\text{Cu}(\text{OAc})_2$ or NaOAc alone is not enough to induce deuteration.

¹⁵⁷ Shriver, D.F.; Weller, M.T.; Overton, T.; Rourke, J. P.; Armstrong, A. A. *Inorganic Chemistry* 6th ed. Ed. Oxford University Press, 2014.



Scheme 127. Competition experiments between electronically biased alkynes.

Control experiments using stoichiometric amount of $[\text{Cp}^*\text{RhCl}_2]_2$ showed that the complex alone is not able to promote the reaction. However, when CsOAc is added to the mixture, a clean formation of the spirocycles is observed. Interestingly, the reaction can be also carried out with a monodentated base such as triethylamine, in the absence of any acetate source, which is further indicating that the C-H activation mechanism is not a classical CMD in which an acetate group acts as the proton shuttle.^{55b}

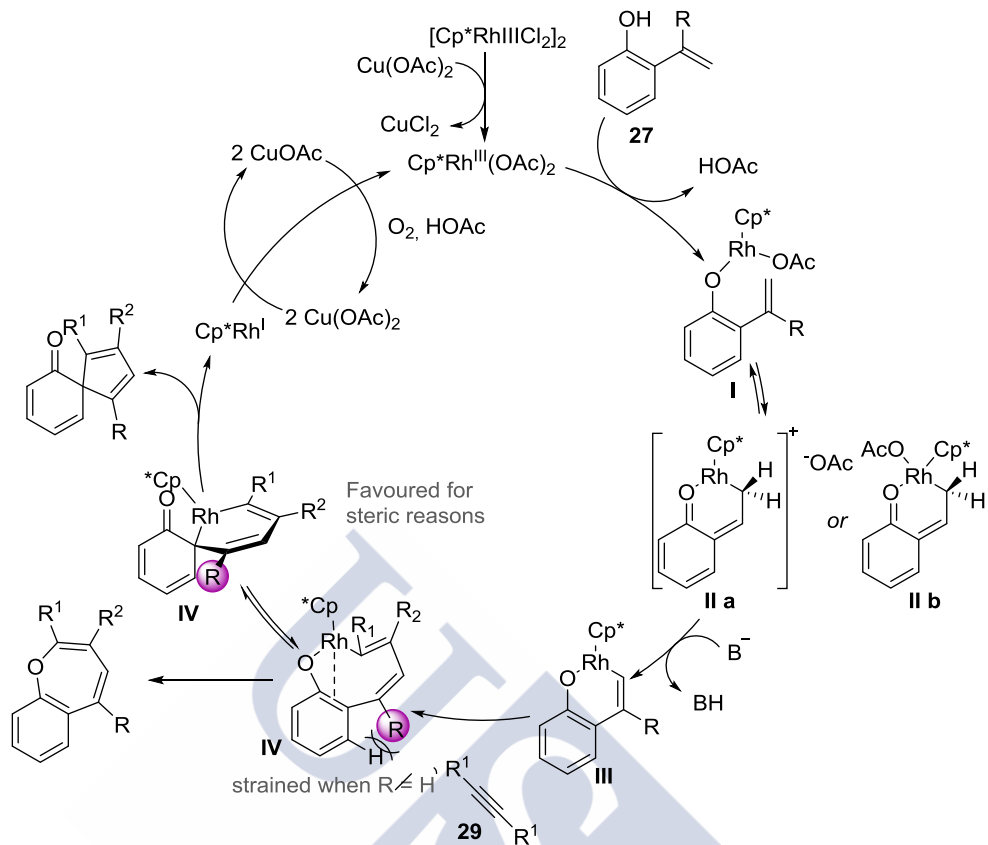


Scheme 128. Studies on the role of the base.

3.5 Mechanistic proposal.

With this data in hand we propose a mechanism similar to the one shown for the oxepines. After the dissociation of the Cp^*Rh dimer, ligand exchange with the O-H group cleavage results in the open intermediate I. C-H activation, presumably, through a dearomatization-rearomatization pathway, leads to rhodacycle IV. This intermediate might evolve by reductive elimination towards the oxepines, only when the alkene is not substituted. However, when the olefin is substituted at the internal position there is a repulsion in the eight-membered rhodacycle between this substituent and the *ortho*-hydrogen from the aromatic ring. Hence, this species is more prone to undergo a keto-tautomerization towards metallacycle V. Reductive elimination and reoxidation of the catalysts deliver the desired compound and the repetition of the catalytic cycle.

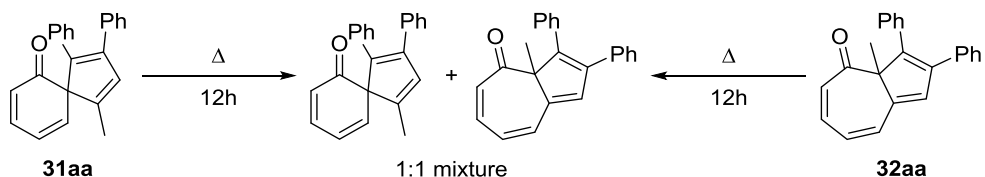
^{55b} Lapointe, D.; Fagnou, K. *Chem. Lett.* **2010**, 39, 1118.



Scheme 129. Mechanistic hypothesis.

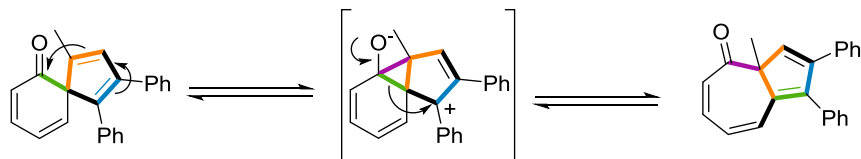
3.6 Formation of the azulenone.

As explained in the beginning of this chapter, at higher temperatures, along with the formation of other products, the reaction also provides a small proportion of interesting azulenone **32aa**. We considered that they could arise from a side reaction suffered by the spirocycles. In order to test our hypothesis we heated compound **31aa** at 85 °C for 12 h. As shown in scheme 130, the substrate evolves to a 1:1 mixture of both products, the spirocycle and the azulenone. Remarkably, independent heating of the azulenone led to the same mixture confirming that the reaction is an equilibrium.



Scheme 130. Proof of the equilibrium.

This interconversion between spirocycle and azuleneone can be explained in terms of the formation of a zwitterionic species and the subsequent ring-opening of the resulting tricycle.¹⁵⁸



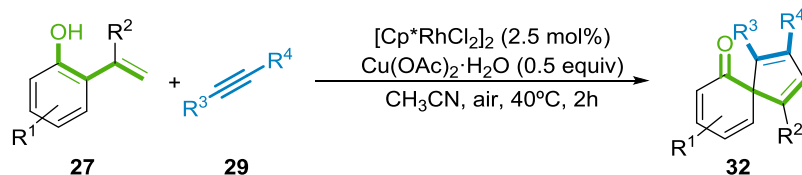
Scheme 131. Formation of the azulenone.



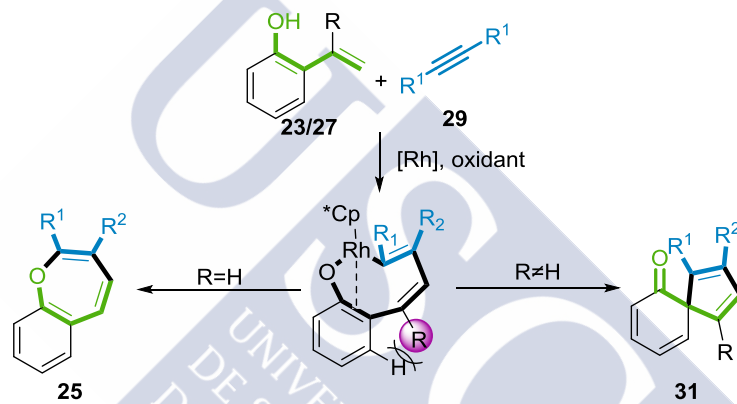
¹⁵⁸ (a) a [1,5] sigmatropic rearrangement or a radical-based mechanism are also plausible: Spangler, C. W. *Chem. Rev.* **1976**, *76*, 187. (b) For a recent, related rearrangement see: Li, X.-Y.; Yang, Y.-F.; Peng, X.-R.; Li, M.-M.; Li, L.-Q.; Deng, X.; Qin, H.-B.; Liu, J.-Q.; Qiu, M.-H. *Org. Lett.* **2014**, *16*, 2196.

4- Conclusions.

In conclusion we have developed a mild formal (3+2) annulation between *o*-vinylphenols and alkynes promoted by rhodium (III) catalysis that provides structurally interesting spirocycles. This transformation conveys a cleavage of the O-H and a C-H bond, and the dearomatization of the phenolic ring. The reaction takes place with excellent chemo and regioselectivity generating chirality from simple, plain structures.

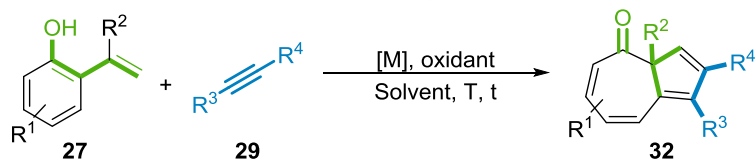


Scheme 132. Oxidative annulation of *o*-vinylphenol.



Scheme 133. Divergence of outcomes depending on the substitution.

Our studies also suggest that from readily available substrates, namely *o*-alkenylphenols and alkynes it is possible to obtain relevant and structurally unrelated products such as azulenones.¹⁵⁹



Scheme 134. Synthesis of azulenones from *o*-alkenylphenols.

¹⁵⁹ These results were published in: Seoane, A.; Casanova, N.; Quiñones, N.; Mascareñas, J. L.; Gulías, M. *J. Am. Chem. Soc.* **2014**, 136, 7607.



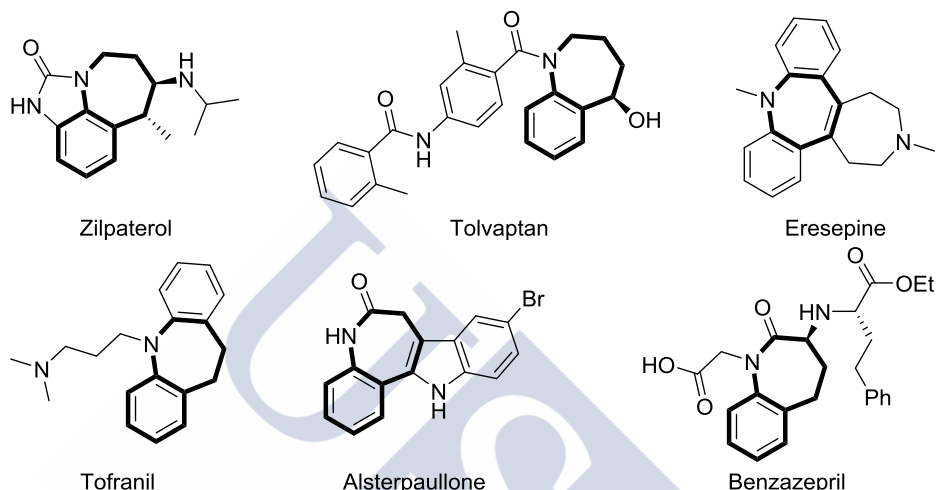
CHAPTER V: Oxidative annulations of *o*-alkenylanilines.





1- Introduction

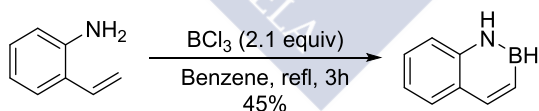
After developing the annulation chemistry of *o*-alkenylphenols, we wondered whether it was possible to translate their chemistry to nitrogen-containing molecules. The motivations behind this goal rely on the prevalence of nitrogen atoms in drugs and bioactive compounds. In fact, if we could replicate the same (5+2) annulation performed with phenols to anilines we would be able to access to benzazepines, a common motif in several pharmaceuticals and natural products.¹⁶⁰



Scheme 135. Biologically active and naturally occurring [1]benzazepines.

1.2 Reactivity of *o*-alkenylanilines.

Unlike previously described *o*-vinylphenols, which were scarcely used in the literature, there are several precedents for the use of *o*-alkenylanilines in synthesis. Their use started with the pioneering work of Dewar and Dietz where they treated them with boron trichloride which allowed the isolation of a cyclic compound isosteric to naphthalene.¹⁶¹



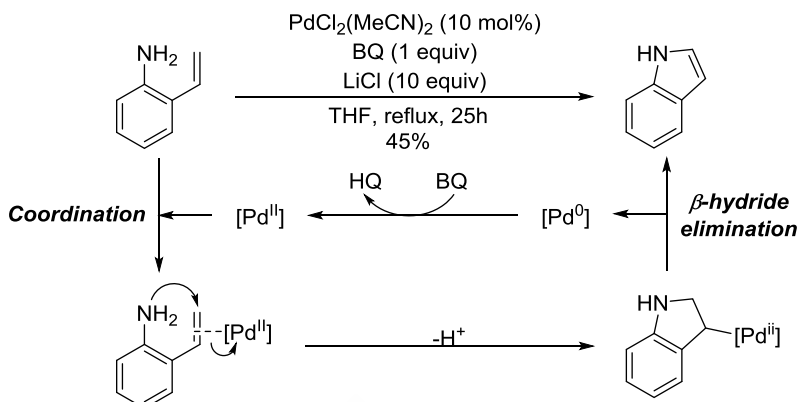
Scheme 136. Synthesis of the naphthalene isostere.

Later, Hegedus and co-workers described that treatment of alkenylanilines, either free or tosyl protected, under Palladium catalysis afforded indoles by cyclization. Their mechanistic hypothesis starts with the coordination of the palladium to the olefin and nucleophilic attack

¹⁶⁰ Shah, J. H.; Hindupur, R. M.; Pati, H. N. *Curr. Bioact. Compd.* **2015**, *11*, 170.

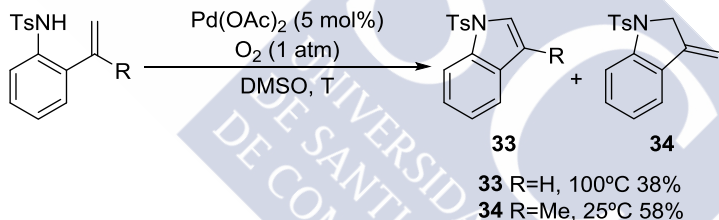
¹⁶¹ Dewar, M. J. S.; Dietz, R. *J. Chem. Soc.* **1959**, 2728.

by the nitrogen. Finally, a β -hydride elimination and reoxidation of the catalyst close the cycle and yields the indoles in a moderate yield.¹⁶²



Scheme 137. Palladium-catalyzed cyclization of *o*-alkenylanilines.

The group of Larock improved the catalytic system by using Palladium acetate and oxygen as oxidant. With those conditions, they were able to expand the scope to different amines albeit in lower yields. Interestingly, when having a methyl at the inner position of the double bond, the reaction can be performed at lower temperatures and the 3-methylene-2,3-dihydroindole **34** is obtained instead of the expected indole.¹⁶³



Scheme 138. Larock's synthesis of indoles.

Following this work, other metals¹⁶⁴ were used to carry out this synthesis. Photocatalytic¹⁶⁵ and even metal-free conditions¹⁶⁶ were also developed by different research groups.

Larock and co-workers also designed a method for synthesizing dihydroquinolinones by using the same tosylanilides and vinylic (pseudo)halides in a formal (5+1) annulation.¹⁶⁷

¹⁶² (a) Hegedus, L. S.; Allen, G. F.; Bozell, J. J.; Waterman, E. L. *J. Am. Chem. Soc.* **1978**, *100*, 5800. (b) Harrington, P. J.; Hegedus, L. S. *J. Org. Chem.* **1984**, *49*, 2657.

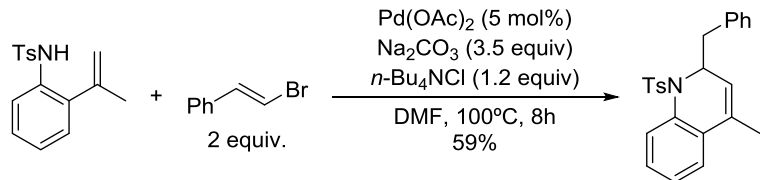
¹⁶³ Larock, R. C.; Hightower, T. R.; Hasvold, L. A.; Peterson, K. P. *J. Org. Chem.* **1996**, *61*, 3584.

¹⁶⁴ (a) Coleman, C. M.; O'Shea, D. F. *J. Am. Chem. Soc.* **2003**, *125*, 4054. (b) Liwosz, T. W.; Chemler, S. R. *Chem. Eur. J.* **2013**, *19*, 12771. (c) Youn, S. W.; Ko, T. Y.; Jang, M. J.; Jang, S. S. *Adv. Synth. Catal.* **2015**, *357*, 227.

¹⁶⁵ Maity, S.; Zheng, N. *Angew. Chemie. Int. Ed.* **2012**, *51*, 9562.

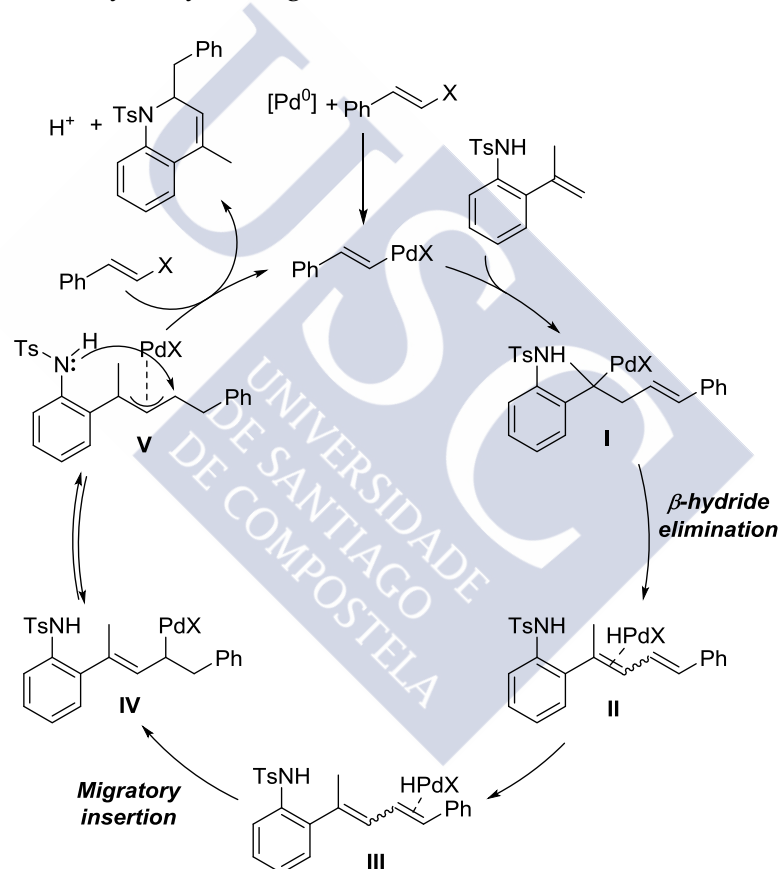
¹⁶⁶ Jang, Y. H.; Youn, S. W. *Org. Lett.* **2014**, *16*, 3720.

¹⁶⁷ (a) Larock, R. C.; Hightower, T. R.; Hasvold, L. A.; Peterson, K. P. *J. Org. Chem.* **1996**, *61*, 3584. (b) Larock, R. C.; Pace, P.; Yang, H. *Tetrahedron Lett.* **1998**, *39*, 2515.



Scheme 139. Larock's formal (5+1) annulation.

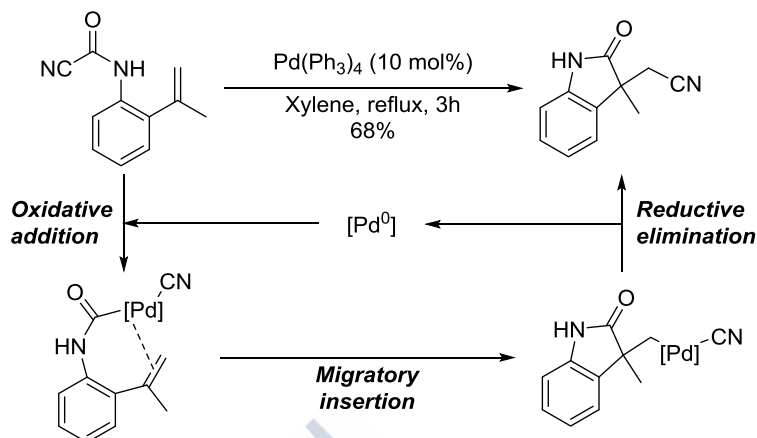
Their mechanistic explanation consists of an initial reduction of palladium acetate and oxidative addition to the aryl (pseudo)halide. Subsequent migratory insertion and β -hydride elimination lead to the diene **II**. From this intermediate, the palladium migrates to the outer olefin, which undergoes a migratory insertion leading to π -allyl **V**. This species suffers a nucleophilic attack from the amine releasing the product and the reduced catalyst, which is now able to reenter the cycle by adding onto the C-X bond.



Scheme 140. Mechanistic hypothesis.

The group of Takemoto employed an oxidative addition to direct the palladium C-H activation in the synthesis of indolinones. Their mechanistic hypothesis starts with the oxidative addition of the Pd (0) into the C-CN bond on the anilide which is followed by the

migratory insertion of the alkenyl unit. A final reductive elimination affords the indolinone and releases the active catalyst.¹⁶⁸

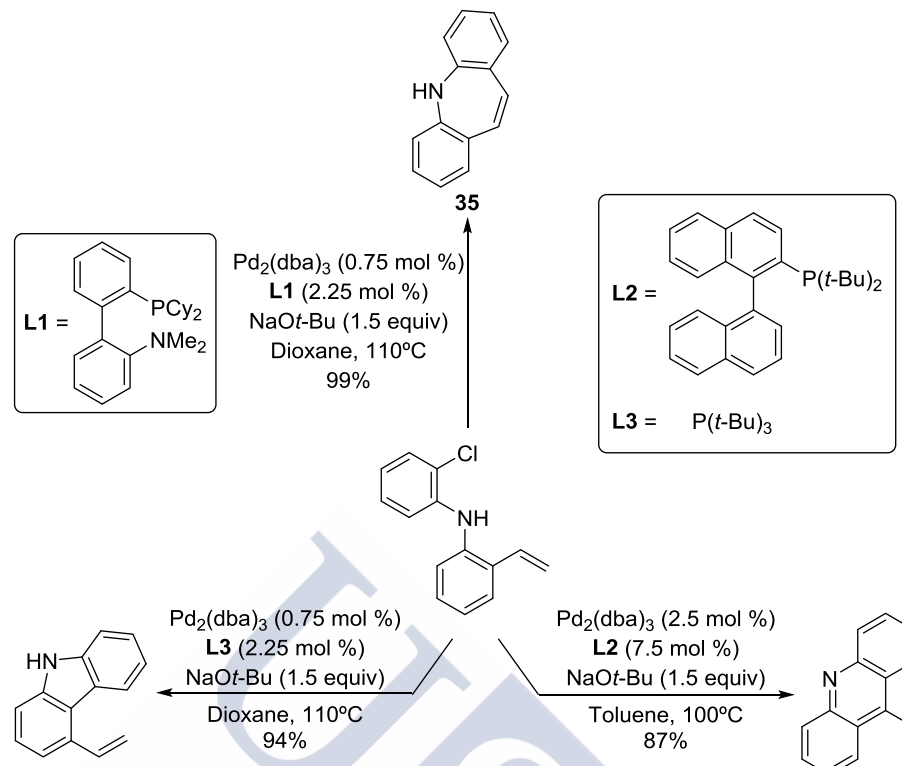


Scheme 141. Palladium-catalyzed synthesis of indolinones.

In 2010, Buchwald and co-workers also took advantage of an oxidative addition-directed strategy to synthesize several nitrogen-containing heterocycles. They were able to control the selectivity of the C-H activation by the use of different phosphines. In their communication, they also explained the formation of the dibenzazepine **35** in terms of a palladium-induced dearomatization/rearomatization mechanism.¹⁶⁹

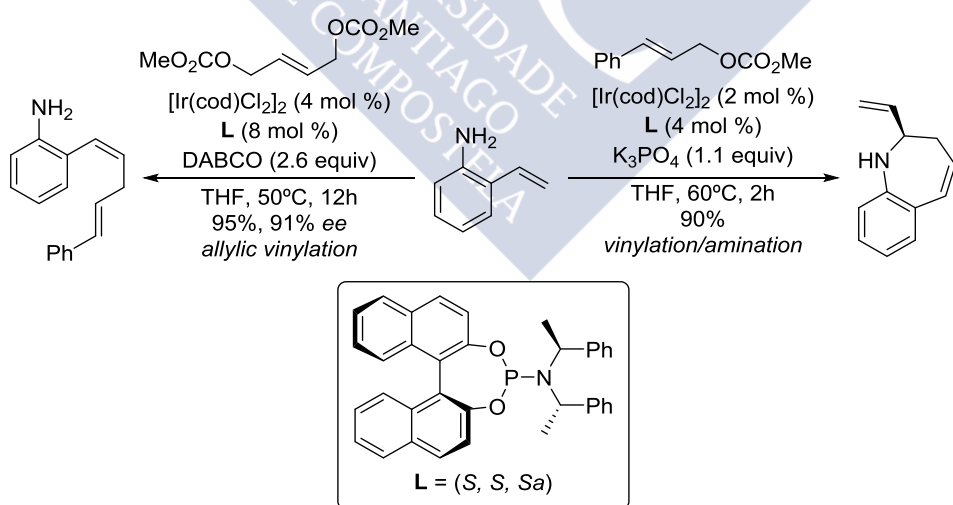
¹⁶⁸ Kobayashi, Y.; Kamisaki, H.; Takeda, H.; Yasui, Y.; Yanada, R.; Takemoto, Y. *Tetrahedron* **2007**, *63*, 2978.

¹⁶⁹ Tsvelikhovsky, D.; Buchwald, S. L. *J. Am. Chem. Soc.* **2010**, *132*, 14048.



Scheme 142. Divergent synthesis of heterocycles from (N-aryl)vinylanilines.

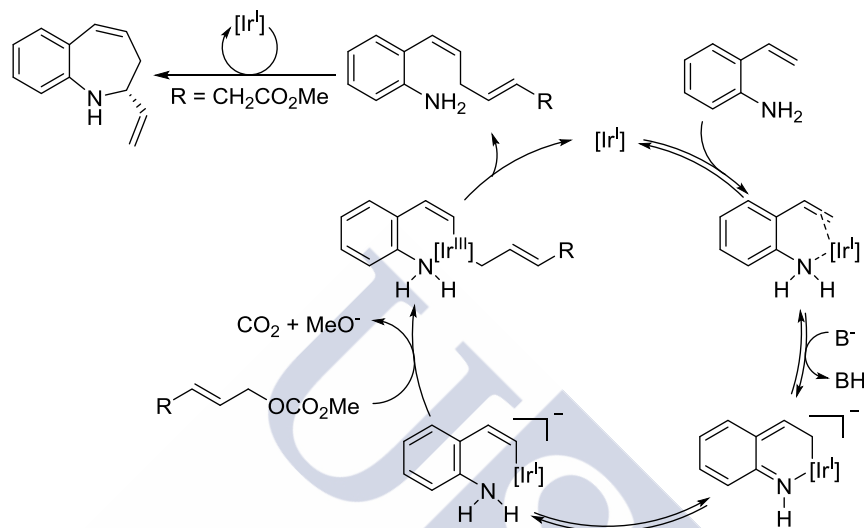
You et al. developed an interesting work on the allylation of vinylanilines by using Ir (I) catalysis and allylic carbonates. They were also able to couple the allylation with an intramolecular amination for the synthesis of dihydrobenzazepines.¹⁷⁰



Scheme 143. Ir(I)-catalyzed allylation and tandem allylation-cyclization of o-vinylanilines with allylic carbonates.

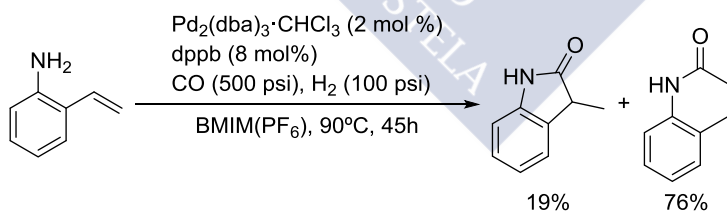
¹⁷⁰ (a) He, H.; Liu, W. B.; Dai, L. X.; You, S. L. *J. Am. Chem. Soc.* **2009**, *131*, 8346. (b) He, H.; Liu, W. B.; Dai, L. X.; You, S. L. *Angew. Chemie. Int. Ed.* **2010**, *49*, 1496. (c) Ye, K.-Y.; Dai, L.-X.; You, S.-L. *Asian J. Org. Chem.* **2013**, *2*, 244.

Their proposed mechanism starts with the coordination of the iridium centre to the amine and the double bond, which is followed by a C-H activation step based on a non-concerted dearomatization/rearomatization pathway. The oxidative addition of the iridium into the carbonate affords intermediate, which upon reductive elimination, yields the allylated vinylaniline and regenerates the catalyst. When R is another carbonate, a second coordination, oxidative addition and reductive elimination affords the cyclized benzazepine.



Scheme 144. Mechanistic hypothesis.

Making use of these substrates, the group of Alper was able to carry out the translation of his *o*-alkenylphenol carbonylation to nitrogen-containing compounds. By using palladium in ionic liquids under high pressure of carbon monoxide and hydrogen (500 psi and 100 psi respectively) they performed the cyclocarbonylation obtaining moderate selectivities when unsubstituted olefins were used as substrates.¹⁷¹



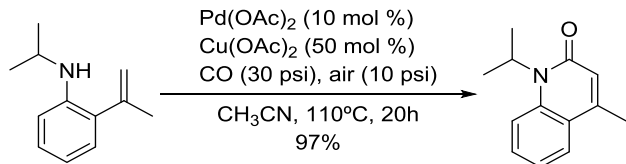
Scheme 145. Cyclocarbonylation of 2-aminostyrenes in ionic liquids.

The same group later described a related work. By blocking the internal position of the double bond and changing the catalytic system for palladium acetate as catalyst and copper acetate as an oxidant as well as acetonitrile as solvent, they were able to reduce the CO

¹³⁰ Ferguson, J.; Zeng, F.; Alper, H. *Org. Lett.* **2012**, *14*, 5602.

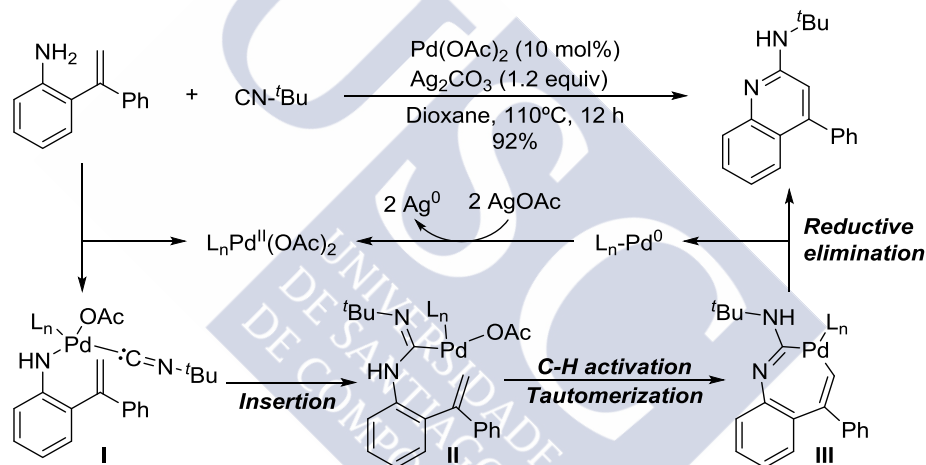
¹⁷¹ Ye, F.; Alper, H. *Adv. Synth. Catal.* **2006**, *348*, 1855.

pressure to a more acceptable value of 30 psi.¹⁷² The proposed mechanism is analogous to the one described when vinylphenols are used.¹³⁰



Scheme 146. Cyclocarbonylation of *N*-substituted 2-aminostyrenes.

More recently, the groups of Zeng¹⁷³ and Peng¹⁷⁴ developed the Palladium-catalyzed (4+2) oxidative annulation of vinylanilines with isocyanides. The mechanism is supposed to occur by the insertion of the cyanide in the Pd-N bond generating intermediate **II** which undergoes C-H activation and isomerization of the double bond to palladacycle **III**. A further reductive elimination releases the aminoquinoline and the reduced catalyst which is reoxidized by the silver salt.¹⁷⁵



Scheme 147. Synthesis of aminoquinolines by oxidative annulation.

An interesting Palladium-catalyzed (5+2) annulation of 2-phenylanilines and alkynes was developed by the group of Luan as an extension of their previous work on the dearomatization of naphthols shown in scheme 111 (scheme 148). The mechanism is supposed to involve the formation of metallacycle **III** which undergoes reductive elimination and isomerization of the double bond towards the imine **36**.¹⁷⁶

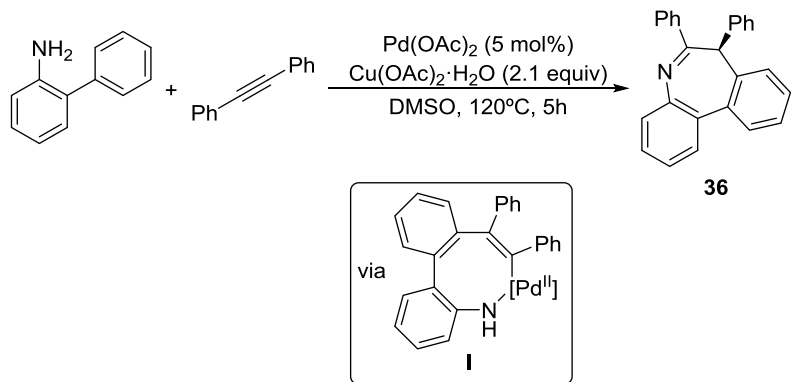
¹⁷² Ferguson, J.; Zeng, F.; Alwis, N.; Alper, H. *Org. Lett.* **2013**, *15*, 1998.

¹⁷³ Wang, L.; Ferguson, J.; Zeng, F. *Org. Biomol. Chem.* **2015**, *13*, 11486.

¹⁷⁴ Zheng, Q.; Ding, Q.; Wang, C.; Chen, W.; Peng, Y. *Tetrahedron* **2016**, *72*, 952.

¹⁷⁵ The work by Prof Peng invokes a migratory insertion form **II** into the olefin, a β -hydride elimination and a [1,3]-H shift followed by rearomatization.

¹⁷⁶ Zuo, Z.; Liu, J.; Nan, J.; Fan, L.; Sun, W.; Wang, Y.; Luan, X. *Angew. Chemie. Int. Ed.* **2015**, *54*, 15385.

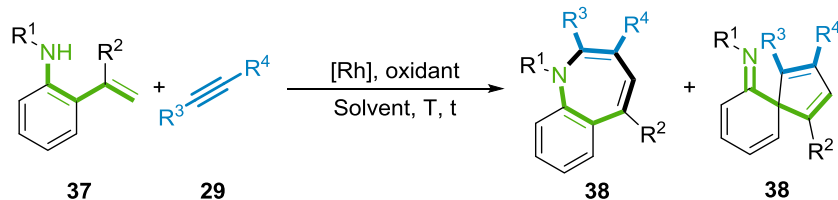


Scheme 148. *Pd*-catalyzed (5+2) oxidative annulation of *o*-phenylanilines.



2- Objectives

Taking into account the precedents shown above, which show that vinylanilines are reactive towards transition-metal catalyzed transformations, our goal was to further study the activation of the olefinic C-H bond of *o*-alkenylanilines by using a system similar to the one we had described for alkenylphenols.



Scheme 149. *Oxidative annulation with alkenylanilines.*

Additionally, we wanted to investigate the effect of the electronic nature of the substituent in the amine in order to maximize the reactivity and see if the replacement of oxygen for nitrogen would affect to the mechanism.



3- Results and discussion.

3.1 Initial studies on the N-substituent.

Our first goal was to identify a functional group, that placed on the nitrogen, would provide the electronic requirements needed for a good reaction performance. For this purpose, we synthesized several N-protected *o*-alkenylanilines derived from commercially available 2-isoprenylaniline. After having tested a variety of electronically tuned groups, only the triflate (entry 7) reacted well enough to be able to isolate coupling products, tosyl and nosyl protected anilines also led to traces of products presenting the aniline and the two phenyls from the alkyne but in a lower yield and harder to purify (entries 6 and 8). However, instead of the expected azepine or spiroimine, two different naphthylamines were isolated arising from a formal (4+2) annulation.

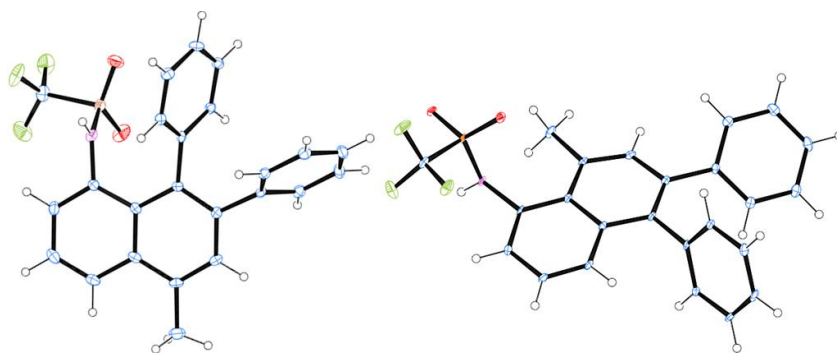
Table 4. Screening of the electronics of the nitrogen centre.¹⁷⁷

Entry	R	Conversion 39 (%)	Conversion 29a (%)	Yield 39 (%) ^b	Yield 39' (%) ^b
1	H	35	100	0	0
2	<i>i</i> -Pr	0	0	-	-
3	Boc	0	0	-	-
4	Ac	0	0	-	-
5	TFAc	0	0	-	-
6	Ts	39	62	Traces of coupling products	
7	Tf	38	75	17	8
8	Ns	48	88	Traces of coupling products	

^a Reaction conditions: **37** (0.33 mmol), **29a** (1 equiv), $[\text{Cp}^*\text{RhCl}_2]$ (2.5 mol %), $\text{Cu}(\text{OAc})_2 \cdot \text{H}_2\text{O}$ (0.5 equiv), solvent (2 mL). ^b Isolated yield.

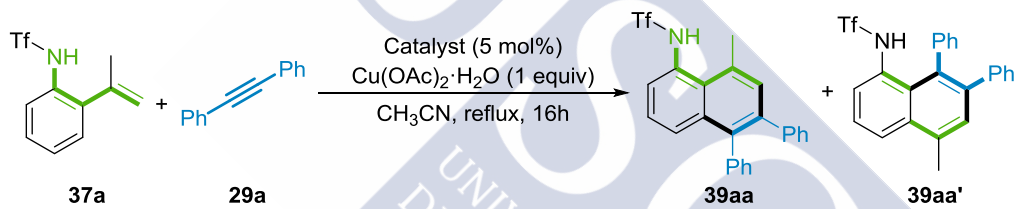
At the beginning we were intrigued by this unusual reactivity, especially for the case where an apparent 1,2-migration of the alkenyl substituent is happening prior to the annulation (**39'**). To fully corroborate the structure of these products we crystallized them and submitted them to X-Ray diffraction which unambiguously confirmed our proposed structures.

¹⁷⁷ In collaboration with Xabier Diz.

**Fig 8.** X-Ray structure of naphthylamides **39aa** and **39aa'**.

3.2 Optimization of the reaction conditions.

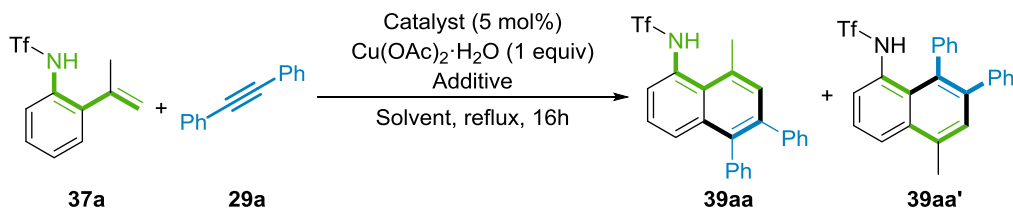
Once established that the triflate group was providing the appropriate electronics for the reactivity, we started to investigate the best conditions to achieve this unusual transformation.

Table 5. Screening of catalyst.^a

Entry	Catalyst	Yield 61aa (%) ^b	Yield 61aa' (%) ^b
1	[Cp*RhCl ₂] ₂	28	16
2	RhCl ₃ · xH ₂ O	0	0 ^c
3	Rh(PPh ₃) ₃ Cl	Traces	Traces ^c
4	[Cp*IrCl ₂] ₂	0	0 ^c
5	[(<i>p</i> -cymene) RuCl ₂] ₂	0	0 ^c
6	Pd(OAc) ₂	0	0 ^c

^a Reaction conditions: **37a** (0.33 mmol), **29a** (1 equiv), catalyst (5 mol %), Cu(OAc)₂·H₂O (1 equiv), acetonitrile (2 mL). ^b Isolated yield. ^c Starting material was mostly recovered.

We started by identifying the appropriate precatalyst for this transformation. To do so, we tested several metal complexes with only [Cp*RhCl₂]₂ leading to appreciable conversions (entry 1). From the other precatalysts screened, Ir and Ru complexes as well as RhCl₃ · xH₂O did not lead to any product and starting materials were mostly recovered (entries 2, 4, 5). Wilkinson's catalyst worked slightly better providing traces of the cycloadducts along with starting material, while palladium acetate led to the decomposition of the anilide and a complex mixture of products.

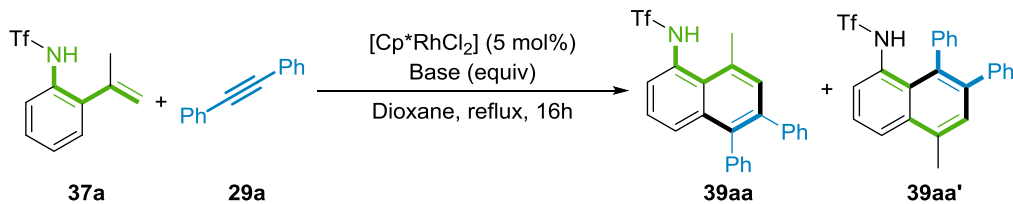
Table 6. Screening of conditions.^a

Entry	Solvent	Catalyst	Additive (equiv)	Yield 39aa (%) ^b	Yield 39aa' (%) ^b
1	Toluene	[Cp*RhCl ₂] ₂	-	32	12
2	EtOH	[Cp*RhCl ₂] ₂	-	32	14
3	TFE	[Cp*RhCl ₂] ₂	-	18	7
4	AcOH	[Cp*RhCl ₂] ₂	-	0	0
5	t-AmOH	[Cp*RhCl ₂] ₂	-	30	16
6 ^{c,d}	DMF	[Cp*RhCl ₂] ₂	-	35	17
7 ^c	DMF	[Cp*RhCl ₂] ₂	-	Traces	Traces
8	Dioxane	[Cp*RhCl ₂] ₂	-	60	19
9	Dioxane	[Cp <i>i</i> BuRhCl ₂] ₂	-	21	9
10	Dioxane	[Cp <i>i</i> PrRhCl ₂] ₂	-	38	29
11	Dioxane	[Cp*RhCl ₂] ₂	AcOH (2)	57	20
12	Dioxane	[Cp*RhCl ₂] ₂	PivOH (2)	56	21
13	Dioxane	[Cp*RhCl ₂] ₂	CsOAc (2)	35	17
14	Dioxane	[Cp*RhCl ₂] ₂	CsOPiv (2)	56	23
15	Dioxane	[Cp*RhCl ₂] ₂	AgSbF ₆ (0.2)	0	0
16 ^e	Dioxane	[Cp*RhCl ₂] ₂		19	5
17 ^f	Dioxane	[Cp*RhCl ₂] ₂		57	24
18 ^f	Dioxane	[Cp*RhCl ₂] ₂		0	0

^a Reaction conditions: 37a (0.33 mmol), 29a (1 equiv), catalyst (5 mol %), Cu(OAc)₂·H₂O (1 equiv), additive, solvent (2 mL). ^b Isolated yield. ^c Reaction performed at 110 °C, starting material was recovered. ^d AgOAc (1 equiv) was used instead of Copper acetate. ^e Reaction performed at 60 °C. ^f 0.5 equiv of Copper acetate were used.

After finding the best catalyst for the transformation, we tested different solvents and additives to further improve the reaction. Among the screened solvents, the best one proved to be dioxane leading to a 79% overall yield in a 3:1 ratio of regioisomers (entry 8) under this conditions, the replacement of the Cp*Rh precatalyst with the analogous Cp*i*Bu and Cp*i*Pr led to lower yields (entries 9, 10). Also, the addition of either acids or bases did not affect the performance of the reaction (entries 11-14) while the use of a silver salt as chlorine scavenger afforded the decomposition of the anilide. Lowering the temperature to 60 °C resulted in the overall yield dropping to a 24% (entry 16) and reducing the amount of copper acetate to 0.5 equivalents does not affect the reaction (entry 17). Finally we confirmed the requirement of the catalyst since, in its absence, starting materials are mostly recovered (entry 18).

We next sought to check the requirement of the oxidant by omitting them from the reaction. To our surprise the reaction could be carried out even in the absence of copper salts as shown below.

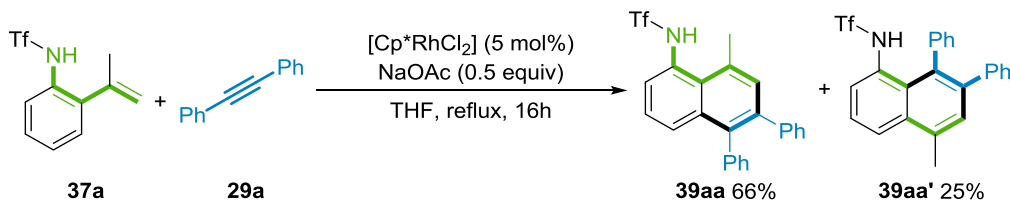
Table 7. Control experiments.^a

Entry	Base (equiv)	Yield 39aa (%) ^b	Yield 39aa' (%) ^b	Observations
1	$\text{Cu}(\text{OAc})_2$ (0.5)	57	24	
2	CsOAc (2)	57	15	
3	CsOAc (1)	54	16	
4	CsOAc (1)	56	15	Under Ar atmosphere
5	NaOAc (2)	57	16	
6	NaOAc (0.5)	53	15	
7	CsCO_3	0	0	Recovery of starting material
8	AcOH	0	0	Recovery of starting material
9	CsOAc (2)	0	0	No Rh, recovery of starting material

^a Reaction conditions: **37a** (0.33 mmol), **29a** (1 equiv), $[\text{Cp}^*\text{RhCl}_2]$ (5 mol %), Base, Dioxane (2 mL). ^b Isolated yield.

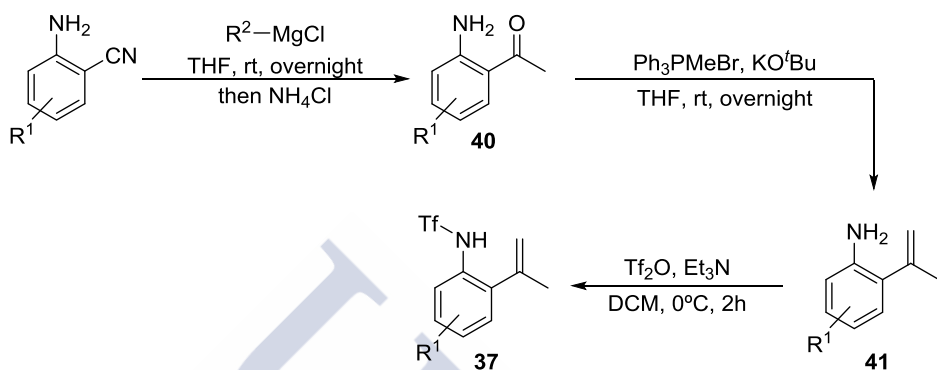
When copper was omitted from the reaction media and cesium acetate was used as base, the reaction still took place catalytically affording the corresponding naphthylamides in similar yield to the one obtained with copper (entries 1, 2). To rule out the possibility that oxygen was acting out as an oxidant, we carried out the reaction with a careful extrusion of air in deoxygenated dioxane, obtaining the same result as before. Sodium acetate was used due to its lower hygroscopicity and, even in a catalytic way, reproduced the previous results (entries 4, 5). Neither cesium carbonate nor acetic acid were able to promote the reaction (entries 6, 7). Finally, when no rhodium catalyst is used under these new conditions, no conversion is observed and the starting material is recovered.

We finally tried the reaction in THF under the copper-free conditions which allowed us to reduce the temperature and still observe a slightly improvement of the yield. These conditions were the ones considered as optimal for the study of the scope.

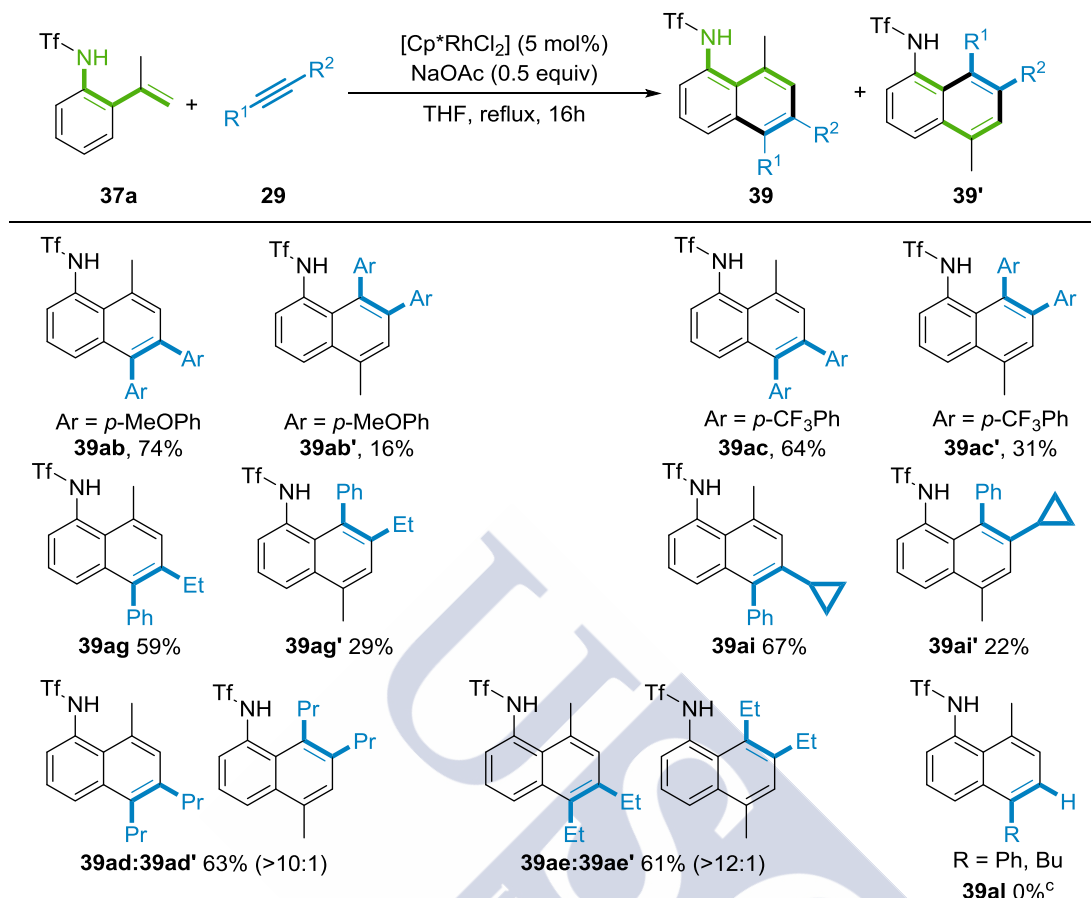
**Scheme 150.** "Copper free" oxidative annulation with alkenylanilides.

3.3 Substrate scope.

For studying the scope of the reaction we synthesized different anilides. The synthetic route used was as follows: When the 2'-aminoacetophenones were available, a Wittig reaction followed by triflation afforded the corresponding annulation precursor. When the ketone was not commercial we synthesized it by the addition of a Grignard to the corresponding benzonitrile.



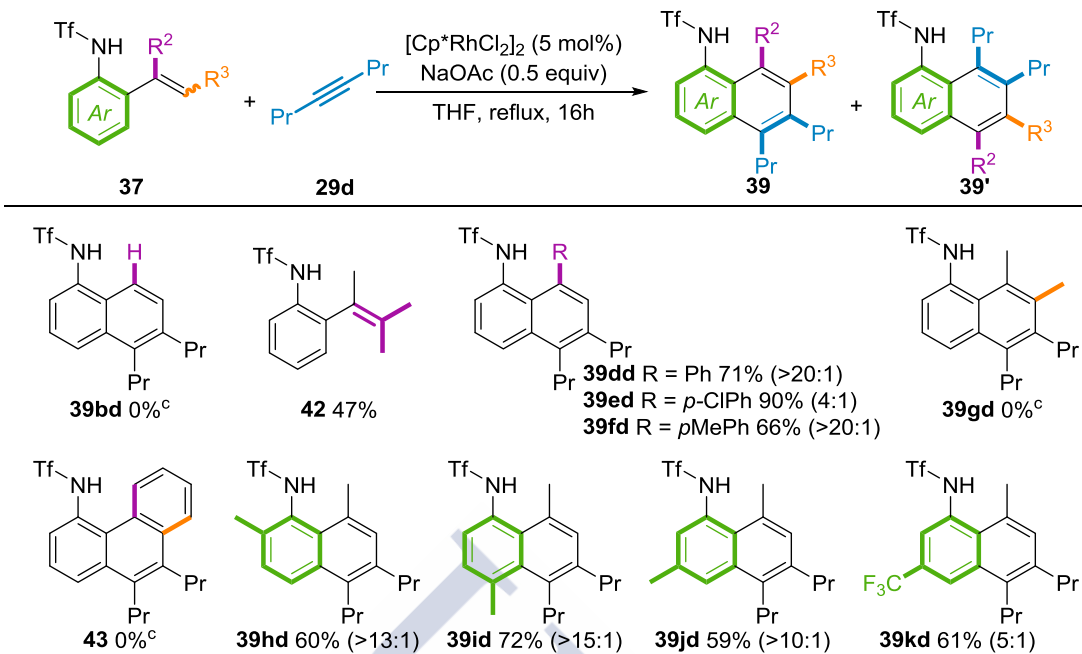
When submitted to the optimized conditions, differently substituted alkynes undergo the oxidative annulation with the model anilide to obtain the corresponding naphthylamides. Electron-rich and electron-poor diarylacetylenes are well tolerated affording the corresponding regioisomers (**39ab** and **39ac**). Interestingly, unsymmetrical aliphatic and aromatic alkynes provide only two of the four possible regioisomers, this preference, probably taking place during the migratory insertion, is similar to the one observed for the annulations with phenols in the previous chapters (**39ai** and **39ag**). Aliphatic alkynes participate in the reaction showing higher regioisomeric ratios, all of them above 10:1 (**39ad** and **39ae**). Despite the lack of copper in the reaction, which might react with terminal alkynes, alkynes with a hydrogen substituent led to no conversion after 16h and the starting materials were mostly recovered (**39al**).



^a Reaction conditions: **39a** (0.33 mmol), **29** (1 equiv), $[\text{Cp}^*\text{RhCl}_2]$ (5 mol %), CsOAc (0.5 equiv), THF (2 mL). ^b Isolated yield. ^c Starting material was recovered.

Scheme 152. Scope of the alkynes.

Regarding the anilides, the reaction requires substitution at the internal position of the olefin since, when *o*-vinylanilide was submitted to the reaction conditions, no progress was observed and starting material was mostly recovered (**39bd**). Mechanistically interesting, when an isopropyl group is replacing the methyl of the alkene, no product is observed instead, we could isolate the isomerized (**42**) in a 47% while when the substituent is an aryl motif, regardless of its electronic nature, the naphthylamides are isolated in 66-90% yield (**39dd-39fd**). If there is a methyl at the terminal position of the alkene, whether *cis* or *trans* the reaction does not proceed at all and starting material is recovered (**39gd**). Same scenario is observed when 2-phenylnanilide is used. When the hydrogen at the *para* position of the amide is replaced by a methyl group, the resulting naphthylamide is isolated in a 72% yield (**39id**). Concerning the *para* position of the double bond, a methyl group affords a satisfactory yield of 59% (**39jd**) and the strongly electron-withdrawing trifluoromethyl also yields **39kd** in a 61% yield although the regiosomeric proportion drops to 5:1. In all of the cases 4-octyne was used as the coupling partner due to the easier identification of the products and the obtention of higher regiosomeric ratios.



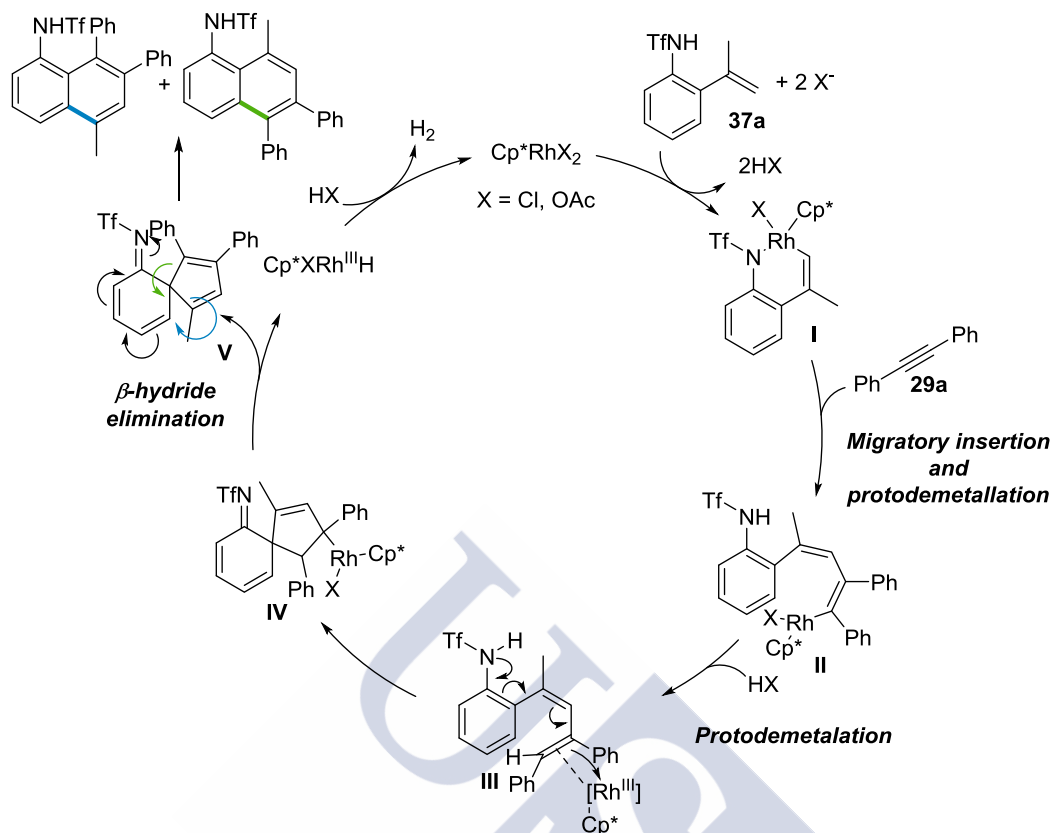
Scheme 153. Scope of the anilides.

3.4 Mechanistic hypothesis.

Although still more studies have to be made in order to establish a plausible mechanism, our current working model consists of the formation of the active catalytic species by cleavage of the rhodium dimer and ligand exchange with the acetates. Another ligand exchange with the NH group followed by the C-H activation would lead to metallacycle **I** which, upon migratory insertion of the alkyne and subsequent protodemettalation, delivers the open alkenylrhodium complex **II**. A second protodemettalation affords the diene **III** which can be coordinated to a Rh (III) species. This intermediate may undergo a nitrogen-mediated nucleophilic attack to the rhodium affording imine **IV** which, after β -hydride elimination yields spirocycle **V**. Rearrangement of this species might lead to both naphthylamines depending on which bond migrates¹⁷⁸. The rhodium hydride complex can now react with the acetic acid formed in the reaction releasing hydrogen and regenerating the catalyst.¹⁷⁹

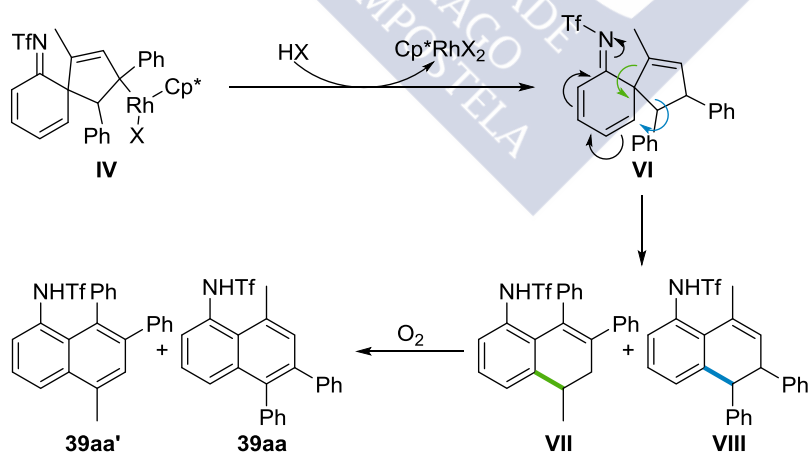
¹⁷⁸ A similar rearrangement has been described in a Palladium-mediated stoichiometric reaction regarding *N,N*-dimethylated *o*-phenylenanilines: Dupont, J.; Pfeffer, M.; Theurel, L.; Rotveel, M. A.; De Cian, A.; Fischer, J. *New J. Chem.* **1991**, *15*, 551.

¹⁷⁹ This protonation of hydrides is described for Manganese in He, R.; Huang, Z. T.; Zheng, Q. Y.; Wang, C. *Angew. Chemie. Int. Ed.* **2014**, *53*, 4950.



Scheme 154. Mechanistic hypothesis.

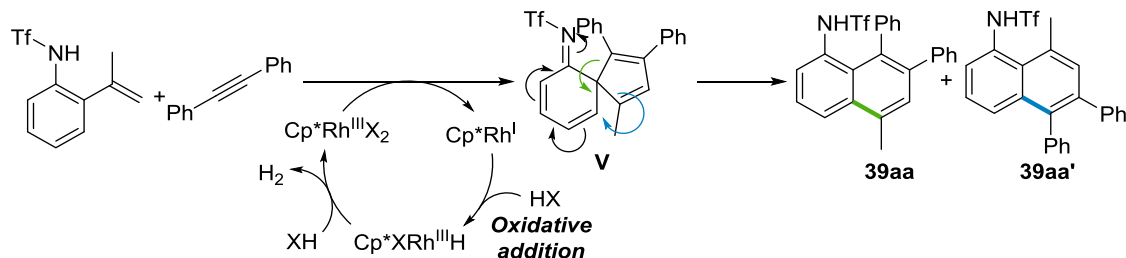
Other mechanisms could also be operating. Another possibility is the protodemetalation of spirocycle **IV** that may release the catalyst and dihydronaphthylamides **VI** and **VII** which, in presence of the oxygen during the workup, rapidly oxidize to the naphthylamides.



Scheme 155. Alternative mechanistic hypothesis.

A third possibility is a mechanism analogous to the one of the obtention of spirocycles with phenols (see in scheme 129 the previous chapter) leading directly to **V** which rearrangement affords the naphthylamines. The reduced complex could be regenerated via oxidative

addition to the acetic acid and protonation of the Rhodium hydride as seen in the first mechanism.



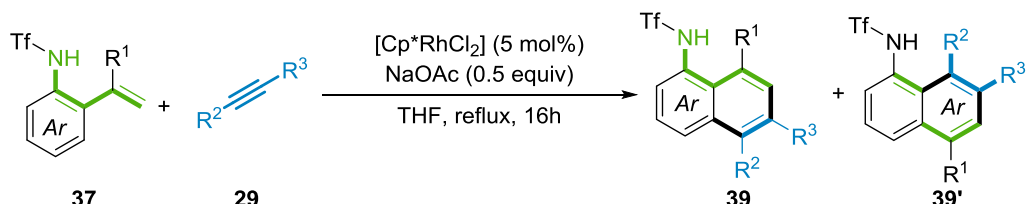
Scheme 156. Oxidation of $\text{Rh}(\text{I})$ by copper acetate.





4- Conclusions

In conclusion, we have developed an unprecedented Rh (III)-catalyzed (4+2) oxidative annulation between triflyl-protected *ortho*-alkenyl anilides to afford naphthylamines. The reaction requires appropriate substitution at the nitrogen and leads to the formation of different regioisomers arising from an apparent 1,2 migration of the alkenyl unit prior to the annulation.



We have also proven that this transformation occurs even in the absence of oxygen or copper salts and sodium acetate alone is able to accomplish this task. Finally, we have proposed different plausible mechanistic pathways for the reaction, although more experiments have to be done in order to distinguish among those possibilities.



CHAPTER VI: Experimental part.





1- General experimental procedures

Reactions were conducted in dry solvents under Argon atmosphere unless otherwise stated. Dry solvents were Aldrich and used without further purification. Dried acetonitrile was also from Aldrich and dried with a solvent system (MBraun, SPS 800 manual), [RhCp*Cl₂]₂ (99%) [12354-85-7] was purchased in Aldrich, and [Ru(p-cymene)Cl₂]₂ was purchased in TCI [52562-29-0] (>95%). All other chemicals were purchased in Aldrich and used without further purification.

The abbreviation "rt" refers to reactions carried out at a temperature between 21-25 °C. Reaction mixtures were stirred using Teflon-coated magnetic stir bars. High reaction temperatures were maintained using Thermowatch-controlled heating blocks. Thin-layer chromatography (TLC) was performed on silica gel plates and components were visualized by observation under UV light, and / or by treating the plates with p-anisaldehyde or cerium nitrate solutions, followed by heating. Flash chromatography was carried out on silica gel. Dryings were performed with anhydrous Na₂SO₄.

Concentration refers to the removal of volatile solvents via distillation using a Büchi rotary evaporator followed by high vacuum.

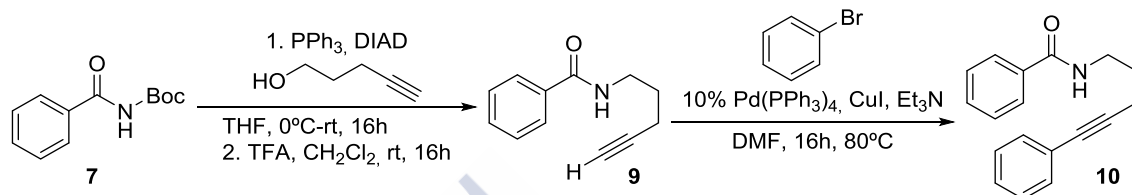
Unless otherwise noted, all Rhodium-catalyzed reactions were carried out without particular precautions to extrude moisture or oxygen.

¹H NMR (300MHz) spectra were recorded at room temperature on a Varian 300MHz spectrometer in CDCl₃ [using CHCl₃ (for 1H, δ = 7.26) as internal standard]. ¹³C NMR (75 MHz) spectra on a Varian spectrometer in CDCl₃ [using CDCl₃ (for 13C, δ = 77.160) as internal standard]. The following abbreviations were used to explain the multiplicities: s = singlet, d = doublet, t = triplet, q = quartet, m = multiplet, br s = broad singlet . Carbon types and structure assignments were determined from DEPT-NMR and two dimensional experiments (HMQC and HMBC, COSY and NOESY). NMR spectra were analyzed using MestReNova© NMR data processing software (www.mestrelab.com). Mass spectra were acquired using electronic impact (EI), chemical ionization (CI) and electrospray (ESI) and were recorded at the CACTUS facility of the University of Santiago de Compostela.



2- CHAPTER II: Intramolecular oxidative annulations of benzamides and acrylamides.

2.1 Procedure for the synthesis of alkynylbenzamides (10-10p), exemplified for 10.



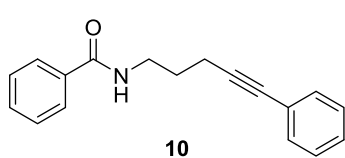
To a solution of *tert*-butyl benzoylcarbamate **7a** (4 g, 17.8 mmol), triphenylphosphine (5.60 g, 21.4 mmol) and 4-pentyn-1-ol (10.0 g, 202 mmol) in THF (90 mL) at 0 °C was added diisopropylazodicarboxylate (DIAD, 4.16 mL, 21.4 mmol) dropwise, very slowly. After complete addition, the yellow solution was stirred at r.t. overnight. The reaction was concentrated, water (40 mL) was added and the mixture was extracted with Et_2O (3x20 mL). The combined organic layers were dried over sodium sulfate and the solvent was evaporated *in vacuo* to afford a viscous oil that was purified by flash chromatography (hexanes:diethylether 1:3) to obtain the *tert*-butyl benzoyl(pent-4-yn-1-yl)carbamate (3.58 g, 70%).

To a solution of *tert*-butyl benzoyl(pent-4-yn-1-yl)carbamate (2.9 g, 10.1 mmol) in CH_2Cl_2 (40 mL) at 0 °C was added trifluoroacetic acid (0.78 mL, 1 eq) dropwise. After complete addition, the solution was stirred at r.t. overnight. Water (15 mL) was added and the mixture was extracted with CH_2Cl_2 (3x10 mL). The combined organic layers were dried over sodium sulfate and the solvent was evaporated *in vacuo* to afford a yellow oil that was purified by flash chromatography (hexanes:diethylether 1:1) to obtain the corresponding *N*-(pent-4-yn-1-yl)benzamide **9a** (1.10 g, 58%). Amorphous white solid. $^1\text{H NMR}$ (300 MHz, CDCl_3) δ 7.76 (dd, $J = 11.3, 4.3$ Hz, 2H), 7.52 – 7.30 (m, 3H), 6.91 (s, 1H), 3.51 (dd, $J = 12.8, 6.7$ Hz, 2H), 2.25 (td, $J = 6.9, 2.6$ Hz, 2H), 1.97 (dd, $J = 3.5, 1.8$ Hz, 1H), 1.90 – 1.73 (m, 2H). $^{13}\text{C NMR}$ (75 MHz, CDCl_3) δ 167.8 (C), 134.6 (C), 131.4 (CH), 128.5 (CH), 127.0 (CH), 83.7 (C), 69.2 (CH), 39.3 (CH₂), 28.1 (CH₂), 16.3 (CH₂).

To a solution of benzamide **9** (100 mg, 0.53 mmol), $\text{Pd}(\text{PPh}_3)_4$ (48 mg, 10 mol%) and CuI (10.17 mg, 10 mol%) in DMF (8 mL), bromobenzene (125 mg, 0.795 mmol) was added Et_3N (0.75 mL, 5.34 mmol). After complete addition, the solution was stirred at 80 °C overnight. The reaction mixture was diluted with EtOAc (30 mL) and washed with water (10 mL) and brine (10mL). The combined organic layers were dried over anhydrous sodium sulfate and the solvents were evaporated *in vacuo* to afford a yellow oil that was purified by flash

chromatography hexanes:ethyl acetate 1:3) to obtain the corresponding arene **10a** (112 mg, 80%).

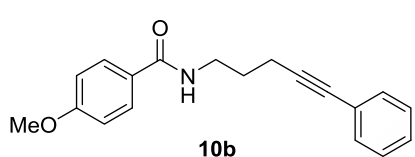
N-(5-Phenylpent-4-yn-1-yl)benzamide (10): white solid. ¹H NMR (300 MHz, CDCl₃) δ 7.86 –



7.60 (m, 2H), 7.51 – 7.13 (m, 8H), 6.53 (br s, 1H), 3.57 (dd, *J* = 12.6, 6.4 Hz, 2H), 2.48 (t, *J* = 6.7 Hz, 2H), 1.99 – 1.77 (m, 2H). ¹³C NMR (75 MHz, CDCl₃) δ 167.5 (C), 134.5 (C), 131.5 (CH), 131.3 (CH), 128.5 (CH), 128.2 (CH), 127.8 (CH), 126.8 (CH), 123.4 (C), 89.2 (C), 81.6 (C), 39.7 (CH₂), 28.2 (CH₂), 17.5 (CH₂). LRMS (*m/z*, *I*) 263 (87), 262 (43) 235 (27) HRMS calculated for C₁₈H₁₇NO 263.1310, found 263.1318.

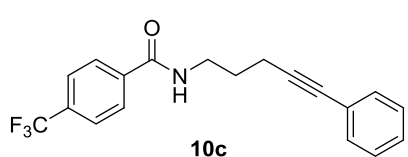
(87), 262 (43) 235 (27) HRMS calculated for C₁₈H₁₇NO 263.1310, found 263.1318.

4-Methoxy-N-(5-phenylpent-4-yn-1-yl)benzamide (10b): yellow solid. ¹H NMR (300 MHz, CDCl₃) δ 7.74 – 7.54 (m, 2H), 7.42 – 7.09 (m, 5H), 6.83 – 6.66 (m, 2H), 6.51 (br s, 1H), 3.73 (s, 3H), 3.53 (dt, *J* = 13.9, 6.9 Hz, 2H), 2.46 (t, *J* = 6.8 Hz, 2H), 1.92 – 1.80 (m, 2H). ¹³C NMR (75 MHz, CDCl₃) δ 167.2 (C), 162.1 (C), 131.7 (CH), 128.8 (CH), 128.4 (CH), 127.9 (CH), 126.9 (C), 123.6 (C), 113.72 (CH), 89.5 (C), 81.7 (C), 55.4 (CH₃), 39.8 (CH₂), 28.4 (CH₂), 17.6 (CH₂). LRMS (*m/z*, *I*) 293 (16), 292 (25), 291 (291), 277 (4).



113.72 (CH), 89.5 (C), 81.7 (C), 55.4 (CH₃), 39.8 (CH₂), 28.4 (CH₂), 17.6 (CH₂). LRMS (*m/z*, *I*) 293 (16), 292 (25), 291 (291), 277 (4).

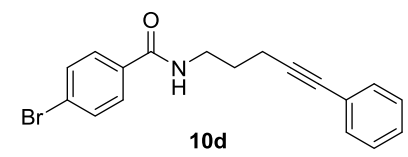
N-(5-Phenylpent-4-yn-1-yl)-4-(trifluoromethyl)benzamide (10c): yellow solid. ¹H NMR (300



MHz, CDCl₃) δ 7.82 (d, *J* = 8.6 Hz, 2H), 7.53 (d, *J* = 8.5 Hz, 2H), 7.40 – 7.22 (m, 5H), 6.90 (br s, 1H), 3.65 (dd, *J* = 12.5, 6.3 Hz, 2H), 2.55 (t, *J* = 6.7 Hz, 2H), 2.08 – 1.83 (m, 2H). ¹³C NMR (75 MHz, CDCl₃) δ 166.4 (C), 137.9 (C), 133.1 (q, *J* = 32.8 Hz, C), 131.6 (CH), 128.4 (CH), 128.1 (CH), 127.5 (CH),

125.6 (q, *J* = 3.5 Hz, CH), 123.4 (C), 120.1 (q, *J* = 272.4 Hz, C), 89.4 (C), 81.9 (C), 40.2 (CH₂), 28.1 (CH₂), 17.7 (CH₂). LRMS (*m/z*, *I*) 331 (74), 330 (27), 312 (13), 302 (23), 277 (15). HRMS calculated for C₁₉H₁₆NOF₃ 331.1184, found 331.1187

4-Bromo-N-(5-phenylpent-4-yn-1-yl)benzamide (10d): white solid. ¹H NMR (300 MHz, CDCl₃) δ 7.66 – 7.06 (m, 8H), 6.80 (br s, 1H), 3.53 (dd, *J* = 12.5, 6.3 Hz, 2H), 2.46 (t, *J* = 6.7 Hz, 2H), 2.03 – 1.64 (m, 2H).



¹³C NMR (75 MHz, CDCl₃) δ 166.7 (C), 133.5 (C), 131.7 (CH), 131.6 (CH), 128.6 (CH), 128.4 (CH), 128.0 (CH), 126.1 (C), 123.4 (C), 89.4 (C), 81.8 (C), 40.0 (CH₂), 28.2(CH₂), 17.6

(CH₂). LRMS (*m/z*, *I*) 341 (28), 313 (9). HRMS calculated for C₁₈H₁₆NOBr 341.0415, found 341.0428.

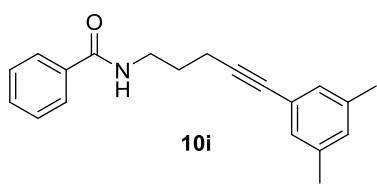
3-methyl-N-(5-phenylpent-4-yn-1-yl)benzamide (10e): white solid. **¹H NMR** (300 MHz, CDCl₃) δ 7.60 – 7.47 (m, 1H), 7.40 – 7.30 (m, J = 6.7, 3.1 Hz, 1H), 7.30 – 7.17 (m, 2H), 6.49 (s, 1H), 3.63 (dd, J = 12.6, 6.4 Hz, 1H), 2.54 (t, J = 6.8 Hz, 1H), 2.30 (s, 1H), 2.01 – 1.86 (m, J = 6.7 Hz, 1H). **¹³C NMR** (75 MHz, CDCl₃) δ 167.9 (C), 138.5 (C), 134.7 (C), 132.2 (CH), 131.7 (CH), 128.4 (CH), 128.4 (CH), 127.9 (CH), 127.7 (CH), 124.0 (CH), 123.6 (C), 89.4 (C), 81.7 (C), 39.8 (CH₂), 28.4 (CH₂), 21.3 (CH₃), 17.6 (CH₂).

3-methoxy-N-(5-phenylpent-4-yn-1-yl)benzamide (10f): white solid. **¹H NMR** (300 MHz, CDCl₃) δ 7.40 – 7.30 (m, 3H), 7.30 – 7.15 (m, 5H), 7.02 – 6.95 (m, 1H), 6.61 (s, 1H), 3.79 (s, 3H), 3.62 (dd, J = 12.6, 6.5 Hz, 2H), 2.53 (t, J = 6.8 Hz, 2H), 1.99 – 1.86 (m, 2H). **¹³C NMR** (75 MHz, CDCl₃) δ 167.6 (C), 159.9 (C), 136.2 (C), 131.7 (CH), 129.6 (CH), 128.3 (CH), 127.9 (CH), 123.6 (C), 118.7 (CH), 117.7 (CH), 112.4 (CH), 89.3 (C), 81.7 (C), 55.5 (CH₃), 39.8 (CH₂), 28.4 (CH₂), 17.5 (CH₂).

N-(5-Phenylpent-4-yn-1-yl)-1-naphthamide (10g): white solid. **¹H NMR** (300 MHz, CDCl₃) δ 8.34 – 8.13 (m, 1H), 7.90 – 7.69 (m, 2H), 7.61 – 7.11 (m, 9H), 6.60 (br s, 1H), 3.59 (dd, J = 12.6, 6.4 Hz, 2H), 2.50 (t, J = 6.9 Hz, 2H), 2.00 – 1.75 (m, 2H). **¹³C NMR** (75 MHz, CDCl₃) δ 170.1 (C), 134.9 (C), 134.0 (C), 131.9 (CH), 130.8 (CH), 130.5 (C), 128.7 (CH), 128.2 (CH), 127.4 (CH), 126.8 (CH), 125.8 (CH), 125.3 (CH), 125.1 (CH), 124.0 (C), 89.6 (C), 82.0 (C), 39.9 (CH₂), 28.8(CH₂), 17.8 (CH₂). **LRMS (m/z, I)** 313 (57), 312 (90), 285 (40).

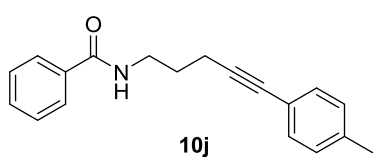
N-(5-(o-Tolyl)pent-4-yn-1-yl)benzamide (10h): brown oil. **¹H NMR** (300 MHz, CDCl₃) δ 7.77 – 7.52 (m, 2H), 7.48 – 6.89 (m, 8H), 6.53 (br s, 1H), 3.58 (dd, J = 12.5, 6.7 Hz, 2H), 2.61 – 2.40 (m, 2H), 2.32 (s, 3H), 1.97 – 1.77 (m 2H). **¹³C NMR** (75 MHz, CDCl₃) δ 167.7 (C), 140.1 (C), 134.6 (C), 132.0 (CH), 131.5 (CH), 129.5 (CH), 128.6 (CH), 127.9 (CH), 127.0 (CH), 125.6 (CH), 123.3 (C), 93.2 (C), 80.6 (C), 39.8 (CH₂), 28.6 (CH₂), 20.9 (CH₃), 17.7 (CH₂). **LRMS (m/z, I)** 277 (59), 259 (28). **HRMS** calculated for C₁₉H₁₉NO 277.1467, found 277.1455.

N-(5-(3,5-Dimethylphenyl)pent-4-yn-1-yl)benzamide (10i): brown solid. **¹H NMR** (300



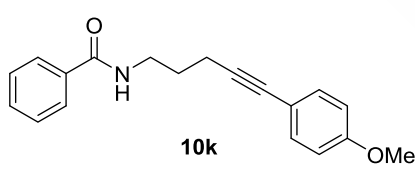
MHz, CDCl₃) δ 7.66 (dd, *J* = 7.9, 6.7 Hz, 2H), 7.42 – 7.32 (m, 1H), 7.31 – 7.20 (m, 2H), 6.92 (s, 2H), 6.84 (s, 1H), 6.59 (brs, 1H), 3.56 (dd, *J* = 12.6, 6.3 Hz, 2H), 2.46 (dd, *J* = 8.4, 5.0 Hz, 2H), 2.18 (s, 3H), 1.92 – 1.78 (m, 2H). **¹³C NMR** (75 MHz, CDCl₃) δ 168.0 (C), 138.3 (C), 135.1 (C), 131.8 (CH), 130.3 (CH), 129.8 (CH), 129.0 (CH), 127.4 (CH), 123.6 (C), 89.0 (C), 82.5 (C), 40.3 (CH₂), 28.8 (CH₃), 21.6 (CH₂), 18.1 (CH₂). **LRMS** (*m/z*, *I*) 291 (55), 263 (20). **HRMS** calculated for C₂₀H₂₁NO 291.1623, found 291.1622.

N-(5-(*p*-Tolyl)pent-4-yn-1-yl)benzamide (10j): brown solid. **¹H NMR** (300 MHz, CDCl₃) 7.66



(dd, *J* = 6.2, 5.2 Hz, 2H), 7.37 (dd, *J* = 10.6, 4.1 Hz, 1H), 7.31 – 7.16 (m, 4H), 7.00 (d, *J* = 8.0 Hz, 2H), 6.54 (brs, 1H), 3.56 (q, *J* = 6.3 Hz, 2H), 2.53 – 2.39 (m, 2H), 2.26 (s, 3H), 1.95 – 1.78 (m, 2H). **¹³C NMR** (75 MHz, CDCl₃) δ 168.1 (C), 138.4 (C), 135.1 (C), 132.0 (CH), 131.9 (CH), 129.6 (CH), 129.0 (CH), 127.4 (CH), 120.9 (C), 89.0 (C), 82.3 (C), 40.3 (CH₂), 28.8 (CH₂), 22.0 (CH₃), 18.0 (CH₂). **LRMS** (*m/z*, *I*) 277 (33), 262 (6) 249 (6) **HRMS** calculated for C₁₉H₁₉NO 277.1467, found 277.1455.

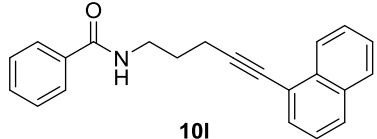
N-(5-(4-Methoxyphenyl)pent-4-yn-1-yl)benzamide (10k): brown solid. **¹H NMR** (300 MHz,



CDCl₃) δ 7.68 (dd, *J* = 8.3, 1.2 Hz, 2H), 7.47 – 7.11 (m, 5H), 6.82 – 6.67 (m, 2H), 6.56 (brs, 1H), 3.69 (d, *J* = 23.8 Hz, 3H), 3.55 (dt, *J* = 22.2, 10.9 Hz, 2H), 2.48 (dd, *J* = 12.6, 6.0 Hz, 2H), 2.03 – 1.77 (m, 2H). **¹³C NMR** (75 MHz, CDCl₃) δ 167.6 (C), 159.3 (C), 134.7 (C), 133.1 (CH), 131.7 (C), 131.5 (CH),

128.6 (CH), 127.0 (CH), 114.0 (CH), 87.8 (C), 81.5 (C), 55.4 (CH₃), 39.9 (CH₂), 28.4 (CH₂), 17.6 (CH₂). **LRMS** (*m/z*, *I*) 293 (45), 262 (6). **HRMS** calculated for C₁₉H₁₉NO₂ 293.1416, found 293.1420.

N-(5-(Naphthalen-1-yl)pent-4-yn-1-yl)benzamide (10l): brown solid. **¹H NMR** (300 MHz, CDCl₃) δ 8.24 (dd, *J* = 7.9, 1.1 Hz, 1H), 7.96 – 7.00 (m, 11H), 6.64 (brs, 1H), 3.72 – 3.46 (m, 2H),



2.56 (dt, *J* = 31.6, 6.8 Hz, 2H), 2.15 – 1.80 (m, 2H). **¹³C NMR** (75 MHz, CDCl₃) δ 167.7 (C), 134.5 (C), 133.4 (C), 133.2 (C), 131.4 (CH), 130.3 (CH), 128.5 (CH), 128.3 (CH), 127.0 (CH), 126.8 (CH), 126.5 (CH), 126.4 (CH), 126.2 (CH), 125.3 (CH), 121.2 (C),

94.4 (C), 79.7 (C), 39.9 (CH₂), 28.6(CH₂), 17.9(CH₂). **LRMS** (*m/z*, *I*) 313 (47), 262 (7). **HRMS** calculated for C₂₂H₁₉NO 313.1467, found 313.1470.

N-(5-(4-(Trifluoromethyl)phenyl)pent-4-yn-1-yl)benzamide (10m): white solid. **¹H NMR** (300 MHz, CDCl₃) δ 7.87 – 7.04 (m, 9H), 6.85 (s, 1H), 3.52 (dd, J = 12.7, 6.7 Hz, 2H), 2.44 (t, J = 6.9 Hz, 2H), 2.00 – 1.70 (m, 2H). **¹³C NMR** (75 MHz, CDCl₃) δ 167.8 (C), 134.5 (C), 131.8 (CH), 131.4 (CH), 129.4 (q, J = 32.6 Hz, C), 128.5 (CH), 127.5 (C), 127.0 (CH), 125.2 (q, J = 3.8 Hz, CH), 124.0 (q, J = 272.3 Hz, C), 92.1 (C), 80.3 (C), 39.6 (CH₂), 28.3 (CH₂), 17.4 (CH₂). **LRMS** (*m/z*, *I*) 331 (44), 330 (33), 303 (8), 262 (9). **HRMS** calculated for C₁₉H₁₆NOF₃ 331.1184, found 331.1182.

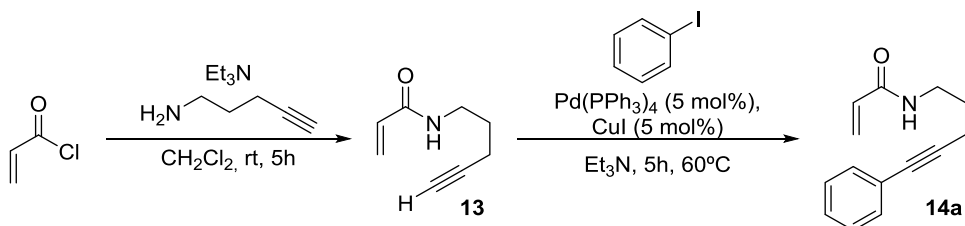
N-(Hex-4-yn-1-yl)benzamide (10o)¹⁸⁰: white solid. **¹H NMR** (300 MHz, CDCl₃) δ 7.88 – 7.65 (m, 2H), 7.55 – 7.30 (m, 3H), 6.55 (d, J = 35.7 Hz, 1H), 3.56 (dd, J = 12.6, 6.5 Hz, 2H), 2.37 – 2.13 (m, 2H), 1.85–1.70 (m, 5H). **¹³C NMR** (75 MHz, CDCl₃) δ 167.5(C), 134.7(C), 131.3 (CH), 128.5 (CH), 126.9 (CH), 78.4 (C), 76.6 (C), 39.7 (CH₂), 28.3 (CH₃), 16.7 (CH₂), 3.5(CH₂). **LRMS** (*m/z*, *I*) 201 (24), 200 (93) 173 (38). **HRMS** calculated for C₁₃H₁₅NO 201.1154, found 201.1114.

N-(6-Phenylhex-5-yn-1-yl)benzamide (10p): white solid. **¹H NMR** (300 MHz, CDCl₃) δ 7.76 – 7.61 (m, 2H), 7.53 – 7.01 (m, 8H), 6.48 (br s, 1H), 3.39 (dt, *J* = 6.7, 3.8 Hz, 2H), 2.35 (dd, *J* = 9.3, 4.2 Hz, 2H), 1.80 – 1.44 (m, 4H). **¹³C NMR** (75 MHz, CDCl₃) δ 167.7 (C), 134.8 (C), 131.7 (CH), 131.5 (CH), 128.7 (CH), 128.3 (CH), 127.8 (CH), 127.0 (CH), 123.9 (C), 89.8 (C), 81.3 (C), 39.7 (CH₂), 29.0 (CH₂), 26.2 (CH₂), 19.2 (CH₂). **LRMS** (*m/z*, *I*) 277 (32), 261 (50), 249 (12). **HRMS** calculated for C₁₉H₁₇NO 275.1310, found 275.1312

N-(7-Phenylhept-6-yn-1-yl)benzamide (10q): yellow oil. **¹H NMR** (300 MHz, CDCl₃) δ 7.79 – 7.54 (m, 2H), 7.47 – 7.22 (m, 5H), 7.23 – 7.12 (m, 3H), 6.31 (br s, 1H), 3.47 – 3.26 (m, 2H), 2.34 (t, *J* = 6.7 Hz, 2H), 1.70 – 1.36 (m, 6H). **¹³C NMR** (75 MHz, CDCl₃) δ 167.7 (C), 134.9 (C), 131.6 (CH), 131.4 (CH), 128.6 (CH), 128.3 (CH), 127.6 (CH), 126.9 (CH), 124.0 (C), 90.0 (C), 80.1(C), 40.0 (CH₂), 29.3 (CH₂), 28.4 (CH₂), 26.2 (CH₂), 19.4 (CH₂). **LRMS** (*m/z*, *I*) 291 (36), 277 (16). **HRMS** calculated for C₂₀H₁₉NO 291.1623, found 291.1624.

¹⁸⁰ This substrate was prepared using 4-hexyn-1-ol as starting material for the Mitsunobu reaction following the general procedure for the synthesis of benzamides.

2.2 Procedure for the synthesis of alkynylbenzamides (**14a-14d**), exemplified for **14a**.



Acryloyl chloride (0.2 mL, 2.4 mmol) was stirred in CH₂Cl₂ (10 mL) with triethylamine (0.46 mL, 0.36 mmol) at rt for 10 min. Addition of commercial available 4-pentynamine (200 mg, 2.40 mmol) was followed by stirring for 5 h. The CH₂Cl₂ was removed in *vacuo*, and the remaining residue was dissolved in ethyl acetate. The solution was washed with 10% HCl and brine, dried over magnesium sulfate and filtered. The solvent was removed and the product was purified by column chromatography (hexanes:EtOAc; 1:1) to afford *N*-(pent-4-yn-1-yl)acrylamide (**13**) (208 mg, 63%).

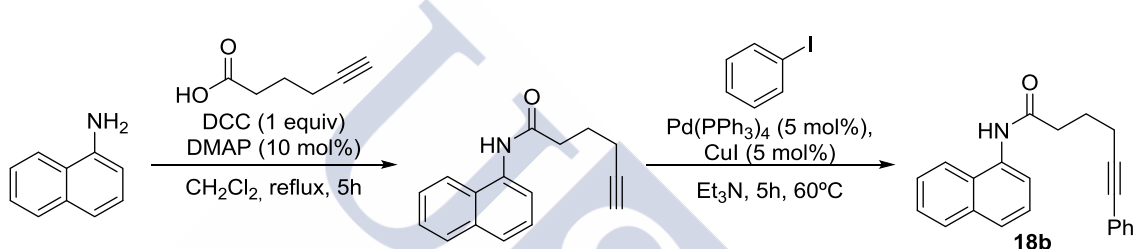
In a Schlenk flask containing Pd(PPh₃)₄ (87 mg, 5 mol %) and CuI (14 mg, 5 mol%) at rt, *N*-(pent-4-yn-1-yl)acrylamide (206 mg, 1.5 mmol) and Et₃N (10 mL) were added with stirring. Then iodobenzene (0.16 mL, 1 equiv.) was added and the mixture was heated to 60 °C. After 5 hours the solvent was removed and the product was purified by column chromatography (hexanes:ethyl acetate; 1:1) to afford the product **14a** (262 mg, 82%).

N-(5-Phenylpent-4-yn-1-yl)acrylamide (14a): yellow oil. ¹H NMR (300 MHz, CDCl₃) δ 7.42 – 7.21 (m, 5H), 6.48 (s, 1H), 6.25 (d, *J* = 17.0 Hz, 1H), 6.11 (dd, *J* = 17.0, 10 Hz, 1H), 5.57 (d, *J* = 10.0 Hz, 1H), 3.47 (q, *J* = 6.4 Hz, 2H), 2.45 (t, *J* = 6.9 Hz, 2H), 1.83 (m, 2H). ¹³C NMR (75 MHz, CDCl₃) δ 165.7 (C), 131.4 (CH), 130.8 (CH), 128.1 (CH), 127.6 (CH), 126.1 (CH₂), 123.5 (C), 88.9 (C), 81.3 (C), 38.8 (CH₂), 28.2 (CH₂), 17.0 (CH₂). LRMS (*m/z*, *I*) 157 (50), 140 (69).

N-(5-Phenylpent-4-yn-1-yl)methacrylamide (14b): yellow solid ¹H NMR (300 MHz, CDCl₃) δ 7.44 – 7.34 (m, 2H), 7.33 – 7.22 (m, 3H), 6.14 (s, 1H), 5.71 – 5.64 (m, 1H), 5.33 – 5.26 (m, 1H), 3.49 (dd, *J* = 12.7, 6.7 Hz, 2H), 2.49 (t, *J* = 6.9 Hz, 2H), 1.99 – 1.92 (m, 3H), 1.86 (p, *J* = 6.9 Hz, 2H). ¹³C NMR (75 MHz, CDCl₃) δ 168.5 (C), 140.1 (C), 131.5 (CH), 128.2 (CH), 127.8 (CH), 123.5 (C), 119.3 (CH₂), 89.0 (C), 81.5 (C), 39.1 (CH₂), 28.2 (CH₂), 18.6 (CH₃), 17.3 (CH₂). LRMS (*m/z*, *I*) 212 (7), 199 (40). HRMS calculated for C₁₅H₁₇NO 227.1310, found 227.1312.

N-(5-Phenylpent-4-yn-1-yl)cyclohex-1-enecarboxamide (14d): yellow oil. **^1H NMR** (300 MHz, CDCl_3) δ 7.41 – 7.34 (m, 2H), 7.31 – 7.24 (m, 3H), 6.66 – 6.54 (m, 1H), 6.03 (s, 1H), 3.49 (dd, J = 12.6, 6.5 Hz, 2H), 2.49 (t, J = 6.8 Hz, 2H), 2.23 – 2.16 (m, 2H), 2.08 (dd, J = 6.1, 2.4 Hz, 2H), 1.85 (p, J = 6.7 Hz, 2H), 1.67 – 1.50 (m, 4H). **^{13}C NMR** (75 MHz, CDCl_3) δ 168.6 (C), 133.3 (CH), 133.1 (C), 131.5 (CH), 128.2 (CH), 127.7 (CH), 123.5 (C), 89.2 (C), 81.5 (C), 39.1 (CH₂), 28.3 (CH₂), 25.3 (CH₂), 24.3 (CH₂), 22.1 (CH₂), 21.5 (CH₂), 17.4 (CH₂). **LRMS** (m/z , *I*) 250 (11), 239 (30).

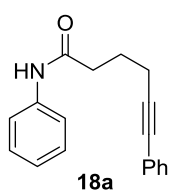
2.3 Procedure for synthesis of hexynamides **18a** and **18b**, exemplified for **18b**.



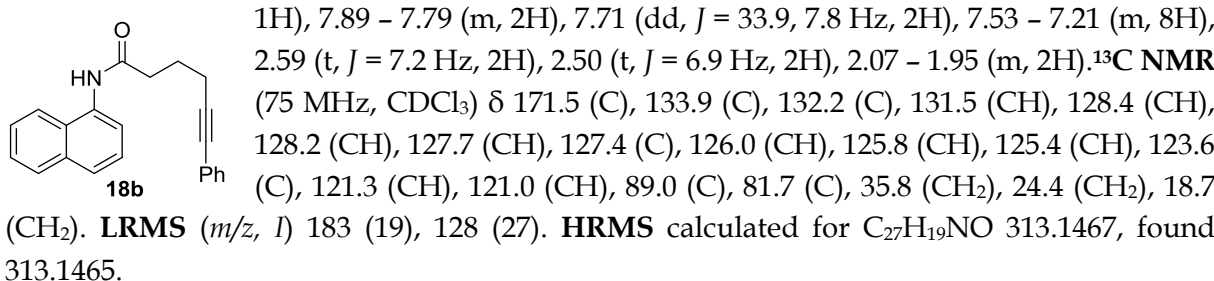
To a solution of hex-5-ynoic acid (1.1 mL, 10 mmol) in CH_2Cl_2 (50 mL) at room temperature under argon were added dimethylaminopyridine (DMAP, 12 mg, 0.10 mmol), *N,N'*-Dicyclohexylcarbodiimide (DCC, 2.06 g, 10 mmol) and naphthalen-1-amine (1.43 g, 10.0 mmol). The mixture was stirred 10 min. at this temperature and then heated at reflux for 5 hours. CH_2Cl_2 (20 ml) was added and the precipitate filtered off. The resulting homogeneous solution was washed with 10% HCl (20 ml) and saturated NaHCO_3 (20 ml). The solvent was evaporated and the crude product purified by flash chromatography (Hexanes:EtOAc; 3:1) to give N-(naphthalen-1-yl)hex-5-ynamide (1.28 g, 54 %) as a white solid.

In a Schlenk flask containing $\text{Pd}(\text{PPh}_3)_4$ (232 mg, 5 mol %) and CuI (37 mg, 5 mol %), N-(naphthalen-1-yl)hex-5-ynamide (744 mg, 4 mmol) and Et_3N (20 mL) were stirred at room temperature. Then iodobenzene (0.43 mL, 1 equiv.) was added and the mixture was heated to 60 °C. After 5 hours the solvent was removed and the crude product was purified by column chromatography (hexanes:diethylether; 1:1) to afford the product **18b** (511 mg, 59%).

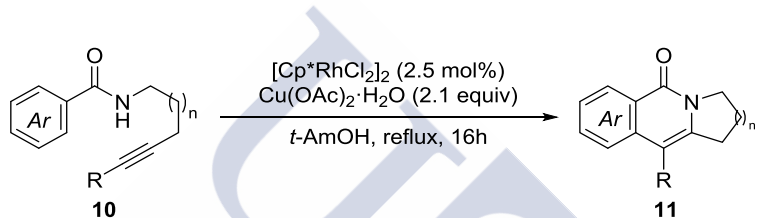
N,6-Diphenylhex-5-ynamide (18a): **^1H NMR** (300 MHz, CDCl_3) δ 7.67 (s, 1H), 7.60 – 7.21 (m, 9H), 7.16 – 6.96 (m, 1H), 2.68 – 2.41 (m, 4H), 2.09 – 1.95 (m, 2H). **^{13}C NMR** (75 MHz, CDCl_3) δ 170.8 (C), 137.9 (C), 131.5 (CH), 128.9 (CH), 128.2 (CH), 127.7 (CH), 124.1 (CH), 123.6 (C), 119.9 (CH), 88.9 (C), 81.6 (C), 36.2(CH₂), 24.2 (CH₂), 18.8 (CH₂). **LRMS** (m/z , *I*) 220 (18), 159 (34). **HRMS** calculated for $\text{C}_{18}\text{H}_{17}\text{NO}$ 263.1310, found 263.1309.



N-(Naphthalen-1-yl)-6-phenylhex-5-ynameide (18b): ¹H NMR (300 MHz, CDCl₃) δ 8.04 (s,

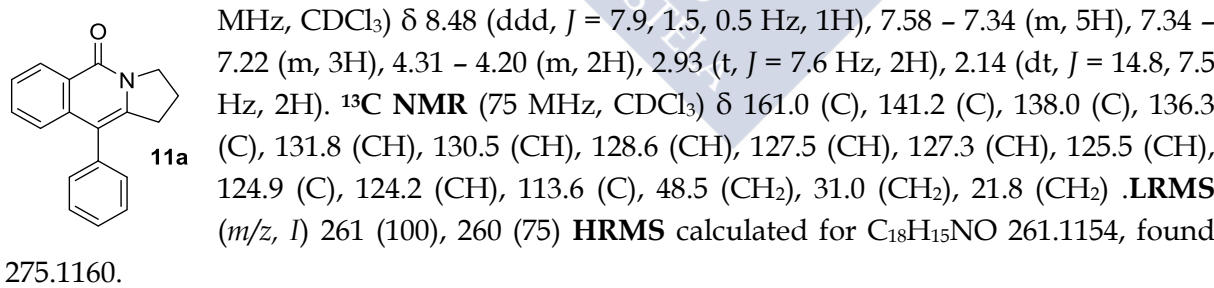


2.4 Procedure for catalytic reactions of alkynylbenzamides 11a-11q.

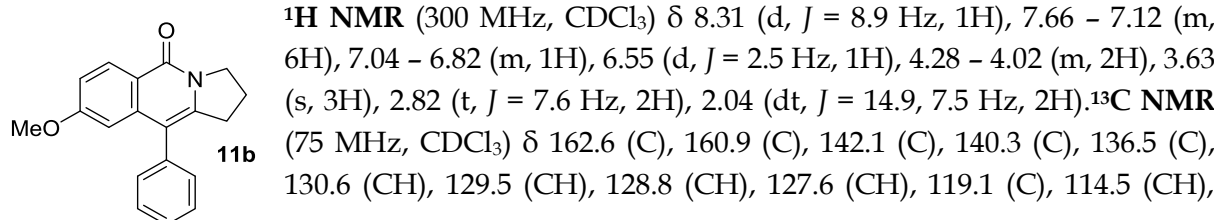


In a Schlenk flask equipped with a stir bar were added **10** (0.25 mmol), [Cp*RhCl₂]₂ (3.9 mg, 2.5% mol) and Cu(OAc)₂ (91 mg, 0.52 mmol) without any particular precautions to extrude oxygen or moisture. *t*-AmOH (2.0 mL) was then added and the flask sealed and placed in a pre-heated (110 °C) block. The reaction was stirred for 16 hours, cooled to room temperature and checked by TLC. The solvent was removed *in vacuo* and the remaining residue was purified by flash column chromatography on silica gel (hexanes:ethyl acetate) to afford the corresponding product **11**.

10-Phenyl-2,3-dihydropyrrolo[1,2-b]isoquinolin-5(1H)-one (11a): white solid. ¹H NMR (300

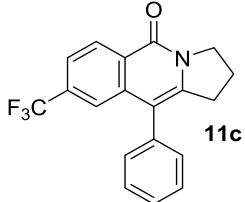


8-Methoxy-10-phenyl-2,3-dihydropyrrolo[1,2-b]isoquinolin-5(1H)-one (11b): brown solid.

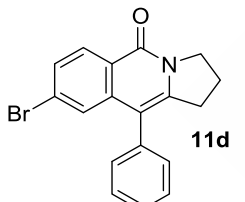


113.4 (C), 106.0 (CH), 55.3 (CH₃), 48.4 (CH₂), 31.2 (CH₂), 21.9 (CH₂). **LRMS** (*m/z*, *I*) 291 (100), 277 (30). **LRMS** (*m/z*, *I*) 341 (28), 313 (9), 212 (38). **HRMS** calculated for C₁₉H₁₇NO₂ 291.1259, found 291.1266

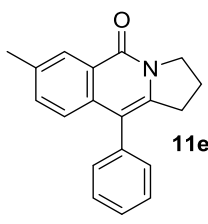
10-Phenyl-8-(trifluoromethyl)-2,3-dihydropyrrolo[1,2-b]isoquinolin-5(1H)-one (11c): green solid. **¹H NMR** (300 MHz, CDCl₃) δ 8.52 (d, *J* = 8.4 Hz, 1H), 7.63 – 7.31 (m, 5H), 7.31 – 7.15 (m, 2H), 4.23 (t, *J* = 7.2 Hz, 2H), 2.89 (t, *J* = 7.6 Hz, 2H), 2.25 – 2.03 (m, 2H). **¹³C NMR** (75 MHz, CDCl₃) δ 160.3 (C), 143.2 (C), 138.1 (C), 135.3 (C), 133.53 (q, *J* = 32.1 Hz, C), 130.4 (CH), 129.1 (CH), 128.6 (CH), 128.1 (CH), 127.0 (C), 123.9 (q, *J* = 273.0 Hz, C), 121.6 (q, *J* = 3.4 Hz, CH), 113.6 (C), 48.8 (CH₂), 31.3 (CH₂), 21.8 (CH₂). **LRMS** (*m/z*, *I*) 329 ([M] 100), 328 (38) **HRMS** calculated for C₁₉H₁₄NOF₃ 329.1027, found 329.1019.



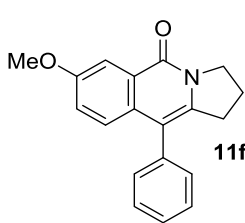
8-Bromo-10-phenyl-2,3-dihydropyrrolo[1,2-b]isoquinolin-5(1H)-one (11d): green solid. **¹H NMR** (300 MHz, CDCl₃) δ 8.23 (d, *J* = 8.6 Hz, 1H), 7.32 (ddd, *J* = 46.4, 25.7, 6.7 Hz, 7H), 4.16 (t, *J* = 7.2 Hz, 2H), 2.84 (t, *J* = 7.6 Hz, 2H), 2.29 – 1.92 (m, 2H). **¹³C NMR** (75 MHz, CDCl₃) δ 160.6 (C), 143.0 (C), 139.7 (C), 135.6 (C), 130.5 (CH), 129.3 (CH), 129.0 (CH), 128.9 (CH), 127.9 (CH), 127.4 (C), 126.8 (CH), 123.7 (C), 112.8 (C), 48.7 (CH₂), 31.3 (CH₂), 21.8 (CH₂). **LRMS** (*m/z*, *I*) 341 (28), 313 (9), 212 (38) **HRMS** calculated for C₁₈H₁₄NOBr 339.0259, found 339.0259.



7-methyl-10-phenyl-2,3-dihydropyrrolo[1,2-b]isoquinolin-5(1H)-one (11e): yellow solid. **¹H NMR** (300 MHz, CDCl₃) δ 8.28 (s, 1H), 7.53 – 7.22 (m, 6H), 7.18 (d, *J* = 8.3 Hz, 1H), 4.30 – 4.22 (m, 2H), 2.92 (t, *J* = 7.6 Hz, 2H), 2.46 (s, 3H), 2.20 – 2.07 (m, 2H). **¹³C NMR** (75 MHz, CDCl₃) δ 161.1 (C), 140.4 (C), 136.6 (C), 135.9 (C), 135.7 (C), 133.5 (CH), 130.7 (CH), 128.8 (CH), 127.5 (CH), 127.1 (CH), 125.0 (C), 124.3 (CH), 113.7 (CH), 48.6 (CH₂), 31.03 (CH₂), 22.1 (CH₂), 21.3 (CH₃).

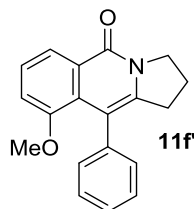


7-methoxy-10-phenyl-2,3-dihydropyrrolo[1,2-b]isoquinolin-5(1H)-one (11f): yellow solid.



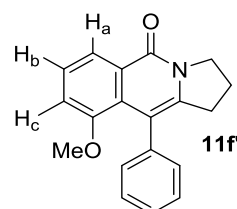
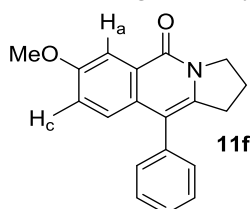
¹H NMR (300 MHz, CDCl₃) δ 7.88 (d, *J* = 2.7 Hz, 1H), 7.58 – 7.33 (m, 3H), 7.33 – 7.10 (m, 4H), 4.32 – 4.23 (m, 2H), 3.93 (s, 3H), 2.92 (t, *J* = 7.6 Hz, 2H), 2.21 – 2.09 (m, 2H). **¹³C NMR** (75 MHz, CDCl₃) δ 160.7 (C), 157.9 (C), 138.8 (C), 136.4 (C), 132.2 (C), 130.5 (CH), 128.6 (CH), 127.4 (C), 126.1 (C), 125.9 (CH), 122.3 (CH), 113.7 (C), 107.1 (CH), 55.6 (CH₃), 48.6 (CH₂), 30.7 (CH₂), 22.0 (CH₂).

9-methoxy-10-phenyl-2,3-dihydropyrrolo[1,2-b]isoquinolin-5(1H)-one (11f'): yellow solid.



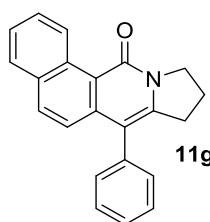
¹H NMR (300 MHz, CDCl₃) δ 8.13 (dd, *J* = 8.1, 1.0 Hz, 1H), 7.47 – 7.12 (m, 6H), 6.97 (dd, *J* = 7.8, 0.7 Hz, 1H), 4.37 – 4.11 (m, 2H), 3.35 (s, 3H), 2.79 (t, *J* = 7.7 Hz, 2H), 2.22 – 1.98 (m, 2H). ¹³C NMR (75 MHz, CDCl₃) δ 160.8 (C), 155.9 (C), 141.9 (C), 141.0 (C), 129.5 (CH), 128.5 (C), 127.5 (CH), 126.9 (C), 126.3 (CH), 126.2 (CH), 120.0 (CH), 114.1 (CH), 112.1 (C), 55.9 (CH₃), 48.9 (CH₂), 31.6 (CH₂), 21.7 (CH₂).

Assignment of regioisomers by ¹H-NMR



The two regioisomers were assigned based on the coupling constants. As expected, in the ¹H-NMR spectrum of 11f, H_a appears as a doublet (d) with a small *J*_{ac} = 2.7 Hz characteristic of this long distant couplings. Meanwhile, in the ¹H-NMR spectrum of 11f', H_a is a double of doublets (dd) with a *J*_{ab} = 8.1 Hz and a small *J*_{ac} = 1 Hz, which are also characteristic of these couplings.

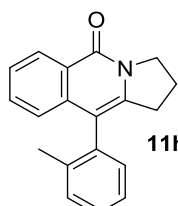
7-Phenyl-9,10-dihydrobenzo[h]pyrrolo[1,2-b]isoquinolin-12(8H)-one (11g): yellow solid. ¹H



¹H NMR (300 MHz, CDCl₃) δ 10.25 (d, *J* = 8.7 Hz, 1H), 8.02 – 6.98 (m, 10H), 4.44 – 4.13 (m, 2H), 2.84 (td, *J* = 7.7, 2.5 Hz, 2H), 2.25 – 1.88 (m, 2H). ¹³C NMR (75 MHz, CDCl₃) δ 161.6 (C), 143.2 (C), 139.5 (C), 136.8 (C), 133.1 (CH), 132.3 (C), 131.7 (C), 130.9 (CH), 128.8 (CH), 128.2 (CH), 128.0 (CH), 127.6 (CH), 127.4 (CH), 126.0 (CH), 122.8 (CH), 117.9 (C), 114.2 (C), 49.5 (CH₂), 31.6 (CH₂), 21.4 (CH₂). LRMS (*m/z*, *I*) 313(57), 312 (89), 285 (40)

HRMS calculated for C₂₂H₁₇NO₃ 311.1309, found 311.1310

10-(*o*-Tolyl)-2,3-dihydropyrrolo[1,2-b]isoquinolin-5(1H)-one (11h): pale yellow solid. ¹H



¹H NMR (300 MHz, CDCl₃) δ 8.54 – 8.38 (m, 1H), 7.71 – 7.20 (m, 5H), 7.16 (d, *J* = 7.0 Hz, 1H), 6.99 (dd, *J* = 8.1, 0.9 Hz, 1H), 4.38 – 4.17 (m, 2H), 2.98 – 2.60 (m, 2H), 2.28 – 2.06 (m, 2H), 2.04 (s, 3H). ¹³C NMR (75 MHz, CDCl₃) δ 161.4 (C), 141.2 (C), 138.1 (C), 137.8 (C), 135.6 (C), 132.1 (CH), 131.0 (CH), 130.4 (CH), 128.2 (CH), 127.6 (CH), 126.4 (CH), 125.7 (CH), 125.0 (C), 124.2 (CH), 113.0 (C), 48.6 (CH₂), 30.8 (CH₂), 21.9 (CH₂), 19.8 (CH₃). LRMS (*m/z*, *I*) 275 (100), 260 (3), 246 (7). HRMS calculated for C₁₉H₁₇NO₂ 275.1310, found 275.1316.

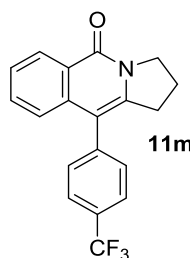
10-(3,5-Dimethylphenyl)-2,3-dihydropyrrolo[1,2-b]isoquinolin-5(1H)-one (11i): yellow solid. **¹H NMR** (300 MHz, CDCl₃) δ 8.40 (d, *J* = 8.0 Hz, 1H), 7.72 – 7.11 (m, 3H), 6.93 (d, *J* = 21.7 Hz, 1H), 6.84 (s, 2H), 4.35 – 4.08 (m, 2H), 2.87 (t, *J* = 7.6 Hz, 2H), 2.54 – 2.17 (m, 6H), 2.07 (dt, *J* = 15.2, 7.5 Hz, 2H). **¹³C NMR** (75 MHz, CDCl₃) δ 161.2 (C), 141.1 (C), 138.3 (2xC), 136.2 (C), 131.9 (CH), 130.7 (C), 129.2 (CH), 128.3 (2xCH), 127.4 (CH), 125.6 (CH), 125.0 (C), 124.5 (CH), 114.1 (C), 48.6 (CH₂), 31.2 (CH₂), 22.0 (CH₂), 21.5 (CH₃). **LRMS** (*m/z*, *I*) 289 (100), 274 (7). **HRMS** calculated for C₂₀H₁₉NO₂ 289.1467, found 289.1467.

10-(Naphthalen-1-yl)-2,3-dihydropyrrolo[1,2-b]isoquinolin-5(1H)-one (11j): brown oil. **¹H NMR** (300 MHz, CDCl₃) δ 8.58 – 8.47 (m, 1H), 7.95 (d, *J* = 7.8 Hz, 2H), 7.63 – 7.32 (m, 7H), 6.98 – 6.88 (m, 1H), 4.42 – 4.24 (m, 2H), 2.94 – 2.78 (m, 1H), 2.63 (ddd, *J* = 17.0, 8.2, 6.8 Hz, 1H), 2.23 – 2.03 (m, 2H). **¹³C NMR** (75 MHz, CDCl₃) δ 161.9 (C), 142.8 (C), 139.2 (C), 134.4 (C), 134.2 (C), 133.2 (C), 132.5 (CH), 129.2 (CH), 129.0 (CH), 128.9 (CH), 127.9 (CH), 126.9 (CH), 126.6 (CH), 126.3 (CH), 126.2 (CH), 126.1 (CH), 125.3 (C), 125.1 (CH), 111.9 (C), 49.1 (CH₂), 31.3 (CH₂), 22.2 (CH₂). **LRMS** (*m/z*, *I*) 311 (100) 282 (5) **HRMS** calculated for C₂₂H₁₇NO₃ 311.1310, found 275.1310

10-(*p*-Tolyl)-2,3-dihydropyrrolo[1,2-b]isoquinolin-5(1H)-one (11k): yellow solid. **¹H NMR** (300 MHz, CDCl₃) δ 8.39 (d, *J* = 7.9 Hz, 1H), 7.48 – 7.27 (m, 3H), 7.21 (dd, *J* = 8.1, 4.3 Hz, 2H), 7.11 (d, *J* = 7.8 Hz, 2H), 4.19 (t, *J* = 7.2 Hz, 2H), 2.85 (t, *J* = 7.6 Hz, 2H), 2.35 (s, 3H), 2.13–1.98 (m 2H). **¹³C NMR** (75 MHz, CDCl₃) δ 161.2 (C), 141.3 (C), 138.4 (C), 137.3 (C), 133.4 (C), 131.9 (CH), 130.5 (CH), 129.5 (CH), 127.5 (CH), 125.6 (CH), 125.1 (C), 124.4 (CH), 113.8 (C), 48.6 (CH₂), 31.2 (CH₂), 22.0 (CH₂), 21.4 (CH₃). **LRMS** (*m/z*, *I*) 275 (100), 261 (24) **HRMS** calculated for C₁₉H₁₇NO₂ 275.1310, found 275.1304.

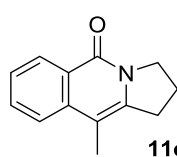
10-(4-Methoxyphenyl)-2,3-dihydropyrrolo[1,2-b]isoquinolin-5(1H)-one (11l): yellow oil. **¹H NMR** (300 MHz, CDCl₃) δ 8.40 (dd, *J* = 8.0, 1.4 Hz, 1H), 7.50 – 7.09 (m, 5H), 7.03 – 6.88 (m, 2H), 4.29 – 4.12 (m, 2H), 3.80 (s, 3H), 2.86 (t, *J* = 7.6 Hz, 2H), 2.07 (dt, *J* = 15.3, 7.6 Hz, 2H). **¹³C NMR** (75 MHz, CDCl₃) δ 161.2 (C), 159.1 (C), 141.5 (C), 138.5 (C), 131.9 (CH), 131.7 (CH), 128.5 (C), 127.5 (CH), 125.6 (CH), 125.0 (C), 124.4 (CH), 114.2 (CH), 113.42 (C), 55.4 (CH₃), 48.6 (CH₂), 31.2 (CH₂), 22.0 (CH₂). **LRMS** (*m/z*, *I*) 275 (100), 261 (24) **HRMS** calculated for C₁₉H₁₇NO₂ 291.1250, found 291.1260.

10-(4-(Trifluoromethyl)phenyl)-2,3-dihydropyrrolo[1,2-b]isoquinolin-5(1H)-one (11m):



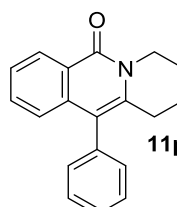
yellow solid. ¹H NMR (300 MHz, CDCl₃) δ 8.41 (dd, *J* = 8.0, 1.3 Hz, 1H), 7.67 (d, *J* = 8.2 Hz, 2H), 7.51 – 7.32 (m, 4H), 7.13 (d, *J* = 8.0 Hz, 1H), 4.24 – 4.16 (m, 2H), 2.85 (t, *J* = 7.6 Hz, 2H), 2.17 – 2.03 (m, 2H). ¹³C NMR (75 MHz, CDCl₃) δ 161.1 (C), 141.8 (C), 140.4 (C), 137.6 (C), 132.2 (CH), 131.2 (2xCH), 129.9 (q, *J* = 33.0 Hz) (C), 127.7 (CH), 126.0 (CH), 125.8 (q, *J* = 3.6 Hz) (2xCH), 125.1 (C), 120.7 (q, *J* = 271.7 Hz) (C), 112.4 (C), 48.7 (CH₂), 31.2 (CH₂), 22.0 (CH₂). LRMS (*m/z*, *I*) 329 (100), 328 (48), 310 (7) HRMS calculated for C₁₉H₁₄NOF₃ 329.1027, found 329.1028.

10-methyl-2,3-dihydropyrrolo[1,2-b]isoquinolin-5(1H)-one (11o): white solid ¹H NMR (300



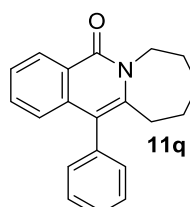
MHz, CDCl₃) δ 8.37 (d, *J* = 8.0 Hz, 1H), 7.57 (ddd, *J* = 12.8, 9.8, 4.7 Hz, 2H), 7.45 – 7.28 (m, 1H), 4.26 – 4.04 (m, 2H), 3.03 (t, *J* = 7.6 Hz, 2H), 2.41 – 2.02 (m, 5H). ¹³C NMR (75 MHz, CDCl₃) δ 161.5 (C), 140.6 (C), 138.9 (C), 132.4 (CH), 128.1 (CH), 125.9 (CH), 125.7 (C), 122.9 (CH), 106.2 (C), 48.9 (CH₂), 30.7 (CH₂), 22.1 (CH₂), 13.9 (CH₃). LRMS (*m/z*, *I*) 199 (100), 184 (8), 170 (9) HRMS calculated for C₁₃H₁₃NO 199.0097, found 199.0098.

11-Phenyl-3,4-dihydro-1H-pyrido[1,2-b]isoquinolin-6(2H)-one (11p): orange solid ¹H NMR



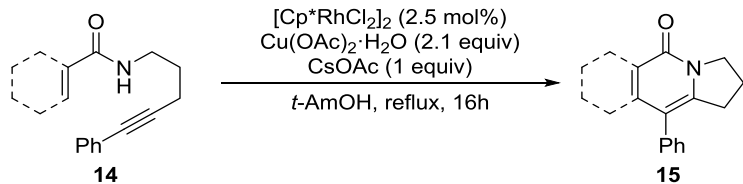
(300 MHz, CDCl₃) δ 8.47 (dd, *J* = 8.0, 1.4 Hz, 1H), 7.78 – 6.78 (m, 8H), 4.40 – 4.04 (m, 2H), 2.73 – 2.38 (m, 2H), 2.11 – 1.84 (m, 2H), 1.84 – 1.59 (m, 2H). ¹³C NMR (75 MHz, CDCl₃) δ 162.5 (C), 138.4 (C), 137.3 (C), 136.9 (C), 131.9 (CH), 131.1 (CH), 128.9 (CH), 127.8 (CH), 127.6 (CH), 125.7 (CH), 124.7 (CH), 124.0 (C), 116.3 (C), 41.2 (CH₂), 26.8 (CH₂), 22.0 (CH₂), 19.1 (CH₂). LRMS (EI) *m/z* 275 (100), 260 (13) 246 (8) LRMS (*m/z*, *I*) 341 (28), 313 (9), 212 (38). HRMS calculated for C₁₉H₁₇NO 275.1310, found 275.1312.

12-Phenyl-8,9,10,11-tetrahydroazepino[1,2-b]isoquinolin-5(7H)-one (11q): white solid. ¹H



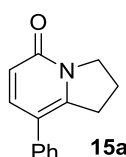
NMR (300 MHz, CDCl₃) δ 8.60 – 8.25 (m, 1H), 7.58 – 7.02 (m, 7H), 7.02 – 6.77 (m, 1H), 4.62 – 4.25 (m, 2H), 2.77 – 2.44 (m, 2H), 1.66 (ddd, *J* = 17.1, 15.4, 11.8 Hz, 6H). ¹³C NMR (75 MHz, CDCl₃) δ 162.5 (C), 142.9 (C), 137.8 (C), 137.6 (C), 132.0 (CH), 131.1 (CH), 128.9 (CH), 128.1 (CH), 127.5 (CH), 125.9 (CH), 125.2 (CH), 124.3 (C), 116.8 (C), 43.8 (CH₂), 30.9 (CH₂), 29.3 (CH₂), 28.6 (CH₂), 27.8 (CH₂). LRMS (*m/z*, *I*) 289 (100), 274 (9), 260 (25), 234 (26) LRMS (*m/z*, *I*) 341 (28), 313 (9), 212 (38). HRMS calculated for C₂₀H₁₉NO 289.1467, found 289.1466.

2.5 Procedure for catalytic reactions of acrylamides 15a-15d.



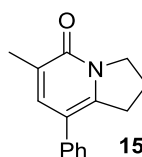
$[\text{Cp}^*\text{RhCl}_2\text{]}_2$ (3.9 mg, 2.5 mol%), $\text{Cu(OAc)}_2 \cdot \text{H}_2\text{O}$ (91 mg, 0.52 equiv.) and CsOAc (58 mg, 0.30 mmol) were added to a Schlenk flask followed by the addition of *t*-AmOH (2.0 mL) and acrylamide **14** (0.25 mmol). The reaction was sealed and placed in a pre-heated (110°C) block. The reaction was stirred for 14 hours, cooled to room temperature and checked by TLC. The solvent was removed and the compound purified by flash column chromatography on silica gel (hexanes:ethyl acetate; 1:1) to afford the product **15a-15d**.

8-Phenyl-2,3-dihydroindolin-5(1H)-one (15a): yellow solid. $^1\text{H NMR}$ (300 MHz, CDCl_3) δ



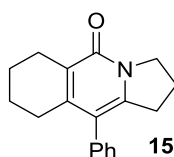
7.47 – 7.08 (m, 6H), 6.44 (d, $J = 9.2$ Hz, 1H), 4.25 – 4.02 (m, 2H), 3.09 (t, $J = 7.6$ Hz, 2H), 2.09 (dt, $J = 14.8, 7.6$ Hz, 2H). $^{13}\text{C NMR}$ (75 MHz, CDCl_3) δ 161.6 (C), 147.4 (C), 141.6 (CH), 137.6 (C), 128.6 (CH), 128.0 (CH), 127.0 (CH), 117.7 (CH), 116.2 (C), 49.0 (CH₂), 32.0 (CH₂), 21.6 (CH₂). **LRMS** (*m/z*, *I*) 210 (100), 181 (25). **HRMS** calculated for $\text{C}_{14}\text{H}_{13}\text{NO}$ 211.0997, found 211.0997.

6-Methyl-8-phenyl-2,3-dihydroindolin-5(1H)-one (15b): yellow liquid. $^1\text{H NMR}$ (300



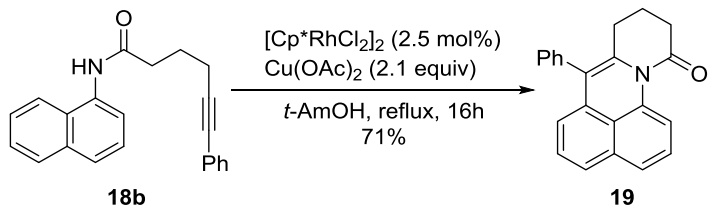
MHz, CDCl_3) δ 7.38 – 7.28 (m, 2H), 7.28 – 7.17 (m, 4H), 4.19 – 4.09 (m, 2H), 3.07 (t, $J = 7.6$ Hz, 2H), 2.12 (s, 3H), 2.11 – 2.05 (m, 2H). $^{13}\text{C NMR}$ (75 MHz, CDCl_3) δ 161.7 (C), 144.3 (C), 139.0 (CH), 137.9 (C), 128.5 (CH), 128.0 (CH), 126.7 (CH), 126.6 (C), 115.5 (C), 49.0 (CH₂), 31.7 (CH₂), 22.0 (CH₂), 16.4 (CH₃). **LRMS** (*m/z*, *I*) 212 (8), 271 (3). **HRMS** calculated for $\text{C}_{15}\text{H}_{15}\text{NO}$ 225.1154, found 225.1149.

10-Phenyl-2,3,6,7,8,9-hexahydropyrrolo[1,2-b]isoquinolin-5(1H)-one (15d): yellow liquid.



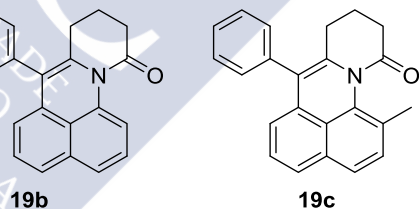
$^1\text{H NMR}$ (300 MHz, CDCl_3) δ 7.48 – 7.29 (m, 3H), 7.22 – 7.11 (m, 2H), 4.19 (t, $J = 7.2$ Hz, 2H), 2.78 (t, $J = 7.7$ Hz, 2H), 2.69 – 2.56 (m, 2H), 2.22 (t, $J = 6.1$ Hz, 2H), 2.17 – 2.01 (m, 2H), 1.82 – 1.66 (m, 2H), 1.66 – 1.53 (m, 2H). $^{13}\text{C NMR}$ (75 MHz, CDCl_3) δ 161.2 (C), 146.7 (C), 143.1 (C), 137.0 (C), 130.0 (CH), 128.4 (CH), 127.2 (CH), 124.4 (C), 117.0 (C), 48.9 (CH₂), 31.1 (CH₂), 28.3 (CH₂), 23.8 (CH₂), 22.3 (CH₂), 22.0 (CH₂), 21.4 (CH₂). **LRMS** (*m/z*, *I*) 250 (21), 236 (5). **HRMS** calculated for $\text{C}_{18}\text{H}_{19}\text{NO}$ 265.1467, found 265.1461.

2.6 Procedure for annulation of hexynamides 18a and 18b. exemplified for 18b.



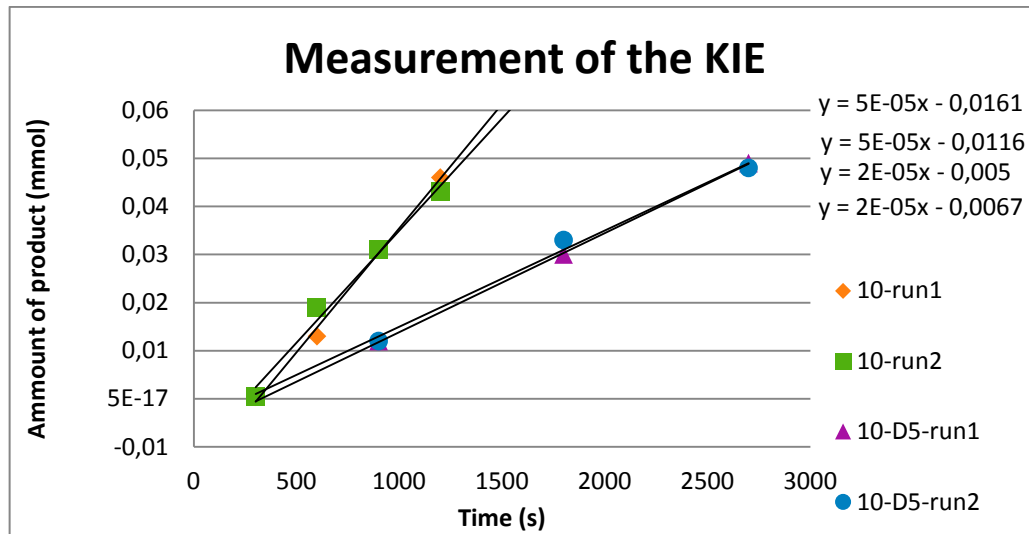
In a Schlenk flask, under argon atmosphere, $[\text{Cp}^*\text{RhCl}_2]_2$ (2.5 mg, 2.5 mol%), and $\text{Cu}(\text{OAc})_2 \cdot \text{H}_2\text{O}$ (64 mg, 2.1 equiv.) were added with stirring followed by the addition of *t*-AmOH (1.12 mL) and hexynamide **18b** (0.15 mmol, 47 mg). The reaction was sealed and placed in a pre-heated (110°C) block. The reaction was stirred for 6 hours and then cooled to room temperature and checked by TLC. The solvent was removed and the remaining residue was purified by flash column chromatography on silica gel (hexanes:ethyl acetate; 3:1) to afford the product **19** (33 mg, 71%). Yellow solid. **1H NMR** (300 MHz, CDCl_3) δ 8.14 (d, J = 7.4 Hz, 1H), 7.37 (ddd, J = 14.9, 11.3, 4.7 Hz, 6H), 7.16 (dd, J = 6.5, 5.1 Hz, 2H), 7.09 – 6.99 (m, 1H), 6.25 (d, J = 7.2 Hz, 1H), 2.71 (t, J = 6.6 Hz, 2H), 2.44 – 2.36 (m, 2H), 1.82 – 1.72 (m, 2H). **13C NMR** (75 MHz, CDCl_3) δ 170.2 (C), 137.3 (C), 134.9 (C), 134.2 (C), 133.8 (C), 131.5 (C), 130.2 (CH), 129.2 (CH), 127.5 (CH), 126.3 (CH), 126.2 (CH), 124.3 (CH), 122.8 (CH), 122.2 (C), 118.3 (CH), 118.0 (CH), 35.2 (CH_2), 28.2 (CH_2), 18.6 (CH_2). **LRMS** (*m/z*, *I*) 282 (57), 253 (69). **HRMS** calculated for $\text{C}_{27}\text{H}_{17}\text{NO}$ 311.1310, found 311.1307.

To fully confirm the regiochemistry of the cycloaddition we have compared the NMR spectra of **19** (1H, 13C, COSY, COSY, HMBC and HMQC) with those of the analogs **19b** and **19c**.



2.7 Kinetic studies.

In a Schlenk flask equipped with a stir bar were added **10** (120 mg, 0.456 mmol) or **10-D5** (122 mg, 0.456 mmol), $[\text{Cp}^*\text{RhCl}_2]_2$ (7.0 mg, 0.011 mmol), and $\text{Cu}(\text{OAc})_2$ (91 mg, 0.52 mmol) without any particular precautions to extrude oxygen or moisture. *t*-AmOH (2.0 mL) was then added and the flask sealed and placed in a pre-heated (110 °C) block. Both reactions were set at the same time in the same heater. Aliquots (0.1 mL) were taken every 5 min for **10** and every 15 min for **10-D5**. The aliquots were diluted in 1 mL of CH_2Cl_2 and immediately filtered through a florisil pad. Volatiles were removed and ^1H NMR of the crude residues were taken. The yield was found by integrating the methylene peaks of the benzamide and the isoquinolone.

**DATA FOR 10a**

Time	Run 1	Run 2
300	0,0004	0,0004
600	0,013	0,019
900	0,031	0,031
1200	0,046	0,043

$$\text{Slope} = 4.96 \times 10^{-5} \text{ M s}^{-1}$$

DATA for 10a-D5

Time	Run 1	Run 2
900	0,012	0,012
1800	0,030	0,033
2700	0,049	0,048

$$\text{Slope} = 2.00 \times 10^{-5} \text{ M s}^{-1}$$

$$\text{KIE} = 2.48$$

2.8 DFT calculations

Methods:

Gas-phase calculations were performed with Gaussian03¹⁸¹ and Gaussian 09¹⁸² at DFT level. The geometries of all complexes here reported were optimized using the B3LYP hybrid functional. Optimizations were carried out using the standard 6-31G(d) basis set for C, H, O, and N. The LANL2DZ basis set, which includes the relativistic effective core potential (ECP) of Hay and Wadt, and employs a split valence (double-zeta) basis set, was used for Rh. Harmonic frequencies were calculated at the same level to characterize the stationary points and to determine the zero-point energies (ZPE). The starting approximate geometries for the transition states (TS) were located graphically. Intrinsic reaction coordinate (IRC) studies were performed to confirm that all transition state structures connect the proposed reactants and products. Single-point PCM calculations (methanol) were performed with Gaussian 09 using the 6-311+G- (2df,2p) basis set for C, H, O, and N, and SDD for Rh. Electronic energy values calculated with the smaller basis set have been corrected using the residual energy at the zero point vibrational energy (ZPE). The evaluation of enthalpy (H) and Gibbs free energy (G) implies the use of the harmonic oscillator / rigid rotor approximation, which introduces some uncertainty in the calculation of the vibrational entropy. Unless otherwise

¹⁸¹ Gaussian 03, Revision C.02, Frisch, M. J.; Trucks, G. W.; Schlegel, H. B.; Scuseria, G. E.; Robb, M. A.; Cheeseman, J. R.; Montgomery, Jr., J. A.; Vreven, T.; Kudin, K. N.; Burant, J. C.; Millam, J. M.; Iyengar, S. S.; Tomasi, J.; Barone, V.; Mennucci, B.; Cossi, M.; Scalmani, G.; Rega, N.; Petersson, G. A.; Nakatsuji, H.; Hada, M.; Ehara, M.; Toyota, K.; Fukuda, R.; Hasegawa, J.; Ishida, M.; Nakajima, T.; Honda, Y.; Kitao, O.; Nakai, H.; Klene, M.; Li, X.; Knox, J. E.; Hratchian, H. P.; Cross, J. B.; Bakken, V.; Adamo, C.; Jaramillo, J.; Gomperts, R.; Stratmann, R. E.; Yazyev, O.; Austin, A. J.; Cammi, R.; Pomelli, C.; Ochterski, J. W.; Ayala, P. Y.; Morokuma, K.; Voth, G. A.; Salvador, P.; Dannenberg, J. J.; Zakrzewski, V. G.; Dapprich, S.; Daniels, A. D.; Strain, M. C.; Farkas, O.; Malick, D. K.; Rabuck, A. D.; Raghavachari, K.; Foresman, J. B.; Ortiz, J. V.; Cui, Q.; Baboul, A. G.; Clifford, S.; Cioslowski, J.; Stefanov, B. B.; Liu, G.; Liashenko, A.; Piskorz, P.; Komaromi, I.; Martin, R. L.; Fox, D. J.; Keith, T.; Al-Laham, M. A.; Peng, C. Y.; Nanayakkara, A.; Challacombe, M.; Gill, P. M. W.; Johnson, B.; Chen, W.; Wong, M. W.; Gonzalez, C.; and Pople, J. A.; Gaussian, Inc., Wallingford CT, 2004.

¹⁸² Gaussian 09, Revision A.1, Frisch, M. J.; Trucks, G. W.; Schlegel, H. B.; Scuseria, G. E.; Robb, M. A.; Cheeseman, J. R.; Scalmani, G.; Barone, V.; Mennucci, B.; Petersson, G. A.; Nakatsuji, H.; Caricato, M.; Li, X.; Hratchian, H. P.; Izmaylov, A. F.; Bloino, J.; Zheng, G.; Sonnenberg, J. L.; Hada, M.; Ehara, M.; Toyota, K.; Fukuda, R.; Hasegawa, J.; Ishida, M.; Nakajima, T.; Honda, Y.; Kitao, O.; Nakai, H.; Vreven, T.; Montgomery, Jr., J. A.; Peralta, J. E.; Ogliaro, F.; Bearpark, M.; Heyd, J. J.; Brothers, E.; Kudin, K. N.; Staroverov, V. N.; Kobayashi, R.; Normand, J.; Raghavachari, K.; Rendell, A.; Burant, J. C.; Iyengar, S. S.; Tomasi, J.; Cossi, M.; Rega, N.; Millam, J. M.; Klene, M.; Knox, J. E.; Cross, J. B.; Bakken, V.; Adamo, C.; Jaramillo, J.; Gomperts, R.; Stratmann, R. E.; Yazyev, O.; Austin, A. J.; Cammi, R.; Pomelli, C.; Ochterski, J. W.; Martin, R. L.; Morokuma, K.; Zakrzewski, V. G.; Voth, G. A.; Salvador, P.; Dannenberg, J. J.; Dapprich, S.; Daniels, A. D.; Farkas, Ö.; Foresman, J. B.; Ortiz, J. V.; Cioslowski, J.; Fox, D. J. Gaussian, Inc., Wallingford CT, 2009.

stated, the energy values included in the main text refer to the single point calculations in methanol performed with the higher quality base on previously optimized structures.

MECHANISTIC PATHWAYS INVESTIGATED BY DFT CALCULATIONS OF THE INTRAMOLECULAR REACTION FOR STANDARD SUBSTRATE 10a.

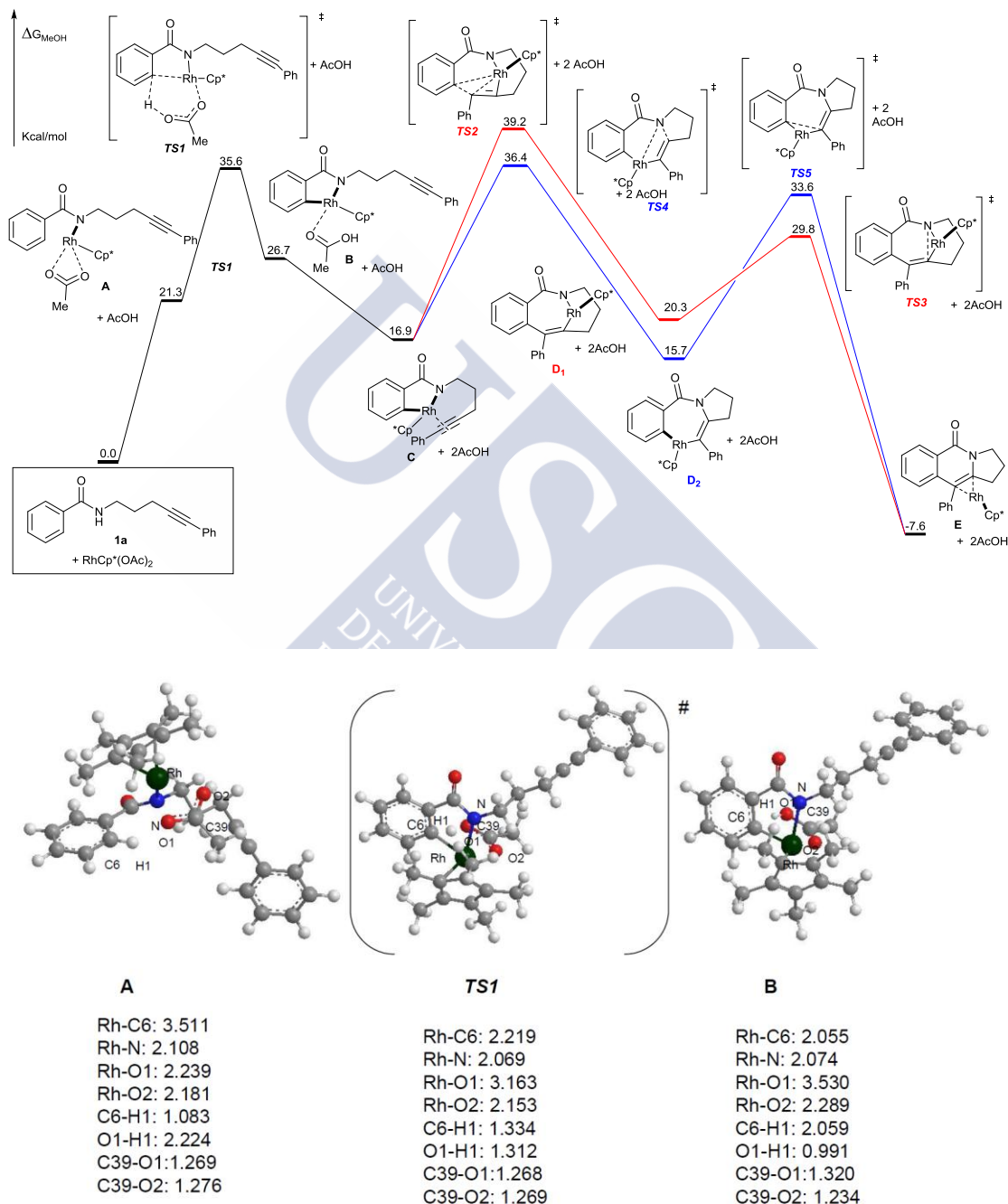


Figure S1: Intermediates involved in the C-H bond cleavage via a concerted metallation-deprotonation transition state. Geometries obtained with B3LYP/6-31G(d) and LANL2DZ for Rh. Distances are given in Å.

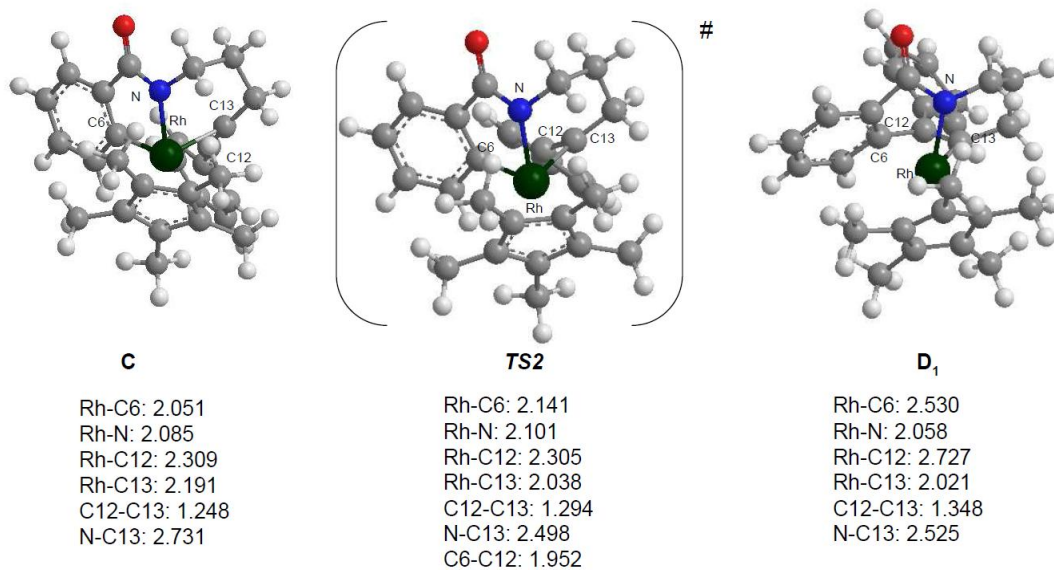


Figure S2: Intermediates involved in the carbometallation step. Geometries obtained with B3LYP/6-31G(d) and LANL2DZ for Rh. Distances are given in Å.¹⁸³

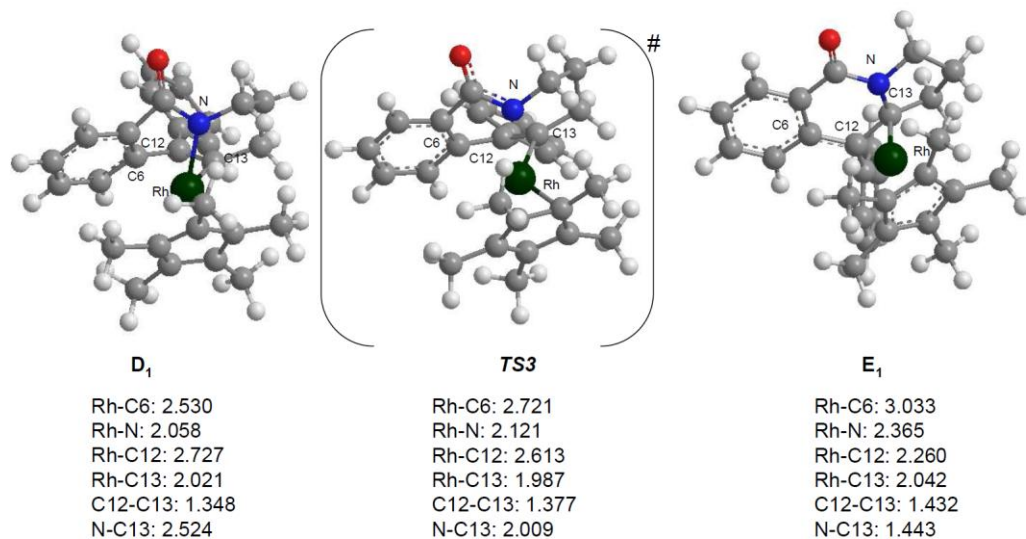


Figure S3: Intermediates involved in the reductive elimination after the carbometallation step. Geometries obtained with B3LYP/6-31G(d) and LANL2DZ for Rh. Distances are given in Å.¹⁸⁴

¹⁸³ Two different conformations were found for intermediate C: one of them (with a lower energy), showing a “pseudo-chair” conformation, evolving through TS2, and another one with a “pseudo-boat” conformation, reacting through TS4. All intends to find a transition state analogous to TS4 starting with a “pseudo-chair” conformation failed, however, if it would exist, the conclusions presented in this paper would be even more enforced.

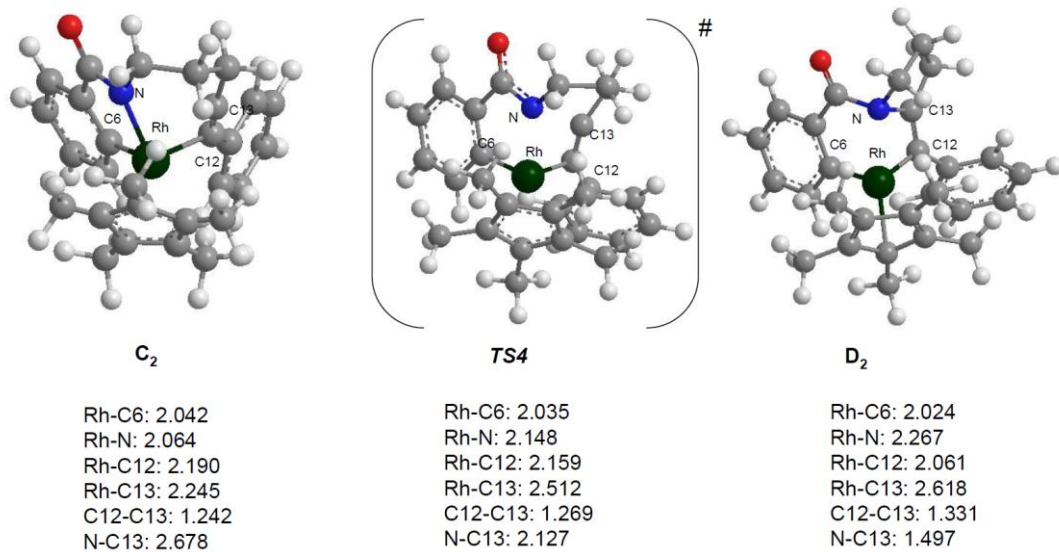


Figure S4: Intermediates involved in the N-metallation step. Geometries obtained with B3LYP/6-31G(d) and LANL2DZ for Rh. Distances are given in Å.⁵

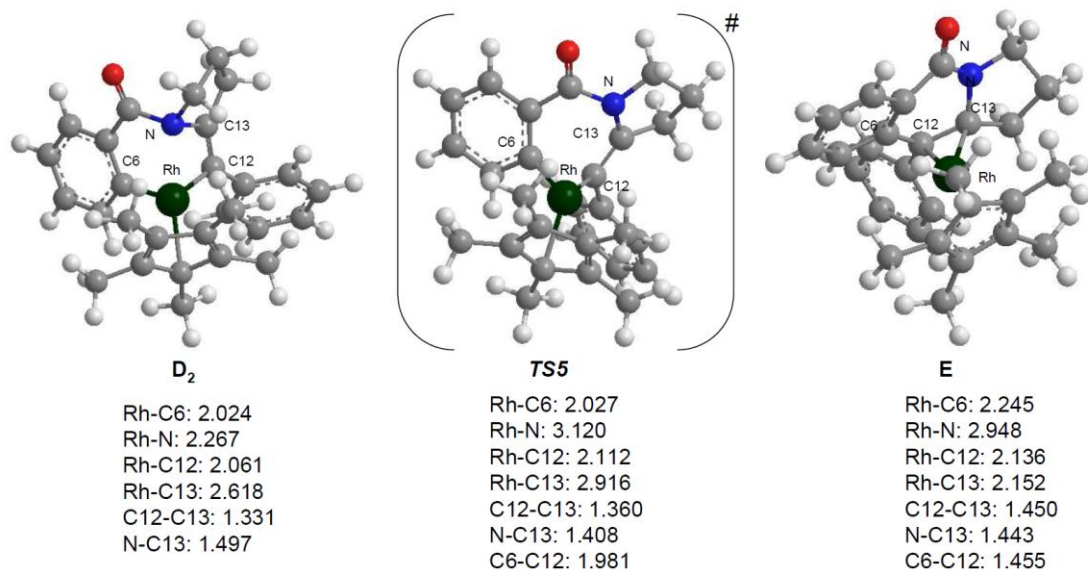


Figure S5: Intermediates involved in the reductive elimination after the N-metallation step. Geometries obtained with B3LYP/6-31G(d) and LANL2DZ for Rh. Distances are given in Å.⁶

¹⁸⁴ Intermediate E₁ was the one obtained by IRC calculations, and has lower energy than E, (figure S5) which is the only one showed in the main text.

ENERGY PROFILESS FOR THE MIGRATORY INSERTION STEP OF THE INTERMOLECULAR REACTION.

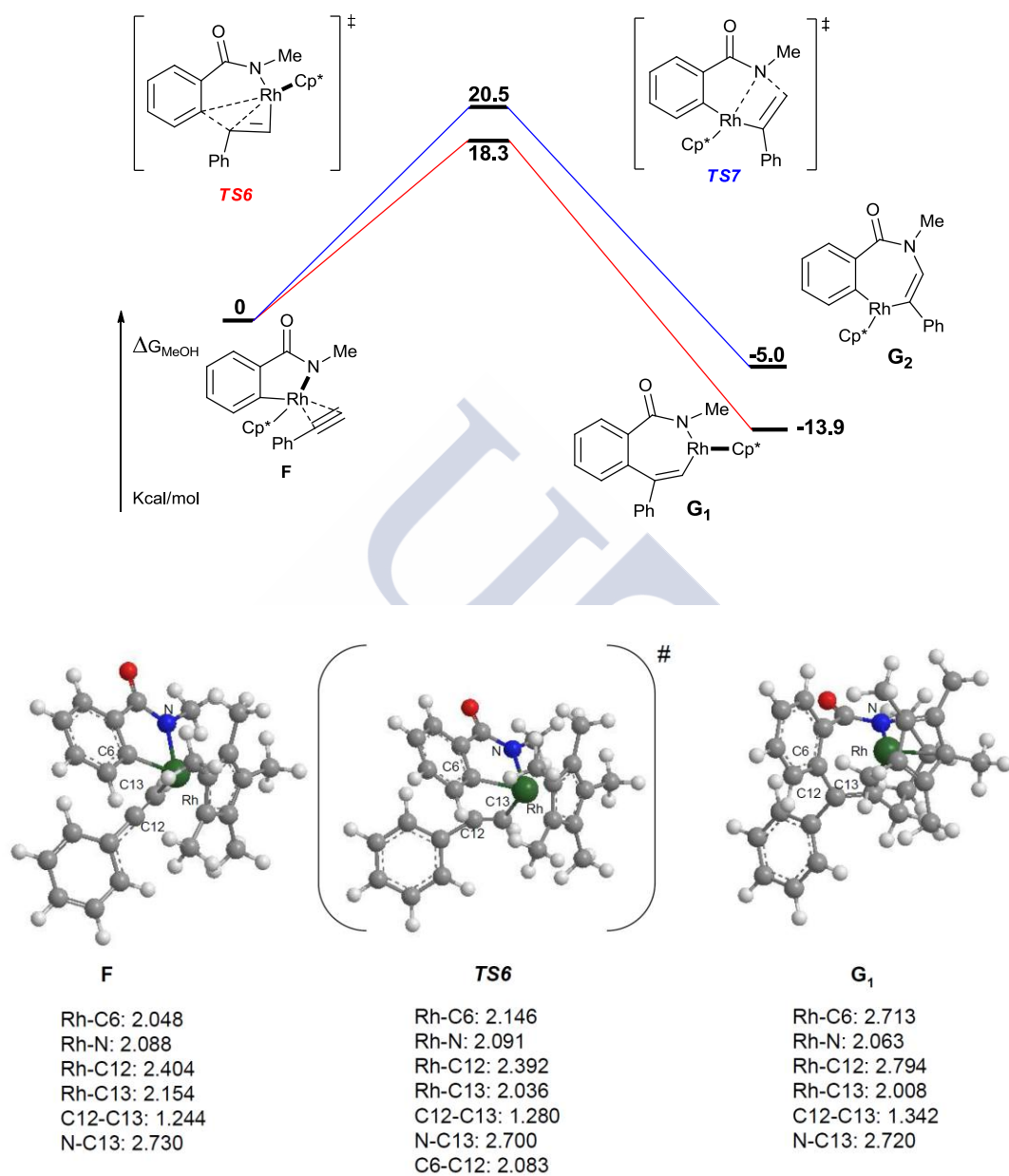


Figure S6: Intermediates involved in the carbometallation step for the intermolecular version. Geometries obtained with B3LYP/6-31G(d) and LANL2DZ for Rh. Distances are given in Å.

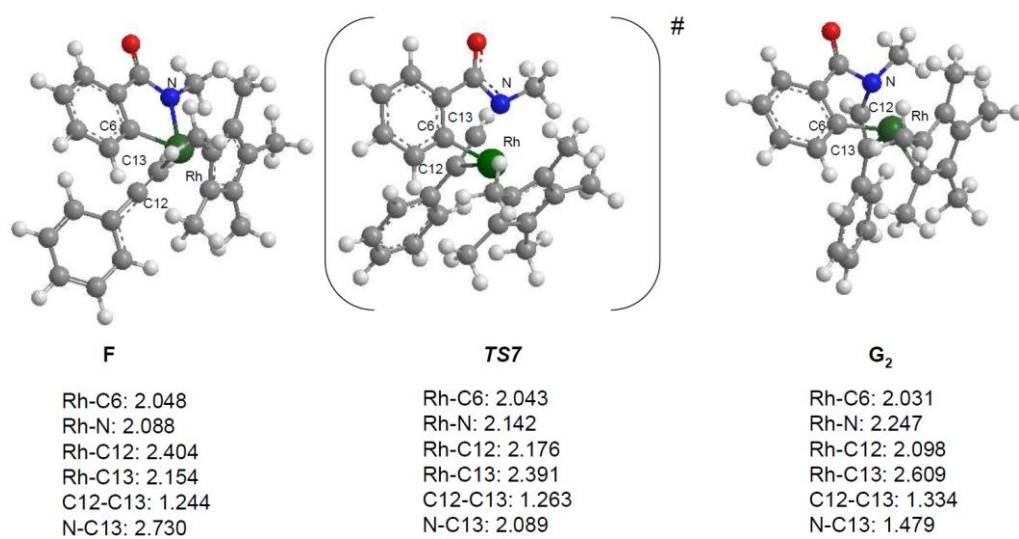


Figure S7: Intermediates involved in the N-metallation step for the intermolecular version. Geometries obtained with B3LYP/6-31G(d) and LANL2DZ for Rh. Distances are given in Å.

ENERGY PROFILES FOR THE MIGRATORY INSERTION STEP OF THE SUBSTRATE WITH AN ELONGATED CONNECTING CHAIN.

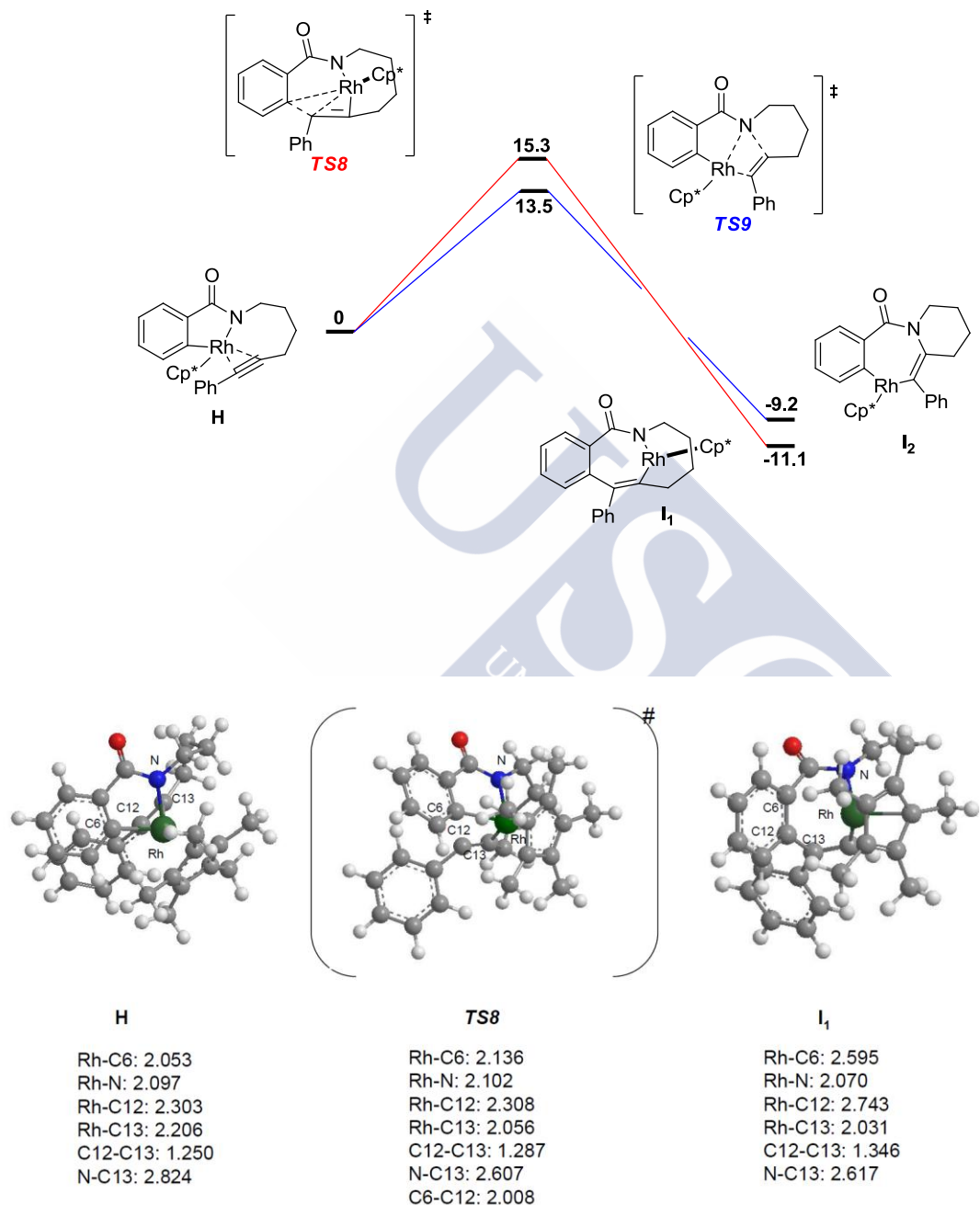


Figure S8: Intermediates involved in the carbometallation step for the substrate with an elongated chain. Geometries obtained with B3LYP/6-31G(d) and LANL2DZ for Rh. Distances are given in Å.

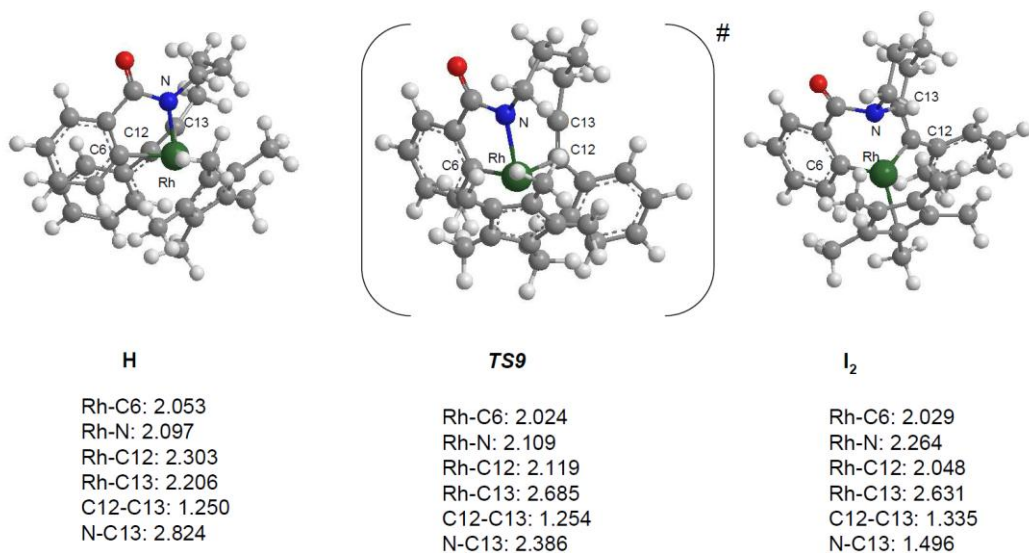


Figure S9: Intermediates involved in the N-metallation step for the substrate with an elongated chain. Geometries obtained with B3LYP/6-31G(d) and LANL2DZ for Rh. Distances are given in Å.

Atomic Cartesian coordinates and computed energies (atomic units) for the stationary points calculated with basis set [B3LYP/6-31G(d) (C, H, O, N) LANL2DZ (Rh)]

1a

Zero-point correction=	0.305399
(Hartree/Particle)	
Thermal correction to Energy=	0.323629
Thermal correction to Enthalpy=	0.324574
Thermal correction to Gibbs Free Energy=	0.252629
Sum of electronic and zero-point Energies=	-825.773279
Sum of electronic and thermal Energies=	-825.755049
Sum of electronic and thermal Enthalpies=	-825.754104
Sum of electronic and thermal Free Energies=	-825.826049

Center Number	Atomic Number	Atomic Type	Coordinates (Angstroms)		
			X	Y	Z
1	7	0	-2.444107	-1.392368	-0.312168
2	6	0	-1.237033	-2.127416	0.040854
3	6	0	-3.094706	-0.613775	0.612733
4	6	0	-4.273085	0.172581	0.107850
5	6	0	-4.984456	-0.157260	-1.054988
6	6	0	-4.680287	1.277550	0.867766
7	6	0	-6.071626	0.617970	-1.460341
8	6	0	-5.761059	2.055589	0.458824
9	6	0	-6.457409	1.729419	-0.708249
10	8	0	-2.741425	-0.565953	1.788497
11	6	0	0.042727	-1.285177	-0.062341
12	6	0	1.294157	-2.096823	0.336056

13	6	0	2.534181	-1.331437	0.213376
14	6	0	3.548493	-0.675542	0.102565
15	6	0	4.747679	0.093029	-0.024626
16	6	0	5.902496	-0.468800	-0.603629
17	6	0	7.068021	0.284101	-0.726734
18	6	0	7.104165	1.606592	-0.277287
19	6	0	5.964469	2.173536	0.298844
20	6	0	4.795485	1.426790	0.426403
21	1	0	-2.613271	-1.208752	-1.290916
22	1	0	-1.369675	-2.478101	1.067754
23	1	0	-1.171200	-3.007675	-0.610796
24	1	0	-4.719643	-1.040716	-1.630113
25	1	0	-4.134346	1.504597	1.777526
26	1	0	-6.622002	0.348346	-2.357660
27	1	0	-6.063649	2.915072	1.050862
28	1	0	-7.302862	2.333807	-1.025943
29	1	0	-0.053086	-0.413459	0.593110
30	1	0	0.164232	-0.910845	-1.086779
31	1	0	1.359724	-3.000895	-0.287251
32	1	0	1.179591	-2.450379	1.371132
33	1	0	5.871852	-1.496634	-0.952216
34	1	0	7.951548	-0.162997	-1.174684
35	1	0	8.014653	2.191525	-0.375298
36	1	0	5.986201	3.201440	0.651048
37	1	0	3.908815	1.864306	0.874954

RhCp*(OAc)₂

Zero-point correction= 0.327269
 (Hartree/Particle)

Thermal correction to Energy= 0.351481

Chapter VI.

Thermal correction to Enthalpy=	0.352425
Thermal correction to Gibbs Free Energy=	0.273184
Sum of electronic and zero-point Energies=	-956.300144
Sum of electronic and thermal Energies=	-956.275931
Sum of electronic and thermal Enthalpies=	-956.274987
Sum of electronic and thermal Free Energies=	-956.354229

Center Number	Atomic Number	Atomic Type	Coordinates (Angstroms)		
			X	Y	Z
1	45	0	0.010241	0.216054	-0.092084
2	6	0	1.251742	-1.149599	1.088793
3	6	0	0.836594	-1.851442	2.344732
4	6	0	1.155407	-1.681973	-0.242964
5	6	0	0.607803	-3.028057	-0.603774
6	6	0	1.675575	-0.699200	-1.153448
7	6	0	1.797894	-0.830334	-2.641290
8	6	0	2.190771	0.416922	-0.364405
9	6	0	2.849282	1.633225	-0.942241
10	6	0	1.929160	0.140619	1.006467
11	6	0	2.256303	1.004326	2.186865
12	8	0	-1.868965	-0.417690	-0.669726
13	6	0	-2.489647	-1.362380	-0.018612
14	8	0	-2.031410	-2.047908	0.898510
15	6	0	-3.927928	-1.552147	-0.498049
16	1	0	-0.158879	-2.283184	2.215991
17	1	0	0.802771	-1.160326	3.191291
18	1	0	1.549158	-2.650800	2.591527
19	1	0	-0.252177	-3.273242	0.021783
20	1	0	1.385172	-3.791588	-0.462096
21	1	0	0.291048	-3.064219	-1.649444

22	1	0	1.687436	0.139309	-3.135442
23	1	0	1.035701	-1.500145	-3.047161
24	1	0	2.782638	-1.235014	-2.913686
25	1	0	2.267872	2.035015	-1.777675
26	1	0	3.851865	1.385982	-1.315354
27	1	0	2.952830	2.427055	-0.198744
28	1	0	3.088599	0.571453	2.757000
29	1	0	1.397341	1.090730	2.859044
30	1	0	2.545019	2.013320	1.882946
31	1	0	-4.548052	-0.739896	-0.100917
32	1	0	-3.986449	-1.505991	-1.589466
33	1	0	-4.319876	-2.505019	-0.135679
34	6	0	-1.274763	2.405363	0.066718
35	8	0	-0.678756	2.092090	-1.012778
36	8	0	-1.117004	1.669903	1.094411
37	6	0	-2.187996	3.602994	0.118992
38	1	0	-3.201288	3.283292	-0.151144
39	1	0	-2.217896	4.018131	1.129325
40	1	0	-1.865783	4.361651	-0.598367

AcOH

Zero-point correction=	0.062022
(Hartree/Particle)	
Thermal correction to Energy=	0.066602
Thermal correction to Enthalpy=	0.067546
Thermal correction to Gibbs Free Energy=	0.034684
Sum of electronic and zero-point Energies=	-229.015588
Sum of electronic and thermal Energies=	-229.011008
Sum of electronic and thermal Enthalpies=	-229.010063
Sum of electronic and thermal Free Energies=	-229.042925

Chapter VI.

Center	Atomic Number	Atomic Number	Type	Coordinates (Angstroms)		
				X	Y	Z
1	8	8	0	0.645495	1.202079	0.000002
2	8	8	0	0.778870	-1.046544	-0.000004
3	6	6	0	0.092467	0.125600	-0.000008
4	6	6	0	-1.397568	-0.110018	0.000000
5	1	1	0	-1.685280	-0.691964	-0.881887
6	1	1	0	-1.685359	-0.691357	0.882263
7	1	1	0	-1.917537	0.848189	-0.000348
8	1	1	0	1.723861	-0.802641	0.000034

A

Zero-point correction=
(Hartree/Particle)

0.570386

Thermal correction to Energy=

0.608136

Thermal correction to Enthalpy=

0.609080

Thermal correction to Gibbs Free Energy=

0.496621

Sum of electronic and zero-point Energies=

-1553.031955

Sum of electronic and thermal Energies=

-1552.994205

Sum of electronic and thermal Enthalpies=

-1552.993261

Sum of electronic and thermal Free Energies=

-1553.105719

Center	Atomic Number	Atomic Number	Type	Coordinates (Angstroms)		
				X	Y	Z
1	45	45	0	1.962382	-0.775810	0.176124
2	7	7	0	0.270829	0.372899	-0.335589
3	6	6	0	-0.744023	-0.421177	-1.045293
4	6	6	0	0.379400	1.654103	-0.802657

5	6	0	1.264199	2.627699	-0.060246
6	6	0	1.547678	2.521952	1.308573
7	6	0	1.737335	3.744660	-0.767720
8	6	0	2.313989	3.501360	1.946555
9	6	0	2.516352	4.712106	-0.134047
10	6	0	2.808454	4.592123	1.228475
11	8	0	-0.259275	2.075622	-1.782953
12	6	0	-2.174136	-0.070278	-0.604839
13	6	0	-3.216567	-0.905986	-1.379886
14	6	0	-4.595572	-0.648346	-0.966415
15	6	0	-5.734431	-0.422655	-0.613781
16	6	0	-9.248562	-0.953072	0.556885
17	6	0	-9.728009	0.358979	0.589001
18	6	0	-8.885345	1.412120	0.223953
19	6	0	-7.573526	1.159584	-0.170919
20	6	0	-7.079127	-0.159455	-0.207144
21	6	0	-7.937830	-1.213396	0.163590
22	1	0	-0.660447	-0.267873	-2.131839
23	1	0	-0.567370	-1.477082	-0.827070
24	1	0	1.164863	1.679472	1.871895
25	1	0	1.462496	3.843675	-1.813204
26	1	0	2.516408	3.413907	3.011362
27	1	0	2.882041	5.567684	-0.696654
28	1	0	3.404529	5.351807	1.728206
29	1	0	-2.358595	0.993485	-0.775996
30	1	0	-2.278681	-0.260193	0.469718
31	1	0	-2.994923	-1.976436	-1.253883
32	1	0	-3.115158	-0.698734	-2.455286
33	1	0	-9.898541	-1.777305	0.839181
34	1	0	-10.751024	0.559315	0.896046
35	1	0	-9.251639	2.435210	0.246456

36	1	0	-6.916864	1.976091	-0.455346
37	1	0	-7.563092	-2.232204	0.137580
38	6	0	3.973138	-0.057229	-0.425002
39	6	0	4.148234	-1.338268	0.261400
40	6	0	3.441583	-2.323857	-0.467833
41	6	0	2.798289	-1.669941	-1.608360
42	6	0	3.206214	-0.288242	-1.613058
43	6	0	4.646981	1.217669	-0.020851
44	6	0	4.938836	-1.516942	1.522416
45	6	0	3.301564	-3.780197	-0.144249
46	6	0	2.024481	-2.366203	-2.686427
47	6	0	2.895960	0.705628	-2.690660
48	1	0	5.685788	1.221885	-0.380552
49	1	0	4.670893	1.326818	1.066648
50	1	0	4.140378	2.094749	-0.427368
51	1	0	4.644998	-0.780479	2.277191
52	1	0	6.011298	-1.385648	1.327322
53	1	0	4.795582	-2.510768	1.953404
54	1	0	3.699655	-4.015711	0.845476
55	1	0	3.841940	-4.389101	-0.880697
56	1	0	2.250502	-4.085583	-0.162260
57	1	0	1.445385	-3.202896	-2.284454
58	1	0	2.703241	-2.767691	-3.451898
59	1	0	1.329417	-1.681760	-3.179614
60	1	0	3.503994	0.485071	-3.578301
61	1	0	3.120697	1.725013	-2.372283
62	1	0	1.843219	0.681853	-2.985997
63	8	0	0.543026	-2.080826	1.194528
64	8	0	1.486095	-0.469912	2.342302
65	6	0	0.640051	-1.413817	2.278504
66	6	0	-0.267009	-1.722747	3.441420

67	1	0	0.207506	-1.436712	4.383031
68	1	0	-1.190470	-1.141791	3.331386
69	1	0	-0.531400	-2.783007	3.452012

TS1

Zero-point correction=	0.564943
(Hartree/Particle)	
Thermal correction to Energy=	0.602174
Thermal correction to Enthalpy=	0.603118
Thermal correction to Gibbs Free Energy=	0.492197
Sum of electronic and zero-point Energies=	-1553.007949
Sum of electronic and thermal Energies=	-1552.970719
Sum of electronic and thermal Enthalpies=	-1552.969774
Sum of electronic and thermal Free Energies=	-1553.080695

Center Number	Atomic Number	Atomic Type	Coordinates (Angstroms)		
			X	Y	Z
1	45	0	1.814789	-0.452572	0.135743
2	7	0	0.523278	0.580796	-1.106593
3	6	0	-0.550875	-0.036867	-1.871683
4	6	0	0.757760	1.901639	-1.308472
5	6	0	1.823219	2.433425	-0.394906
6	6	0	2.175037	1.654745	0.730278
7	6	0	2.441677	3.656021	-0.655308
8	6	0	3.189119	2.143857	1.579374
9	6	0	3.451259	4.112022	0.193703
10	6	0	3.823004	3.358940	1.315461
11	8	0	0.171168	2.616791	-2.133364
12	6	0	-1.936474	0.194500	-1.247292
13	6	0	-3.068228	-0.409881	-2.107296

14	6	0	-4.386151	-0.280723	-1.485879
15	6	0	-5.462759	-0.163155	-0.938509
16	6	0	-8.775140	-1.014748	0.579712
17	6	0	-9.227445	0.246424	0.976228
18	6	0	-8.434719	1.371986	0.737264
19	6	0	-7.198941	1.241790	0.107454
20	6	0	-6.732317	-0.025098	-0.296182
21	6	0	-7.540343	-1.152965	-0.050212
22	1	0	-0.543009	0.371330	-2.892006
23	1	0	-0.362234	-1.115210	-1.937081
24	1	0	2.122850	4.225344	-1.523860
25	1	0	3.446223	1.592696	2.481503
26	1	0	3.943132	5.060614	-0.007558
27	1	0	4.591360	3.731573	1.988904
28	1	0	-2.098891	1.271139	-1.135990
29	1	0	-1.958766	-0.254372	-0.249226
30	1	0	-2.859908	-1.474130	-2.295020
31	1	0	-3.075452	0.077309	-3.093051
32	1	0	-9.386841	-1.894562	0.761954
33	1	0	-10.190944	0.351482	1.467710
34	1	0	-8.780469	2.356098	1.042722
35	1	0	-6.581153	2.114883	-0.079252
36	1	0	-7.186735	-2.132076	-0.359067
37	6	0	3.812155	-0.810965	-0.760572
38	6	0	3.883419	-1.325717	0.603345
39	6	0	2.920154	-2.355338	0.726451
40	6	0	2.264428	-2.534916	-0.565226
41	6	0	2.865344	-1.619193	-1.486062
42	6	0	4.734045	0.212458	-1.356088
43	6	0	4.875744	-0.897087	1.643516
44	6	0	2.598727	-3.158466	1.951036

45	6	0	1.249788	-3.598036	-0.865048
46	6	0	2.572278	-1.500796	-2.951244
47	1	0	5.685042	-0.249793	-1.655707
48	1	0	4.957174	1.011845	-0.644584
49	1	0	4.295127	0.675696	-2.243666
50	1	0	5.176265	0.143340	1.504603
51	1	0	5.781335	-1.516394	1.581214
52	1	0	4.475176	-0.998087	2.656475
53	1	0	3.117499	-2.774286	2.833069
54	1	0	2.896495	-4.206612	1.816213
55	1	0	1.523067	-3.138776	2.156130
56	1	0	0.532691	-3.700552	-0.044772
57	1	0	1.733912	-4.574079	-1.009510
58	1	0	0.684959	-3.372939	-1.773996
59	1	0	3.322396	-2.055704	-3.530864
60	1	0	2.595755	-0.458806	-3.280227
61	1	0	1.590286	-1.907662	-3.203447
62	8	0	0.121234	-0.918427	1.380065
63	8	0	0.180426	1.103114	2.352694
64	6	0	-0.312294	-0.056032	2.203952
65	6	0	-1.518290	-0.422968	3.043373
66	1	0	-1.457876	0.055607	4.023503
67	1	0	-2.417940	-0.050294	2.539520
68	1	0	-1.603701	-1.506553	3.146192
69	1	0	1.163048	1.241149	1.494724

B

Zero-point correction= 0.569929
 (Hartree/Particle)

Thermal correction to Energy= 0.607018

Thermal correction to Enthalpy= 0.607962

Chapter VI.

Thermal correction to Gibbs Free Energy=	0.497764
Sum of electronic and zero-point Energies=	-1553.022684
Sum of electronic and thermal Energies=	-1552.985595
Sum of electronic and thermal Enthalpies=	-1552.984651
Sum of electronic and thermal Free Energies=	-1553.094848

Center Number	Atomic Number	Atomic Type	Coordinates (Angstroms)		
			X	Y	Z
1	45	0	1.917165	-0.373288	0.131874
2	7	0	0.592945	0.388867	-1.271351
3	6	0	-0.470857	-0.370987	-1.911868
4	6	0	0.758571	1.674650	-1.680417
5	6	0	1.796172	2.375174	-0.858010
6	6	0	2.406500	1.622278	0.163244
7	6	0	2.076313	3.732129	-1.033885
8	6	0	3.277084	2.285696	1.041920
9	6	0	2.972753	4.368999	-0.174995
10	6	0	3.559526	3.648167	0.869398
11	8	0	0.106177	2.236122	-2.572146
12	6	0	-1.853867	-0.077137	-1.305922
13	6	0	-2.986680	-0.824596	-2.042382
14	6	0	-4.298679	-0.618970	-1.429055
15	6	0	-5.373523	-0.431560	-0.897807
16	6	0	-8.245236	1.295376	0.766353
17	6	0	-9.135522	0.234190	0.949786
18	6	0	-8.781188	-1.047467	0.520672
19	6	0	-7.547276	-1.269807	-0.086407
20	6	0	-6.641210	-0.207467	-0.276333
21	6	0	-7.009847	1.081008	0.159216
22	1	0	-0.493927	-0.130370	-2.984064

23	1	0	-0.255861	-1.440308	-1.810754
24	1	0	1.570719	4.262041	-1.836884
25	1	0	3.741054	1.754691	1.869818
26	1	0	3.198723	5.424579	-0.302506
27	1	0	4.238598	4.146195	1.558287
28	1	0	-2.037891	1.000545	-1.355963
29	1	0	-1.854974	-0.371147	-0.249700
30	1	0	-2.762972	-1.901781	-2.068145
31	1	0	-3.014289	-0.495098	-3.090980
32	1	0	-8.514935	2.295156	1.096359
33	1	0	-10.098882	0.405052	1.422597
34	1	0	-9.469471	-1.877280	0.658297
35	1	0	-7.270545	-2.264662	-0.421964
36	1	0	-6.317682	1.904670	0.013300
37	6	0	3.519434	-1.340393	-0.944994
38	6	0	4.029353	-1.141958	0.402870
39	6	0	3.199660	-1.879456	1.280002
40	6	0	2.280963	-2.694957	0.470192
41	6	0	2.516663	-2.408718	-0.880374
42	6	0	4.158969	-0.835671	-2.206032
43	6	0	5.257637	-0.357309	0.754316
44	6	0	3.307706	-1.971928	2.773880
45	6	0	1.288485	-3.656914	1.052224
46	6	0	1.898358	-3.059830	-2.080511
47	1	0	4.925412	-1.536086	-2.567732
48	1	0	4.638422	0.133537	-2.045296
49	1	0	3.418892	-0.707830	-3.000918
50	1	0	5.332536	0.565906	0.174985
51	1	0	6.152412	-0.959803	0.544768
52	1	0	5.284439	-0.091434	1.814530
53	1	0	3.858667	-1.124636	3.191111

Chapter VI.

54	1	0	3.830115	-2.890442	3.075821
55	1	0	2.317975	-1.988532	3.241611
56	1	0	0.658333	-3.163558	1.800729
57	1	0	1.794952	-4.495858	1.548225
58	1	0	0.629797	-4.072621	0.285010
59	1	0	2.587997	-3.804510	-2.501851
60	1	0	1.684932	-2.333130	-2.869293
61	1	0	0.966166	-3.576371	-1.835929
62	8	0	0.247077	-0.258828	1.693333
63	8	0	-0.086268	1.966368	1.856059
64	6	0	-0.388351	0.708406	2.120330
65	6	0	-1.610644	0.553237	2.983925
66	1	0	0.701411	1.992301	1.255750
67	1	0	-1.625069	1.310929	3.771445
68	1	0	-2.500023	0.701226	2.359841
69	1	0	-1.641562	-0.449865	3.410622

C

Zero-point correction= 0.506868
(Hartree/Particle)

Thermal correction to Energy=	0.538133
Thermal correction to Enthalpy=	0.539077
Thermal correction to Gibbs Free Energy=	0.445450
Sum of electronic and zero-point Energies=	-1323.997559
Sum of electronic and thermal Energies=	-1323.966294
Sum of electronic and thermal Enthalpies=	-1323.965350
Sum of electronic and thermal Free Energies=	-1324.058976

Center Number	Atomic Number	Atomic Type	Coordinates (Angstroms)		
			X	Y	Z

1	45	0	-0.650891	-0.202761	-0.030164
2	7	0	-1.560665	1.365937	0.999016
3	6	0	-2.375337	1.142801	2.179552
4	6	0	-1.065264	2.624987	0.813596
5	6	0	0.005224	2.640395	-0.222483
6	6	0	0.429611	1.400968	-0.714464
7	6	0	0.606605	3.830267	-0.642555
8	6	0	1.483405	1.362670	-1.632460
9	6	0	1.639691	3.789650	-1.578364
10	6	0	2.076995	2.555087	-2.068646
11	8	0	-1.432191	3.632874	1.432168
12	6	0	0.119531	-0.544372	1.992111
13	6	0	1.176928	-0.576219	1.330134
14	6	0	-1.534727	0.746208	3.402007
15	6	0	-0.752099	-0.565132	3.185641
16	6	0	2.572011	-0.727559	1.004238
17	6	0	3.136171	-2.015308	0.904322
18	6	0	4.493589	-2.174378	0.633394
19	6	0	5.310073	-1.054221	0.458835
20	6	0	4.761189	0.226432	0.561452
21	6	0	3.404063	0.395104	0.829326
22	1	0	-2.911827	2.070973	2.403322
23	1	0	-3.119107	0.361861	1.974241
24	1	0	0.249691	4.764612	-0.217237
25	1	0	1.865038	0.416121	-2.006043
26	1	0	2.110063	4.709084	-1.917743
27	1	0	2.892479	2.514036	-2.788079
28	1	0	-2.182045	0.620548	4.280518
29	1	0	-0.834969	1.560154	3.622341
30	1	0	-1.462363	-1.399568	3.097966

31	1	0	-0.123296	-0.775735	4.062001
32	1	0	2.504618	-2.884854	1.060775
33	1	0	4.915045	-3.173679	0.564476
34	1	0	6.368825	-1.179101	0.248774
35	1	0	5.392187	1.101424	0.432238
36	1	0	2.977620	1.388487	0.906237
37	6	0	-1.273922	-0.800790	-2.174383
38	6	0	-0.462725	-1.858158	-1.646864
39	6	0	-1.191429	-2.461640	-0.549341
40	6	0	-2.416284	-1.768045	-0.376902
41	6	0	-2.447583	-0.696752	-1.350943
42	6	0	-1.021025	-0.021476	-3.431231
43	6	0	0.792666	-2.414672	-2.255441
44	6	0	-0.732306	-3.671698	0.209062
45	6	0	-3.539446	-2.139686	0.548471
46	6	0	-3.595403	0.244928	-1.566395
47	1	0	-1.454677	-0.548062	-4.292948
48	1	0	0.045593	0.113062	-3.623649
49	1	0	-1.472021	0.973119	-3.387257
50	1	0	1.274508	-1.687990	-2.915033
51	1	0	0.574468	-3.307612	-2.858665
52	1	0	1.524180	-2.704063	-1.494302
53	1	0	0.327187	-3.601390	0.474843
54	1	0	-0.854710	-4.578570	-0.398966
55	1	0	-1.300769	-3.814615	1.132102
56	1	0	-3.179480	-2.650493	1.447172
57	1	0	-4.248345	-2.817095	0.051450
58	1	0	-4.106931	-1.261879	0.870808
59	1	0	-4.369674	-0.221989	-2.191191
60	1	0	-3.272747	1.163501	-2.062905
61	1	0	-4.057488	0.533055	-0.618359

TS2

Zero-point correction= 0.506154
 (Hartree/Particle)

Thermal correction to Energy= 0.536416
 Thermal correction to Enthalpy= 0.537361
 Thermal correction to Gibbs Free Energy= 0.446224
 Sum of electronic and zero-point Energies= -1323.968903
 Sum of electronic and thermal Energies= -1323.938640
 Sum of electronic and thermal Enthalpies= -1323.937696
 Sum of electronic and thermal Free Energies= -1324.028833

Center Number	Atomic Number	Atomic Type	Coordinates (Angstroms)		
			X	Y	Z
1	45	0	-0.862977	-0.124952	0.018270
2	7	0	-0.919370	1.574852	1.251649
3	6	0	-1.418490	1.477837	2.618012
4	6	0	-0.008960	2.558436	1.002855
5	6	0	0.770758	2.284386	-0.242012
6	6	0	0.851607	0.945748	-0.685967
7	6	0	1.400795	3.310103	-0.948993
8	6	0	1.522800	0.678379	-1.895175
9	6	0	2.060415	3.031565	-2.146809
10	6	0	2.105602	1.714983	-2.623838
11	8	0	0.192274	3.555546	1.710039
12	6	0	0.389231	-0.528776	1.574771
13	6	0	1.327612	-0.340733	0.703368

14	6	0	-0.416928	0.754162	3.541184
15	6	0	0.009605	-0.637195	3.001720
16	6	0	3.759421	0.021906	0.197151
17	6	0	5.055558	-0.475674	0.084091
18	6	0	5.302804	-1.843985	0.230287
19	6	0	4.245480	-2.714350	0.500951
20	6	0	2.947444	-2.218633	0.624940
21	6	0	2.687374	-0.844676	0.475257
22	1	0	-1.586629	2.488521	3.006411
23	1	0	-2.379192	0.951289	2.615024
24	1	0	1.335245	4.319446	-0.552092
25	1	0	1.620494	-0.344937	-2.248078
26	1	0	2.533689	3.831418	-2.710196
27	1	0	2.614859	1.492952	-3.558855
28	1	0	-0.841363	0.635733	4.547530
29	1	0	0.474607	1.384337	3.631928
30	1	0	-0.816766	-1.351269	3.115076
31	1	0	0.854853	-1.017949	3.592483
32	1	0	3.569654	1.084124	0.086226
33	1	0	5.876717	0.207011	-0.117071
34	1	0	6.314822	-2.228255	0.134469
35	1	0	4.429580	-3.779234	0.616255
36	1	0	2.121043	-2.890051	0.839659
37	6	0	-2.037571	-0.507339	-1.994192
38	6	0	-1.497206	-1.756082	-1.486193
39	6	0	-2.150828	-2.059443	-0.244679
40	6	0	-2.988568	-0.954796	0.083848
41	6	0	-2.924578	0.004574	-1.021256
42	6	0	-1.707393	0.094318	-3.328564
43	6	0	-0.589071	-2.681180	-2.246418
44	6	0	-1.990101	-3.322601	0.550706

45	6	0	-3.972067	-0.885145	1.216007
46	6	0	-3.738170	1.263502	-1.094876
47	1	0	-2.208946	-0.452660	-4.138849
48	1	0	-0.631551	0.070719	-3.530284
49	1	0	-2.024191	1.138938	-3.387726
50	1	0	0.068751	-2.131767	-2.926432
51	1	0	-1.169454	-3.387925	-2.856853
52	1	0	0.043234	-3.271041	-1.575606
53	1	0	-0.982107	-3.738459	0.453077
54	1	0	-2.694622	-4.094737	0.211173
55	1	0	-2.179009	-3.156061	1.615831
56	1	0	-3.620245	-1.426510	2.099680
57	1	0	-4.933887	-1.329548	0.921712
58	1	0	-4.172165	0.148126	1.513649
59	1	0	-4.797105	1.036571	-1.280621
60	1	0	-3.392601	1.919406	-1.898048
61	1	0	-3.675778	1.830573	-0.160548

D₁

Zero-point correction= 0.508498
(Hartree/Particle)

Thermal correction to Energy= 0.538850

Thermal correction to Enthalpy= 0.539794

Thermal correction to Gibbs Free Energy= 0.448500

Sum of electronic and zero-point Energies= -1324.011068

Sum of electronic and thermal Energies= -1323.980716

Sum of electronic and thermal Enthalpies= -1323.979771

Sum of electronic and thermal Free Energies= -1324.071066

Center	Atomic	Atomic	Coordinates (Angstroms)
--------	--------	--------	-------------------------

Chapter VI.

Number	Number	Type	X	Y	Z
<hr/>					
1	45	0	-0.986001	-0.183280	0.030688
2	7	0	-0.373250	-0.622464	1.945659
3	6	0	-0.110952	-1.980490	2.403752
4	6	0	0.461667	0.382665	2.298460
5	6	0	0.436887	1.476103	1.224746
6	6	0	1.088501	1.262873	-0.034833
7	6	0	-0.063545	2.760890	1.535550
8	6	0	1.204500	2.358070	-0.924653
9	6	0	0.040762	3.804860	0.630957
10	6	0	0.684000	3.601826	-0.605834
11	8	0	1.173759	0.479361	3.297219
12	6	0	0.809160	-1.071504	-0.239298
13	6	0	1.715223	-0.077822	-0.328678
14	6	0	1.068290	-2.644807	1.657062
15	6	0	1.019460	-2.514499	0.107362
16	6	0	-3.132277	0.820539	-0.537556
17	6	0	-2.340826	0.489877	-1.734652
18	6	0	-2.152247	-0.910040	-1.777791
19	6	0	-2.667584	-1.446025	-0.527829
20	6	0	-3.361494	-0.356754	0.174676
21	6	0	-3.581774	2.211823	-0.202045
22	6	0	-1.974666	1.489223	-2.792269
23	6	0	-1.562704	-1.712483	-2.901239
24	6	0	-2.856921	-2.901474	-0.212420
25	6	0	-4.106161	-0.533132	1.464899
26	6	0	3.182793	-0.184683	-0.519113
27	6	0	3.732972	-1.046873	-1.484339
28	6	0	5.114282	-1.152640	-1.646521
29	6	0	5.975615	-0.388311	-0.856287

30	6	0	5.442598	0.481890	0.098193
31	6	0	4.062325	0.585445	0.264307
32	1	0	0.119143	-1.956334	3.476014
33	1	0	-1.026575	-2.570392	2.275148
34	1	0	-0.505544	2.921012	2.515056
35	1	0	1.734323	2.209249	-1.861666
36	1	0	-0.344859	4.788295	0.886908
37	1	0	0.791517	4.429665	-1.302135
38	1	0	1.121555	-3.706590	1.934877
39	1	0	1.995487	-2.172240	2.000681
40	1	0	0.221603	-3.147426	-0.301267
41	1	0	1.968781	-2.891045	-0.294764
42	1	0	-4.288715	2.588925	-0.953563
43	1	0	-2.736000	2.909430	-0.173261
44	1	0	-4.077204	2.253422	0.771566
45	1	0	-1.544962	2.396211	-2.353800
46	1	0	-2.861107	1.791028	-3.367909
47	1	0	-1.244644	1.082288	-3.497407
48	1	0	-0.856198	-1.122587	-3.492079
49	1	0	-2.350163	-2.067428	-3.580790
50	1	0	-1.028560	-2.592212	-2.530903
51	1	0	-2.881787	-3.080348	0.867035
52	1	0	-2.059091	-3.517705	-0.636722
53	1	0	-3.808443	-3.265375	-0.627152
54	1	0	-4.956169	-1.216767	1.339274
55	1	0	-4.496884	0.417320	1.838027
56	1	0	-3.456230	-0.950106	2.243121
57	1	0	3.065457	-1.621288	-2.121152
58	1	0	5.518138	-1.824349	-2.400038
59	1	0	7.051839	-0.466641	-0.985602
60	1	0	6.104334	1.077727	0.721749

Chapter VI.

61	1	0	3.656369	1.246939	1.024810
----	---	---	----------	----------	----------

TS3

Zero-point correction=	0.507061
(Hartree/Particle)	
Thermal correction to Energy=	0.537165
Thermal correction to Enthalpy=	0.538110
Thermal correction to Gibbs Free Energy=	0.446812
Sum of electronic and zero-point Energies=	-1323.991913
Sum of electronic and thermal Energies=	-1323.961808
Sum of electronic and thermal Enthalpies=	-1323.960864
Sum of electronic and thermal Free Energies=	-1324.052162

Center Number	Atomic Number	Atomic Type	Coordinates (Angstroms)		
			X	Y	Z
1	45	0	-0.973925	-0.203704	-0.014176
2	7	0	-0.415993	0.493839	1.910014
3	6	0	-0.623980	-0.277921	3.131240
4	6	0	0.122019	1.758122	1.990256
5	6	0	0.628635	2.233799	0.668381
6	6	0	1.261800	1.329489	-0.244332
7	6	0	0.528618	3.594487	0.360137
8	6	0	1.707630	1.863997	-1.476903
9	6	0	0.973516	4.090836	-0.861737
10	6	0	1.558366	3.212185	-1.782967
11	8	0	0.202711	2.426308	3.023986
12	6	0	0.705413	-0.803138	0.863366
13	6	0	1.629753	-0.067447	0.156103

14	6	0	0.544550	-1.272232	3.266732
15	6	0	0.859567	-1.892697	1.877183
16	6	0	-2.686049	0.306699	-1.661930
17	6	0	-1.881378	-0.894770	-1.961185
18	6	0	-2.153138	-1.885928	-0.977919
19	6	0	-2.911549	-1.229755	0.056934
20	6	0	-3.311339	0.107764	-0.438431
21	6	0	-2.723279	1.523654	-2.538242
22	6	0	-1.110379	-1.085665	-3.235674
23	6	0	-1.721999	-3.323445	-0.996339
24	6	0	-3.525417	-1.893312	1.254341
25	6	0	-4.214068	1.043087	0.310711
26	6	0	2.966912	-0.602253	-0.200435
27	6	0	4.114349	0.214362	-0.140673
28	6	0	5.377017	-0.300334	-0.425030
29	6	0	5.531692	-1.643636	-0.780807
30	6	0	4.405143	-2.464171	-0.856656
31	6	0	3.139055	-1.947575	-0.579883
32	1	0	-0.656621	0.409916	3.981424
33	1	0	-1.581538	-0.806368	3.071757
34	1	0	0.087307	4.248578	1.106350
35	1	0	2.199372	1.202665	-2.184400
36	1	0	0.870357	5.146473	-1.096582
37	1	0	1.911682	3.584601	-2.741593
38	1	0	0.334332	-2.051821	4.009618
39	1	0	1.428865	-0.720342	3.606615
40	1	0	0.170775	-2.720168	1.665539
41	1	0	1.879225	-2.294827	1.872549
42	1	0	-3.219661	1.307648	-3.494489
43	1	0	-1.714015	1.882900	-2.772723
44	1	0	-3.262518	2.347047	-2.062295

45	1	0	-0.574229	-0.173743	-3.516881
46	1	0	-1.782753	-1.339805	-4.067813
47	1	0	-0.374714	-1.890291	-3.146541
48	1	0	-0.784154	-3.455537	-1.544880
49	1	0	-2.477762	-3.957755	-1.481227
50	1	0	-1.571179	-3.714082	0.015254
51	1	0	-3.660724	-1.188111	2.080070
52	1	0	-2.913840	-2.725275	1.616271
53	1	0	-4.517663	-2.297292	1.005785
54	1	0	-5.244829	0.663269	0.337885
55	1	0	-4.238468	2.034253	-0.150186
56	1	0	-3.886008	1.171232	1.348351
57	1	0	4.010178	1.256751	0.145354
58	1	0	6.246787	0.348627	-0.359803
59	1	0	6.517680	-2.042279	-1.003788
60	1	0	4.508126	-3.506766	-1.147339
61	1	0	2.264127	-2.585381	-0.673788

E₁

Zero-point correction=	0.509924
(Hartree/Particle)	
Thermal correction to Energy=	0.540110
Thermal correction to Enthalpy=	0.541054
Thermal correction to Gibbs Free Energy=	0.450189
Sum of electronic and zero-point Energies=	-1324.047336
Sum of electronic and thermal Energies=	-1324.017151
Sum of electronic and thermal Enthalpies=	-1324.016207
Sum of electronic and thermal Free Energies=	-1324.107071

Center Number	Atomic Number	Atomic Type	Coordinates (Angstroms)		
			X	Y	Z
<hr/>					
1	45	0	-0.857330	-0.059080	-0.034731
2	7	0	-0.218498	1.584712	1.476090
3	6	0	-1.040682	1.755694	2.697408
4	6	0	0.209613	2.741031	0.794400
5	6	0	1.329260	2.545216	-0.147812
6	6	0	1.898221	1.260017	-0.341352
7	6	0	1.820663	3.671127	-0.815059
8	6	0	2.999087	1.178389	-1.215873
9	6	0	2.893537	3.558815	-1.694368
10	6	0	3.478923	2.304027	-1.884119
11	8	0	-0.336880	3.813573	1.023541
12	6	0	0.447202	0.306632	1.482209
13	6	0	1.349502	0.081863	0.379504
14	6	0	-0.992163	0.377206	3.378669
15	6	0	0.330126	-0.246263	2.886343
16	6	0	-1.641164	-1.043044	-2.011120
17	6	0	-1.663147	-1.958892	-0.860774
18	6	0	-2.684367	-1.513419	0.053822
19	6	0	-3.114211	-0.243240	-0.409376
20	6	0	-2.508707	0.017858	-1.720917
21	6	0	-0.874442	-1.263361	-3.282994
22	6	0	-1.012193	-3.311065	-0.823205
23	6	0	-3.189193	-2.266988	1.250321
24	6	0	-4.149470	0.641420	0.224831
25	6	0	-2.833215	1.198156	-2.591266
26	6	0	3.101716	-3.090401	-0.822647
27	6	0	2.296661	-1.952036	-0.789264
28	6	0	2.178973	-1.171081	0.373133

29	6	0	2.921042	-1.566952	1.498264
30	6	0	3.716076	-2.715546	1.475565
31	6	0	3.809439	-3.484424	0.315614
32	1	0	-0.580505	2.541633	3.306345
33	1	0	-2.047794	2.084602	2.435691
34	1	0	1.341635	4.625544	-0.621450
35	1	0	3.488884	0.224472	-1.371829
36	1	0	3.272736	4.432397	-2.216437
37	1	0	4.327639	2.197314	-2.555515
38	1	0	-1.834185	-0.236672	3.048046
39	1	0	-1.038462	0.464958	4.468048
40	1	0	0.333475	-1.337883	2.914197
41	1	0	1.167752	0.107682	3.507957
42	1	0	-1.462243	-1.853719	-4.001329
43	1	0	0.055037	-1.812586	-3.106229
44	1	0	-0.613479	-0.318512	-3.769659
45	1	0	-0.879593	-3.661515	0.205037
46	1	0	-0.026382	-3.305386	-1.293363
47	1	0	-1.628197	-4.054532	-1.350614
48	1	0	-2.388559	-2.822100	1.750457
49	1	0	-3.960305	-2.998682	0.966722
50	1	0	-3.640921	-1.598782	1.990928
51	1	0	-4.257141	0.438142	1.294987
52	1	0	-5.135917	0.494068	-0.237967
53	1	0	-3.896682	1.701342	0.110060
54	1	0	-3.803924	1.069656	-3.092514
55	1	0	-2.078889	1.342851	-3.370391
56	1	0	-2.890984	2.127140	-2.013616
57	1	0	3.172660	-3.673097	-1.737855
58	1	0	1.748143	-1.649186	-1.675542
59	1	0	2.892636	-0.961855	2.398985

60	1	0	4.273850	-2.999537	2.364482
61	1	0	4.431559	-4.375174	0.294668

C₂

Zero-point correction=	0.507267
(Hartree/Particle)	
Thermal correction to Energy=	0.538257
Thermal correction to Enthalpy=	0.539201
Thermal correction to Gibbs Free Energy=	0.445987
Sum of electronic and zero-point Energies=	-1323.991468
Sum of electronic and thermal Energies=	-1323.960478
Sum of electronic and thermal Enthalpies=	-1323.959533
Sum of electronic and thermal Free Energies=	-1324.052748

Center Number	Atomic Number	Atomic Type	Coordinates (Angstroms)		
			X	Y	Z
1	45	0	-0.592862	-0.200204	0.004959
2	7	0	-1.452661	1.351988	1.105769
3	6	0	-2.253820	1.176436	2.313037
4	6	0	-1.050542	2.623377	0.818737
5	6	0	0.005603	2.645421	-0.228850
6	6	0	0.470898	1.412427	-0.700265
7	6	0	0.559352	3.848578	-0.675324
8	6	0	1.530203	1.397119	-1.610789
9	6	0	1.596726	3.829226	-1.605436
10	6	0	2.083440	2.602118	-2.065182
11	8	0	-1.479432	3.637754	1.384285
12	6	0	1.259463	-0.631242	1.209034
13	6	0	0.293999	-0.488558	1.992850

14	6	0	-1.968069	-0.139358	3.043036
15	6	0	-0.466034	-0.375259	3.255406
16	6	0	2.663748	-0.776193	0.898338
17	6	0	3.126257	-1.406892	-0.267958
18	6	0	4.491716	-1.560969	-0.499375
19	6	0	5.421234	-1.083129	0.426715
20	6	0	4.974121	-0.448755	1.588686
21	6	0	3.610426	-0.294639	1.825025
22	1	0	-3.330487	1.229843	2.090678
23	1	0	-2.039733	2.021843	2.979434
24	1	0	0.164121	4.775872	-0.268941
25	1	0	1.949319	0.462912	-1.969765
26	1	0	2.034787	4.758578	-1.960542
27	1	0	2.906547	2.575780	-2.776458
28	1	0	-2.470653	-0.118306	4.018001
29	1	0	-2.381091	-0.989064	2.489297
30	1	0	-0.307735	-1.289418	3.844413
31	1	0	-0.043274	0.454195	3.840560
32	1	0	2.404507	-1.773476	-0.988165
33	1	0	4.830946	-2.053396	-1.406913
34	1	0	6.485692	-1.200113	0.243166
35	1	0	5.689807	-0.068256	2.312476
36	1	0	3.263089	0.204695	2.724302
37	6	0	-0.850527	-1.214682	-2.069603
38	6	0	-0.790925	-2.289760	-1.130564
39	6	0	-1.951674	-2.217124	-0.270490
40	6	0	-2.698526	-1.077523	-0.650051
41	6	0	-1.996400	-0.408172	-1.731398
42	6	0	0.000543	-1.046906	-3.293883
43	6	0	0.163271	-3.450178	-1.136498
44	6	0	-2.318029	-3.265388	0.741544

45	6	0	-4.033211	-0.643275	-0.121641
46	6	0	-2.527113	0.756159	-2.517279
47	1	0	-0.472651	-1.543972	-4.152411
48	1	0	0.994475	-1.486972	-3.170339
49	1	0	0.135491	0.005822	-3.552153
50	1	0	0.989950	-3.298769	-1.834904
51	1	0	-0.358192	-4.367195	-1.444197
52	1	0	0.588166	-3.636537	-0.144391
53	1	0	-1.460687	-3.548304	1.362389
54	1	0	-2.672782	-4.180594	0.246686
55	1	0	-3.116239	-2.928999	1.408993
56	1	0	-4.252977	-1.079240	0.856405
57	1	0	-4.831096	-0.956219	-0.809504
58	1	0	-4.087927	0.444608	-0.029387
59	1	0	-3.263304	0.427002	-3.264399
60	1	0	-1.724951	1.278839	-3.044279
61	1	0	-3.017017	1.484895	-1.864792

TS4

Zero-point correction=	0.506380
(Hartree/Particle)	
Thermal correction to Energy=	0.536787
Thermal correction to Enthalpy=	0.537731
Thermal correction to Gibbs Free Energy=	0.446474
Sum of electronic and zero-point Energies=	-1323.976009
Sum of electronic and thermal Energies=	-1323.945601
Sum of electronic and thermal Enthalpies=	-1323.944657
Sum of electronic and thermal Free Energies=	-1324.035914

Chapter VI.

Center Number	Atomic Number	Atomic Type	Coordinates (Angstroms)		
			X	Y	Z
<hr/>					
1	45	0	-0.457446	-0.371446	-0.177873
2	7	0	-1.658754	0.426571	1.413657
3	6	0	-2.268235	-0.312601	2.511845
4	6	0	-2.038407	1.755099	1.262357
5	6	0	-1.432346	2.373712	0.058726
6	6	0	-0.641226	1.564969	-0.774694
7	6	0	-1.659594	3.725144	-0.231367
8	6	0	-0.071924	2.156285	-1.911859
9	6	0	-1.093530	4.295416	-1.367751
10	6	0	-0.297648	3.505991	-2.205256
11	8	0	-2.792072	2.350092	2.037610
12	6	0	1.146163	0.367352	1.063893
13	6	0	0.365988	0.407343	2.063463
14	6	0	-1.194936	-0.737478	3.539570
15	6	0	-0.074566	0.311931	3.464355
16	6	0	2.575490	0.456131	0.768437
17	6	0	3.503013	-0.275962	1.534559
18	6	0	4.870035	-0.186196	1.273446
19	6	0	5.336849	0.640547	0.249096
20	6	0	4.424861	1.373164	-0.514566
21	6	0	3.055795	1.278418	-0.265466
22	1	0	-2.803393	-1.191233	2.130661
23	1	0	-2.995506	0.353184	2.985127
24	1	0	-2.285794	4.298817	0.446446
25	1	0	0.562326	1.576541	-2.577795
26	1	0	-1.264831	5.342669	-1.602437
27	1	0	0.155054	3.943931	-3.092832
28	1	0	-1.612297	-0.790631	4.550884

29	1	0	-0.782356	-1.724086	3.296628
30	1	0	0.786763	0.025960	4.082566
31	1	0	-0.447941	1.281909	3.817216
32	1	0	3.142389	-0.916079	2.334990
33	1	0	5.570838	-0.759135	1.875168
38	6	0	0.382479	-1.596035	-1.872003
39	6	0	0.417348	-2.515440	-0.745329
40	6	0	-0.904263	-2.733555	-0.302928
41	6	0	-1.792539	-1.958764	-1.155556
42	6	0	-1.534433	-0.608768	-3.371784
43	6	0	1.558203	-1.275165	-2.751198
44	6	0	1.669233	-3.137989	-0.200443
45	6	0	-1.355344	-3.664109	0.785869
46	6	0	-3.292181	-1.981853	-1.087273
47	1	0	-1.657698	-1.313975	-4.205737
48	1	0	-0.864533	0.186432	-3.707062
49	1	0	-2.508131	-0.152015	-3.175058
50	1	0	1.356524	-0.411200	-3.391279
51	1	0	1.797247	-2.120032	-3.413490
52	1	0	2.455811	-1.050244	-2.166627
53	1	0	2.481036	-2.408494	-0.119763
54	1	0	2.019109	-3.943206	-0.861479
55	1	0	1.510733	-3.572581	0.790957
56	1	0	-0.540070	-3.916014	1.470499
57	1	0	-1.732491	-4.607359	0.366155
58	1	0	-2.168079	-3.233501	1.380089
59	1	0	-3.696342	-2.859117	-1.612585
60	1	0	-3.729537	-1.090702	-1.545628
61	1	0	-3.647889	-2.028658	-0.053670

D₂

Zero-point correction=	0.508604
(Hartree/Particle)	
Thermal correction to Energy=	0.538964
Thermal correction to Enthalpy=	0.539908
Thermal correction to Gibbs Free Energy=	0.448728
Sum of electronic and zero-point Energies=	-1324.011344
Sum of electronic and thermal Energies=	-1323.980985
Sum of electronic and thermal Enthalpies=	-1323.980040
Sum of electronic and thermal Free Energies=	-1324.071220

Center	Atomic Number	Atomic Number	Atomic Type	Coordinates (Angstroms)		
Number	X	Y	Z			
1	45	0	0	-0.457031	0.495321	-0.077740
2	7	0	0	-0.840069	-1.300397	-1.407022
3	6	0	0	-0.981533	-1.405215	-2.879489
4	6	0	0	-1.748864	-2.178964	-0.667980
5	6	0	0	-1.656598	-2.016625	0.794162
6	6	0	0	-1.033740	-0.859265	1.311025
7	6	0	0	-2.215175	-2.998497	1.628665
8	6	0	0	-0.943112	-0.755123	2.707582
9	6	0	0	-2.122554	-2.863798	3.008924
10	6	0	0	-1.475843	-1.742055	3.542621
11	8	0	0	-2.504468	-2.931415	-1.256266
12	6	0	0	1.162335	-0.749579	-0.353768
13	6	0	0	0.604985	-1.623096	-1.189603
14	6	0	0	-0.075283	-2.597056	-3.287829
15	6	0	0	0.992051	-2.719768	-2.154949
16	6	0	0	3.622521	-0.591412	-0.806997
17	6	0	0	4.940895	-0.499335	-0.359760

18	6	0	5.220012	-0.472600	1.008312
19	6	0	4.167137	-0.531067	1.925768
20	6	0	2.848273	-0.613301	1.480986
21	6	0	2.551491	-0.658715	0.105019
22	1	0	-0.617040	-0.465729	-3.303880
23	1	0	-2.027726	-1.550651	-3.149084
24	1	0	-2.712492	-3.851627	1.175413
25	1	0	-0.446754	0.099969	3.159217
26	1	0	-2.541419	-3.621018	3.665792
27	1	0	-1.385136	-1.635998	4.621919
28	1	0	-0.674560	-3.508325	-3.351483
29	1	0	0.382673	-2.424079	-4.266576
30	1	0	2.014893	-2.591179	-2.519560
31	1	0	0.941881	-3.709699	-1.683095
32	1	0	3.412215	-0.602359	-1.873158
33	1	0	5.751692	-0.447669	-1.082292
34	1	0	6.247071	-0.402674	1.356470
35	1	0	4.374346	-0.511451	2.992853
36	1	0	2.029594	-0.659635	2.192913
37	6	0	-1.465228	2.395391	0.817007
38	6	0	-0.011574	2.420345	0.898167
39	6	0	0.496799	2.604348	-0.455047
40	6	0	-0.596439	2.534385	-1.339467
41	6	0	-1.818282	2.393926	-0.549189
42	6	0	-2.400757	2.411485	1.990099
43	6	0	0.794681	2.637386	2.147147
44	6	0	1.933980	2.862194	-0.800823
45	6	0	-0.565292	2.679278	-2.833915
46	6	0	-3.204715	2.378933	-1.128191
47	1	0	-2.464922	3.421109	2.419404
48	1	0	-2.072580	1.735037	2.784939

Chapter VI.

49	1	0	-3.411651	2.108803	1.703198
50	1	0	0.286715	2.233873	3.028325
51	1	0	0.959518	3.709446	2.330614
52	1	0	1.776614	2.158485	2.079019
53	1	0	2.612344	2.243465	-0.206505
54	1	0	2.193828	3.913209	-0.610082
55	1	0	2.141096	2.659432	-1.855766
56	1	0	0.429148	2.473143	-3.240924
57	1	0	-0.840719	3.698414	-3.140460
58	1	0	-1.273050	1.999259	-3.320815
59	1	0	-3.527868	3.391834	-1.408176
60	1	0	-3.937136	1.984280	-0.418497
61	1	0	-3.258977	1.763802	-2.033011

TS5

Zero-point correction= (Hartree/Particle)

Thermal correction to Energy=

0.507423

Thermal correction to Enthalpy=

0.537468

Thermal correction to Gibbs Free Energy=

0.538412

Sum of electronic and zero-point Energies=

0.447527

Sum of electronic and thermal Energies=

-1323.987655

Sum of electronic and thermal Enthalpies=

-1323.957610

Sum of electronic and thermal Free Energies=

-1323.956666

Center	Atomic	Atomic	Coordinates (Angstroms)		
Number	Number	Type	X	Y	Z

1	45	0	0.825921	-0.094480	-0.169353
2	7	0	-0.950028	2.184922	-1.346943

3	6	0	-1.447978	2.886836	-2.546731
4	6	0	-0.222544	2.941218	-0.413855
5	6	0	-0.138323	2.373299	0.946628
6	6	0	-0.211285	0.971349	1.207564
7	6	0	-0.063923	3.288283	2.012300
8	6	0	-0.341178	0.560754	2.558852
9	6	0	-0.156064	2.857608	3.328862
10	6	0	-0.319072	1.486995	3.593803
11	8	0	0.190159	4.057668	-0.734144
12	6	0	-1.278879	0.075520	-0.200281
13	6	0	-1.709430	1.033370	-1.064724
14	6	0	-2.508403	1.927394	-3.113870
15	6	0	-2.978379	1.124834	-1.883487
16	6	0	2.676753	-1.013881	0.871965
17	6	0	1.645189	-1.977161	0.500385
18	6	0	1.696386	-2.164114	-0.962314
19	6	0	2.543990	-1.181550	-1.464441
20	6	0	3.129242	-0.438702	-0.326433
21	6	0	3.091309	-0.682138	2.274451
22	6	0	0.963936	-2.918185	1.448715
23	6	0	1.006539	-3.261848	-1.714782
24	6	0	2.890891	-0.920034	-2.900800
25	6	0	4.132257	0.666506	-0.485432
26	6	0	-2.181502	-1.046974	0.168061
27	6	0	-2.329704	-2.145093	-0.700706
28	6	0	-3.193504	-3.198013	-0.396881
29	6	0	-3.926804	-3.183831	0.792319
30	6	0	-3.798664	-2.098557	1.660636
31	6	0	-2.943184	-1.039074	1.349858
32	1	0	-0.625719	3.090328	-3.238025
33	1	0	-1.865335	3.854139	-2.245444

34	1	0	0.035478	4.341415	1.767390
35	1	0	-0.446259	-0.496407	2.783927
36	1	0	-0.123841	3.574411	4.144339
37	1	0	-0.409797	1.142403	4.622010
38	1	0	-3.320218	2.462793	-3.614290
39	1	0	-2.051979	1.249027	-3.844060
40	1	0	-3.398924	0.148161	-2.131690
41	1	0	-3.746889	1.687184	-1.330631
42	1	0	3.637454	-1.517891	2.733274
43	1	0	2.226948	-0.459721	2.910589
44	1	0	3.747332	0.192560	2.299658
45	1	0	-0.040670	-3.181901	1.104782
46	1	0	0.877230	-2.482590	2.448264
47	1	0	1.539851	-3.850577	1.544732
48	1	0	0.029993	-3.498189	-1.283425
49	1	0	1.602933	-4.185762	-1.687250
50	1	0	0.856470	-3.003066	-2.767845
51	1	0	2.907802	0.152720	-3.123407
52	1	0	2.175096	-1.390239	-3.581522
53	1	0	3.888593	-1.311938	-3.145799
54	1	0	5.110809	0.272265	-0.794641
55	1	0	4.273727	1.220568	0.446245
56	1	0	3.818710	1.385169	-1.250821
57	1	0	-1.767653	-2.154375	-1.629905
58	1	0	-3.296249	-4.028521	-1.091253
59	1	0	-4.596241	-4.005045	1.034176
60	1	0	-4.375763	-2.067879	2.581612
61	1	0	-2.866423	-0.192105	2.023678

E

Zero-point correction= 0.509084
 (Hartree/Particle)
 Thermal correction to Energy= 0.539501
 Thermal correction to Enthalpy= 0.540445
 Thermal correction to Gibbs Free Energy= 0.448728
 Sum of electronic and zero-point Energies= -1324.054768
 Sum of electronic and thermal Energies= -1324.024351
 Sum of electronic and thermal Enthalpies= -1324.023407
 Sum of electronic and thermal Free Energies= -1324.115124

Center Number	Atomic Number	Atomic Type	Coordinates (Angstroms)		
			X	Y	Z
1	45	0	0.602860	-0.246958	-0.064514
2	7	0	-0.163108	2.367867	-1.189780
3	6	0	-0.171307	2.934222	-2.535693
4	6	0	0.665750	2.778534	-0.185550
5	6	0	0.568389	1.904175	1.033357
6	6	0	-0.599226	1.082208	1.286976
7	6	0	1.435879	2.218558	2.120336
8	6	0	-0.857848	0.667389	2.635941
9	6	0	1.179707	1.762388	3.390609
10	6	0	0.010248	0.993864	3.648177
11	8	0	1.396430	3.763693	-0.260255
12	6	0	-1.342651	0.613086	0.127350
13	6	0	-0.749981	1.051220	-1.121651
14	6	0	-0.498363	1.717053	-3.419529
15	6	0	-1.344720	0.812749	-2.501099
16	6	0	-2.979518	-1.256700	-0.402453
17	6	0	-4.262164	-1.801698	-0.334370

Chapter VI.

18	6	0	-5.271521	-1.144638	0.372048
19	6	0	-4.987041	0.066763	1.004855
20	6	0	-3.706235	0.615040	0.928961
21	6	0	-2.677323	-0.038669	0.226542
22	1	0	0.795674	3.398355	-2.746517
23	1	0	-0.944016	3.710984	-2.619303
24	1	0	2.270253	2.880804	1.913015
25	1	0	-1.747254	0.079403	2.838125
26	1	0	1.844249	2.021506	4.210310
27	1	0	-0.201420	0.665891	4.662788
28	1	0	-1.018919	1.995543	-4.340331
29	1	0	0.428987	1.202686	-3.695482
30	1	0	-1.324445	-0.236456	-2.800991
31	1	0	-2.396782	1.134357	-2.512791
32	1	0	-2.197409	-1.784195	-0.938532
33	1	0	-4.470613	-2.747511	-0.828194
34	1	0	-6.268659	-1.572646	0.429284
35	1	0	-5.763950	0.591051	1.555339
36	1	0	-3.496725	1.565517	1.412528
37	6	0	1.928590	-2.012938	0.927023
38	6	0	0.997875	-2.627639	0.074447
39	6	0	1.169849	-2.051835	-1.256735
40	6	0	2.317724	-1.172684	-1.229926
41	6	0	2.719014	-1.076106	0.133333
42	6	0	2.121516	-2.251903	2.397071
43	6	0	0.018693	-3.707543	0.433565
44	6	0	0.501394	-2.562446	-2.501771
45	6	0	3.005376	-0.554912	-2.414633
46	6	0	3.876421	-0.287431	0.673680
47	1	0	3.042284	-2.819490	2.593882
48	1	0	1.289140	-2.818821	2.824524

49	1	0	2.196466	-1.309765	2.951989
50	1	0	-0.247522	-3.675530	1.494496
51	1	0	0.433938	-4.705195	0.229015
52	1	0	-0.910933	-3.623658	-0.137467
53	1	0	-0.543224	-2.836433	-2.322376
54	1	0	1.010893	-3.460719	-2.879385
55	1	0	0.518817	-1.818480	-3.303924
56	1	0	2.319576	-0.422210	-3.257454
57	1	0	3.834346	-1.185375	-2.768975
58	1	0	3.421246	0.428571	-2.174742
59	1	0	4.746004	-0.937702	0.846203
60	1	0	3.626227	0.184308	1.630108
61	1	0	4.184233	0.503050	-0.016679

2a

Zero-point correction=
(Hartree/Particle)

0.286555

Thermal correction to Energy= 0.301718

Thermal correction to Enthalpy= 0.302662

Thermal correction to Gibbs Free Energy= 0.243386

Sum of electronic and zero-point Energies= -824.663563

Sum of electronic and thermal Energies= -824.648401

Sum of electronic and thermal Enthalpies= -824.647457

Sum of electronic and thermal Free Energies= -824.706732

Center	Atomic	Atomic	Coordinates (Angstroms)		
Number	Number	Type	X	Y	Z

1	7	0	-1.657605	-1.430834	0.084401
---	---	---	-----------	-----------	----------

2	6	0	-2.093958	-2.830861	0.169651
3	6	0	-2.572002	-0.383593	0.070660
4	6	0	-1.949490	0.948368	-0.014012
5	6	0	-0.537113	1.105510	-0.047541
6	6	0	-2.795245	2.068808	-0.067598
7	6	0	-0.022766	2.418695	-0.149292
8	6	0	-2.265762	3.345965	-0.159364
9	6	0	-0.871200	3.513936	-0.202650
10	8	0	-3.781898	-0.605423	0.119596
11	6	0	0.320884	-0.069125	0.009265
12	6	0	-0.280181	-1.290990	0.072927
13	6	0	-0.826511	-3.606184	-0.226186
14	6	0	0.328580	-2.670800	0.192915
15	6	0	2.564104	-0.315707	-1.115158
16	6	0	3.956980	-0.219956	-1.106973
17	6	0	4.620386	0.250438	0.027830
18	6	0	3.882583	0.624108	1.153332
19	6	0	2.490709	0.522269	1.145161
20	6	0	1.809914	0.047712	0.011869
21	1	0	-2.948553	-2.989284	-0.490989
22	1	0	-2.420093	-3.052810	1.193792
23	1	0	-3.865950	1.894672	-0.036674
24	1	0	1.051625	2.564155	-0.188008
25	1	0	-2.921961	4.210719	-0.200803
26	1	0	-0.449435	4.512850	-0.281059
27	1	0	-0.773837	-4.588900	0.249572
28	1	0	-0.808646	-3.756507	-1.311439
29	1	0	1.228856	-2.789045	-0.413715
30	1	0	0.619930	-2.851773	1.237359
31	1	0	2.048843	-0.667314	-2.005424
32	1	0	4.522663	-0.506601	-1.989753

33	1	0	5.704324	0.327944	0.034549
34	1	0	4.391050	0.991072	2.041154
35	1	0	1.920121	0.808479	2.024854

F

Zero-point correction=	0.467853
(Hartree/Particle)	
Thermal correction to Energy=	0.498968
Thermal correction to Enthalpy=	0.499912
Thermal correction to Gibbs Free Energy=	0.405593
Sum of electronic and zero-point Energies=	-1246.598040
Sum of electronic and thermal Energies=	-1246.566924
Sum of electronic and thermal Enthalpies=	-1246.565980
Sum of electronic and thermal Free Energies=	-1246.660299

Center Number	Atomic Number	Atomic Type	Coordinates (Angstroms)		
			X	Y	Z
1	45	0	0.683165	-0.240669	-0.217272
2	7	0	1.692371	1.216530	-1.321110
3	6	0	2.698587	0.922775	-2.320364
4	6	0	1.384154	2.522104	-1.092972
5	6	0	0.303205	2.651430	-0.072995
6	6	0	-0.216157	1.468719	0.464699
7	6	0	-0.174021	3.899547	0.335146
8	6	0	-1.235713	1.546060	1.418120
9	6	0	-1.181121	3.974676	1.297576
10	6	0	-1.709244	2.797768	1.836755
11	8	0	1.919182	3.491092	-1.647980
12	6	0	-1.341520	-0.501593	-1.487712

13	6	0	-0.276041	-0.493164	-2.129440
14	6	0	-2.698090	-0.576523	-1.034424
15	6	0	-3.324291	-1.833273	-0.898410
16	6	0	-4.658161	-1.917349	-0.507095
17	6	0	-5.386987	-0.753729	-0.246143
18	6	0	-4.776750	0.495614	-0.385104
19	6	0	-3.443050	0.591529	-0.775722
20	1	0	2.436402	0.020852	-2.889210
21	1	0	3.693661	0.751649	-1.879211
22	1	0	2.787516	1.768974	-3.009486
23	1	0	0.263169	4.787244	-0.114500
24	1	0	-1.682476	0.646491	1.834857
25	1	0	-1.555796	4.940977	1.625805
26	1	0	-2.498812	2.848093	2.584023
27	1	0	0.286800	-0.485178	-3.043343
28	1	0	-2.760102	-2.733295	-1.123479
29	1	0	-5.130917	-2.890934	-0.411155
30	1	0	-6.427802	-0.820483	0.058478
31	1	0	-5.342333	1.402397	-0.189969
32	1	0	-2.966902	1.558672	-0.883883
33	6	0	1.330051	-0.898280	1.896149
34	6	0	0.429218	-1.892665	1.401756
35	6	0	1.068608	-2.538852	0.267852
36	6	0	2.328508	-1.934189	0.046703
37	6	0	2.470866	-0.865099	1.018910
38	6	0	1.186606	-0.105921	3.161661
39	6	0	-0.839749	-2.350806	2.062097
40	6	0	0.502787	-3.704861	-0.488525
41	6	0	3.363617	-2.377105	-0.946608
42	6	0	3.691309	-0.015306	1.220772
43	1	0	1.611899	-0.666159	4.006183

44	1	0	0.141889	0.110368	3.396490
45	1	0	1.711299	0.850708	3.098906
46	1	0	-1.224397	-1.594651	2.751803
47	1	0	-0.671327	-3.268210	2.643690
48	1	0	-1.630620	-2.562974	1.335881
49	1	0	-0.587783	-3.739798	-0.415464
50	1	0	0.887031	-4.651653	-0.084453
51	1	0	0.767095	-3.670001	-1.549892
52	1	0	2.905622	-2.828748	-1.832428
53	1	0	4.032354	-3.129908	-0.505803
54	1	0	3.987243	-1.545377	-1.283836
55	1	0	4.351756	-0.462456	1.976763
56	1	0	3.427721	0.990419	1.558645
57	1	0	4.265631	0.089593	0.297328

TS6

Zero-point correction= 0.467773
 (Hartree/Particle)

Thermal correction to Energy= 0.497641

Thermal correction to Enthalpy= 0.498585

Thermal correction to Gibbs Free Energy= 0.408184

Sum of electronic and zero-point Energies= -1246.574583

Sum of electronic and thermal Energies= -1246.544716

Sum of electronic and thermal Enthalpies= -1246.543772

Sum of electronic and thermal Free Energies= -1246.634172

Center	Atomic	Atomic	Coordinates (Angstroms)		
Number	Number	Type	X	Y	Z

1	45	0	0.904209	-0.147940	-0.244726
---	----	---	----------	-----------	-----------

Chapter VI.

2	7	0	0.844405	1.593693	-1.401094
3	6	0	1.645044	1.782742	-2.594384
4	6	0	-0.068020	2.546365	-1.093621
5	6	0	-0.880934	2.160158	0.102916
6	6	0	-0.840501	0.823903	0.539905
7	6	0	-1.607233	3.117819	0.816092
8	6	0	-1.508426	0.472424	1.725124
9	6	0	-2.263322	2.761356	1.994796
10	6	0	-2.199858	1.439712	2.455662
11	8	0	-0.234512	3.623945	-1.684580
12	6	0	-0.350670	-0.807792	-1.705434
13	6	0	-1.348056	-0.542778	-0.948037
14	6	0	-3.741507	0.091554	-0.556881
15	6	0	-5.077393	-0.281226	-0.436079
16	6	0	-5.438105	-1.632313	-0.446011
17	6	0	-4.454657	-2.613529	-0.583728
18	6	0	-3.115605	-2.246036	-0.713212
19	6	0	-2.744579	-0.888933	-0.705074
20	1	0	1.200886	2.569063	-3.213191
21	1	0	2.677117	2.088059	-2.359875
22	1	0	1.698615	0.850848	-3.172238
23	1	0	-1.617398	4.135405	0.435379
24	1	0	-1.520706	-0.561992	2.059882
25	1	0	-2.819582	3.506678	2.557499
26	1	0	-2.707667	1.158863	3.375476
27	1	0	-0.140663	-1.205823	-2.686862
28	1	0	-3.459251	1.138854	-0.544360
29	1	0	-5.840864	0.484978	-0.333791
30	1	0	-6.481848	-1.917848	-0.345875
31	1	0	-4.728530	-3.665141	-0.591431
32	1	0	-2.345286	-3.003061	-0.826945

33	6	0	2.129658	-0.450583	1.740736
34	6	0	1.651838	-1.731352	1.256893
35	6	0	2.275958	-1.991321	-0.009730
36	6	0	3.055048	-0.847454	-0.362625
37	6	0	2.967964	0.105914	0.742596
38	6	0	1.807640	0.139021	3.082651
39	6	0	0.820302	-2.706794	2.040199
40	6	0	2.152409	-3.260344	-0.802864
41	6	0	3.991821	-0.733728	-1.530253
42	6	0	3.721778	1.401756	0.810638
43	1	0	2.356847	-0.382389	3.878611
44	1	0	0.740003	0.065367	3.312900
45	1	0	2.078179	1.196952	3.132015
46	1	0	0.168207	-2.196681	2.754927
47	1	0	1.457114	-3.394920	2.614390
48	1	0	0.188621	-3.315756	1.385961
49	1	0	1.162026	-3.712637	-0.690954
50	1	0	2.890837	-4.002321	-0.469006
51	1	0	2.321291	-3.087593	-1.869870
52	1	0	3.634163	-1.299953	-2.395614
53	1	0	4.986567	-1.123321	-1.270111
54	1	0	4.119350	0.305091	-1.845069
55	1	0	4.777319	1.225400	1.059982
56	1	0	3.307020	2.070622	1.569011
57	1	0	3.689932	1.931919	-0.145490

G₁

Zero-point correction= 0.470625
(Hartree/Particle)

Thermal correction to Energy= 0.500723

Thermal correction to Enthalpy= 0.501667

Chapter VI.

Thermal correction to Gibbs Free Energy=	0.409852
Sum of electronic and zero-point Energies=	-1246.628247
Sum of electronic and thermal Energies=	-1246.598150
Sum of electronic and thermal Enthalpies=	-1246.597206
Sum of electronic and thermal Free Energies=	-1246.689021

Center Number	Atomic Number	Atomic Type	Coordinates (Angstroms)		
			X	Y	Z
1	45	0	-0.970149	-0.242097	0.175103
2	7	0	-0.534069	0.424201	2.078738
3	6	0	-0.718817	-0.251044	3.347145
4	6	0	0.338896	1.443297	1.995033
5	6	0	0.574666	1.858010	0.543578
6	6	0	1.342672	1.071474	-0.361409
7	6	0	0.141305	3.140993	0.145285
8	6	0	1.644184	1.610799	-1.632294
9	6	0	0.425925	3.636762	-1.118588
10	6	0	1.190523	2.866527	-2.010900
11	8	0	0.886229	2.061533	2.913200
12	6	0	0.816050	-1.149063	0.317442
13	6	0	1.817356	-0.314624	-0.003762
14	6	0	4.237779	0.331569	0.189388
15	6	0	5.595280	0.013035	0.161832
16	6	0	6.009142	-1.289347	-0.124848
17	6	0	5.050059	-2.271439	-0.386619
18	6	0	3.693913	-1.952922	-0.362804
19	6	0	3.260960	-0.647952	-0.064603
20	1	0	-0.455071	0.431272	4.161842
21	1	0	-1.761517	-0.565923	3.471604
22	1	0	-0.082016	-1.145253	3.428239

23	1	0	-0.396654	3.748124	0.867989
24	1	0	2.256847	1.024741	-2.311992
25	1	0	0.085268	4.627943	-1.406274
26	1	0	1.439646	3.259029	-2.993580
27	1	0	0.956767	-2.180878	0.638021
28	1	0	3.927423	1.344620	0.429199
29	1	0	6.331346	0.785136	0.370991
30	1	0	7.067228	-1.536068	-0.149406
31	1	0	5.360144	-3.286582	-0.622199
32	1	0	2.955200	-2.716513	-0.591511
33	6	0	-3.035767	0.324410	-0.966590
34	6	0	-2.137840	-0.511700	-1.784692
35	6	0	-1.967809	-1.756350	-1.137347
36	6	0	-2.599070	-1.642172	0.172370
37	6	0	-3.350531	-0.375696	0.197258
38	6	0	-3.485623	1.695681	-1.375843
39	6	0	-1.646014	-0.122244	-3.147734
40	6	0	-1.289567	-2.980471	-1.678641
41	6	0	-2.793128	-2.765250	1.147981
42	6	0	-4.232174	0.058578	1.329734
43	1	0	-4.117884	1.649598	-2.272771
44	1	0	-2.630979	2.339992	-1.613780
45	1	0	-4.060947	2.186299	-0.586644
46	1	0	-1.265458	0.904726	-3.159016
47	1	0	-2.457642	-0.179697	-3.886649
48	1	0	-0.839994	-0.778358	-3.486726
49	1	0	-0.531761	-2.725699	-2.424471
50	1	0	-2.021307	-3.645567	-2.157494
51	1	0	-0.795348	-3.550858	-0.886729
52	1	0	-1.943872	-3.454352	1.140813
53	1	0	-3.694069	-3.344740	0.898526

Chapter VI.

54	1	0	-2.913245	-2.391897	2.169045
55	1	0	-5.116385	-0.588099	1.407983
56	1	0	-4.581207	1.086061	1.198890
57	1	0	-3.703407	0.010453	2.287452

TS7

Zero-point correction=	0.468360
(Hartree/Particle)	
Thermal correction to Energy=	0.498208
Thermal correction to Enthalpy=	0.499152
Thermal correction to Gibbs Free Energy=	0.408855
Sum of electronic and zero-point Energies=	-1246.575463
Sum of electronic and thermal Energies=	-1246.545614
Sum of electronic and thermal Enthalpies=	-1246.544670
Sum of electronic and thermal Free Energies=	-1246.634967

Center	Atomic	Atomic	Coordinates (Angstroms)		
Number	Number	Type	X	Y	Z

1	45	0	0.494025	-0.385879	-0.077050
2	7	0	1.639572	0.470306	-1.672304
3	6	0	2.276672	-0.234670	-2.772310
4	6	0	2.018457	1.787354	-1.497513
5	6	0	1.424917	2.382983	-0.275600
6	6	0	0.664894	1.547314	0.559833
7	6	0	1.643501	3.729728	0.038305
8	6	0	0.117287	2.104711	1.723421
9	6	0	1.097454	4.268479	1.200078
10	6	0	0.333526	3.451328	2.040165
11	8	0	2.780810	2.371791	-2.270890

12	6	0	-1.203994	0.371830	-1.206710
13	6	0	-0.386728	0.363920	-2.169935
14	6	0	-2.612778	0.453412	-0.847202
15	6	0	-3.567190	-0.264112	-1.595191
16	6	0	-4.922028	-0.188431	-1.275859
17	6	0	-5.349669	0.610384	-0.212652
18	6	0	-4.411402	1.330045	0.531154
19	6	0	-3.053170	1.248544	0.225222
20	1	0	1.918027	-1.266023	-2.800347
21	1	0	3.366211	-0.233375	-2.652977
22	1	0	2.064375	0.244230	-3.740515
23	1	0	2.247810	4.324842	-0.641196
24	1	0	-0.492288	1.503030	2.392924
25	1	0	1.260799	5.312790	1.452746
26	1	0	-0.101177	3.863794	2.948614
27	1	0	-0.122286	0.374734	-3.212024
28	1	0	-3.234346	-0.878201	-2.426908
29	1	0	-5.644636	-0.749045	-1.863013
30	1	0	-6.406319	0.672747	0.032900
31	1	0	-4.737558	1.958921	1.355349
32	1	0	-2.323933	1.810606	0.797929
33	6	0	1.130451	-1.372374	1.868421
34	6	0	-0.261834	-1.656456	1.621561
35	6	0	-0.327632	-2.548618	0.474380
36	6	0	0.980099	-2.741171	-0.020803
37	6	0	1.888728	-1.976044	0.817276
38	6	0	1.696603	-0.673847	3.069534
39	6	0	-1.408357	-1.369049	2.549504
40	6	0	-1.590114	-3.173073	-0.042388
41	6	0	1.395163	-3.635233	-1.154078
42	6	0	3.384359	-1.964997	0.688568

Chapter VI.

43	1	0	1.845300	-1.390905	3.889013
44	1	0	1.036813	0.116268	3.435296
45	1	0	2.663884	-0.213826	2.850262
46	1	0	-1.183077	-0.532594	3.217392
47	1	0	-1.627842	-2.240160	3.183687
48	1	0	-2.323488	-1.119226	2.003524
49	1	0	-2.415651	-2.454918	-0.066555
50	1	0	-1.900954	-4.005507	0.604300
51	1	0	-1.462909	-3.572161	-1.052882
52	1	0	0.585603	-3.781175	-1.875758
53	1	0	1.688480	-4.628559	-0.786130
54	1	0	2.255007	-3.230007	-1.696721
55	1	0	3.828376	-2.833052	1.196251
56	1	0	3.819008	-1.064455	1.130744
57	1	0	3.698872	-2.002422	-0.358498

G₂

Zero-point correction= (Hartree/Particle)

0.471814

Thermal correction to Energy=

0.501193

Thermal correction to Enthalpy=

0.502137

Thermal correction to Gibbs Free Energy=

0.413067

Sum of electronic and zero-point Energies=

-1246.628427

Sum of electronic and thermal Energies=

-1246.599048

Sum of electronic and thermal Enthalpies=

-1246.598104

Sum of electronic and thermal Free Energies=

-1246.687174

Center Atomic Atomic Coordinates (Angstroms)

Number Number Type X Y Z

1	45	0	0.428111	-0.394764	-0.072082
---	----	---	----------	-----------	-----------

2	7	0	0.835028	0.731993	-1.973383
3	6	0	1.242580	0.054198	-3.215915
4	6	0	1.693786	1.873305	-1.634041
5	6	0	1.546526	2.306160	-0.233071
6	6	0	0.938392	1.419582	0.684403
7	6	0	2.052885	3.555669	0.158912
8	6	0	0.814005	1.865009	2.009126
9	6	0	1.922959	3.967610	1.480062
10	6	0	1.294373	3.119028	2.399588
11	8	0	2.451575	2.341444	-2.461488
12	6	0	-1.186048	0.579373	-0.871131
13	6	0	-0.599536	1.093024	-1.953238
14	6	0	-2.592738	0.678924	-0.479028
15	6	0	-3.623540	0.444549	-1.409516
16	6	0	-4.962776	0.545361	-1.032888
17	6	0	-5.301527	0.883078	0.279369
18	6	0	-4.288977	1.116127	1.214328
19	6	0	-2.949779	1.005607	0.843025
20	1	0	0.601123	-0.818236	-3.351321
21	1	0	2.286713	-0.257927	-3.137459
22	1	0	1.145447	0.722975	-4.078814
23	1	0	2.540629	4.180813	-0.584045
24	1	0	0.330204	1.238467	2.753994
25	1	0	2.300105	4.936488	1.795185
26	1	0	1.175569	3.438879	3.432990
27	1	0	-0.986306	1.711058	-2.765485
28	1	0	-3.362413	0.173345	-2.428900
29	1	0	-5.743546	0.357673	-1.765739
30	1	0	-6.345186	0.960061	0.572326
31	1	0	-4.544027	1.383785	2.236657
32	1	0	-2.160466	1.192523	1.564390

Chapter VI.

33	6	0	1.461211	-1.772777	1.516069
34	6	0	0.008523	-1.788547	1.594526
35	6	0	-0.484790	-2.485113	0.416396
36	6	0	0.618407	-2.754855	-0.420248
37	6	0	1.828822	-2.304026	0.261596
38	6	0	2.381345	-1.311153	2.607370
39	6	0	-0.801428	-1.521738	2.831862
40	6	0	-1.917022	-2.870068	0.185492
41	6	0	0.600854	-3.486213	-1.732494
42	6	0	3.222378	-2.495589	-0.267151
43	1	0	2.419646	-2.050146	3.419780
44	1	0	2.055375	-0.360578	3.040414
45	1	0	3.401664	-1.169343	2.240685
46	1	0	-0.316619	-0.784259	3.478658
47	1	0	-0.926568	-2.439304	3.425612
48	1	0	-1.801034	-1.148382	2.588686
49	1	0	-2.604505	-2.078451	0.497213
50	1	0	-2.170910	-3.773553	0.757761
51	1	0	-2.115125	-3.082399	-0.869141
52	1	0	-0.382090	-3.439041	-2.210945
53	1	0	0.848856	-4.548689	-1.598035
54	1	0	1.333510	-3.076259	-2.435954
55	1	0	3.567764	-3.526998	-0.107695
56	1	0	3.937859	-1.829038	0.222406
57	1	0	3.278223	-2.303755	-1.344360

H

Zero-point correction=	0.536345
(Hartree/Particle)	
Thermal correction to Energy=	0.568566
Thermal correction to Enthalpy=	0.569510

Thermal correction to Gibbs Free Energy=	0.474392				
Sum of electronic and zero-point Energies=	-1363.269276				
Sum of electronic and thermal Energies=	-1363.237055				
Sum of electronic and thermal Enthalpies=	-1363.236111				
Sum of electronic and thermal Free Energies=	-1363.331229				
<hr/>					
Center Number	Atomic Number	Atomic Type	Coordinates (Angstroms)		
X	Y	Z			
<hr/>					
1	45	0	-0.603708	-0.195052	-0.143345
2	7	0	-1.557735	1.450262	0.740027
3	6	0	-2.887958	0.421916	2.633449
4	6	0	-1.000961	2.681004	0.549895
5	6	0	0.219971	2.605763	-0.299521
6	6	0	0.610755	1.343666	-0.754545
7	6	0	0.930604	3.754837	-0.659223
8	6	0	1.736640	1.237904	-1.576274
9	6	0	2.043273	3.648466	-1.492938
10	6	0	2.441390	2.389304	-1.952117
11	8	0	-1.440912	3.751290	0.994150
12	6	0	0.096242	-0.507639	1.924885
13	6	0	1.169309	-0.543004	1.284182
14	6	0	-1.659710	0.462634	3.555772
15	6	0	-0.620531	-0.620961	3.219442
16	6	0	-2.823370	1.401310	1.451890
17	6	0	2.586858	-0.699875	1.071374
18	6	0	3.150056	-1.991453	1.035043
19	6	0	4.526372	-2.161848	0.900092
20	6	0	5.363690	-1.047992	0.801602
21	6	0	4.816423	0.236827	0.845688
22	6	0	3.440782	0.416012	0.977360

Chapter VI.

23	1	0	-3.795237	0.663844	3.203280
24	1	0	-3.024076	-0.606094	2.274927
25	1	0	0.582331	4.711026	-0.277977
26	1	0	2.092066	0.269301	-1.917002
27	1	0	2.599171	4.536446	-1.783326
28	1	0	3.312616	2.295406	-2.597307
29	1	0	-1.967455	0.286643	4.594138
30	1	0	-1.190764	1.452641	3.524865
31	1	0	-1.118802	-1.600816	3.256885
32	1	0	0.155474	-0.639034	3.998219
33	1	0	-3.650328	1.166079	0.760813
34	1	0	-3.005651	2.417245	1.818264
35	1	0	2.500533	-2.855907	1.136833
36	1	0	4.945202	-3.164377	0.878740
37	1	0	6.437177	-1.180647	0.697817
38	1	0	5.463659	1.106896	0.778085
39	1	0	3.016829	1.412700	1.011409
40	6	0	-0.921743	-0.914570	-2.328295
41	6	0	-0.290197	-1.975401	-1.606600
42	6	0	-1.229798	-2.449267	-0.604544
43	6	0	-2.408189	-1.670468	-0.686304
44	6	0	-2.191188	-0.660564	-1.708657
45	6	0	-0.429056	-0.260437	-3.585011
46	6	0	0.997842	-2.658029	-1.966888
47	6	0	-0.977215	-3.621047	0.298097
48	6	0	-3.714513	-1.925114	0.008457
49	6	0	-3.218291	0.315800	-2.203264
50	1	0	-0.830899	-0.789354	-4.460770
51	1	0	0.660075	-0.275344	-3.660160
52	1	0	-0.747566	0.782890	-3.650878
53	1	0	1.639033	-2.013467	-2.574392

54	1	0	0.806994	-3.571398	-2.548362
55	1	0	1.570492	-2.945524	-1.080673
56	1	0	-0.010314	-3.530693	0.805543
57	1	0	-0.960749	-4.559058	-0.273078
58	1	0	-1.748439	-3.714867	1.067414
59	1	0	-3.588022	-2.517774	0.918571
60	1	0	-4.393889	-2.482477	-0.652171
61	1	0	-4.222007	-0.996356	0.281990
62	1	0	-3.818295	-0.128655	-3.010011
63	1	0	-2.751251	1.223174	-2.595248
64	1	0	-3.904521	0.616081	-1.407572

TS8

Zero-point correction= 0.535264
(Hartree/Particle)

Thermal correction to Energy= 0.566707

Thermal correction to Enthalpy= 0.567651

Thermal correction to Gibbs Free Energy= 0.474529

Sum of electronic and zero-point Energies= -1363.250406

Sum of electronic and thermal Energies= -1363.218963

Sum of electronic and thermal Enthalpies= -1363.218019

Sum of electronic and thermal Free Energies= -1363.311141

Center	Atomic	Atomic	Coordinates (Angstroms)		
Number	Number	Type	X	Y	Z

1	45	0	-0.806223	-0.155924	-0.102786
2	7	0	-1.022227	1.661313	0.930359
3	6	0	-2.018597	0.884891	3.131987
4	6	0	-0.148197	2.661672	0.640090
5	6	0	0.804308	2.267934	-0.441597

6	6	0	0.917224	0.906800	-0.782907
7	6	0	1.514145	3.240148	-1.151474
8	6	0	1.714592	0.549422	-1.885736
9	6	0	2.303401	2.875325	-2.242194
10	6	0	2.388730	1.528085	-2.616325
11	8	0	-0.119410	3.788054	1.159461
12	6	0	0.336006	-0.467808	1.578068
13	6	0	1.324912	-0.296339	0.771853
14	6	0	-0.643701	0.505416	3.707376
15	6	0	0.010195	-0.707303	3.004702
16	6	0	-1.996596	1.909159	1.980790
17	6	0	2.719030	-0.731493	0.654811
18	6	0	3.028938	-2.091314	0.836508
19	6	0	4.354812	-2.525658	0.827078
20	6	0	5.388792	-1.606804	0.640692
21	6	0	5.091085	-0.252114	0.462290
22	6	0	3.768492	0.184240	0.460670
23	1	0	-2.639139	1.320999	3.926874
24	1	0	-2.533116	-0.032630	2.821103
25	1	0	1.403449	4.275213	-0.840695
26	1	0	1.844539	-0.497023	-2.148858
27	1	0	2.845660	3.631875	-2.803373
28	1	0	2.999750	1.236400	-3.467499
29	1	0	-0.751024	0.238559	4.766746
30	1	0	0.037583	1.363617	3.663117
31	1	0	-0.667324	-1.568245	3.090633
32	1	0	0.938552	-0.976741	3.530033
33	1	0	-3.012395	1.964854	1.554786
34	1	0	-1.773074	2.902394	2.385487
35	1	0	2.219789	-2.800298	0.987289
36	1	0	4.578366	-3.579996	0.966939

37	1	0	6.422274	-1.942834	0.634990
38	1	0	5.893713	0.467308	0.324545
39	1	0	3.537131	1.234870	0.320855
40	6	0	-1.739717	-0.722915	-2.193029
41	6	0	-1.191462	-1.904335	-1.554908
42	6	0	-1.956804	-2.170879	-0.368765
43	6	0	-2.893980	-1.109819	-0.205194
44	6	0	-2.752315	-0.209515	-1.349373
45	6	0	-1.320002	-0.185758	-3.529634
46	6	0	-0.167339	-2.823368	-2.158321
47	6	0	-1.803646	-3.378100	0.511042
48	6	0	-4.027564	-1.055825	0.778118
49	6	0	-3.625956	0.984527	-1.600476
50	1	0	-1.691613	-0.828561	-4.339498
51	1	0	-0.231076	-0.128793	-3.623813
52	1	0	-1.713632	0.819911	-3.699054
53	1	0	0.492551	-2.290632	-2.848661
54	1	0	-0.651719	-3.628957	-2.728686
55	1	0	0.458291	-3.295368	-1.394204
56	1	0	-0.754820	-3.678831	0.603047
57	1	0	-2.353567	-4.236467	0.100678
58	1	0	-2.186747	-3.195940	1.519386
59	1	0	-3.824359	-1.654109	1.670586
60	1	0	-4.947434	-1.450347	0.322609
61	1	0	-4.240587	-0.032885	1.101581
62	1	0	-4.609244	0.676548	-1.982798
63	1	0	-3.181154	1.664136	-2.331846
64	1	0	-3.791406	1.555294	-0.682017

I₁

Zero-point correction=	0.537209
(Hartree/Particle)	
Thermal correction to Energy=	0.568988
Thermal correction to Enthalpy=	0.569933
Thermal correction to Gibbs Free Energy=	0.475371
Sum of electronic and zero-point Energies=	-1363.296162
Sum of electronic and thermal Energies=	-1363.264383
Sum of electronic and thermal Enthalpies=	-1363.263439
Sum of electronic and thermal Free Energies=	-1363.358000

Center Number	Atomic Number	Atomic Type	Coordinates (Angstroms)		
			X	Y	Z
1	45	0	-0.997637	-0.111832	-0.030169
2	7	0	-0.455526	-0.756779	1.860664
3	6	0	-0.221700	-3.249648	1.558312
4	6	0	0.343937	0.194446	2.371593
5	6	0	0.442593	1.388741	1.423815
6	6	0	1.154446	1.321921	0.187092
7	6	0	-0.025851	2.641977	1.882050
8	6	0	1.367222	2.522337	-0.532815
9	6	0	0.169924	3.795841	1.141696
10	6	0	0.879364	3.734725	-0.073490
11	8	0	0.935127	0.212251	3.456693
12	6	0	0.807813	-0.954199	-0.422436
13	6	0	1.728429	0.020608	-0.300707
14	6	0	1.101226	-3.183790	0.772289
15	6	0	1.054122	-2.424739	-0.580541
16	6	0	-0.523463	-2.064388	2.491549
17	6	0	3.199483	-0.078167	-0.510597
18	6	0	3.742258	-0.588936	-1.701908

19	6	0	5.123694	-0.677701	-1.880172
20	6	0	5.990513	-0.245687	-0.874550
21	6	0	5.464737	0.276124	0.310441
22	6	0	4.084754	0.361860	0.490399
23	1	0	-0.211735	-4.146497	2.193859
24	1	0	-1.049537	-3.393311	0.853741
25	1	0	-0.512755	2.684016	2.852257
26	1	0	1.944763	2.477696	-1.452262
27	1	0	-0.190892	4.751360	1.513386
28	1	0	1.062557	4.643693	-0.641068
29	1	0	1.421974	-4.209825	0.546619
30	1	0	1.887226	-2.742718	1.398515
31	1	0	0.283762	-2.885563	-1.213920
32	1	0	2.014836	-2.588071	-1.086401
33	1	0	-1.521128	-2.221371	2.931592
34	1	0	0.190997	-2.057201	3.324137
35	1	0	3.071071	-0.903324	-2.496946
36	1	0	5.522558	-1.075247	-2.810236
37	1	0	7.066385	-0.311280	-1.013920
38	1	0	6.131479	0.612295	1.100476
39	1	0	3.680930	0.752443	1.421064
40	6	0	-2.193774	0.926117	-1.700063
41	6	0	-2.050350	-0.448842	-1.998505
42	6	0	-2.680091	-1.184888	-0.914841
43	6	0	-3.382998	-0.213308	-0.062506
44	6	0	-3.067242	1.064443	-0.521633
45	6	0	-1.714646	2.086914	-2.520522
46	6	0	-1.413504	-1.050467	-3.217129
47	6	0	-2.975270	-2.656398	-0.928719
48	6	0	-4.250355	-0.587358	1.102800
49	6	0	-3.510312	2.385091	0.035299

Chapter VI.

50	1	0	-2.545835	2.528253	-3.088309
51	1	0	-0.945812	1.785418	-3.237001
52	1	0	-1.290338	2.875535	-1.890271
53	1	0	-0.645700	-0.394343	-3.636583
54	1	0	-2.164710	-1.227592	-3.999486
55	1	0	-0.939924	-2.010981	-2.993969
56	1	0	-2.154016	-3.235455	-1.360486
57	1	0	-3.872481	-2.856668	-1.533048
58	1	0	-3.166836	-3.040351	0.076979
59	1	0	-3.757041	-1.319922	1.749937
60	1	0	-5.195051	-1.032794	0.761671
61	1	0	-4.495895	0.281727	1.718647
62	1	0	-4.184857	2.898239	-0.663768
63	1	0	-2.659389	3.052304	0.214516
64	1	0	-4.043003	2.265643	0.982499

TS9

Zero-point correction= 0.535093
(Hartree/Particle)

Thermal correction to Energy=	0.566756
Thermal correction to Enthalpy=	0.567700
Thermal correction to Gibbs Free Energy=	0.473558
Sum of electronic and zero-point Energies=	-1363.256829
Sum of electronic and thermal Energies=	-1363.225166
Sum of electronic and thermal Enthalpies=	-1363.224222
Sum of electronic and thermal Free Energies=	-1363.318364

Center	Atomic Number	Atomic Type	Coordinates (Angstroms)		
			X	Y	Z

1	45	0	-0.223965	0.530402	0.067630
2	7	0	-1.865484	-0.456740	-0.880515
3	6	0	-2.642136	-1.181722	-3.170746
4	6	0	-2.653312	-1.204711	-0.042903
5	6	0	-1.997813	-1.441272	1.272608
6	6	0	-0.803601	-0.750267	1.539044
7	6	0	-2.553916	-2.326190	2.203168
8	6	0	-0.162278	-0.989916	2.761736
9	6	0	-1.910271	-2.548999	3.418369
10	6	0	-0.710811	-1.883013	3.690895
11	8	0	-3.771982	-1.642793	-0.345232
12	6	0	0.981995	-1.104180	-0.743863
13	6	0	0.059875	-1.621438	-1.424441
14	6	0	-1.347383	-1.915626	-3.532301
15	6	0	-0.648471	-2.547799	-2.309031
16	6	0	-2.443057	-0.042250	-2.158628
17	6	0	4.274487	-1.833693	0.947956
18	6	0	5.172487	-1.676000	-0.110849
19	6	0	4.691894	-1.321785	-1.373124
20	6	0	3.325149	-1.129185	-1.577512
21	6	0	2.416085	-1.279523	-0.513978
22	6	0	2.908430	-1.629498	0.755121
23	1	0	-3.082374	-0.759722	-4.084870
24	1	0	-3.367605	-1.887784	-2.756112
25	1	0	-3.487690	-2.821143	1.949311
26	1	0	0.772128	-0.490376	3.007632
27	1	0	-2.332140	-3.236372	4.147062
28	1	0	-0.196173	-2.057618	4.633859
29	1	0	-1.572815	-2.722915	-4.240299
30	1	0	-0.643783	-1.239170	-4.036961
31	1	0	0.137422	-3.243142	-2.650048

Chapter VI.

32	1	0	-1.368137	-3.143544	-1.733421
33	1	0	-1.775180	0.708362	-2.593362
34	1	0	-3.415526	0.438698	-1.977840
35	1	0	4.638502	-2.115743	1.932468
36	1	0	6.236493	-1.829972	0.046073
37	1	0	5.380327	-1.201032	-2.205494
38	1	0	2.951275	-0.862407	-2.561788
39	1	0	2.210749	-1.752233	1.576433
40	6	0	-0.133594	2.341488	1.424303
41	6	0	1.183137	2.116501	0.898556
42	6	0	1.142216	2.423555	-0.525376
43	6	0	-0.180084	2.757575	-0.876692
44	6	0	-0.998937	2.646332	0.320470
45	6	0	-0.522291	2.385918	2.872792
46	6	0	2.440365	1.917847	1.696293
47	6	0	2.344887	2.444214	-1.421633
48	6	0	-0.664179	3.237973	-2.214407
49	6	0	-2.455673	2.999075	0.410514
50	1	0	-1.567511	2.102972	3.022395
51	1	0	-0.392648	3.405789	3.261655
52	1	0	0.087842	1.718187	3.484919
53	1	0	3.144522	1.252103	1.188622
54	1	0	2.226333	1.483395	2.677088
55	1	0	2.954066	2.874923	1.868795
56	1	0	2.065113	2.412091	-2.478812
57	1	0	3.011868	1.599865	-1.223208
58	1	0	2.927148	3.362885	-1.262694
59	1	0	-0.043020	2.863879	-3.034467
60	1	0	-0.644398	4.335917	-2.265308
61	1	0	-1.695314	2.928905	-2.409178
62	1	0	-2.997373	2.696691	-0.490654

63	1	0	-2.593813	4.083160	0.531433
64	1	0	-2.934806	2.506310	1.260825

I₂

Zero-point correction=	0.537935
(Hartree/Particle)	
Thermal correction to Energy=	0.569211
Thermal correction to Enthalpy=	0.570155
Thermal correction to Gibbs Free Energy=	0.477334
Sum of electronic and zero-point Energies=	-1363.304802
Sum of electronic and thermal Energies=	-1363.273526
Sum of electronic and thermal Enthalpies=	-1363.272582
Sum of electronic and thermal Free Energies=	-1363.365403

Center Number	Atomic Number	Atomic Type	Coordinates (Angstroms)		
			X	Y	Z
1	45	0	0.499684	-0.497577	-0.166395
2	7	0	0.726803	1.675808	-0.759561
3	6	0	0.468779	3.492285	-2.482748
4	6	0	1.609440	2.259445	0.245592
5	6	0	1.478484	1.626085	1.572542
6	6	0	0.943299	0.320927	1.636100
7	6	0	1.944135	2.299254	2.712589
8	6	0	0.846476	-0.266325	2.906299
9	6	0	1.837747	1.693000	3.959607
10	6	0	1.280984	0.411419	4.050254
11	8	0	2.398485	3.140618	-0.045617
12	6	0	-1.205151	0.630244	-0.045965
13	6	0	-0.731947	1.809324	-0.457289

14	6	0	-1.034473	3.593497	-2.178782
15	6	0	-1.327964	3.161952	-0.725175
16	6	0	1.026788	2.098280	-2.153160
17	6	0	-4.956959	0.140722	-0.192925
18	6	0	-3.655670	0.496099	-0.550641
19	6	0	-2.576221	0.270444	0.325884
20	6	0	-2.846503	-0.337910	1.567367
21	6	0	-4.148511	-0.683318	1.926202
22	6	0	-5.210182	-0.447853	1.047549
23	1	0	0.659147	3.701820	-3.543390
24	1	0	1.021645	4.237372	-1.901225
25	1	0	2.383436	3.286705	2.599659
26	1	0	0.420227	-1.260046	3.016615
27	1	0	2.180747	2.207244	4.853063
28	1	0	1.184325	-0.065273	5.023788
29	1	0	-1.386729	4.618196	-2.350176
30	1	0	-1.595055	2.941908	-2.864268
31	1	0	-2.404565	3.134717	-0.528941
32	1	0	-0.892625	3.905743	-0.038783
33	1	0	0.570050	1.345311	-2.803760
34	1	0	2.110660	2.070471	-2.289523
35	1	0	-5.774035	0.322425	-0.886781
36	1	0	-3.463168	0.942933	-1.522396
37	1	0	-2.021448	-0.517904	2.249775
38	1	0	-4.336124	-1.139345	2.895146
39	1	0	-6.223469	-0.724924	1.325824
40	6	0	1.698895	-2.501167	0.020468
41	6	0	0.254936	-2.679932	0.077736
42	6	0	-0.270101	-2.418213	-1.254089
43	6	0	0.792336	-1.949478	-2.052998
44	6	0	2.016977	-1.993970	-1.256688

45	6	0	2.657734	-2.839814	1.124272
46	6	0	-0.496143	-3.393380	1.166193
47	6	0	-1.689906	-2.658995	-1.675695
48	6	0	0.733026	-1.578791	-3.507209
49	6	0	3.382977	-1.649324	-1.779261
50	1	0	2.802281	-3.927104	1.192550
51	1	0	2.297847	-2.493065	2.097769
52	1	0	3.638982	-2.386107	0.959010
53	1	0	-0.001460	-3.281505	2.135766
54	1	0	-0.561729	-4.471695	0.958800
55	1	0	-1.517902	-3.013521	1.265554
56	1	0	-2.397188	-2.373669	-0.891926
57	1	0	-1.851784	-3.723811	-1.896029
58	1	0	-1.949380	-2.093619	-2.575643
59	1	0	-0.277415	-1.287146	-3.809618
60	1	0	1.036061	-2.421177	-4.145293
61	1	0	1.404745	-0.745669	-3.741273
62	1	0	3.796583	-2.470807	-2.381478
63	1	0	4.088249	-1.448008	-0.968087
64	1	0	3.358128	-0.762108	-2.421257

**Single Point energies (atomic units) in solution (methanol) calculated with
PCM and the basis set [B3LYP/6-311+G(2df,2p) (C, H, O, N) SDD (Rh)] for
the stationary points calculated with basis set [B3LYP/6-31G(d) (C, H, O,
P) LANL2DZ (Rh)]**

1a

SCF Done: E (RB3LYP) = -826.383854445

RhCp*(OAc)₂

SCF Done: E (RB3LYP) = -958.034208475

AcOH

SCF Done: E (RB3LYP) = -229.184617354

A

SCF Done: E (RB3LYP) = -1555.20491705

TS1

SCF Done: E (RB3LYP) = -1555.17823861

B

SCF Done: E (RB3LYP) = -1555.19747310

C

SCF Done: E (RB3LYP) = -1326.01092398

TS2

SCF Done: E (RB3LYP) = -1325.97607810

D₁

SCF Done: E (RB3LYP) = -1326.01578781

TS3

SCF Done: E (RB3LYP) = -1325.99167880

E₁

SCF Done: E (RB3LYP) = -1326.04167573

C₂

SCF Done: E (RB3LYP) = -1326.00656776

TS4

SCF Done: E (RB3LYP) = -1325.98087699

D₂

SCF Done: E (RB3LYP) = -1326.00869134

TS5

SCF Done: E (RB3LYP) = -1325.98637592

E

SCF Done: E (RB3LYP) = -1326.05323034

2a:

SCF Done: E (RB3LYP) = -825.235899617

F:

SCF Done: E (RB3LYP) = -1248.55309852

TS6:

SCF Done: E (RB3LYP) = -1248.52655976

G₁

SCF Done: E (RB3LYP) = -1248.57956030

TS7:

SCF Done: E (RB3LYP) = -1248.52362053

G₂

SCF Done: E (RB3LYP) = -1248.56847424

H

SCF Done: E (RB3LYP) = -1365.32606176

TS8:

SCF Done: E (RB3LYP) = -1365.30182313

I₁

SCF Done: E (RB3LYP) = -1365.34481675

TS9:

SCF Done: E (RB3LYP) = -1365.30375982

I₂

SCF Done: E (RB3LYP) = -1365.34370592

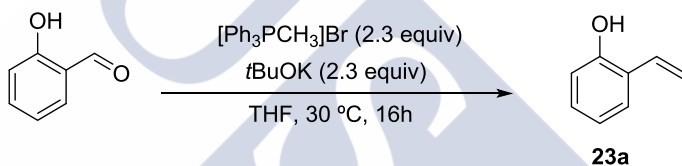
3- CHAPTER III: Assembly of benzoxepines and coumarins by oxidative annulations of *o*-vinylphenols.

3.1 General considerations.

2-(prop-1-en-1-yl)phenol (*E*:*Z* = 14:1) was prepared according to the procedure described by Hanessian, Stephen et al in *Organic Letters* **2006**, *8*, 5481-5484.

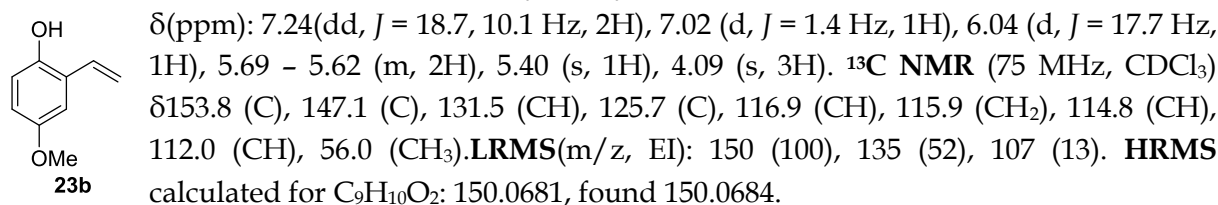
Alkynes **29b** (1,2-bis(4-methoxyphenyl)ethyne) and **29c** (1,2-bis(4-(trifluoromethyl)phenyl)ethyne) were prepared according to the procedure reported in *Tetrahedron* **2005**, *61*, 9878–9885. Alkyne **29e** was prepared according to the procedure from Wender et. al. *Angew. Chem. Int. Ed.* **2004**, *43*, 3076-3079. All the other alkynes were purchased from Aldrich.

3.2 Procedure A for the synthesis of *o*-vinylphenols exemplified for **23a**.

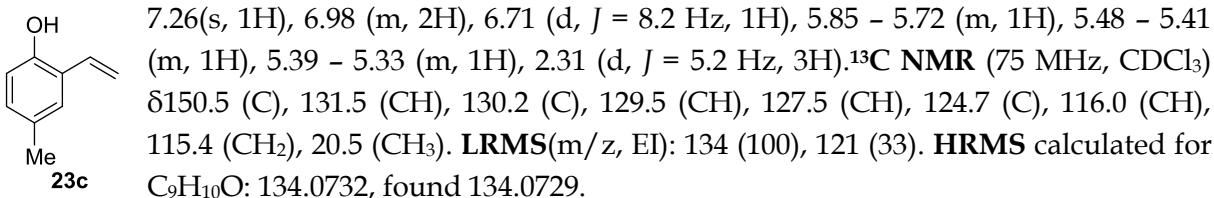


To a solution of methyltriphenylphosphonium bromide (2.04 g, 2.3 equiv) and potassium *tert*-butoxide (0.699 g, 2.3 equiv) in THF (26 mL) under Ar atmosphere was added the aldehyde derivative (0.50 g, 4.09 mmol). The reaction was heated at $30\text{ }^\circ\text{C}$ and stirred for 12 hours and then cooled to room temperature. Solvents were removed *in vacuo* and the resulting mixture was extracted with diethyl ether. The combined organic layers were washed with brine, and dried over anhydrous sodium sulfate. Evaporation of the solvent followed by purification by flash chromatography on silica gel (hexanes:diethylether; 4:6) gave the 2-hydroxystyrene (**23a**) (1.89 g, 96%), as a yellow liquid. ¹H NMR (300 MHz, $CDCl_3$) δ (ppm): 7.60 – 7.50 (m, 1H), 7.32 – 7.21 (m, 1H), 7.18 – 7.02 (m, 2H), 6.92 – 6.86 (m, 1H), 5.94 – 5.83 (m, 1H), 5.61 (s, 1H), 5.47 (dd, J = 11.2, 4.3 Hz, 1H). ¹³C NMR (75 MHz, $CDCl_3$) δ 152.7 (C), 131.5 (CH), 129.0 (CH), 127.3 (CH), 125.1 (C), 121.1 (CH), 116.1 (CH), 115.8 (CH₂). LRMS (m/z, EI): 225 (100), 121 (87), 107 (37). HRMS calculated for C_8H_8O : 121.0653, found 121.0653.

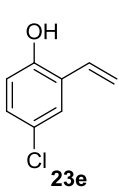
4-methoxy-2-vinylphenol (23b): 56% yield, yellow liquid. ¹H NMR (300 MHz, $CDCl_3$)



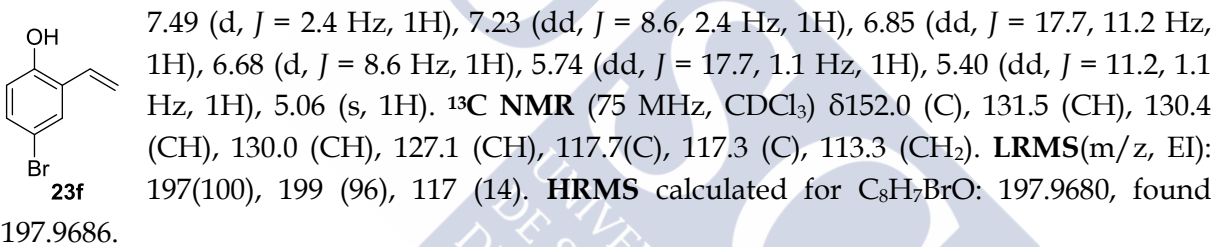
4-methyl-2-vinylphenol (23c): 65% yield, yellow liquid. **¹H NMR** (300 MHz, CDCl₃) δ(ppm):



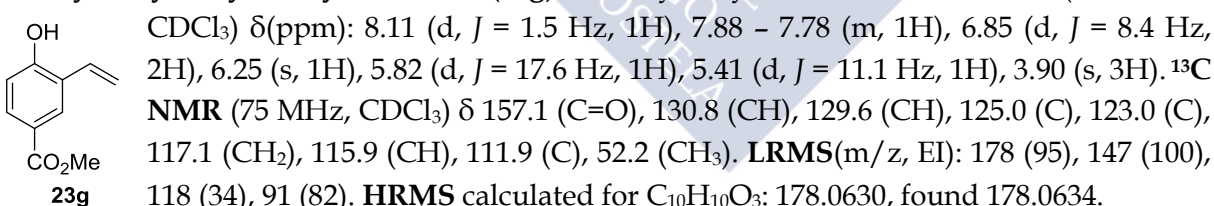
4-chloro-2-vinylphenol (23e): 71% yield, white solid. **¹H NMR** (300 MHz, CDCl₃) δ(ppm): 7.42 – 7.32 (m, 1H), 7.15 – 7.03 (m, 1H), 6.95 – 6.80 (m, 1H), 6.73 (dd, J = 8.6, 4.8 Hz, 1H), 5.75 (ddd, J = 17.7, 4.6, 1.0 Hz, 1H), 5.41 (ddd, J = 11.1, 4.7, 1.0 Hz, 1H), 5.04 (s, 1H). **¹³C NMR** (75 MHz, CDCl₃) δ151.4 (C), 130.5 (CH), 128.6 (CH), 127.1 (CH), 126.5 (C), 126.1 (C), 117.3 (CH), 117.2 (CH₂). **LRMS(m/z, EI):** 154 (37), 153 (100). **HRMS** calculated for C₈H₇ClO: 154.0186 found, 154.0185.



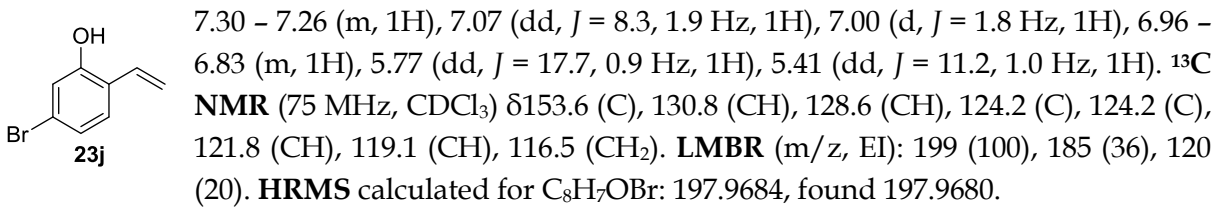
4-bromo-2-vinylphenol (23f): 97% yield, white solid. **¹H NMR** (300 MHz, CDCl₃) δ(ppm):



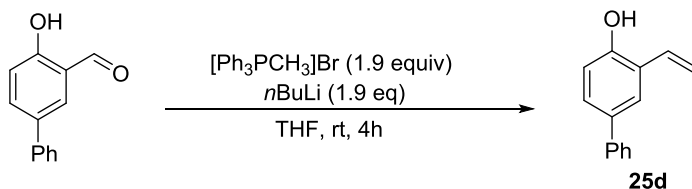
Methyl-4-hydroxy-3-vinylbenzoate (23g): 88% yield, yellow solid. **¹H NMR** (300 MHz, CDCl₃) δ(ppm):



5-bromo-2-vinylphenol (23j): 70% yield, white solid. **¹H NMR** (300 MHz, CDCl₃) δ(ppm):



3.3 Procedure B for the synthesis of o-vinylphenols exemplified for 25d.



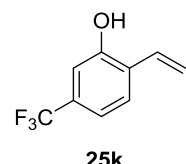
To a solution of methyltriphenylphosphoniumbromide (0.7 g, 1.9 equiv) in THF (15mL) was added butyllithium solution in THF (1.1 mL, 2.3M) dropwise to -78 °C. The resulting mixture was stirred 15 minutes, allowed to reach rt and added dropwise to 4-hydroxy-[1.1']biphenyl-3-carbaldehyde¹⁸⁵ (0.25 g, 1.26 mmol) at -78°C. The reaction was stirred for 4 hours at rt and quenched with saturated NH₄Cl aqueous solution. The solvent was removed *in vacuo* and the resulting mixture was extracted with diethyl ether. The combined organic layer was washed with brine, and dried over anhydrous Na₂SO₄. Evaporation of the solvents followed by flash column chromatography purification on silica gel (hexanes:diethylether; 8:2) yielded the 3-vinylbiphenyl-4-ol (**25d**) (0.22g, 88%), as a white solid. ¹H NMR (300 MHz, CDCl₃) δ(ppm): 7.66 – 7.54 (m, 1H), 7.47 – 7.30 (m, 6H), 7.00 (dd, *J* = 17.7, 11.2 Hz, 1H), 6.87 (d, *J* = 8.3 Hz, 1H), 5.83 (dd, *J* = 17.7, 1.2 Hz, 1H), 5.43 (dd, *J* = 11.2, 1.2 Hz, 1H), 5.09 (d, *J* = 5.0 Hz, 1H). ¹³C NMR (75 MHz, CDCl₃) δ(ppm): ¹³C NMR (75 MHz, cdcl₃) δ 152.5(C), 140.9(C), 134.3(C), 131.7(CH), 129.9(CH), 128.9(CH), 127.8(CH), 126.9(CH), 126.8(CH), 125.8(C), 116.4(CH), 116.4(CH₂). LRMS (m/z, EI): 196 (100), 167 (41), 152 (25), 115 (10). HRMS calculated for C₁₄H₁₂O: 196.0888 found, 196.0887.

5-methoxy-2-vinylphenol (25h): 92% yield, white solid. ¹H NMR (300 MHz, CDCl₃) δ 7.33 – 7.29 (d, 1H), 6.93 – 6.81 (m, 1H), 6.52 – 6.48 (m, 1H), 6.37 (d, *J* = 2.5 Hz, 1H), 5.66 – 5.60 (m, 1H), 5.47 (s, 1H), 5.28 – 5.22 (m, 1H), 3.77 (s, 3H). ¹³C NMR (75 MHz, CDCl₃) δ 160.3 (C), 154.0 (C), 131.2 (CH), 128.3 (CH), 118.0 (C), 113.8 (CH₂), 106.9 (CH), 101.8 (CH), 55.5 (CH₃). LRMS (m/z, EI): 150 (100), 137 (34), 121 (9). HRMS calculated for C₉H₁₀O₂: 150.0661 found, 150.0681.

5-methyl-2-vinylphenol (25i): 72% yield, yellow solid. ¹H NMR (300 MHz, CDCl₃) δ 7.28 (d, *J* = 7.8 Hz, 1H), 6.91 (dd, *J* = 17.7, 11.2 Hz, 1H), 6.74 (ddd, *J* = 5.1, 2.8, 0.5 Hz, 1H), 6.60 (d, *J* = 9.8 Hz, 1H), 5.70 (dd, *J* = 17.7, 1.3 Hz, 1H), 5.31 (dd, *J* = 11.2, 1.3 Hz, 1H), 5.14 (s, 1H), 2.30 (s, 3H). ¹³C NMR (75 MHz, CDCl₃) δ 152.8 (C), 139.3 (C), 131.5 (CH), 127.3 (CH), 122.1 (CH), 121.9 (C), 116.6 (CH), 114.9 (CH₂), 21.3 (CH₃). LRMS (m/z, EI): 134 (100), 121 (51), 105 (67), 91 (99). HRMS calculated for C₉H₁₀O: 134.0732 found, 134.0732.

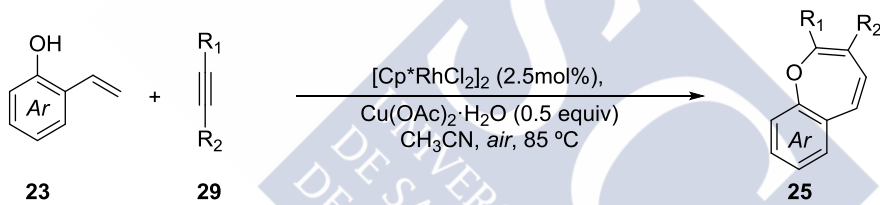
¹⁸⁵ The synthesis of 4-hydroxybiphenyl-3-carbaldehyde was carried out following the procedure reported in *Bioorg. Med. Chem.* **2010**, *18*, 358–365. All spectral data obtained was according to the previously reported.

5-(trifluoromethyl)-2-vinylphenol (25k): 94% yield, orange liquid. **¹H NMR** (300 MHz, CDCl₃) δ 7.48 (d, *J* = 8.0 Hz, 1H), 7.17 (d, *J* = 8.0 Hz, 1H), 7.05 (s, 1H), 6.94 (dd, *J* = 17.8, 11.2 Hz, 1H), 5.87 – 5.79 (m, 1H), 5.52 – 5.45 (m, 1H). **LRMS** (m/z, EI): 188 (100), 169 (16), 159 (27), 119 (18). **HRMS** calculated for C₉H₇OF₃: 188.0449 found, 188.0449. This compound is instable and start to decompose quite readily. It was used just after preparation.



2-methyl-6-vinylphenol (25l): 46% yield, yellow solid. **¹H NMR** (300 MHz, CDCl₃) δ 7.24 – 7.20 (m, 1H), 7.05 (d, *J* = 7.4 Hz, 1H), 6.93 (dd, *J* = 17.7, 11.2 Hz, 1H), 6.82 (t, *J* = 7.6 Hz, 1H), 5.71 (dd, *J* = 17.7, 1.4 Hz, 1H), 5.38 (dd, *J* = 11.2, 1.4 Hz, 1H), 4.96 (s, 1H), 2.26 (s, 3H). **¹³C NMR** (75 MHz, CDCl₃) δ 151.3 (C), 132.1 (CH), 130.4 (CH), 125.4 (CH), 124.5 (C), 123.8 (C), 120.5 (CH), 116.3 (CH₂), 16.0 (CH₃). **LRMS** (m/z, EI): 134 (100). **HRMS** calculated for C₉H₁₀O: 134.0731 found, 134.0732.

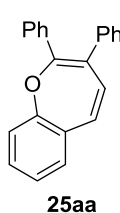
3.4 General procedure for the Rh-catalyzed reaction leading to oxepines 25.



To a solution of [Cp^{*}RhCl₂]₂ (5.2 mg, and Cu(OAc)₂ · H₂O (33 mg, 0.5 equiv, 0.165 mmol) in CH₃CN (2 mL) under air atmosphere was added the alkyne **29** (0.333 mmol) followed by the addition of corresponding *ortho*-vinylphenols **25** (0.50 mmol, 1.5 equiv). The reaction was sealed with a rubber septum and an air atmosphere was injected in the flask with a balloon and a needle. The reaction was heated at 85 °C, stirred overnight and then cooled to room temperature. The reaction was filtered through celite and washed first with hexanes and then with diethyl ether. The solvents were removed *in vacuo* and the remaining residue was purified by flash column chromatography on silica gel to afford the corresponding oxepines **25**.

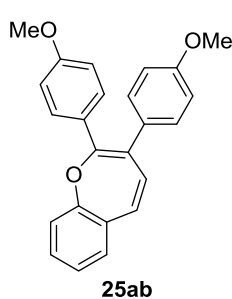
¹⁸⁶ The corresponding aldehyde precursor for the Wittig reaction was prepared by treatment of the 2-methoxy-4-(trifluoromethyl)-1-vinylbenzene with 3 equivalents of LiCl in DMF at 130 °C (53% yield).

2,3-Diphenylbenzo[*b*]oxepine (25aa): 97% yield, yellow solid. **¹H NMR** (300 MHz, CDCl₃) δ



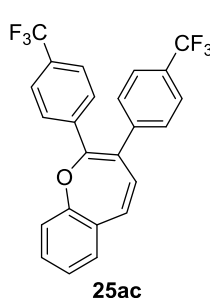
7.51 – 7.42 (m, 2H), 7.40 – 7.11 (m, 11H), 7.05 – 6.91 (m, 2H), 6.46 (d, J = 11.1 Hz, 1H). **NMR** (75 MHz, CDCl₃) δ 154.9 (C), 148.5 (C), 139.4 (C), 135.7 (C), 132.5 (CH), 131.7 (C), 131.0 (CH), 130.6 (CH), 130.4 (CH), 130.1 (CH), 128.6 (CH), 128.4 (CH), 127.8 (CH), 127.6 (C), 127.5 (CH), 124.9 (CH), 121.34 (CH). **LRMS** (*m/z*, *I*) 296 (82) 194 (80) **HRMS** calculated for C₂₂H₁₆O₂ 296.1201, found 296.1203.

2,3-Bis(4-methoxyphenyl)benzo[*b*]oxepine (25ab): 85% yield, yellow liquid. **¹H NMR** (300



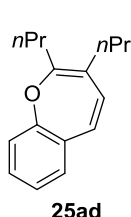
MHz, CDCl₃) δ 7.42 (d, J = 8.9 Hz, 2H), 7.34 (dd, J = 7.5, 1.3 Hz, 1H), 7.26 (td, J = 7.9, 1.6 Hz, 1H), 7.20 – 7.09 (m, 3H), 6.93 (dd, J = 14.9, 9.5 Hz, 2H), 6.80 (d, J = 8.7 Hz, 2H), 6.73 (d, J = 8.9 Hz, 2H), 6.42 (d, J = 11.1 Hz, 1H), 3.79 (d, J = 3.7 Hz, 6H). **¹³C NMR** (75 MHz, CDCl₃) δ 159.3 (C), 158.9 (C), 154.6 (C), 147.4 (C), 132.7 (CH), 131.9 (C), 131.6 (C), 131.4 (CH), 130.3 (CH), 130.1 (CH), 128.3 (CH), 125.6 (CH), 124.6 (CH), 121.2 (CH), 113.9 (CH), 113.1 (CH), 55.3 (CH₃), 55.2 (CH₃). **LRMS** (*m/z*, *I*) 356 (79), 341 (8), 224 (100) **HRMS** calculated for C₂₄H₂₀O₃ 356.1412, found 356.1412

2,3-Bis(4-(trifluoromethyl)phenyl)benzo[*b*]oxepine (25ac): 71% yield, yellow solid. **¹H NMR**



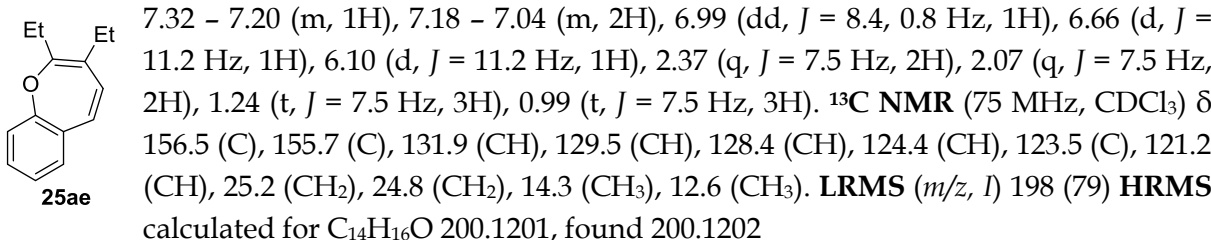
(300 MHz, CDCl₃) δ 7.60 – 7.41 (m, 6H), 7.40 – 7.17 (m, 5H), 7.06 (d, J = 11.2 Hz, 1H), 6.89 (d, J = 8.0 Hz, 1H), 6.37 (d, J = 11.1 Hz, 1H). **¹³C NMR** (75 MHz, CDCl₃) δ 154.7 (C), 147.6 (C), 142.5 (C), 138.5 (C), 132.5 (CH), 131. (CH), 131.1 (CH), 130.6 (CH), 130.2 (CH), 128.8 (CH), 128.1 (C), 127.9 (C, q, *J* = 291.3 Hz), 125.7 (CH, q, *J* = 3.6 Hz), 125.3 (CH), 125.0 (CH, q, *J* = 3.6 Hz), 122.3 (C, q, *J* = 10.8 Hz), 121.1 (CH). **LRMS** (*m/z*, *I*) 432 (64), 363 (8), 334 (14), 262 (78) **HRMS** calculated for C₂₄H₁₄OF₃ 432.0949, found 432.0951.

2,3-Dipropylbenzo[*b*]oxepine (25ad): 56% yield, yellow liquid. **¹H NMR** (300 MHz, CDCl₃) δ

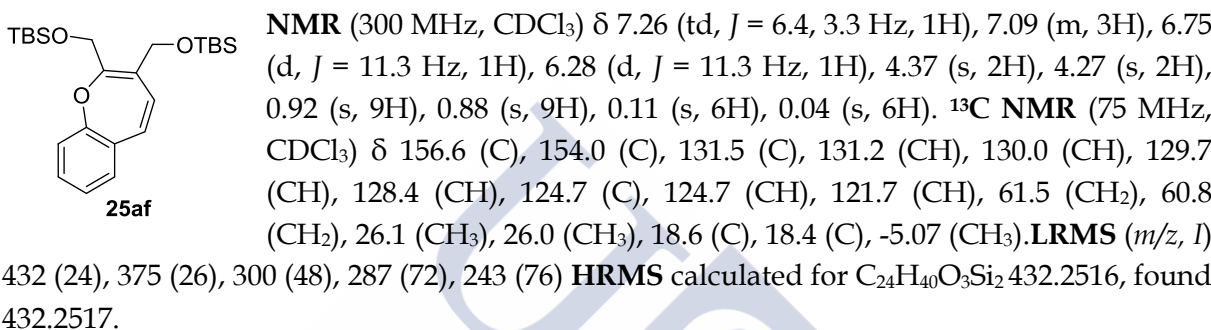


7.30 – 7.20 (m, 1H), 7.17 – 7.04 (m, 2H), 6.98 (d, *J* = 8.0 Hz, 1H), 6.65 (d, *J* = 11.2 Hz, 1H), 6.12 (s, 1H), 2.34 (t, 2H), 2.05 (t, *J* = 7.4 Hz, 2H), 1.83 – 1.65 (m, 2H), 1.48 – 1.32 (m, 2H), 0.99 (t, *J* = 7.4 Hz, 3H), 0.86 (t, *J* = 7.4 Hz, 3H). **¹³C NMR:** (75 MHz, CDCl₃) δ 156.4 (C), 154.7 (C), 132.3 (CH), 131.9 (C), 129.5 (CH), 129.3 (CH), 128.3 (CH), 124.4 (CH), 122.8 (C), 121.1 (CH), 33.9 (CH₂), 33.6 (CH₂), 22.8 (CH₂), 20.9 (CH₂), 14.1 (CH₃), 13.9 (CH₃). **LRMS** (*m/z*, *I*) 228 (100), 199 (90), 185 (27) **HRMS** calculated for C₁₆H₂₀O₂ 228.1514, found 228.1511

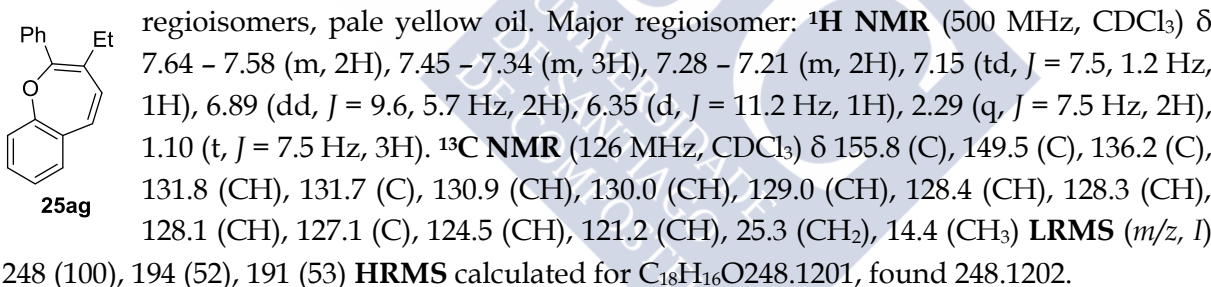
2,3-Diethylbenzo[*b*]oxepine (25ae): 52% yield, yellow liquid. **¹H NMR** (300 MHz, CDCl₃) δ



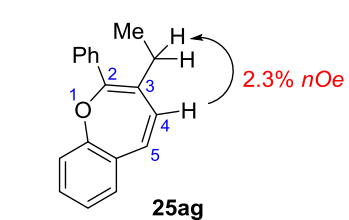
((Benzo[*b*]oxepine-2,3-diylbis(methylene))bis(oxy))bis(tert-butyldimethylsilane) (25af): **¹H**



3-Ethyl-2-phenylbenzo[*b*]oxepine (25ag): 85% yield, 14:1 inseparable mixture of regioisomers, pale yellow oil. Major regioisomer:

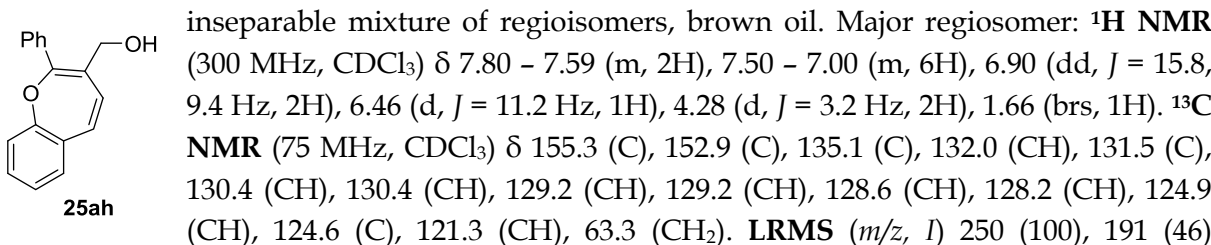


Assignment of the regiochemistry.

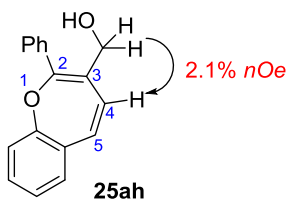


The major regioisomer was assigned based on the HMBC, HSQC, COSY experiments, nOe between the ethyl chain and the hydrogen of the C₄ of the oxepine unit.

2-Phenylbenzo[*b*]oxepin-3-yl)metanol (25ah) (major regiosomer): 65% yield, 11:1



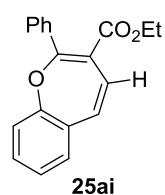
HRMS calculated for C₁₇H₁₄O₂ 250.0994, found 250.0992.



Assignment of the regiochemistry.

The major regioisomer was assigned based on the HMBC, HSQC, COSY experiments, as well as by the observation of nOe between the CH₂OH chain and the hydrogen of the C₄ of the oxepine unit.

Ethyl 2-phenylbenzo[b]oxepine-3-carboxylate (25ai): 99% yield, 8:1 inseparable mixture of regioisomers, yellow oil. Major regiosomer: (300 MHz, CDCl₃) δ 7.58 (dd, J = 7.8, 1.6 Hz, 2H), 7.48 – 7.27 (m, 5H), 7.21 (m, 2H), 6.99 (d, J = 8.1 Hz, 1H), 6.88 (d, J = 11.3 Hz, 1H), 6.61 (d, J = 11.3 Hz, 1H), 4.05 (q, J = 7.1 Hz, 2H), 1.00 (t, J = 7.1 Hz, 3H). ¹³C NMR (75 MHz, CDCl₃) δ 167.8 (C), 161.2 (C), 155.6 (C), 136.2 (C), 131.3 (C), 131.2 (CH), 130.5 (CH), 129.7 (CH), 129.0 (CH), 128.8 (CH), 128.1 (C), 128.0 (CH), 127.6 (CH), 125.5 (CH), 121.4 (CH), 61.1 (CH₂), 13.6 (CH₃). LRMS (m/z, I) 292 (100), 219 (28), 191 (59) HRMS calculated for C₁₉H₁₆O₃ 292.1099, found 292.1100



Assignment of the regiochemistry.

The major regioisomer was assigned based on bidimensional experiments including HMBC, HSQC, COSY.

7-Methoxy-2,3-diphenylbenzo[b]oxepine (25ba): 84% yield, yellow crystals. ¹H NMR (300 MHz, CDCl₃) δ 7.46 – 7.37 (m, 2H), 7.27 – 7.10 (m, 8H), 6.93 (d, J = 11.1 Hz, 1H), 6.86 – 6.76 (m, 3H), 6.43 (d, J = 11.1 Hz, 1H), 3.78 (s, 3H). ¹³C NMR (75 MHz, CDCl₃) δ 156.5 (C), 148.8 (C), 139.3 (C), 135.5 (C), 132.8 (CH), 132.0 (C), 130.7 (CH), 130.3 (CH), 130.0 (CH), 128.4 (CH), 128.3 (CH), 127.7 (CH), 127.4 (CH), 127.2 (C), 121.8 (CH), 116.2 (CH), 112.3 (CH), 55.7 (CH₃). LRMS (m/z, I) 326 (100), 224 (48), 221 (53) HRMS calculated for C₂₃H₁₈O₂ 326.1307, found 326.1307

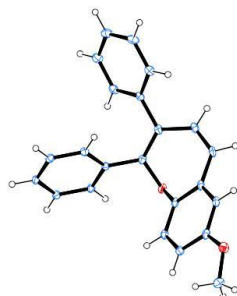
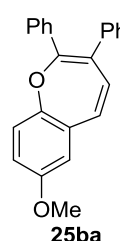
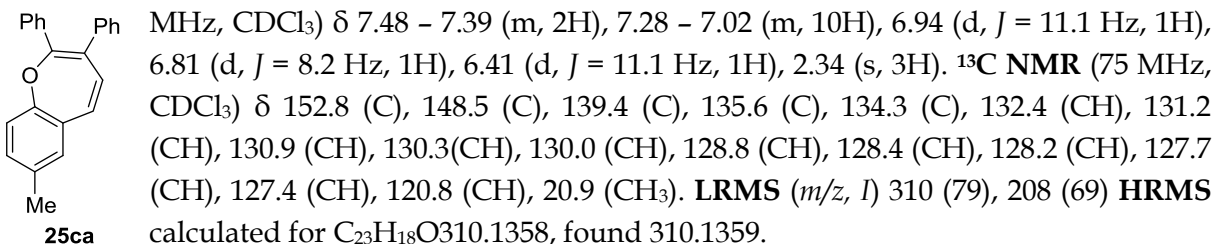
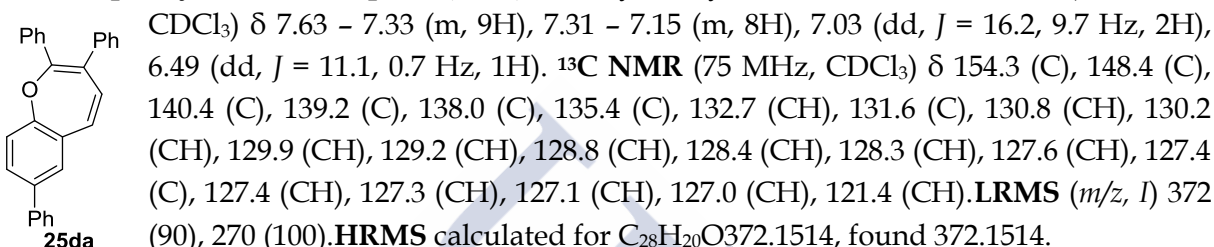


Fig 1. 3-D structure of oxepine 25ba obtained by X-Ray diffractometry

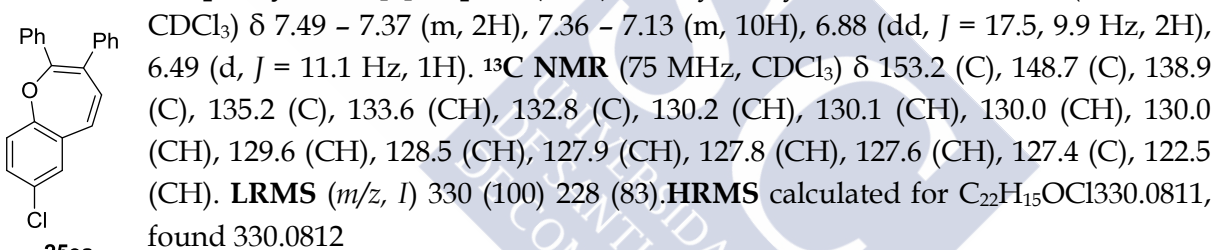
7-Methyl-2,3-diphenylbenzo[b]oxepine (25ca): 63% yield, pale yellow oil. ¹H NMR (300



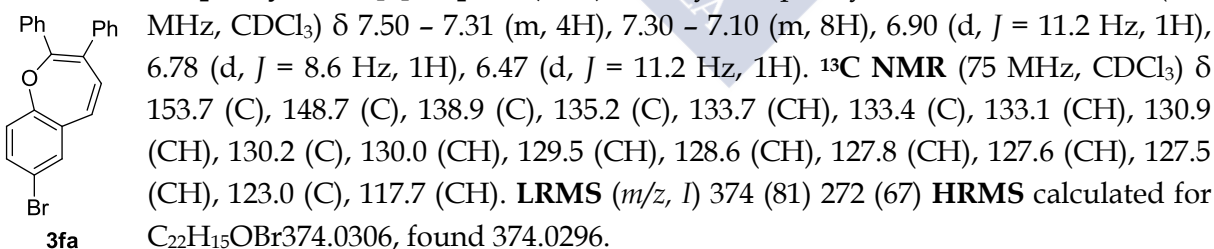
2,3,7-Triphenylbenzo[b]oxepine (25da): 89% yield, yellow crystals. ¹H NMR (300 MHz,



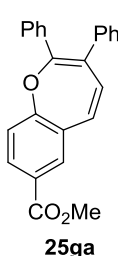
7-Chloro-2,3-diphenylbenzo[b]oxepine (25ea): 78% yield, yellow oil. ¹H NMR (300 MHz,



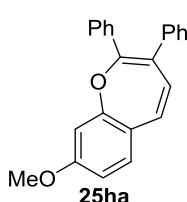
7-Bromo-2,3-diphenylbenzo[b]oxepine (25fa): 80% yield, pale yellow solid. ¹H NMR (300



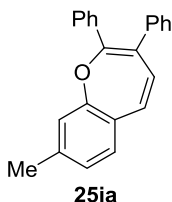
Methyl 2,3-diphenylbenzo[b]oxepine-7-carboxylate (25ga): 69% yield, yellow solid. ¹H NMR (300 MHz, CDCl₃) δ 8.06 (d, *J* = 2.1 Hz, 1H), 7.95 (dd, *J* = 8.4, 2.1 Hz, 1H), 7.47 – 7.37 (m, 2H), 7.27 – 7.13 (m, 8H), 6.97 (dd, *J* = 16.9, 9.8 Hz, 2H), 6.47 (d, *J* = 11.1 Hz, 1H), 3.91 (s, 3H). ¹³C NMR (75 MHz, CDCl₃) δ 166.5 (C), 158.3 (C), 148.2 (C), 138.9 (C), 135.2 (C), 133.2 (CH), 131.8 (CH), 131.4 (C), 130.3 (CH), 130.1 (CH), 129.9 (CH), 128.5 (CH), 127.8 (CH), 127.7 (CH), 127.6 (CH), 126.9 (C), 121.4 (CH), 52.2 (CH₃). LRMS (*m/z*, *I*) 354 (100), 252 (82) HRMS calculated for C₂₄H₁₈O₃ 354.1256, found 354.1258



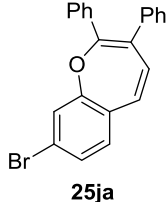
8-Methoxy-2,3-diphenylbenzo[b]oxepines (25ha): 88% yield, yellow oil. ¹H NMR (300 MHz, CDCl₃) δ 7.47 – 7.39 (m, 2H), 7.28 – 7.13 (m, 9H), 6.93 (d, *J* = 11.1 Hz, 1H), 6.74 (dd, *J* = 8.5, 2.5 Hz, 1H), 6.47 (d, *J* = 2.4 Hz, 1H), 6.31 (d, *J* = 11.1 Hz, 1H), 3.72 (s, 3H). ¹³C NMR (75 MHz, CDCl₃) δ 162.0 (C), 156.0 (C), 147.2 (C), 139.5 (C), 135.6 (C), 130.6 (CH), 130.3 (CH), 130.2 (CH), 130.0 (CH), 129.2 (CH), 128.4 (CH), 128.2 (CH), 127.8 (C), 127.7 (CH), 127.4 (CH), 124.7 (C), 110.9 (CH), 106.4 (CH), 55.6 (CH₃). LRMS (*m/z*, *I*) 326 (72), 310 (13), 224 (60) HRMS calculated for C₂₃H₁₈O₂ 326.1307, found 326.1308



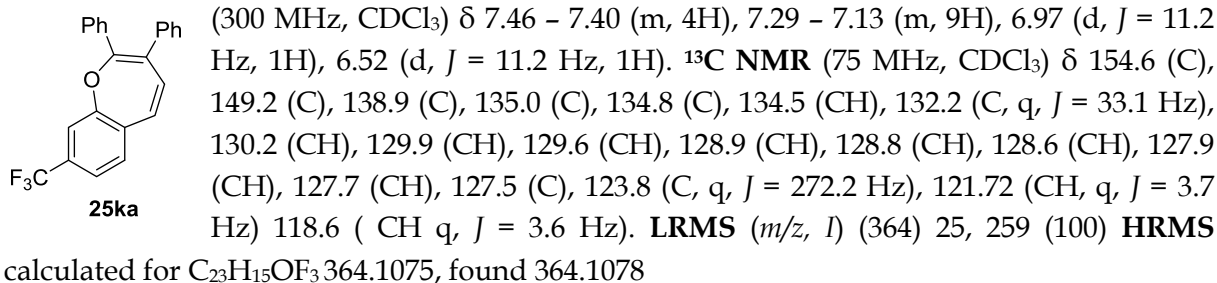
8-Methyl-2,3-diphenylbenzo[b]oxepine (25ia): 90% yield, yellow solid. ¹H NMR (300 MHz, CDCl₃) δ 7.52 – 7.43 (m, 2H), 7.32 – 7.15 (m, 9H), 7.01 (dd, *J* = 12.3, 6.0 Hz, 2H), 6.78 (s, 1H), 6.40 (d, *J* = 11.1 Hz, 1H), 2.31 (s, 3H). ¹³C NMR (75 MHz, CDCl₃) δ 154.8 (C), 148.0 (C), 141.1 (C), 139.5 (C), 135.6 (C), 131.5 (CH), 130.8 (CH), 130.3 (CH), 130.0 (CH), 128.8 (C), 128.4 (CH), 128.2 (CH), 128.2 (CH), 127.6 (CH), 127.4 (CH), 125.7 (CH), 121.6 (CH), 21.3 (CH₃). LRMS (*m/z*, *I*) 310 (87), 265 (26), 208 (89) HRMS calculated for C₂₃H₁₈O₃ 310.1358, found 310.1356



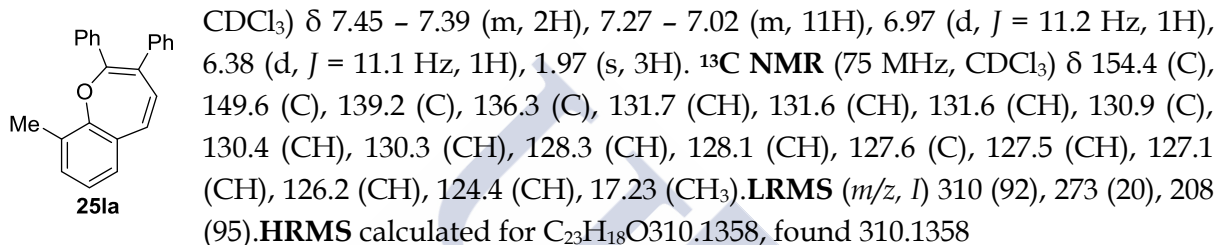
8-Bromo-2,3-diphenylbenzo[b]oxepine (25ja): 78% yield, brown solid. ¹H NMR (300 MHz, CDCl₃) δ 7.48 – 7.37 (m, 2H), 7.34 – 7.13 (m, 10H), 7.08 (d, *J* = 1.9 Hz, 1H), 6.90 (d, *J* = 11.1 Hz, 1H), 6.43 (d, *J* = 11.2 Hz, 1H). ¹³C NMR (75 MHz, CDCl₃) δ 155.0 (C), 148.4 (C), 139.0 (C), 135.1 (C), 132.9 (CH), 130.6 (C), 130.2 (CH), 129.9 (CH), 129.4 (CH), 128.6 (CH), 128.5 (CH), 128.1 (CH), 127.8 (CH), 127.7 (C), 127.6 (CH), 124.5 (CH), 123.3 (C). LRMS (*m/z*, *I*) 374 (94), 272 (100). HRMS calculated for C₂₂H₁₅OBr 374.0306, found 374.0305



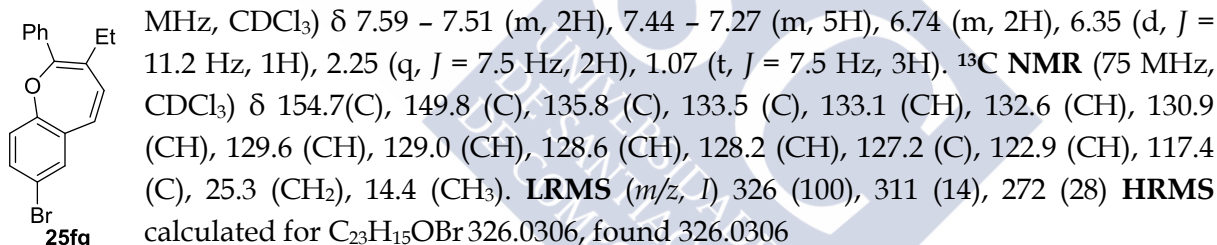
2,3-diphenyl-8-(trifluoromethyl)benzo[b]oxepine (25ka): 86% yield, yellow oil. **¹H NMR**



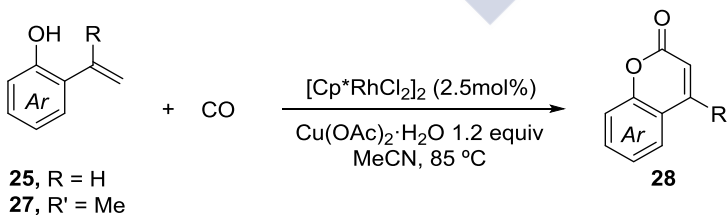
9-Methyl-2,3-diphenylbenzo[b]oxepine (25la): 78% yield, yellow solid. **¹H NMR** (300 MHz,



7-bromo-3-ethyl-2-phenylbenzo[b]oxepine (25fg): 80% yield, brown solid. **¹H NMR** (300



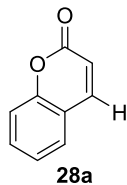
3.5 General procedure for the Rh-catalyzed synthesis of coumarines 28.



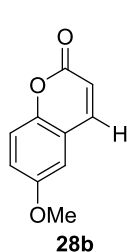
To a solution of [Cp*RhCl₂]₂ (7.7 mg, 0.0125 mmol, 2.5 mol%) and Cu(OAc)₂ · H₂O (120 mg, 0.60 mmol, 1.2 eq) in MeCN (2 mL) purged with CO was added 2-alkenyl phenols **25 (a, b, c)** or **27** (0.5 mmol, 1.0 equiv). The reaction was sealed with a rubber septum and a CO atmosphere was injected in the flask with a balloon and a needle. The reaction was heated at 85 °C and stirred for 16 hours and then cooled to room temperature. The reaction was filtered through celite and washed first with hexanes and then with diethyl ether. The

solvents were removed *in vacuo* and the remaining residue was purified by flash column chromatography on silica gel to afford the corresponding coumarin products **28**.

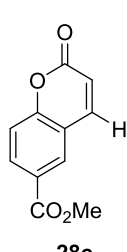
2H-Chromen-2-one (28a): 60% yield, white solid. **¹H NMR** (300 MHz, CDCl₃) δ 7.68 (d, *J* = 9.6 Hz, 1H), 7.56 – 7.37 (m, 2H), 7.34 – 7.16 (m, 2H), 6.37 (d, *J* = 9.6 Hz, 1H). **¹³C NMR** (75 MHz, CDCl₃) δ 160.8 (C), 154.0 (C), 143.5 (CH), 131.8 (CH), 127.9 (CH), 124.4 (CH), 118.8 (C), 116.8 (CH), 116.6 (CH). **LRMS** (*m/z*, *I*) 146 (100), 127 (18), 118 (88) **HRMS** calculated for C₉H₆O₂ 146.0368, found 146.0366



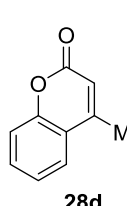
6-Methoxy-2H-chromen-2-one (28b): 85% yield, brown solid. **¹H NMR** (300 MHz, CDCl₃) δ 7.64 (d, *J* = 9.5 Hz, 1H), 7.22 (d, *J* = 9.1 Hz, 1H), 7.07 (dd, *J* = 9.1, 2.9 Hz, 1H), 6.89 (d, *J* = 2.9 Hz, 1H), 6.39 (d, *J* = 9.5 Hz, 1H), 3.82 (s, 3H). **¹³C NMR** (75 MHz, CDCl₃) δ 161.1 (C), 156.1 (C), 148.5 (C), 143.3 (CH), 119.5 (CH), 119.2 (C), 117.9 (CH), 117.1 (CH), 110.1 (CH), 55.9 (CH₃). **LRMS** (*m/z*, *I*) 176 (100), 161 (12), 148 (69), 133 (82) **HRMS** calculated for C₁₀H₈O₃ 176.0473, found 176.0473



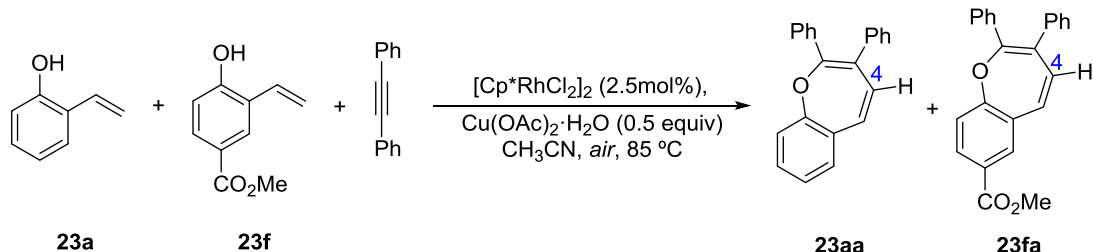
Methyl 2-oxo-2H-chromene-6-carboxylate (28c): 78% yield, brown solid. **¹H NMR** (300 MHz, CDCl₃) δ 8.21 – 8.11 (m, 2H), 7.74 (d, *J* = 9.6 Hz, 1H), 7.34 (d, *J* = 8.5 Hz, 1H), 6.46 (d, *J* = 9.6 Hz, 1H), 3.93 (s, 3H). **¹³C NMR** (75 MHz, CDCl₃) δ 165.7 (C), 160.0 (C), 156.9 (C), 143.2 (CH), 132.9 (CH), 130.0 (CH), 126.6 (C), 118.6 (C), 117.6 (CH), 117.2 (CH), 52.5 (CH₃). **LRMS** (*m/z*, *I*) 204 (85), 173 (100) 145 (55) **HRMS** calculated for C₁₁H₈O₄ 204.0423, found 204.0425



4-Methyl-2H-chromen-2-one (28d): 84% yield, red solid. **¹H NMR** (300 MHz, CDCl₃) δ 7.63 – 7.48 (m, 2H), 7.37 – 7.24 (m, 2H), 6.28 (d, *J* = 1.1 Hz, 1H), 2.44 (d, *J* = 1.2 Hz, 3H). **¹³C NMR** (75 MHz, CDCl₃) δ 160.9 (C), 153.6 (C), 152.5 (C), 131.9 (CH), 124.7 (CH), 124.3 (CH), 120.1 (C), 117.2 (CH), 115.2 (CH), 18.7 (CH₃). **LRMS** (*m/z*, *I*) 160 (100), 132 (92) **HRMS** calculated for C₁₀H₈O₂ 160.0524, found 160.0523

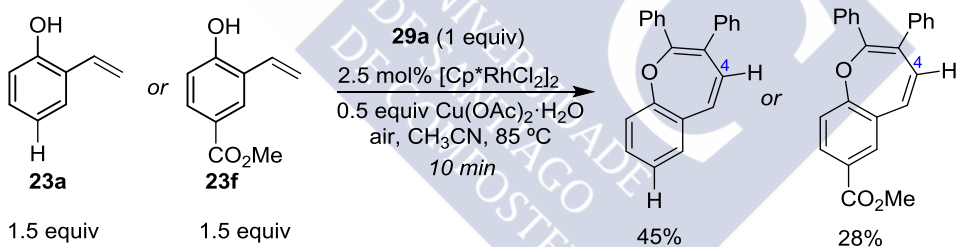


3.6 Competition experiment between 23a and 23f.



To a solution of $[\text{Cp}^*\text{RhCl}_2]_2$ (5.2 mg, 2.5 mol%) and $\text{Cu}(\text{OAc})_2 \cdot \text{H}_2\text{O}$ (33 mg, 0.165 mmol, 0.5 equiv) and diphenylacetylene (59 mg, 0.333 mmol) in MeCN (1.5 mL) under air atmosphere was added 2-vinylphenol (**23a**) (80 mg, 2 equiv, 0.66 mmol) and methyl 4-hydroxy-3-vinylbenzoate (**23f**) (119 mg, 2 equiv, 0.66 mmol) dissolved in MeCN (0.5 mL). The reaction was sealed with a rubber septum and an air atmosphere was injected in the flask with a balloon and a needle. The reaction was heated at 85 °C and stirred at that temperature. After 105 min an aliquot was filtered through silica, washing with diethylether; the solvents were evaporated *in vacuo* and the residue was analyzed by ^1H NMR in CDCl_3 . The ratio of oxepines **23fa** and **23aa** of the crude mixture was determined to be 8:1 by integration of the H_4 of the oxepines.

3.7 Procedure for comparing reaction rates.



RATE of 25aa: To a solution of $[\text{Cp}^*\text{RhCl}_2]_2$ (5.2 mg, 0.125 mmol/2.5 mol%) and $\text{Cu}(\text{OAc})_2 \cdot \text{H}_2\text{O}$ (33 mg, 0.165 mmol, 0.5 equiv) and diphenylacetylene (59 mg, 0.333 mmol) in MeCN (2 mL) under air atmosphere was added 2-vinylphenol (60 mg, 0.50 mmol). The reaction was sealed with a rubber septum and an air atmosphere was injected in the flask with a balloon and a needle. The reaction was heated at 85 °C. After 10 minutes an aliquot of 0.2 mL of the reaction mixture was taken filtered through silica (washing with diethylether) and the solvents were evaporated *in vacuo*. 0.75 mL of a solution of 3 μL of dioxane (as internal standard) in 5 mL of CDCl_3 was added and the residue analyzed by ^1H NMR. The yield was found by integrating the H_4 of the oxepine **25aa**.

RATE of 25fa: To a solution of $[\text{Cp}^*\text{RhCl}_2]_2$ (5.2 mg, 0.125 mmol/2.5 mol%) and $\text{Cu}(\text{OAc})_2 \cdot \text{H}_2\text{O}$ (33 mg, 0.165 mmol, 0.5 equiv) and diphenylacetylene (59 mg, 0.333 mmol) in MeCN (2

mL) under air atmosphere was added 4-hydroxy-3-vinylbenzoate (89 mg, 0.50 mmol). The reaction was sealed with a rubber septum and an air atmosphere was injected in the flask with a balloon and a needle. The reaction was heated at 85 °C. After 10 minutes an aliquot of 0.2 mL of the reaction mixture was taken filtered through silica (washing with diethylether) and the solvents were evaporated *in vacuo*. 0.75 mL of a solution of 3 µL of MeOH (as internal standard) in 5 mL of CDCl₃ was added and the residue analyzed by ¹H NMR. The yield was found by integrating the H₄ of the oxepine **25fa**.





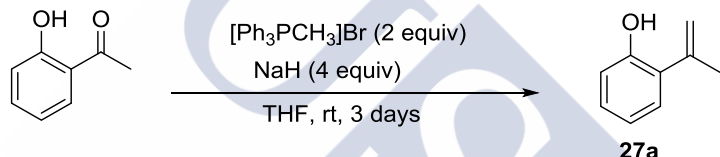
4- CHAPTER IV: Dearomatizing (3+2) oxidative annulations of *o*-alkenylphenols and alkynes for the synthesis of spirocycles.

4.1 General considerations.

Alkenylphenols **27j** 2-(1-(4-(fluoromethyl)phenyl)vinyl)phenol and **27i** 2-(1-(4-methoxyphenyl) vinyl)phenol were prepared according to the procedure reported by Sasano, K.; Takaya, J.; Iwasawa, N., *J. Am. Chem. Soc.* **2013**, *135*, 10954. All the data recorded match with the reported data.

All Alkenylphenols substrates were kept under Argon at -60 °C and used freshly within 2-3 days after made.

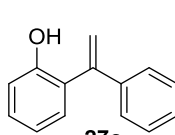
4.2 Procedure A for the synthesis of *o*-vinylphenols exemplified for **27a**.



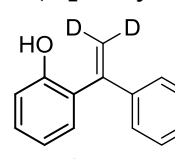
To a solution of sodium hydride (0.588 g, 14.7 mmol) in THF (15 mL) under Ar atmosphere was added methyltriphenylphosphoniumbromide (2.62 g, 7.35 mmol) at 0 °C. The reaction mixture was stirred for 1h at that temperature. Then 1-(2-hydroxyphenyl)ethanone (0.50 g, 3.67 mmol) was added at 0 °C and the reaction was stirred for 3 days at room temperature and quenched with saturated NH₄Cl aqueous solution. The solvent was removed in vacuo and the resulting mixture was extracted with diethyl ether. The combined organic layer was washed with brine, and dried over anhydrous sodium sulfate. Evaporation of the solvent followed by purification by flash chromatography on silica gel (hexanes:diethylether; 8:2) gave 2-(prop-1-en-2-yl)phenol (**27a**) (0.44 g, 91%), yellow liquid. ¹H NMR (300 MHz, CDCl₃) δ 7.25 – 7.15 (m, 2H), 7.01 – 6.87 (m, 2H), 5.76 (s, 1H), 5.47 – 5.40 (m, 1H), 5.21 – 5.15 (m, 1H), 2.15 (dd, *J* = 1.6, 0.9 Hz, 3H). ¹³C NMR (75 MHz, CDCl₃) δ 152.0 (C), 142.2 (C), 129.0 (C), 128.7 (CH), 127.9 (CH), 120.3 (CH), 115.9 (CH₂), 115.7 (CH), 24.3 (CH₃). LRMS (CI) (*m/z*, *I*): 135(100). HRMS calculated for C₉H₁₁O 135.0810, found 135.0810.

2-(but-1-en-2-yl)phenol (27b): 68%, pale yellow liquid. ¹H NMR (300 MHz, CDCl₃) δ 7.25 – 7.07 (m, 2H), 7.02 – 6.86 (m, 2H), 5.70 (dd, *J* = 1.9, 1.1 Hz, 1H), 5.41 (dd, *J* = 1.6, 0.8 Hz, 1H), 5.16 (dd, *J* = 1.8, 0.9 Hz, 1H) 2.45 (q, *J* = 7.4 Hz, 2H), 1.10 (t, *J* = 7.4 Hz, 3H). ¹³C NMR (75 MHz, CDCl₃) δ 152.3 (C), 148.1 (C), 128.6 (CH), 128.0 (CH), 120.2 (CH), 115.5 (CH), 114.1 (CH₂), 30.8 (CH₂), 12.6 (CH₃). LRMS (CI) (*m/z*, *I*): 149 (100), 133 (59), 107 (83). HRMS calculated for C₁₀H₁₃O 149.0966, found 149.0965.

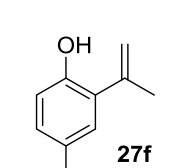
2-(1-phenylvinyl)phenol (27c): 91% yield, yellow liquid. **¹H NMR** (300 MHz, CDCl₃) δ(ppm):


 7.45 – 7.33 (m, 5H), 7.28 (dd, *J* = 6.2, 4.4 Hz, 1H), 7.20 – 7.16 (m, 1H), 6.98 (ddd, *J* = 8.6, 5.8, 2.1 Hz, 2H), 5.91 (d, *J* = 1.2 Hz, 1H), 5.46 (d, *J* = 1.2 Hz, 1H), 5.24 (d, *J* = 1.2 Hz, 1H). **¹³C NMR** (75 MHz, CDCl₃) δ 153.2 (C), 145.4 (C), 139.5 (C), 130.6 (CH), 129.6 (CH), 128.8 (CH), 128.8 (CH), 127.7 (C), 127.2 (CH), 120.6 (CH), 116.9 (CH₂), 116 (CH). **LRMS (CI)** (*m/z*, *I*): 197 (98), 195 (92), 181 (96), 103 (100). **HRMS** calculated for C₁₄H₁₂O 195.0810 found, 195.0809.

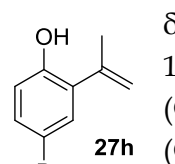
2-(1-phenylvinyl)phenol-d₂ (27c-d₂, 88% deuteration):¹⁸⁷ 94%, pale yellow liquid. **¹H NMR**


 (300 MHz, CDCl₃) δ 7.51 – 7.24 (m, 6H), 7.19 (dd, *J* = 4.1, 3.4 Hz, 1H), 7.07 – 6.93 (m, 2H), 5.90 (s, 0.12H), 5.46 (s, 0.12H), 5.27 (s, 1H). **¹³C NMR** (75 MHz, CDCl₃) δ 153.2(C), 145.2 (C), 139.5 (C), 130.5 (CH), 129.6 (CH), 128.8 (CH), 128.7 (CH), 127.6 (C), 127.1 (CH), 120.6 (CH), 115.9 (CH) **LRMS (CI)** (*m/z*, *I*): 199(100), 181 (27). **HRMS** calculated for C₁₄H₁₀D₂ O198.1014, found 198.1016.

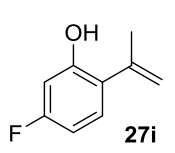
4-methyl-2-(prop-1-en-2-yl)phenol (27f): 80%, yellow liquid. **¹H NMR** (300 MHz, CDCl₃) δ


 (ppm): δ 7.09 – 6.98 (m, 2H), 6.94 – 6.86 (m, 1H), 5.79 (s, 1H), 5.48 – 5.36 (m, 1H), 5.19 (dd, *J* = 1.9, 0.9 Hz, 1H), 2.34 (d, *J* = 0.5 Hz, 3H), 2.23 – 2.16 (m, 3H). **¹³C NMR** (75 MHz, CDCl₃) δ 149.7 (C), 142.4 (C), 129.3 (C), 129.1 (CH), 128.8 (C), 128.3 (CH), 115.6 (CH₂), 115.5 (CH), 24.16 (CH₃), 20.5 (CH₃). **LRMS (EI)** (*m/z*, *I*): 148 (100), 133 (50), 105 (61). **HRMS** calculated for C₁₀H₁₂O: 148.0888 found, 148.0889.

4-bromo -2-(prop-1-en-2-yl)phenol (27h): 79% yield, red liquid. **¹H NMR** (300 MHz, CDCl₃)


 δ(ppm): 7.29 – 7.24 (m, 2H), 6.83 (dd, *J* = 6.8, 2.3 Hz, 1H), 5.70 (s, 1H), 5.44 (d, *J* = 1.3 Hz, 1H), 5.18 (s, 1H), 2.12 (s, 3H). **¹³C NMR** (75 MHz, CDCl₃) δ 151.2 (C), 141.2 (C), 131.5 (CH), 131.0 (C), 130.6 (CH), 117.5 (CH), 116.9 (CH₂), 112.4 (C), 24.2 (CH₃). **LRMS (EI)** (*m/z*, *I*): 212 (16), 149 (64), 118 (23), 5 (100). **HRMS** calculated for C₉H₉OBr: 211.9837 found, 211.9820.

5-fluoro-2-(prop-1-en-2-yl)phenol (27j): 36% yield, yellow liquid. **¹H NMR** (300 MHz,


 CDCl₃) δ(ppm): 7.09 (ddd, *J* = 8.3, 6.5, 1.5 Hz, 1H), 6.69 – 6.58 (m, 2H), 5.91 (s, 1H), 5.41 41 (dt, *J* = 3.0, 1.5 Hz, 1H), 5.12 (dd, *J* = 1.7, 0.8 Hz, 1H), 2.10 (d, *J* = 0.9 Hz, 3H). **¹³C NMR** (75 MHz, CDCl₃) δ 162.7 (C, d, *J* = 245.5 Hz), 153.3 (C,d, *J* = 11.7 Hz), 141.6 (C), 128.8 (CH, d, *J* = 9.9 Hz), 125.0 (C, d, *J* = 3.1 Hz), 116.0

¹⁸⁷This compound was synthesized using trideutated methyltriphenylphosphoniumiodide instead of methyltriphenylphosphoniumbromide.

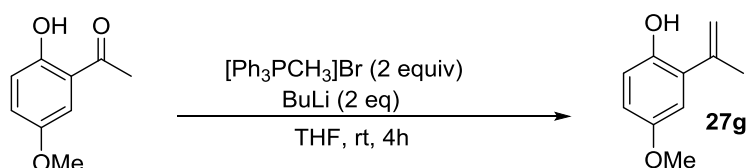
(CH₂), 107.3 (CH, d, *J* = 21.7 Hz), 103.1 (CH, d, *J* = 24.9 Hz), 24.4(CH₃). **LRMS (EI)** (*m/z*, *I*): 148 (73), 139 (38), 85 (75), 57 (100).

5-chloro-2-(prop-1-en-2-yl)phenol (27k): 73%, yellow liquid. **¹H NMR** (300 MHz, CDCl₃) δ (ppm): 7.06 (d, *J* = 8.2 Hz, 1H), 6.95 (d, *J* = 2.1 Hz, 1H), 6.90 – 6.85 (m, 1H), 5.82 (s, 1H), 5.43 – 5.40 (m, 1H), 5.15 – 5.13 (m, 1H), 2.11 – 2.08 (m, 3H). **¹³C NMR** (75 MHz, CDCl₃) δ 152.8 (C), 141.4 (C), 133.8 (C), 128.8 (CH), 127.5 (C), 120.6 (CH), 116.4 (CH₂), 116.0 (CH), 24.3 (CH₃). **LRMS (EI)** (*m/z*, *I*): 168 (45), 155 (50), 104 (64), 91 (100). **HRMS** calculated for C₉H₉OCl: 168.0342 found, 169.0344.

2-(prop-1-en-2-yl)-5,6,7,8-tetrahydronaphthalen-1-ol (27m): 62 %, yellow liquid. **¹H NMR** (300 MHz, CDCl₃) δ (ppm): 6.93 (d, *J* = 7.8 Hz, 1H), 6.68 (d, *J* = 7.8 Hz, 1H), 5.85 (s, 1H), 5.43 – 5.40 (m, 1H), 5.15 (s, 1H), 2.80 – 2.70 (m, 4H), 2.14 – 2.12 (m, 3H), 1.90 – 1.76 (m, 4H). **¹³C NMR** (75 MHz, CDCl₃) δ 149.6 (C), 142.8 (C), 138.1 (C), 125.3 (C), 124.3 (CH), 124.1 (CH), 120.6 (C), 115.3 (CH), 29.7 (CH₂), 24.6 (CH₂), 23.5 (CH₃), 23 (CH₂), 22.9 (CH₂), 22.9 (CH₂). **LRMS (EI)** (*m/z*, *I*): 188 (100), 173 (90), 160 (32), 145(67). **HRMS** calculated for C₁₃H₁₆O: 188.1201 found, 188.1200.

4, 5-dimethyl-2-(prop-1-en-2-yl)phenol (27n): 25% yield, white solid. **¹H NMR** (300 MHz, CDCl₃) δ(ppm): 6.92 (d, *J* = 4.6 Hz, 1H), 6.76 (d, *J* = 4.8 Hz, 1H), 5.54 (dd, *J* = 4.1, 2.5 Hz, 1H), 5.37 (ddt, *J* = 4.8, 3.3, 1.6 Hz, 1H), 5.13 (s, 1H), 2.25 – 2.22 (m, 3H), 2.22 – 2.19 (m, 3H), 2.12 (dd, *J* = 3.3, 1.3 Hz, 3H). **¹³C NMR** (75 MHz, CDCl₃) δ 149.9 (C), 142.3 (C), 137.2 (C), 128.7 (CH), 128.1 (C), 126.1 (C), 116.8 (CH), 115.3 (CH₂), 77.1 (C), 24.4 (CH₃), 19.7 (CH₃), 18.9 (CH₃). **LRMS (CI)** (*m/z*, *I*): 163 (100), 162 (79), 147 823). **HRMS** calculated for C₁₁H₁₅O: 163.1123 found, 163.1125.

4.3 Procedure B for the synthesis of *o*-vinylphenols exemplified for 27g.

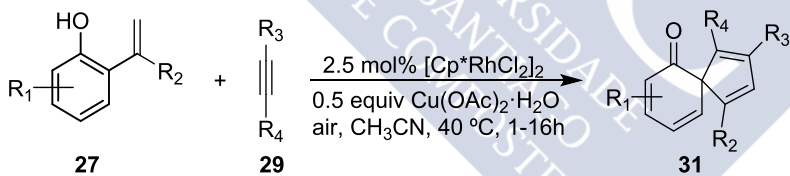


To a solution of methyltriphenylphosphoniumbromide (2.10 g, 6.02 mmol) in THF (25mL) was added dropwise a butyllithium solution in THF (2.6 mL, x 2.3 M, 6.02 mmol) at -78 °C.

The resulting mixture was stirred 15 minutes and allowed to reach rt. After cooling the mixture again to -78 °C, 1-(2-hydroxy-4-methoxyphenyl)ethanone (0.5 g, 3.01 mmol) was added and the reaction was stirred for 4 hours at room temperature and quenched with saturated NH₄Cl aqueous solution. The solvent was removed *in vacuo* and the resulting mixture was extracted with diethyl ether. The combined organic layer was washed with brine, and dried over anhydrous sodium sulfate. Solvent evaporation followed by flash column chromatography purification on silica gel (hexanes:diethylether; 8:3) yielded 4-methoxy-2-(prop-1-en-2-yl)phenol (**27g**) (0.16 g, 32%), yellow liquid. ¹H NMR (300 MHz, CDCl₃) δ (ppm): 7.07 (d, *J* = 7.9 Hz, 1H), 6.58 – 6.48 (m, 2H), 5.94 (s, 1H), 5.35 (dt, *J* = 3.2, 1.5 Hz, 1H), 5.11 (dd, *J* = 1.8, 0.9 Hz, 1H), 3.79 (d, *J* = 3.4 Hz, 3H), 2.11 – 2.10 (m, 3H). ¹³C NMR (75 MHz, CDCl₃) δ 160.0 (C), 153.2 (C), 142.1 (C), 128.5 (CH), 121.5 (C), 114.9 (CH₂), 106.4 (CH), 101.1 (CH), 55.3 (CH₃), 24.5 (CH₃). LRMS (EI) (*m/z*, *I*): 164 (100), 149 (23), 137 (10). HRMS calculated for C₁₀H₁₂O₂: 165.0916 found, 165.0916.

5-methoxy-2-(prop-1-en-2-yl)phenol (27i): 42 %, yellow liquid. ¹H NMR (300 MHz, CDCl₃) δ (ppm): 7.06 (d, *J* = 8.3 Hz, 1H), 6.52 – 6.44 (m, 2H), 5.91 (s, 1H), 5.37 – 5.32 (m, 1H), 5.13 – 5.07 (m, 1H), 3.78 (s, 3H), 2.10 (dd, *J* = 1.4, 0.9 Hz, 3H). ¹³C NMR (75 MHz, CDCl₃) δ 160.1 (C), 153.2 (C), 142.1 (C), 128.5 (CH), 121.5 (C), 114.9 (CH₂), 106.5 (CH), 101.1 (CH), 55.4 (CH₃), 24.6 (CH₃). LRMS (CI) (*m/z*, *I*): 164 (100), 152 (85), 149 (72), 108 (64). HRMS calculated for C₁₀H₁₂O₂: 164.1 found, 164.1.

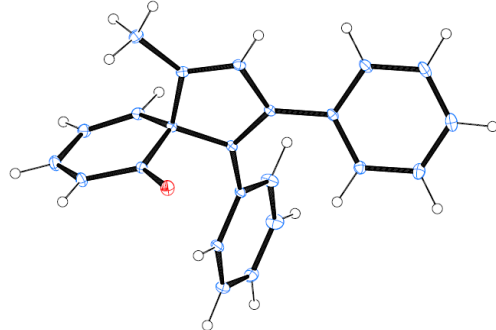
4.4 Procedure A for the Rh-catalyzed annulations.



To a solution of [Cp*RhCl₂]₂ (5.2 mg, 2.5 mol%) and Cu(OAc)₂ · H₂O (33 mg, 0.5 equiv, 0.165 mmol) in CH₃CN (2 mL) under air atmosphere was added the alkyne **2** (0.333 mmol) followed by the addition of corresponding *ortho*-alkenylphenols **27** (0.50 mmol, 1.5 equiv). The reaction was sealed with a rubber septum and an air atmosphere was injected in the flask with a balloon and a needle. The reaction was heated at 40 °C, stirred until full conversion as followed by TLC and then cooled to room temperature. The solvents were removed *in vacuo* and the remaining residue was purified by flash column chromatography on silica gel to afford the corresponding spirocycles **31**. In some cases we also isolated small proportions of products **25** and **32**.

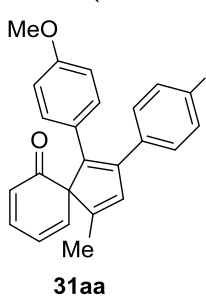
4-methyl-1,2-diphenylspiro[4.5]deca-1,3,7,9-tetraen-6-one (31aa): 97% yield, brown solid. ¹H NMR (500 MHz, CDCl₃) δ 7.39 – 7.33 (m, 2H), 7.32 – 7.23 (m, 3H), 7.22 – 7.17 (m, 1H), 7.16 – 7.11 (m, 3H), 7.10 – 7.04 (m, 2H), 6.63 – 6.59 (m, 1H), 6.55 – 6.49 (m, 1H), 6.29 (dd, *J* = 9.9, 0.5 Hz, 1H), 6.11 – 6.07 (m, 1H), 1.89 – 1.74 (m, 3H). ¹³C NMR (126 MHz, CDCl₃) δ 197.3 (C), 145.6 (C), 143.3 (CH), 141.9 (CH), 141.2 (C), 135.9 (C), 135.7 (C), 135.6 (CH), 128.7 (CH), 128.6 (CH), 128.4 (CH), 128.3 (CH), 128.3 (CH), 127.6 (CH), 127.0 (CH), 122.8 (CH), 77.2 (C), 13.1 (CH₃). LRMS (CI) (*m/z*, *I*): 311 (29), 137 (100). HRMS calculated for C₂₃H₁₉O 311.1436, found 311.1438.

The structure of this compound was further confirmed by XR-anaylysis. CCDC 995495 contains the crystallographic data of **31aa**, which can be obtained via www.ccdc.cam.ac.uk/data_request/cif.

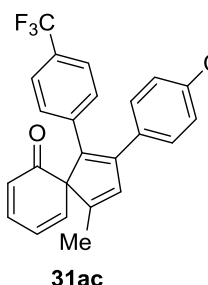


3a-methyl-1,2-diphenylazulen-4(3aH)-one (32aa): yellow oil. ¹H NMR (500 MHz, CDCl₃) δ 7.27 – 7.20 (m, 4H), 7.16 – 7.09 (m, 3H), 7.05 – 6.99 (m, 4H), 6.72 (d, *J* = 11.2 Hz, 1H), 6.62 (dd, *J* = 12.3, 8.3 Hz, 1H), 6.07 (dd, *J* = 11.1, 8.3 Hz, 1H), 5.70 (d, *J* = 12.3 Hz, 1H), 1.32 (s, 3H). ¹³C NMR (126 MHz, CDCl₃) δ 199.7 (C), 150.3 (C), 145.4 (C), 144.0 (CH), 140.9 (C), 137.1 (CH), 134.9 (C), 134.4 (C), 132.0 (CH), 130.5 (CH), 128.4 (CH), 128.3 (CH), 128.0 (CH), 127.5 (CH), 123.1 (CH), 122.7 (CH), 67.7 (C), 24.6 (CH₃). LRMS (EI) (*m/z*, *I*): 310 (100), 295 (10), 282 (53), 267 (71). HRMS calculated for C₂₃H₁₈O 310.1358, found 310.1359.

1,2-bis(4-methoxyphenyl)-4-methylspiro[4.5]deca-1,3,7,9-tetraen-6-one (31ab): 93% yield, brown solid. ¹H NMR (300 MHz, CDCl₃) δ 7.32 – 7.23 (m, 2H), 7.19 – 7.12 (m, 1H), 7.04 – 6.94 (m, 2H), 6.83 – 6.75 (m, 2H), 6.70 – 6.61 (m, 2H), 6.55 (d, *J* = 1.5 Hz, 1H), 6.47 (dd, *J* = 9.2, 6.0 Hz, 1H), 6.24 (d, *J* = 9.8 Hz, 1H), 6.08 – 6.01 (m, 1H), 3.77 (s, 3H), 3.71 (s, 3H), 1.78 (d, *J* = 1.4 Hz, 3H). ¹³C NMR (75 MHz, CDCl₃) δ 197.7 (C), 158.9 (C), 158.3 (C), 144.5 (C), 143.8 (C), 143.4 (CH), 142.3 (CH), 139.5 (C), 135.6 (CH), 129.7 (CH), 129.4 (CH), 128.5 (CH), 128.3 (C), 122.5 (CH), 113.7 (CH), 113.7 (CH), 77.1 (C), 55.2 (CH₃), 55.1 (CH₃), 13.0 (CH₃). LRMS (CI) (*m/z*, *I*): 371 (100). HRMS calculated for C₂₅H₂₃O₃ 371.1647, found 371.1647

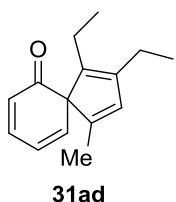


4-methyl-1,2-bis(4-(trifluoromethyl)phenyl)spiro[4.5]deca-1,3,7,9-tetraen-6-one (31ac): 71%



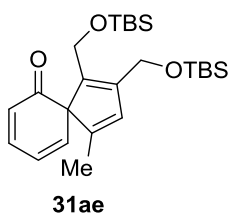
yield, brown solid. **¹H NMR** (300 MHz, CDCl₃) δ 7.55 (d, *J* = 8.1 Hz, 2H), 7.45 – 7.35 (m, 4H), 7.26 – 7.18 (m, 1H), 7.13 – 7.07 (m, 2H), 6.60 – 6.51 (m, 2H), 6.29 (d, *J* = 9.9 Hz, 1H), 6.08 – 6.01 (m, 1H), 1.83 (d, *J* = 1.6 Hz, 3H). **¹³C NMR** (75 MHz, CDCl₃) δ 196.4 (C), 147.6 (C), 146.1 (C), 143.5 (CH), 141.2 (C), 140.7 (CH), 139.0 (C), 138.7 (C), 134.9 (CH), 130.0 (C, q, *J* = 31.9 Hz), 128.9 (CH), 128.8 (CH), 128.4 (CH), 125.7 (CH, q, *J* = 3.7 Hz), 125.5 (CH, q, *J* = 3.7 Hz), 124.1 (q, *J* = 272.0 Hz), 123.5 (CH), 13.1 (CH₃) **LRMS (CI)** (*m/z*, *I*): 447 (99), 427 (100). **HRMS** calculated for C₂₅H₁₇OF₆ 447.1194, found 447.1194.

1,2-diethyl-4-methylspiro[4.5]deca-1,3,7,9-tetraen-6-one (31ad): 93% yield, yellow oil. **¹H NMR**



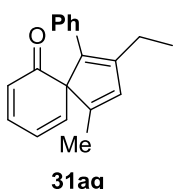
(300 MHz, CDCl₃) δ 7.20 – 7.11 (m, 1H), 6.41 (dd, *J* = 9.1, 5.9 Hz, 1H), 6.24 – 6.14 (m, 2H), 5.73 (dd, *J* = 9.1, 1.1 Hz, 1H), 2.26 (q, *J* = 7.6 Hz, 2H), 2.05 (q, *J* = 7.6 Hz, 2H), 1.64 (d, *J* = 1.3 Hz, 3H), 1.06 (t, *J* = 7.6 Hz, 3H), 0.88 (t, *J* = 7.6 Hz, 3H). **¹³C NMR** (75 MHz, CDCl₃) δ 198.8 (C), 146.4 (C), 143.3 (CH), 143.2 (C), 142.7 (CH), 141.9 (C), 134.1 (CH), 128.3 (CH), 122.1 (CH), 76.1 (C), 20.6 (CH₂), 20.0 (CH₂), 14.7 (CH₃), 13.9 (CH₃), 13.2 (CH₃). **LRMS (CI)** (*m/z*, *I*): 215 (100), 199 (17), 185 (98). **HRMS** calculated for C₁₅H₁₉O₂ 215.1436, found 215.1439.

1,2-bis(((tert-butyldimethylsilyl)oxy)methyl)-4-methylspiro[4.5]deca-1,3,7,9-tetraen-6-one (31ae): 81% yield, yellow oil. **¹H NMR**

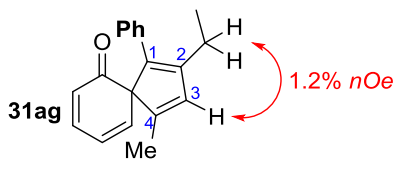


(300 MHz, CDCl₃) δ 7.14 – 7.05 (m, 1H), 6.38 (dd, *J* = 9.2, 5.9 Hz, 1H), 6.27 (d, *J* = 1.6 Hz, 1H), 6.17 (d, *J* = 9.8 Hz, 1H), 5.84 – 5.74 (m, 1H), 4.46 (q, *J* = 13.5 Hz, 2H), 4.25 (q, *J* = 13.2 Hz, 2H), 1.67 (d, *J* = 1.3 Hz, 3H), 0.90 (s, 9H), 0.81 (s, 9H), 0.07 (d, *J* = 3.3 Hz, 6H), -0.05 (d, *J* = 4.1 Hz, 6H). **¹³C NMR** (75 MHz, CDCl₃) δ 197.3 (C), 145.0 (C), 144.8 (C), 142.6 (CH), 141.6 (CH), 141.2 (C), 132.5 (CH), 128.4 (CH), 121.8 (CH), 74.9 (C), 59.0 (CH₂), 58.2 (CH₂), 26.04 (CH₃), 26.00 (CH₃), 18.5 (C), 13.0 (CH₃), -5.1 (CH₃), -5.49 (CH₃), -5.53 (CH₃). **LRMS (CI)** (*m/z*, *I*): 446 (7), 389 (13), 314 (19), 301 (63). **HRMS** calculated for C₂₅H₄₂O₃Si₂ 446.2673, found 446.2673.

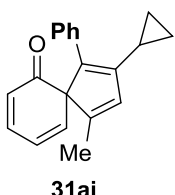
2-ethyl-4-methyl-1-phenylspiro[4.5]deca-1,3,7,9-tetraen-6-one (31ag): 89% yield, yellow oil.



¹H NMR (300 MHz, CDCl₃) δ 7.27 – 7.07 (m, 6H), 6.48 – 6.34 (m, 2H), 6.22 (d, *J* = 9.8 Hz, 1H), 5.99 – 5.91 (m, 1H), 2.49 (q, *J* = 7.5 Hz, 2H), 1.74 (d, *J* = 1.4 Hz, 3H), 1.18 (t, *J* = 7.6 Hz, 3H). **¹³C NMR** (75 MHz, CDCl₃) δ 197.9 (C), 148.8 (C), 145.2 (C), 143.3 (CH), 142.6 (CH), 140.0 (C), 135.7 (CH), 134.9 (CH), 128.5 (CH), 128.2 (CH), 128.0 (CH), 126.6 (CH), 122.4 (CH), 76.5 (C), 21.7 (CH₂), 13.8 (CH₃), 12.9 (CH₃). **LRMS (EI)** (*m/z*, *I*): 262 (100), 247 (67), 233 (27), 219 (28), 205 (58). **HRMS** calculated for C₁₉H₁₈O₂ 262.1358, found 262.1358.

Assignment of the regiochemistry

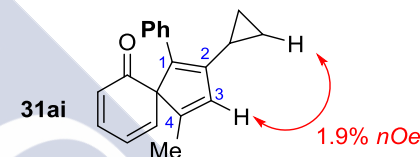
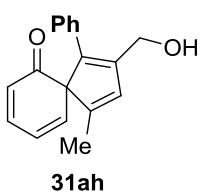
The major regioisomer was assigned based on the HMBC, HSQC, COSY experiments, as well as by the observation of nOe between the ethyl chain and the C3 hydrogen of the spiro unit.

2-cyclopropyl-4-methyl-1-phenylspiro[4.5]deca-1,3,7,9-tetraen-6-one (31ai): 78%

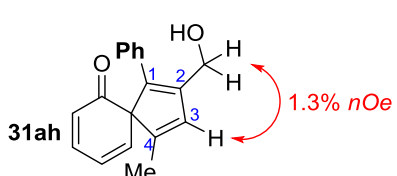
yield, yellow oil. **¹H NMR** (300 MHz, CDCl₃) δ 7.35 – 7.23 (m, 4H), 7.22 – 7.13 (m, 2H), 6.50 – 6.43 (m, 1H), 6.27 (dd, J = 9.8, 0.6 Hz, 1H), 6.05 – 5.95 (m, 2H), 2.03 – 1.91 (m, 1H), 1.74 (d, J = 1.6 Hz, 3H), 0.99 – 0.81 (m, 3H), 0.79 – 0.63 (m, 1H). **¹³C NMR** (75 MHz, CDCl₃) δ 197.9 (C), 148.5 (C), 145.4 (C), 143.3 (CH), 142.8 (CH), 139.8 (C), 135.9 (C), 131.2 (CH), 128.6 (CH), 128.3 (CH), 128.0 (CH), 126.5 (CH), 122.4 (CH), 76.6 (C), 13.0 (CH₃), 10.5 (CH), 7.7 (CH₂), 7.6 (CH₂). **LRMS (EI)** (m/z, I): 274 (100), 259 (48), 246 (27), 231 (47), 215 (79). **HRMS** calculated for C₂₀H₁₈O₂ 274.1349, found 274.1358.

Assignment of the regiochemistry

The major regioisomer was assigned based on the HMBC, HSQC, COSY experiments, as well as by the observation of nOe between the cyclopropyl chain and the hydrogen of the C3 of the spiro unit.

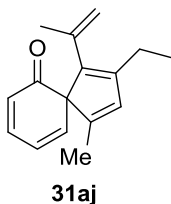
**2-(hydroxymethyl)-4-methyl-1-phenylspiro[4.5]deca-1,3,7,9-tetraen-6-one (31ah): 78% yield,**

yellow oil. **¹H NMR** (500 MHz, CDCl₃) δ 7.27 – 7.17 (m, 4H), 7.09 – 7.04 (m, 2H), 6.57 (q, J = 1.5 Hz, 1H), 6.50 (dd, J = 9.2, 5.9 Hz, 1H), 6.29 (d, J = 9.7 Hz, 1H), 6.01 – 5.97 (m, 1H), 4.53 (dd, J = 51.2, 13.0 Hz, 2H), 3.00 (br s, 1H), 1.73 (d, J = 1.5 Hz, 3H). **¹³C NMR** (75 MHz, CDCl₃) δ 197.7 (C), 146.2 (C), 145.5 (C), 143.8 (CH), 142.2 (C), 141.9 (CH), 134.4 (C), 133.8 (CH), 128.2 (CH), 127.7 (CH), 127.0 (CH), 122.5 (CH), 76.3 (C), 58.5 (CH₂), 12.7 (CH₃). **LRMS (EI)** (m/z, I): 264 (100), 247 (30), 234 (31), 219 (27), 202 (50). **HRMS** calculated for C₂₂H₁₆O₂ 264.1150, found 264.1150

Assignment of the regiochemistry

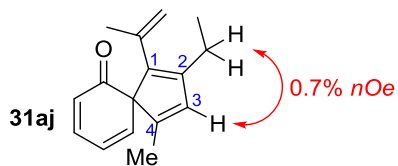
The major regioisomer was assigned based on the HMBC, HSQC, COSY experiments, as well as by the observation of nOe between the CH₂OH chain and the hydrogen of the C3.

2-ethyl-4-methyl-1-(prop-1-en-2-yl)spiro[4.5]deca-1,3,7,9-tetraen-6-one (31aj): 80% yield, yellow oil. ¹H NMR (300 MHz, CDCl₃) δ 7.21 – 7.11 (m, 1H), 6.47 – 6.38 (m, 1H), 6.27 – 6.21 (m, 2H), 5.89 – 5.80 (m, 1H), 4.77 (s, 1H), 4.46 (s, 1H), 2.63 – 2.38 (m, 2H), 1.86 – 1.81 (m, 3H), 1.64 (d, *J* = 1.3 Hz, 3H), 1.12 (dd, *J* = 7.8, 7.3 Hz, 3H). ¹³C NMR (75 MHz, CDCl₃) δ 197.9 (C), 148.8 (C), 144.2 (C), 143.9 (CH), 143.0 (CH), 142.0 (C), 139.1 (C), 135.7 (C), 128.4 (CH), 121.8 (CH), 114.1 (CH), 75.6 (C), 23.4 (CH₃), 22.3 (CH₂), 14.2 (CH₃), 12.5 (CH₃). LRMS (EI) (*m/z*, *I*): 226 (67), 211 (65), 198 (100), 183 (72). HRMS calculated for C₁₆H₁₈O 226.1358, found 226.1356.



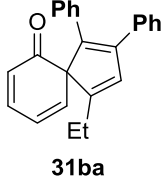
I: 226 (67), 211 (65), 198 (100), 183 (72). HRMS calculated for C₁₆H₁₈O 226.1358, found 226.1356.

Assignment of the regiochemistry.

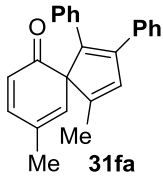


The major regioisomer was assigned based on the HMBC, HSQC, COSY experiments, as well as by the observation of nOe between the CH₂CH₃ chain and the hydrogen of the C3.

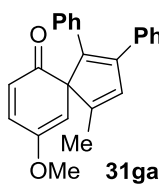
4-ethyl-1,2-diphenylspiro[4.5]deca-1,3,7,9-tetraen-6-one (31ba): 94% yield, brown solid. ¹H NMR (300 MHz, CDCl₃) δ 7.40 – 7.33 (m, 2H), 7.30 – 7.21 (m, 3H), 7.20 – 7.01 (m, 6H), 6.62 (t, *J* = 1.9 Hz, 1H), 6.48 (dd, *J* = 9.1, 6.0 Hz, 1H), 6.25 (d, *J* = 9.8 Hz, 1H), 6.15 – 5.98 (m, 1H), 2.21 – 2.00 (m, 2H), 1.16 (t, *J* = 7.4 Hz, 3H). ¹³C NMR (75 MHz, CDCl₃) δ 197.4 (C), 152.1 (C), 145.4 (C), 143.3 (CH), 142.1 (CH), 140.9 (C), 135.9 (C), 135.6 (C), 133.2 (CH), 128.7 (CH), 128.6 (CH), 128.4 (CH), 128.3 (CH), 128.2 (CH), 127.6 (CH), 127.0 (CH), 122.7 (CH), 77.1 (C), 20.6 (CH₂), 12.1 (CH₃). LRMS (EI) (*m/z*, *I*): 324 (100), 309 (45), 296 (21), 279 (18), 267 (86). HRMS calculated for C₂₄H₂₀O 324.1514, found 324.1523.



4,9-dimethyl-1,2-diphenylspiro[4.5]deca-1,3,7,9-tetraen-6-one (31fa): 89% yield, Red oil. ¹H NMR (300 MHz, CDCl₃) δ (ppm): 7.31 (dt, *J* = 8.5, 4.4 Hz, 2H), 7.27 – 7.2 (m, 3H), 7.14 – 7.08 (m, 3H), 7.01 (dd, *J* = 6.3, 3.4 Hz, 3H), 6.53 (d, *J* = 1.6 Hz, 1H), 6.20 (d, *J* = 9.9 Hz, 1H), 5.73 (s, 1H), 2.03 (d, *J* = 1.4 Hz, 3H), 1.79 (d, *J* = 1.5 Hz, 3H). ¹³C NMR (75 MHz, CDCl₃) δ (ppm): 197.5 (C), 147.6 (CH), 146.3 (C), 145.1 (C), 141.5 (C), 136.0 (C), 135.8 (C), 135.4 (CH), 134.9 (CH), 130.6 (C), 128.6 (CH), 128.4 (CH), 128.3 (CH), 128.2 (CH), 127.5 (CH), 126.9 (CH), 76.5 (C), 21.2 (CH₃), 13.2 (CH₃). HRMS (m/z, ESI) for C₂₈H₂₁O [M+H]⁺ 325.1639.

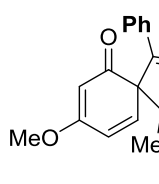


9-methoxy-4-methyl-1,2-diphenylspiro[4,5]deca-1,3,7,9-tetraen-6-one (31ga): 43% yield,



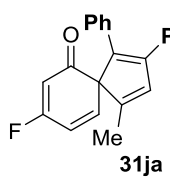
yellow solid. **¹H NMR** (300 MHz, CDCl₃) δ (ppm) 7.37 (d, *J* = 1.4, 2H), 7.33 – 7.25 (m, 3H), 7.19 – 7.10 (m, 5H), 6.67 – 6.63 (m, 1H), 6.43 – 6.37 (m, 1H), 6.13 – 6.05 (m, 1H), 5.74 (d, *J* = 1.8 Hz, 1H), 3.83 (s, 3H), 1.90 – 1.83 (m, 3H). **¹³C NMR** (75 MHz, CDCl₃) δ (ppm): 195.5 (C), 173.0 (C), 145.8 (C), 145.5 (C), 142.3 (CH), 141.4 (C), 135.8 (C), 135.2 (CH), 128.6 (CH), 128.4 (CH), 128.3 (CH), 128.3 (CH), 127.5 (CH), 127 (CH), 122.9 (CH), 102.9 (CH), 75.4 (C), 56.0 (CH₃), 13.1(CH₃). **HRMS** (m/z, ESI) calculated for C₂₄H₂₁O₂ [M+H]⁺ found, 341.1638.

8-methoxy-4-methyl-1,2-diphenylspiro[4,5] deca-1,3,7,9-tetraen-6-one (31ia): 43% yield,



yellow solid. **¹H NMR** (300 MHz, CDCl₃) δ (ppm): 7.39 – 7.33 (m, 2H), 7.31 – 7.23 (m, 3H), 7.17 – 7.09 (m, 5H), 6.63 (d, *J* = 1.6 Hz, 1H), 6.41 – 6.36 (m, 1H), 6.08 (d, *J* = 9.8 Hz, 1H), 5.73 (d, *J* = 1.8 Hz, 1H), 3.82 (s, 3H), 1.85 (d, *J* = 1.5 Hz, 3H). **¹³C NMR** (75 MHz, CDCl₃) δ (ppm): 195.6 (C), 173.1 (C), 145.8 (C), 145.5 (C), 142.4 (CH), 141.4 (C), 135.8 (C), 135.3 (CH), 128.6 (CH), 128.4 (CH), 128.3 (CH), 128.3 (CH), 128 (C), 127.5 (CH), 127 (CH), 123 (CH), 103 (CH), 75.4 (C), 56.0 (CH₃), 13.1 (CH₃). **HRMS** (m/z, ESI) calculated for C₂₄H₂₁O₂ [M+H]⁺ found, 341.1536.

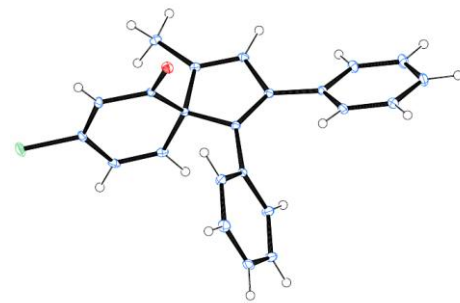
8-fluoro-4-methyl-1,2-diphenylspiro[4,5]deca-1,3,7,9-tetraen-6-one(31ja): 97% yield, red oil.



¹H NMR (500 MHz, CDCl₃) δ (ppm): 7.38 – 7.30 (m, 2H), 7.31 – 7.22 (m, 3H), 7.19 – 7.12 (m, 3H), 7.08 – 7.02 (m, 2H), 6.65 (q, *J* = 1.5 Hz, 1H), 6.55 – 6.48 (m, 1H), 6.24 – 6.20 (m, 1H), 6.04 (dd, *J* = 12.5, 2.0 Hz, 1H), 1.84 (t, *J* = 2.0 Hz, 3H). **¹³C NMR** (500 MHz, CDCl₃) δ (ppm): 196.1 (C, d, *J* = 18.1 Hz), 175 (C, d, *J* = 279.2 Hz), 146.2 (C), 145.2 (CH, d, *J* = 13.8 Hz), 144.9 (C), 140.7 (C), 136.3 (CH), 135.4 (C), 135.3 (C), 128.6 (CH), 128.5 (CH), 128.3 (CH), 127.8 (CH), 127.3 (CH), 119.7 (CH, d, *J* = 33.1 Hz), 109.8 (CH, d, *J* = 12.6 Hz), 76.5 (C), 13.1 (CH₃). **HRMS** (m/z, ESI) calculated for C₂₃H₁₈FO [M+H]⁺ found, 329.1336.

8-chloro-4-methyl-1,2-diphenylspiro[4,5]deca-1,3,7,9-tetraen-6-one (31ka): 85% yield, red

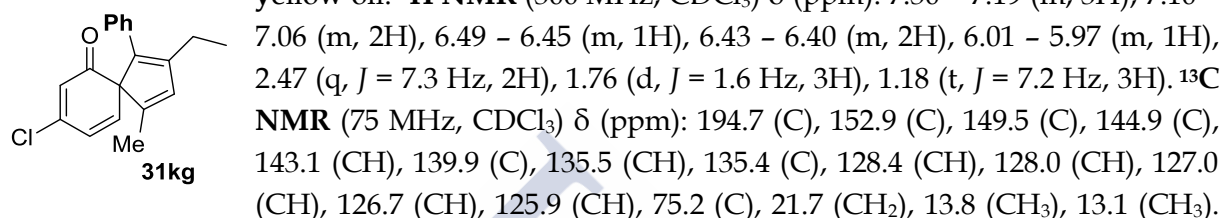
solid. **¹H NMR** (300 MHz, CDCl₃) δ (ppm): 7.29 (dd, *J* = 5.2, 3.3 Hz, 1H), 7.24 (dd, *J* = 5.1, 2.0 Hz, 3H), 7.11 (t, *J* = 3.2 Hz, 3H), 7.00 (dd, *J* = 6.6, 3.0 Hz, 3H), 6.60 (d, *J* = 1.5 Hz, 1H), 6.51 (dd, *J* = 9.6, 1.3 Hz, 1H), 6.44 (s, 1H), 6.07 (s, 1H), 1.81 (d, *J* = 1.4 Hz, 3H). **¹³C NMR** (75 MHz, CDCl₃) δ (ppm): 194.2 (C), 152.9 (C), 146.1 (C), 145.2 (C), 142.4 (CH), 140.9 (C), 136.2 (CH),



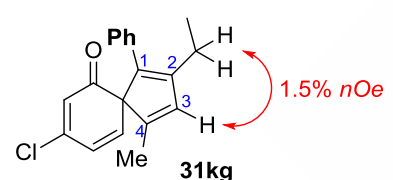
135.5 (C), 135.4 (C), 128.6 (CH), 128.5 (CH), 128.3 (CH), 127.8 (CH), 127.3 (CH), 126.8 (CH), 126.3 (CH), 75.9 (C), 13.2 (CH₃). **HRMS** (m/z, ESI) calculated for C₂₃H₁₈ClO [M+H]⁺ 345.1047 found, 345.1041.

confirmed by XR-analysis. CCDC 995496 contains the crystallographic data of **31ka**, which can be obtained via www.ccdc.cam.ac.uk/data_request/cif.

8-chloro-2-ethyl-4-methyl-1-phenylspiro[4,5]deca-1,3,7,9-tetraen-6-one (31kg): 73% yield, yellow oil. ¹H NMR (300 MHz, CDCl₃) δ (ppm): 7.30 – 7.19 (m, 3H), 7.10 –



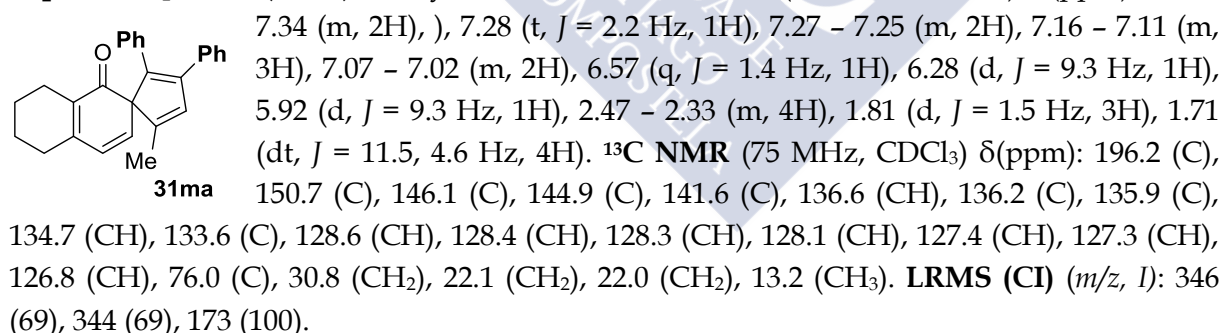
HRMS (m/z, ESI) calculated for C₁₉H₁₈ClO [M+H]⁺ 297.1036 found, 297.1041.



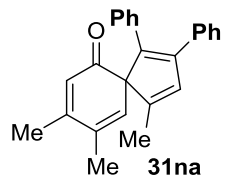
Assignment of the regiochemistry

The major regiosomer was assigned based on the HMBC, HSQC, COSY experiments, as well as by the observation of nOe between the CH₂OH chain and the hydrogen of the C3.

5-methyl-2,3-diphenyl-5', 6', 7', 8'-tetrahydro-1'H-spiro[cyclopenta[2,4]diene-1,2-naphthalen]1'-one (31ma): 78% yield, Yellow oil. ¹H NMR (300 MHz, CDCl₃) δ (ppm): 7.39 –

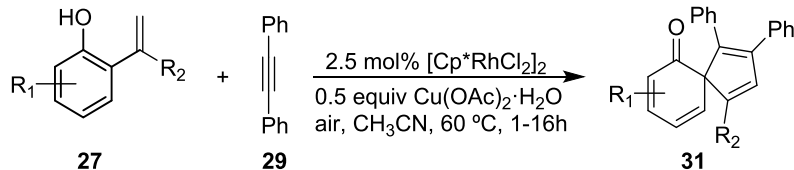


4,8,9-Trimethyl-1,2-diphenylspiro[4,5] deca-1,3,7,9-tetraen-6-one (31na): 77% yield, yellow solid. ¹H NMR (300 MHz, CDCl₃) δ (ppm): 7.37 – 7.28 (m, 2H), 7.24 (ddd, *J* = 6.5, 3.7, 1.1 Hz, 3H), 7.16 – 7.07 (m, 3H), 7.07 – 7.00 (m, 2H), 6.59 – 6.51 (m, 1H), 6.15 (s, 1H), 5.76 (s, 1H), 2.13 (s, 3H), 2.03 (d, *J* = 1.0 Hz, 3H), 1.81 – 1.78 (m, 3H). ¹³C NMR (75 MHz, CDCl₃) δ (ppm): 197.1 (C), 157.3 (C), 146.3 (C), 145.0 (C), 141.6 (C), 136.1 (C), 136 (CH), 135.9 (C), 134.8 (CH), 132.4 (C), 128.6 (CH), 128.4 (CH), 128.2 (CH), 127.4 (CH), 127 (CH), 126.8 (CH), 21.7 (CH₃),



19.2 (CH₃), 13.2 (CH₃). **LRMS (CI)** (*m/z*, *I*): 339 (60), 338 (39), 275 (71), 257 (100), 246 (86), 149 (91). **HRMS** calculated for C₂₅H₂₃O: 339.1749, found, 339.1749.

4.5 Procedure B for the Rh-catalyzed annulations.

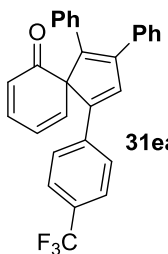


To a solution of [Cp*RhCl₂]₂ (5.2 mg, 2.5 mol%) and Cu(OAc)₂·H₂O (33 mg, 0.5 equiv, 0.165 mmol) in CH₃CN (2 mL) under air atmosphere was added the alkyne **2** (0.333 mmol) followed by the addition of corresponding *ortho*-vinylphenols **27** (0.50 mmol, 1.5 equiv). The reaction flask was sealed with a rubber septum and an air atmosphere was injected in the flask with a balloon and a needle. The reaction was heated at 60 °C, stirred until completion followed by TLC and then cooled to room temperature. The solvents were removed *in vacuo* and the remaining residue was purified by flash column chromatography on silica gel to afford the corresponding spirocycles **31**.

1,2,4-triphenylspiro[4,5]deca-1,3,7,9-tetraen-6-one (31ca): 92% yield, orange solid. **¹H NMR** (300 MHz, CDCl₃) δ(ppm): 7.51 (s, 1H), 7.36 – 7.32 (m, 6H), 7.28 – 7.18 (m, 7H), 7.17 – 7.09 (m, 3H), 6.53 (dd, *J* = 9.2, 6.0 Hz, 1H), 6.33 (d, *J* = 9.9 Hz, 1H), 6.28 – 6.23 (m, 1H). **¹³C NMR** (75 MHz, CDCl₃) δ(ppm): 196.5(C), 148.2(C), 145.7(C), 143.1(CH), 142.3(C), 141.5(CH), 135(C), 134.9(C), 134.1(CH), 133.6(C), 129.4(CH), 129.2(CH), 128.8(CH), 128.5(CH), 128.3(CH), 128.1(CH), 127.7(CH), 127.7(CH), 125.7(CH), 123.2(CH), 75.5(C). **HRMS (m/z, ESI)** calculated for C₂₈H₂₁O [M+H]⁺ 373.1587 found, 373.1577.

4-(4-methoxyphenyl)-1,2-diphenylspiro[4,5]deca-1,3,7,9-tetraen-6-one (31da): 70% yield, brown foam. **¹H NMR** (300 MHz, CD₂Cl₂) δ 7.35 – 7.15 (m, 11H), 7.14 – 7.06 (m, 3H), 6.89 – 6.80 (m, 2H), 6.48 (dd, *J* = 9.0, 6.0 Hz, 1H), 6.27 – 6.17 (m, 2H), 3.78 (s, 3H). **¹³C NMR** (75 MHz, CD₂Cl₂) δ 196.8 (C), 159.8 (C), 148.6 (C), 146.3 (C), 143.6 (CH), 142.1 (CH), 141.9 (C), 135.7 (C), 135.6 (C), 132.5 (CH), 129.8 (CH), 129.5 (CH), 128.9 (CH), 128.8 (CH), 128.5 (CH), 128.1 (CH), 128.0 (CH), 127.4 (CH), 127.1 (C), 123.6 (CH), 114.7 (CH), 75.9 (C), 55.8 (CH₃). **LRMS (CI)** (*m/z*, *I*): 403 (49), 271 (50), 228 (100). **HRMS** calculated for C₂₉H₂₃O₂ 403.1698, found 403.1712

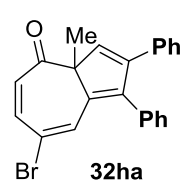
1,2-diphenyl-4-(4-(trifluoromethyl)phenyl)spiro[4.5]deca-1,3,7,9-tetraen-6-one (31ea): 98%



yield, brown foam. **¹H NMR** (300 MHz, CDCl₃) δ 7.62 – 7.51 (m, 3H), 7.39 (d, J = 8.2 Hz, 2H), 7.36 – 7.16 (m, 8H), 7.16 – 7.07 (m, 3H), 6.52 (dd, J = 9.2, 6.0 Hz, 1H), 6.34 – 6.28 (m, 1H), 6.24 – 6.18 (m, 1H). **¹³C NMR** (75 MHz, CDCl₃) δ 196.0 (C), 146.5 (C), 145.6 (C), 143.7 (C), 143.2 (CH), 140.8 (CH), 136.8 (C), 136.5 (CH), 134.6 (C), 134.5 (C), 129.21 (CH), 129.19 (CH), 128.5 (CH), 128.4 (CH), 128.2 (CH), 127.9 (CH), 125.7 (CH), 124.2 (q, J = 271.8 Hz, C) 123.6 (CH), 75.3 (C). **LRMS (CI)** (*m/z*, *I*): 440 (100), 421 (50), 412 (58). **HRMS** calculated for C₂₉H₂₀OF₃ 441.1480, found 441.1466.

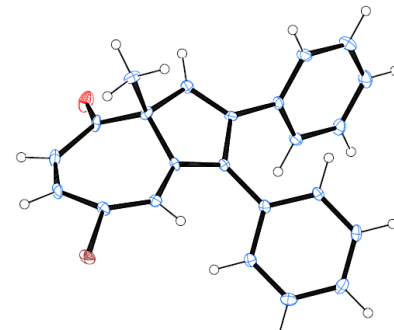
8-bromo -4-methyl-1,2-diphenylspiro[4.5] deca-1,3,7,9-tetraen-6-one (31ha): 67% yield, red oil. **¹H NMR** (300 MHz, CDCl₃) δ (ppm): 7.32 – 7.22 (m, 4H), 7.17 – 7.13 (m, 4H), 7.11 (d, J = 2.7 Hz, 1H), 7.04 – 7.01 (m, 2H), 6.58 (t, J = 1.6 Hz, 1H), 6.30 (d, J = 2.6 Hz, 1H), 6.15 (d, J = 10.1 Hz, 1H), 1.86 (d, J = 1.6 Hz, 3H). **¹³C NMR** (75 MHz, CDCl₃) δ (ppm): 194.9 (C), 146.7 (CH), 145.7 (C), 145.0 (C), 140.4 (C), 139.6 (CH), 135.7 (CH), 135.4 (C), 135.2 (C), 130.0 (CH), 128.5 (CH), 128.5 (CH), 128.3 (CH), 127.8 (CH), 127.3 (CH), 114.5 (C), 78.7 (C), 13.4 (CH₃). **HRMS** (*m/z*, ESI) calculated for C₂₃H₁₈BrO [M+H]⁺ 389.0536 found, 389.0551.

1,2-triphenylazulen-7-bromo-4(3aH)-one (32ha):¹⁸⁸ 18% yield, red solid. **¹H NMR** (300 MHz,



CDCl₃) δ(ppm): 7.41 – 7.35 (m, 2H), 7.30 (dd, J = 2.9, 2.3 Hz, 2H), 7.27 – 7.24 (m, 3H), 7.20 (d, J = 0.7 Hz, 1H), 7.15 – 7.08 (m, 4H), 7.00 – 6.94 (m, 1H), 5.68 (d, J = 12.9 Hz, 1H), 1.46 (s, 3H). **¹³C NMR** (75 MHz, CDCl₃) δ (ppm): 197.8 (C), 151.2 (C), 145.8 (C), 143.9 (CH), 140.8 (CH), 139.4 (C), 134.5 (C), 133.9 (C), 133.8 (CH), 130.4 (CH), 128.8 (CH), 128.4 (CH), 128.3 (CH), 128.2 (CH), 127.8 (CH), 122.2 (CH), 117.1 (C), 67.6 (C), 24.3 (CH₃). **LRMS (CI)** (*m/z*, *I*): 390 (52), 311 (68), 310 (100). calculated for C₂₃H₁₈BrO [M+H]⁺ 389.0536 found, 389.0530.

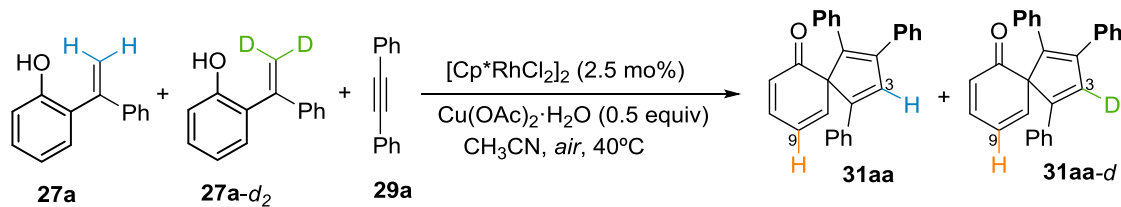
The structure of this compound was further confirmed by XR-anaylsis. CCDC 995497 contains the crystallographic data of **5ha**, which can be obtained via www.ccdc.cam.ac.uk/data_request/cif.



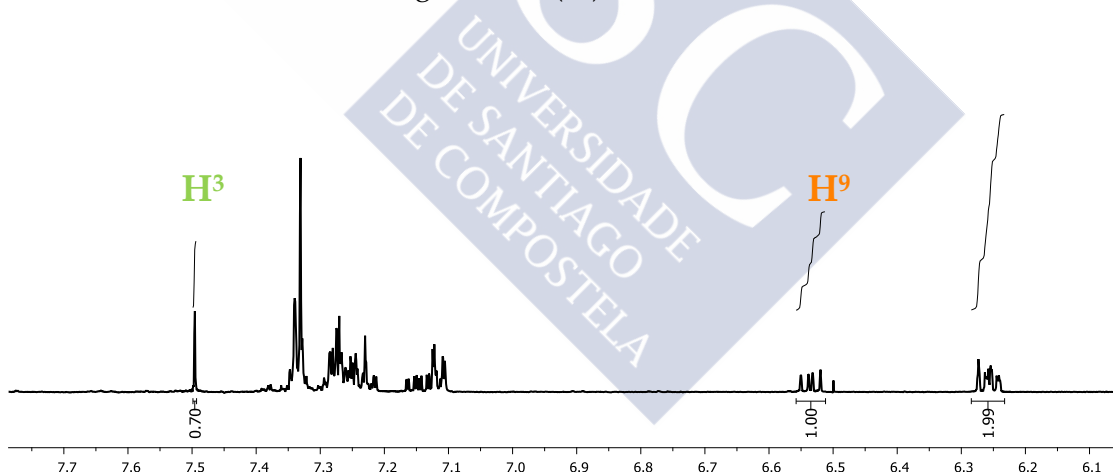
¹⁸⁸This compound was isolated as minor product in the reaction of **xx** and **xx** following general procedure B.

4.6 Mechanistic experiments.

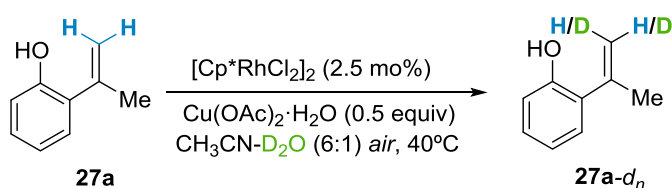
4.1 KIE measurements.



To a solution of $[\text{Cp}^*\text{RhCl}_2]_2$ (4.5 mg, 2.5 mol%) and $\text{Cu}(\text{OAc})_2 \cdot \text{H}_2\text{O}$ (29 mg, 0.146 mmol, 0.5 equiv) and diphenylacetylene (52 mg, 0.293 mmol) in MeCN (1 mL) under air atmosphere was added a equimolar solution of **27** and **27-d2** (0.386 mmol each) in MeCN (1 mL). This solution was prepared by mixing 75 mg of **31** and 99 mg of **31-d2** (88% deuterated). The reaction mixture was heated at 40°C . After 45 minutes the reaction was poured in to Et_2O (10mL), the solvents were evaporated *in vacuo* and the remaining residue was purified by flash column chromatography on silica gel to remove the remaining starting material. The residue was analyzed by H NMR. The KIE value (approx 2.3) was obtained by integrating the H3 of the spiro **31** and the H9 of the spiro **31** and **31-d**. The conversion (approx 10%) was determined based on the starting material (**27**) recovered.



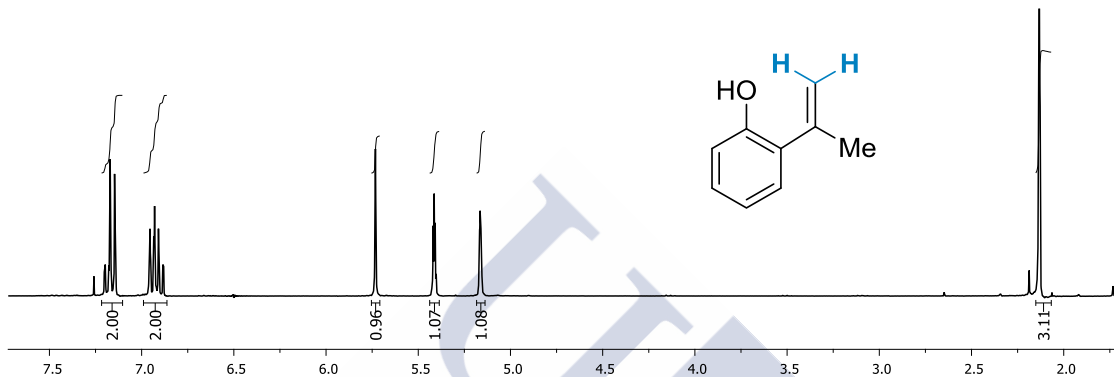
4.1 Deuterium exchange (without alkyne).



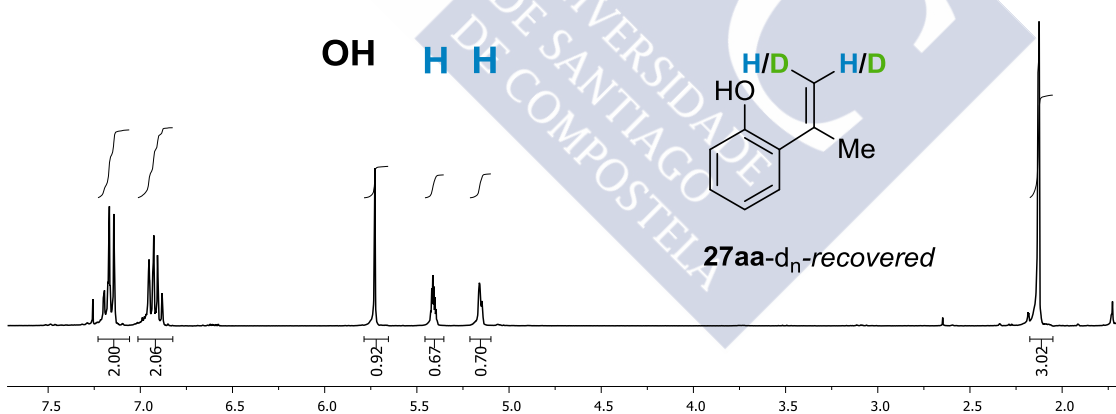
To a solution of $[\text{Cp}^*\text{RhCl}_2]_2$ (5.2 mg, 2.5 mol%) and $\text{Cu}(\text{OAc})_2 \cdot \text{H}_2\text{O}$ (33 mg, 0.5 equiv, 0.165 mmol) in CH_3CN (1.7 mL) under air atmosphere was added 2-(prop-1-en-2-yl)phenol **27a**

(0.50 mmol, 1.5 equiv) and D₂O (0.3 mL). The reaction was sealed with a rubber septum and an air atmosphere was injected in the flask with a balloon and a needle. The reaction was heated at 40 °C, stirred for 4 h and then cooled to room temperature. The solvents were removed *in vacuo* and the remaining residue was purified by flash column chromatography on silica gel to give **27a** and **27a-d_n** (26 mg, 39% recovery). 30% deuteration on both olefinic protons based on ¹H-NMR.¹⁸⁹

1) ¹H-NMR of starting material **27a**

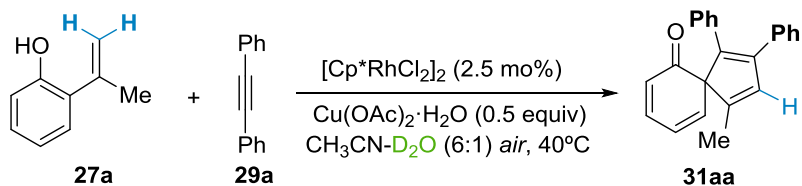


2) ¹H-NMR of the starting material **27a-d_n**-recovered (30% deuteration)

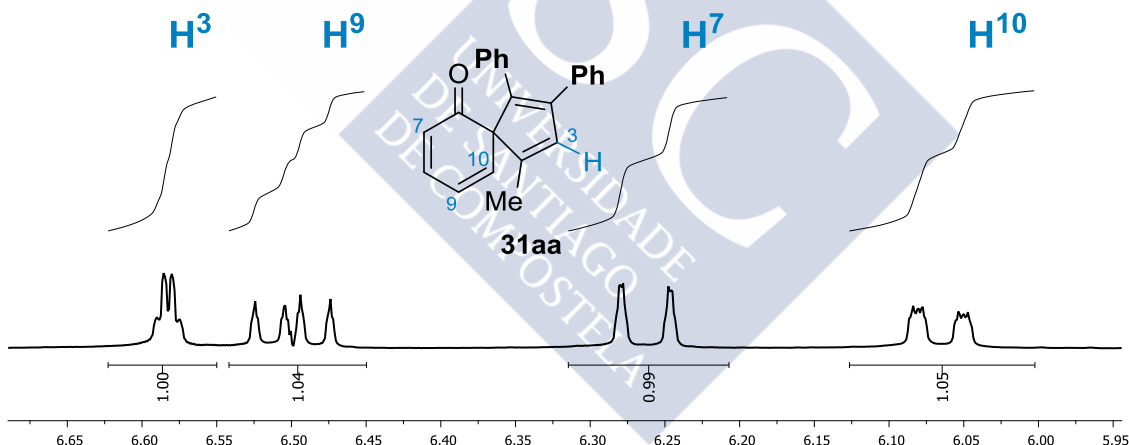
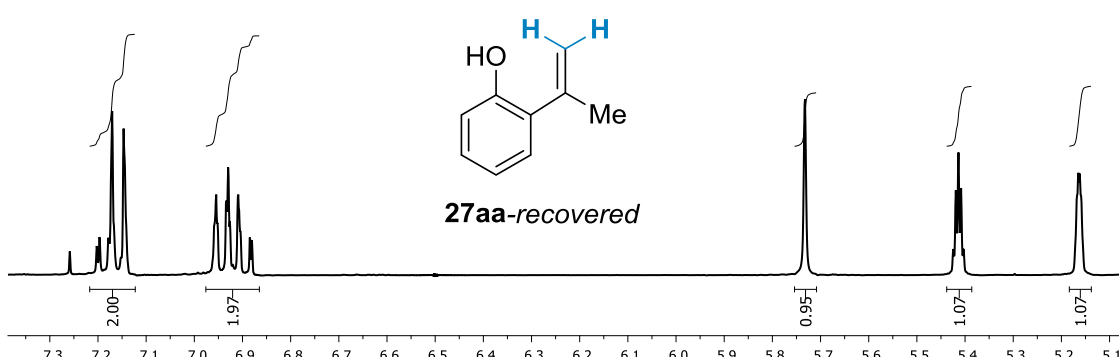


¹⁸⁹No deuteration was observed in absence of the either the rhodium catalyst or copper acetate.

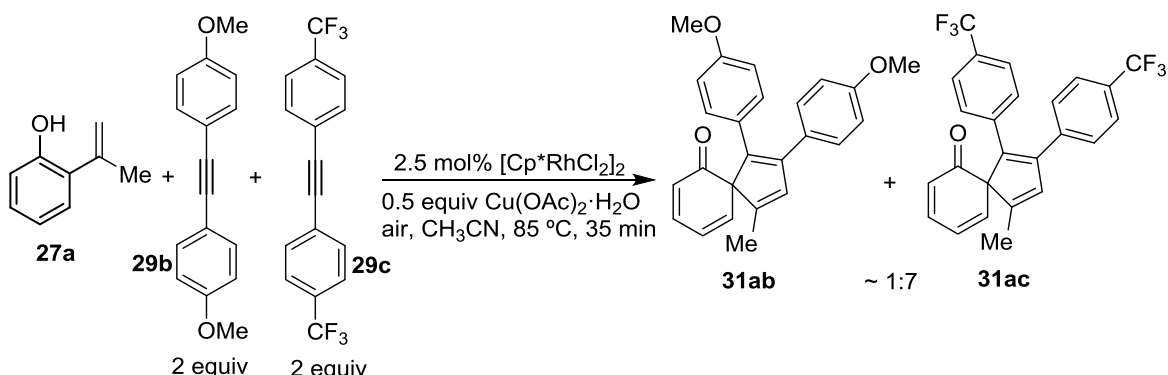
4.2 Deuterium exchange (with alkyne).



To a solution of $[\text{Cp}^*\text{RhCl}_2]_2$ (5.2 mg, 2.5 mol%) and $\text{Cu}(\text{OAc})_2 \cdot \text{H}_2\text{O}$ (33 mg, 0.5 equiv, 0.165 mmol) in CH_3CN (1.7 mL) under air atmosphere was added diphenylacetylene (59 mg, 1 equiv, 0.333 mmol) followed by the addition of 2-(prop-1-en-2-yl)phenol **27a** (0.50 mmol, 1.5 equiv) and D_2O (0.3 mL). The reaction was sealed with a rubber septum and an air atmosphere was injected in the flask with a balloon and a needle. The reaction was heated at 40 °C, stirred for 4 h and then cooled to room temperature. The solvents were removed *in vacuo* and the remaining residue was purified by flash column chromatography on silica gel to afford the 4-methyl-1,2-diphenylspiro[4.5]deca-1,3,7,9-tetraen-6-one **31aa** (12 mg, 11%), diphenylacetylene **29a** (49 mg, 83% recovered) and 2-(prop-1-en-2-yl)phenol **27a** (44 mg, 66% recovered).

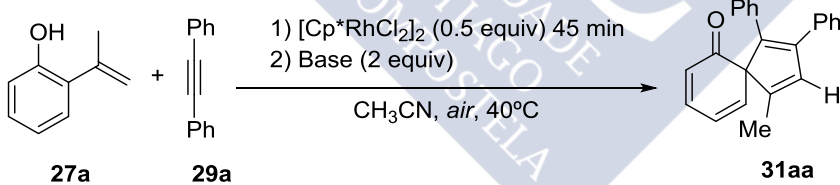
3) 1-H-NMR of product **31aa** recovered4) 1H-NMR of **27a**-recovered

4.3 Competition between alkynes **29b** and **29c**.



To a solution of $[\text{Cp}^*\text{RhCl}_2]_2$ (4.6 mg, 2.5 mol%) and $\text{Cu}(\text{OAc})_2 \cdot \text{H}_2\text{O}$ (30 mg, 0.150 mmol, 0.5 equiv) and alkynes **29b** (143 mg, 2 equiv, 0.6 mmol) and **29c** (189 mg, 2 equiv, 0.6 mmol) in MeCN (2 mL) under air atmosphere was added 2-(prop-1-en-2-yl)phenol (**27a**) (40 mg, 1 equiv, 0.3 mmol). The reaction was sealed with a rubber septum and an air atmosphere was injected in the flask with a balloon and a needle. The reaction was heated at 40°C and stirred at that temperature. After 2 h, the resulting mixture was filtered through silica, washing with diethylether; the solvents were evaporated *in vacuo* and the residue was analyzed by ^1H NMR in CDCl_3 indicating ~1:7 mixture of **31ab**:**31ac** and a conversion of approx 35%, based on the amount of starting materials recovered.

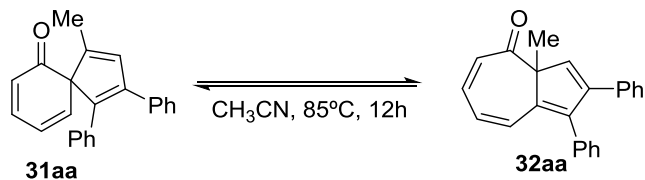
4.4 Stoichiometric experiment.



To a solution of $[\text{Cp}^*\text{RhCl}_2]_2$ (50 mg, 0.5 equiv) in CH_3CN (1 mL) under air atmosphere was added diphenylacetylene (**29a**) (29 mg, 1 equiv, 0.162 mmol) followed by the addition of 2-(prop-1-en-2-yl)phenol **27a** (22 mg, 1 equiv, 0.162 mmol). The reaction was sealed with a rubber septum and an air atmosphere was injected in the flask with a balloon and a needle. The solution was stirred for 45 min at 40°C and no conversion was observed through TLC, after that, CsOAc (62 mg, 2 equiv) was added and the mixture stirred 1 h. The solvents were removed *in vacuo* and the remaining residue was purified by flash column chromatography on silica gel to afford the 4-methyl-1,2-diphenylspiro[4.5]deca-1,3,7,9-tetraen-6-one **31aa** (43 mg, 86%).

A similar experiment was carried out using Et₃N (41 µL, 2 equiv) instead of CsOAc to afford the 4-methyl-1,2-diphenylspiro[4.5]deca-1,3,7,9-tetraen-6-one **31aa** (32 mg, 64%) after 5h of reaction.

4.7 Thermal rearrangement.



A solution of **31aa** (31 mg, 0.10 mmol) or **32aa** (31 mg, 0.10 mmol) in CH₃CN (2 mL) was refluxed for 12h. The solvents were removed *in vacuo* and the product was isolated in quantitative yield without further manipulation. Analysis of the ¹H-NMR shows approx. 1:1 mixture of **31aa** and **32aa**.

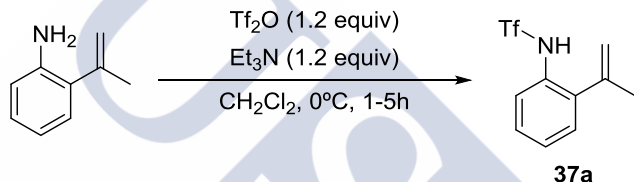


5- CHAPTER V: Oxidative annulations of *o*-alkenylanilines

5.1 General considerations

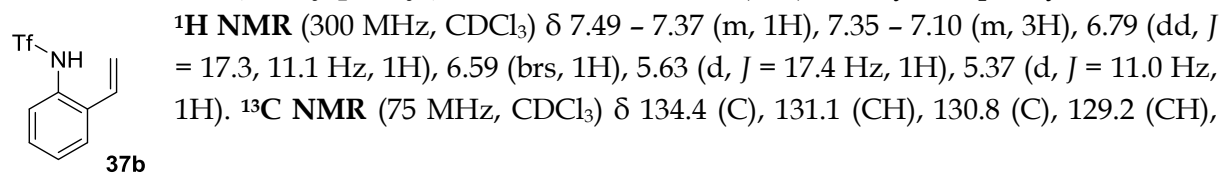
All non commercial vinylanilines were synthesized from the corresponding ketone *via* Wittig reaction, if the ketone was not available, then an addition of the corresponding Grignard reagent was done to the appropriately substituted 2-aminobenzonitrile.¹⁹⁰ Boc¹⁹¹, acetyl, tosyl, isopropyl¹⁷³, trifluoroacetyl¹⁹² and nosyl¹⁹³ protected *o*-alkenylanilines were synthesized as previously described in the literature. All spectral data recorded was in agreement with those in the corresponding communication.

5.2 Procedure for the synthesis of triflyl protected *o*-alkenylanilides (37a-37k) exemplified for 37a.



To a solution of *o*-isopropenylaniline (1 mL, 7.34 mmol) in dichloromethane (25 mL) under Ar atmosphere was added triethylamine (1.228 ml, 1.2 equiv) at 0 °C. Then trifluoromethanesulfonic anhydride (1.489 ml, 1.2 equiv) was added dropwise. The reaction was stirred at 0 °C for 1.5 hours and quenched with saturated NH4Cl aqueous solution. The resulting mixture was extracted with dichloromethane and dried over anhydrous sodium sulfate. Evaporation of the solvent followed by purification column flash chromatography on silica gel (hexanes:diethylether; 8:2) affording 1,1,1-trifluoro-N-(2-(prop-1-en-2-yl)phenyl)methanesulfonamide (**37a**), (1.84g, 94%), as a white solid upon freezing. **1H NMR** (300 MHz, CDCl₃) δ 7.49 (d, *J* = 7.9 Hz, 1H), 7.25 – 7.09 (m, 4H), 5.36 (dd, *J* = 2.7, 1.2 Hz, 1H), 4.92 (s, 1H), 2.00 (d, *J* = 1.0 Hz, 3H). **13C NMR** (75 MHz, CDCl₃) δ 142.2 (C), 135.9 (C), 130.8 (C), 128.7 (CH), 128.6 (CH), 126.4 (CH), 121.1 (CH), 119.9 (q, *J* = 323.4 Hz, C), 118.1 (CH₂), 24.5 (CH₃).

1,1,1-trifluoro-N-(2-vinylphenyl)methanesulfonamide (37b): 59% yield, pale yellow solid.



¹⁹⁰ Jana, S.; Ashokan, A.; Kumar, S.; Verma, A.; Kumar, S. *Org. Biomol. Chem.* **2015**, *13*, 8411.

¹⁹¹ Kobayashi, K.; Fukamachi, S.; Nakamura, D.; Morikawa, O.; Konishi, H. *Heterocycles* **2007**, *75*, 95.

¹⁷³ Ferguson, J.; Zeng, F.; Alwis, N.; Alper, H. *Org. Lett.* **2013**, *15*, 1998.

¹⁹² Kobayashi, K.; Miyamoto, K.; Morikawa, O.; Konishi, H. *Bull. Chem. Soc. Jpn.* **2005**, *78*, 886.

¹⁹³ Liwosz, T. W.; Chemler, S. R. *Synlett* **2015**, *26*, 335.

128.7 (CH), 127.3 (CH), 126.5 (CH), 119.9 (q, $J = 322.9$ Hz, C), 119.6 (CH₂).

1,1,1-trifluoro-N-(2-(3-methylbut-1-en-2-yl)phenyl)methanesulfonamide (37c): 76% yield, white solid. **¹H NMR** (300 MHz, CDCl₃) δ 7.61 (d, $J = 8.2$ Hz, 1H), 7.37 – 7.08 (m, 4H), 5.44 (s, 1H), 5.04 (s, 1H), 2.68 – 2.43 (m, 1H), 1.12 (d, $J = 1.7$ Hz, 3H), 1.10 (d, $J = 1.7$ Hz, 3H). **¹³C NMR** (75 MHz, CDCl₃) δ 152.3 (C), 134.6 (C), 131.9 (C), 129.2 (CH), 128.5 (CH), 125.6 (CH), 119.8 (q, $J = 322.8$ Hz, C), 119.4 (C), 115.1 (CH), 35.3 (CH), 21.1 (CH₃).

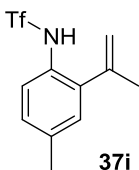
1,1,1-trifluoro-N-(2-(1-phenylvinyl)phenyl)methanesulfonamide (37d): 85% yield, white solid. **¹H NMR** (300 MHz, CDCl₃) δ 7.61 (d, $J = 8.0$ Hz, 1H), 7.53 – 7.26 (m, 8H), 6.47 (brs, 1H), 5.96 (s, 1H), 5.42 (s, 1H). **¹³C NMR** (75 MHz, CDCl₃) δ 145.5 (C), 138.7 (C), 135.3 (C), 132.2 (C), 131.2 (CH), 129. (CH), 129.4 (CH), 129.3 (CH), 127.3 (CH), 126.7 (CH), 123.0 (CH), 119.74 (q, $J = 323.5$ Hz, C), 118.3 (CH₂).

N-(2-(1-(4-chlorophenyl)vinyl)phenyl)-1,1,1-trifluoromethanesulfonamide (37e): 94% yield, white solid. **¹H NMR** (300 MHz, CDCl₃) δ 7.58 (d, $J = 8.0$ Hz, 1H), 7.51 – 7.15 (m, 7H), 6.47 (brs, 1H), 5.93 (s, 1H), 5.38 (s, 1H). **¹³C NMR** (75 MHz, CDCl₃) δ 144.3 (C), 137.2 (C), 135.3 (C), 134.9 (C), 132.1 (C), 131.2 (CH), 129.7 (CH), 129.5 (CH), 128.0 (CH), 127.4 (CH), 123.1 (CH), 119.7 (q, $J = 323.0$ Hz, C), 118.6 (CH₂).

1,1,1-trifluoro-N-(2-(1-(p-tolyl)vinyl)phenyl)methanesulfonamide (37f): 87% yield, yellow liquid. **¹H NMR** (300 MHz, CDCl₃) δ 7.58 (d, $J = 8.0$ Hz, 1H), 7.46 – 7.28 (m, 3H), 7.17 (s, 4H), 6.48 (brs, 1H), 5.88 (s, 1H), 5.33 (s, 1H), 2.37 (s, 3H). **¹³C NMR** (75 MHz, CDCl₃) δ 145.3 (C), 139.4 (C), 135.9 (C), 135.6 (C), 132.1 (C), 131.2 (CH), 130.1 (CH), 129.4 (CH), 127.2 (CH), 126.6 (CH), 123.0 (CH), 119.8 (q, $J = 323.4$ Hz, C), 117.3 (CH₂), 21.21 (CH₃).

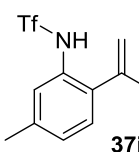
1,1,1-trifluoro-N-(5-methyl-2-(prop-1-en-2-yl)phenyl)methanesulfonamide (37h): 86% yield, white solid. **¹H NMR** (300 MHz, CDCl₃) δ 7.33 – 7.08 (m, 3H), 6.61 (brs, 1H), 5.38 – 5.28 (m, 1H), 4.94 (s, 1H), 2.44 (s, 3H), 2.12 (s, 3H). **¹³C NMR** (75 MHz, CDCl₃) δ 144.2(C), 142.9 (C), 138.5 (C), 130.4 (CH), 129.1 (C), 128.5 (C), 127.0 (CH), 119.6 (q, $J = 322.4$ Hz, C), 117.4 (CH₂), 24.01, 19.12 (CH₃).

1,1,1-trifluoro-N-(4-methyl-2-(prop-1-en-2-yl)phenyl)methanesulfonamide (37i): 47% yield,



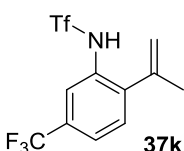
white solid. **¹H NMR** (300 MHz, CDCl₃) δ 7.45 (d, *J* = 8.3 Hz, 1H), 7.17 – 6.96 (m, 3H), 5.40 (s, 1H), 4.98 (s, 1H), 2.34 (s, 3H), 2.09 (s, 3H). **¹³C NMR** (75 MHz, CDCl₃) δ 142.3 (C), 136.4 (C), 129.1 (CH), 128.0 (C), 121.7 (CH), 119.8 (q, *J* = 324.3 Hz, C), 117.7 (CH₂), 24.54 (CH₃), 20.92 (CH₃).

1,1,1-trifluoro-N-(5-methyl-2-(prop-1-en-2-yl)phenyl)methanesulfonamide (37j): 72% yield,

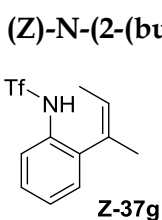


white solid. **¹H NMR** (300 MHz, CDCl₃) δ 7.41 (s, 1H), 7.31 (s, 1H), 7.14 – 7.03 (m, 2H), 5.43 (s, 1H), 4.99 (s, 1H), 2.37 (s, 4H), 2.09 (s, 4H). **¹³C NMR** (75 MHz, CDCl₃) δ 142.2 (C), 138.8 (C), 133.4 (C), 130.5 (C), 128.4 (CH), 127.3 (CH), 121.9 (CH), 119.9 (q, *J* = 323.5 Hz, C), 117.8 (CH₂), 24.5 (CH₃), 21.2(CH₃).

1,1,1-trifluoro-N-(2-(prop-1-en-2-yl)-5-(trifluoromethyl)phenyl)methanesulfonamide (37k):



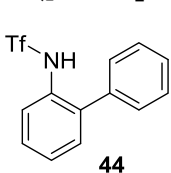
56% yield, white solid. **¹H NMR** (300 MHz, CDCl₃) δ 7.86 (s, 1H), 7.54 – 7.27 (m, 3H), 5.56 – 5.49 (m, 1H), 5.10 – 5.03 (m, 1H), 2.16 – 2.04 (m, 3H). **¹³C NMR** (75 MHz, CDCl₃) δ 141.1 (C), 139.2 (C) 131.6 (C), 131.13 (q, *J* = 33.2 Hz, C), 129.4 (CH), 123.11 (q, *J* = 3.7 Hz, CH), 119.8 (q, *J* = 323.0 Hz, C) 119.3 (CH₂), 117.95 (q, *J* = 3.8 Hz, CH) 24.2 (CH₃).



(Z)-N-(2-(but-2-en-2-yl)phenyl)-1,1,1-trifluoromethanesulfonamide (Z-37g): 23% yield, white solid. **¹H NMR** (300 MHz, CDCl₃) δ 7.60 (d, *J* = 8.1 Hz, 1H), 7.34 – 7.18 (m, 2H), 7.12 (dd, *J* = 7.5, 1.6 Hz, 1H), 6.90 (brs, 1H), 5.88 – 5.76 (m, 1H), 2.02 – 1.96 (m, 3H), 1.47 – 1.42 (m, 3H). **¹³C NMR** (75 MHz, CDCl₃) δ 132.9 (C), 132.7 (C), 131.4 (C), 129.1 (CH), 128.4 (CH), 126.7 (CH), 126.1 (CH), 119.8 (q, *J* = 322.6 Hz, C) 119.1 (CH₂), 25.0 (CH₃), 14.66 (CH₃).

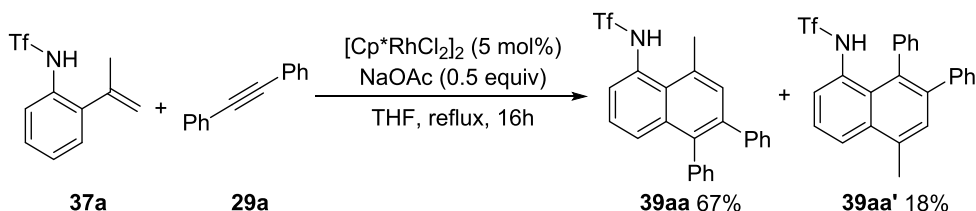
(E)-N-(2-(but-2-en-2-yl)phenyl)-1,1,1-trifluoromethanesulfonamide (E/Z 5.5:1) (E-37g): 47% yield, white solid. **¹H NMR** (300 MHz, CDCl₃) δ 7.69 – 7.46 (m, 1H), 7.57 – 7.52 (m, 3H), 7.06 (brs, 1H), 5.60 – 5.43 (m, 1H), 2.03 – 1.87 (m, 3H), 1.82 (dd, *J* = 6.7, 1.1 Hz, 3H). **¹³C NMR** (75 MHz, CDCl₃) δ 137.9 (C), 133.0 (C), 131.1 (C), 129.3 (CH), 128.1 (CH), 127.8 (CH), 126.3 (CH), 120.9 (CH), 119.9 (q, *J* = 323.3 Hz, C), 17.9 (CH₃), 14.06 (CH₃).

N-([1,1'-biphenyl]-2-yl)-1,1,1-trifluoromethanesulfonamide (44): 86% yield, white solid. **¹H NMR** (300 MHz, CDCl₃) δ 7.74 – 7.70 (m, 1H), 7.61 – 7.55 (m, 2H), 7.55 – 7.50 (m, 1H), 7.50 – 7.44 (m, 1H), 7.43 – 7.36 (m, 4H), 6.79 (brs, 1H). **¹³C NMR** (75 MHz, CDCl₃) δ 137.0 (C), 135.1 (C), 131.8 (C), 131.0 (CH), 129.6 (CH), 129.3



(CH), 129.2 (CH), 128.9 (CH), 126.8 (CH), 121.8 (CH) 119.73 (q, $J = 323.2$ Hz, C).

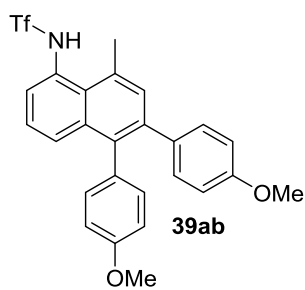
5.3 General Procedure for the [4+2] C-H annulation leading to naphthylamides 39aa-39kd exemplified for 39aa.



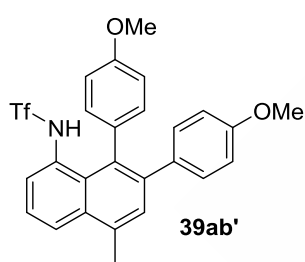
To a solution of $[\text{Cp}^*\text{RhCl}_2]_2$ (4.6 mg, 5 mol%), *o*-alkenylaniline **37a** (40 mg, 0.15 mmol) and NaOAc (6.1 mg, 0.5 equiv, 0.75 mmol) in THF (2 mL) under air atmosphere was added the alkyne **29a** (27 mg, 1 equiv). The reaction was sealed with a rubber septum and an air atmosphere was injected in the flask with a balloon and a needle. The reaction was heated at 70 °C, stirred until completion followed by TLC and then cooled to room temperature. The solvents were removed *in vacuo* and the remaining residue was purified by flash column chromatography on silica gel to afford the corresponding naphthylamides **39aa**, **39aa'**.

1,1,1-trifluoro-N-(8-methyl-5,6-diphenylnaphthalen-1-yl)methanesulfonamide (39aa): 57% yield, brown solid. $^1\text{H NMR}$ (500 MHz, CDCl_3) δ 7.78 (dd, $J = 8.6, 1.2$ Hz, 1H), 7.54 – 7.50 (m, 2H), 7.37 – 7.28 (m, 5H), 7.23 – 7.11 (m, 7H), 3.10 (s, 3H). $^{13}\text{C NMR}$ (126 MHz, CDCl_3) δ 141.2 (C), 139.0 (C), 137.2 (C), 135.6 (C), 134.1 (CH), 131.8 (C), 131.6 (CH), 130.2 (CH), 130.0 (CH), 129.8 (C), 129.1 (C), 128.1 (CH), 127.8 (CH), 127.6 (CH), 127.1 (CH), 126.6 (CH), 125.0 (CH), 119.8 (q, $J = 322.6$ Hz, C), 25.6 (CH₃). **LRMS** (m/z, EI): 441 (84), 309 (53), 308 (100). **HRMS** calculated for $\text{C}_{24}\text{H}_{18}\text{NO}_2\text{F}_3\text{S}$: 441.1019 found, 441.1010.

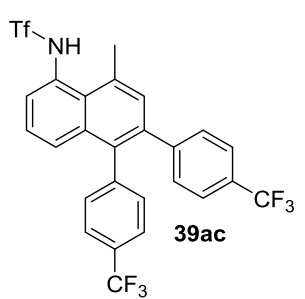
1,1,1-trifluoro-N-(5-methyl-7,8-diphenylnaphthalen-1-yl)methanesulfonamide (39aa'): 24% yield brown solid. $^1\text{H NMR}$ (500 MHz, CDCl_3) δ 8.05 (dd, $J = 8.5, 1.2$ Hz, 1H), 7.69 (dd, $J = 7.6, 1.2$ Hz, 1H), 7.54 (dd, $J = 8.3, 7.7$ Hz, 1H), 7.43 (d, $J = 0.8$ Hz, 1H), 7.37 – 7.30 (m, 3H), 7.23 – 7.11 (m, 5H), 7.05 – 6.96 (m, 2H), 6.77 (brs, 1H), 2.79 (d, $J = 0.8$ Hz, 3H). $^{13}\text{C NMR}$ (126 MHz, CDCl_3) δ 141.5 (C), 141.3 (C), 139.8 (C), 134.9 (C), 133.9 (C), 132.0 (C), 131.2 (C), 130.9 (CH), 130.0 (CH), 129.8 (CH), 129.3 (CH), 128.5 (CH), 127.6 (CH), 126.5 (CH), 125.63 (CH), 125.57 (C), 124.0 (CH), 121.7 (CH), 119.7 (q, $J = 323.5$ Hz, C). $^{20}\text{F NMR}$ (376 MHz, CDCl_3) δ 119.7 (q, $J = 323.5$ Hz, C). **LRMS (m/z, EI): 441 (34), 306 (75), 292 (100). **HRMS** calculated for $\text{C}_{24}\text{H}_{18}\text{NO}_2\text{F}_3\text{S}$: 441.0998 found, 441.1010.**

N-(5,6-bis(4-methoxyphenyl)-8-methylnaphthalen-1-yl)-1,1,1-

trifluoromethanesulfonamide (39ab): 74% yield, brown solid. **¹H NMR** (300 MHz, CDCl₃) δ 7.79 (dd, J = 8.6, 1.3 Hz, 1H), 7.52 – 7.45 (m, 2H), 7.35 – 7.25 (m, 2H), 7.09 – 7.02 (m, 4H), 6.89 – 6.83 (m, 2H), 6.77 – 6.70 (m, 2H), 3.83 (s, 3H), 3.77 (s, 3H), 3.07 (s, 3H). **¹³C NMR** (75 MHz, CDCl₃) δ 158.7 (C), 158.4 (C), 138.8 (C), 136.8 (C), 136.2 (C), 134.4 (CH), 133.9 (C), 132.7 (CH), 131.6 (C), 131.5 (C), 131.2 (CH), 130.2 (CH), 129.8 (C), 129.2 (C), 127.5 (CH), 124.9 (CH), 119.9 (q, J = 323.8 Hz, C), 113.7 (CH), 113.4 (CH), 55.3 (CH₃), 55.3 (CH₃), 25.5 (CH₃). **LRMS** (m/z, EI): 501 (66), 368 (100). **HRMS** calculated for C₂₆H₂₂NO₄F₃S: 501.1222 found, 501.1219.

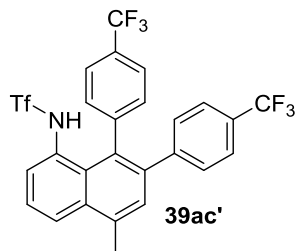
1N-(7,8-bis(4-methoxyphenyl)-5-methylnaphthalen-1-yl)-1,1-

trifluoromethanesulfonamide (39ab'): 22% yield, brown solid. ¹H NMR (300 MHz, CDCl₃) δ 8.01 (dd, J = 8.4, 1.1 Hz, 1H), 7.68 (dd, J = 7.6, 1.1 Hz, 1H), 7.50 (t, J = 8.0 Hz, 1H), 7.39 (s, 1H), 7.08 (d, J = 8.6 Hz, 2H), 7.00 (brs, 1H), 6.96 – 6.84 (m, 4H), 6.77 – 6.67 (m, 2H), 3.82 (s, 3H), 3.77 (s, 3H), 2.76 (s, 3H). **¹³C NMR** (75 MHz, CDCl₃) δ 159.8 (C), 158.3 (C), 141.3 (C), 134.7 (C), 134.0 (C), 133.8 (C), 132.1 (CH), 131.7 (C), 131.6 (C), 131.4 (C), 130.9 (CH), 130.5 (CH), 125.5 (CH), 123.8 (CH), 121.0(C), 119.5 (d, J = 323.9 Hz, C), 115.0 (CH), 113.2 (CH), 55.5 (CH₃), 55.3 (CH₃), 20.3 (CH₃). **LRMS** (m/z, EI): 501 (100), 368 (50), 353 (43), 337 (57). **HRMS** calculated for C₂₆H₂₂NO₄F₃S: 501.1222 found, 501.1222.

N-(7,8-bis(4-methoxyphenyl)-5-methylnaphthalen-1-yl)-1,1,1-

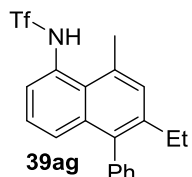
trifluoromethanesulfonamide (39ac): 64% yield, white solid. **¹H NMR** (300 MHz, CDCl₃) δ 8.15 (dd, J = 7.3, 2.4 Hz, 1H), 7.66 – 7.57 (m, 4H), 7.49 – 7.37 (m, 3H), 7.33 – 7.27 (m, 2H), 7.10 (d, J = 8.1 Hz, 2H), 6.15 (brs, 1H), 2.81 (s, 3H). **¹³C NMR** (75 MHz, CDCl₃) δ 144.8 (C), 143.9 (C), 140.2 (C), 136.0 (C), 134.3 (C), 131.1 (CH), 130.3 (C), 130.1 (CH), 130.1 (q, J = 30.1 Hz, C), 129.7 (d, J = 38.1 Hz, C), 129.6 (CH), 128.7 (d, J = 39.6 Hz, C), 126.2 (CH), 126.1 (CH), 126.0 (C), 125.3 (CH), 125.2 (q, J = 3.6 Hz, CH), 124.8 (q, J = 3.6 Hz, CH), 123.8 (q, J = 271.2 Hz, C), 119.5 (d, J = 323.1 Hz, C), 20.4 (CH₃). **LRMS** (m/z, EI): 577 (40), 444 (100). **HRMS** calculated for C₂₆H₁₆NO₂F₉S: 577.0758 found, 577.0756.

N-(5,6-bis(4-methoxyphenyl)-8-methylnaphthalen-1-yl)-1,1,1-trifluoromethanesulfonamide (39ac'):



31% yield, white solid. **¹H NMR** (300 MHz, CDCl₃) δ 7.72 – 7.53 (m, 4H), 7.54 – 7.34 (m, 4H), 7.33 – 7.15 (m, 5H), 3.11 (s, 3H). **¹³C NMR** (75 MHz, CDCl₃) δ 144.5 (C), 142.6 (C), 137.8 (C), 136.0 (C), 135.2 (C), 133.5 (CH), 133.3 (C), 132.0 (CH), 130.4 (C), 130.3 (CH), 129.9 (CH), 129.9 (q, *J* = 32.3 Hz, C), 129.5 (C), 129.3 (d, *J* = 32.5 Hz, C), 128.6 (CH), 125.8 (CH), 125.4 (q, *J* = 3.7 Hz, CH), 125.1 (q, *J* = 3.6 Hz, CH), 124.27 (q, *J* = 272.7 Hz, C), 119.92 (q, *J* = 323.2 Hz, C), 25.5 (CH₃). **LRMS** (m/z, EI): 577 (100), 444 (83), 429 (42), 375 (72). **HRMS** calculated for C₂₆H₁₆NO₂F₉S: 577.0758 found, 577.0760.

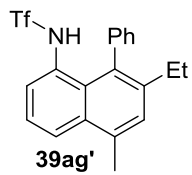
N-(6-ethyl-8-methyl-5-phenylnaphthalen-1-yl)-1,1,1-trifluoromethanesulfonamide (39ag):



59% yield brown solid. **¹H NMR** (300 MHz, CDCl₃) δ 7.63 – 7.14 (m, 9H), 3.04 (s, 3H), 2.57 – 2.32 (m, 2H), 1.19 – 0.96 (m, 3H). **¹³C NMR** (75 MHz, CDCl₃) δ 140.3 (C), 139.6 (C), 137.3 (C), 136.0 (C), 133.3 (CH), 131.7 (C), 130.5 (CH), 129.8 (CH), 129.1 (C), 128.9 (C) 128.6 (CH), 127.5 (CH), 126.7 (CH), 124.6 (CH), 119.7 (d, *J* = 323.7 Hz, C), 26.8 (CH₂), 25.6 (CH₃), 15.7 (CH₃).

LRMS (m/z, EI): 393 (40), 260 (100), 231 (22), 230 (29). **HRMS** calculated for C₂₀H₁₈NO₂F₃S: 393.1010 found, 393.1017.

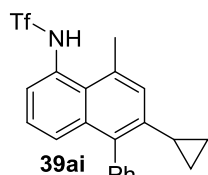
N-(7-ethyl-5-methyl-8-phenylnaphthalen-1-yl)-1,1,1-trifluoromethanesulfonamide (39ag'):



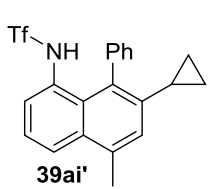
29% yield brown solid. **¹H NMR** (300 MHz, CDCl₃) δ 7.97 (d, *J* = 8.4 Hz, 1H), 7.66 – 7.53 (m, 4H), 7.44 (dd, *J* = 16.0, 1.6 Hz, 1H), 7.40 – 7.33 (m, 3H), 6.71 (brs, 1H), 2.75 (s, 3H), 2.41 (q, *J* = 7.5 Hz, 2H), 1.07 (t, *J* = 7.5 Hz, 3H). **¹³C NMR** (75 MHz, CDCl₃) 142.2 (C), 140.4 (C), 135.3 (C), 133.2 (C), 131.8 (C), 130.9 (C), 130.1 (CH), 130.0 (CH), 129.1 (CH), 129.0 (CH), 125.6 (C), 124.9 (CH), 123.9 (CH), 120.8 (CH), 119.8 (q, *J* = 324.1 Hz, C), 26.9 (CH₂), 20.5 (CH₃), 15.9 (CH₃).

LRMS (m/z, EI): 393 (68), 260 (39), 231 (100). **HRMS** calculated for C₂₀H₁₈NO₂F₃S: 393.1010 found, 393.1021.

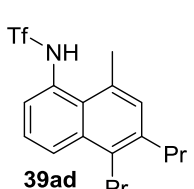
N-(6-cyclopropyl-8-methyl-5-phenylnaphthalen-1-yl)-1,1,1-trifluoromethanesulfonamide (39ai):



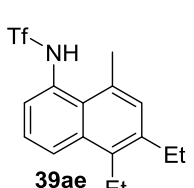
67% yield brown solid. **¹H NMR** (300 MHz, CDCl₃) δ 7.58 – 7.36 (m, 5H), 7.35 – 7.19 (m, 3H), 6.84 (brs, 1H), 2.99 (s, 3H), 1.83 – 1.52 (m, 1H), 1.15 – 0.65 (m, 4H). **¹³C NMR** (75 MHz, CDCl₃) δ 139.7 (C), 139.2 (C), 138.1 (C), 135.7 (C), 131.9 (C), 130.9 (CH), 129.5 (CH), 129.1 (C), 128.7 (CH), 127.5 (CH), 127.4 (CH), 126.75 (CH), 126.72 (CH) 124.8 (CH), 119.9 (q, *J* = 323.3 Hz, C), 25.7 (CH₂), 13.5 (CH), 9.4 (CH₂). **LRMS** (m/z, EI): 405 (57), 272 (100). **HRMS** C₂₁H₁₈NO₂F₃S: 405.1010 found, 405.1028.

N-(7-cyclopropyl-5-methyl-8-phenylnaphthalen-1-yl)-1,1,1-trifluoromethanesulfonamide (39ai')

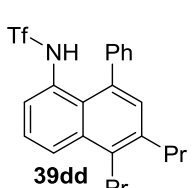
(39ai'): 22% yield, brown solid. **¹H NMR** (300 MHz, CDCl₃) δ 7.94 (dd, *J* = 8.4, 1.1 Hz, 1H), 7.66 – 7.51 (m, 4H), 7.42 (dt, *J* = 7.7, 4.1 Hz, 3H), 6.92 (s, 1H), 6.76 (brs, 1H), 2.71 (s, 3H), 1.64 – 1.50 (m, 1H), 0.84 – 0.67 (m, 4H). **¹³C NMR** (75 MHz, CDCl₃) δ 140.8 (C), 140.6 (C), 135.2 (C), 132.9 (C), 132.8 (C), 130.4 (CH), 129.9 (CH), 128.8 (CH), 125.3 (C), 124.6 (CH), 123.84 (CH), 123.79 (CH), 120.9 (CH), 119.5 (q, *J* = 323.9 Hz, C), 20.8 (CH₃), 13.9 (CH), 9.5 (CH₂). **LRMS** (m/z, EI): 405 (26), 272 (34), 271 (42), 257 (54), 256 (100). **HRMS** (m/z, EI): 405 (26), 272 (34), 271 (42), 257 (54), 256 (100). **HRMS** calculated for C₂₁H₁₈NO₂F₃S: 405.1010 found, 405.1010.

1,1,1-trifluoro-N-(8-methyl-5,6-dipropylnaphthalen-1-yl)methanesulfonamide (39ad)

major regioisomer: 63% yield >10:1 inseparable mixture of regioisomers, white solid. **¹H NMR** (300 MHz, CDCl₃) δ 8.04 (dd, *J* = 8.3, 1.0 Hz, 1H), 7.62 – 7.36 (m, 2H), 7.22 (s, 1H), 7.09 (brs, 1H), 3.45 – 3.24 (m, 2H), 2.85 – 2.70 (m, *J* = 8.9, 6.9 Hz, 2H), 2.65 (s, 3H), 1.78 – 1.61 (m, 2H), 1.59 – 1.45 (m, 2H), 1.17 – 0.98 (m, 6H). **¹³C NMR** (75 MHz, CDCl₃) δ 141.2 (C), 134.4 (C), 132.8 (C), 132.2 (C), 131.1 (CH), 129.6 (C), 128.9 (C), 127.5 (CH), 127.0 (CH), 123.9 (CH), 119.9 (q, *J* = 323.7 Hz, C), 36.8 (CH₂), 31.6 (CH₂), 25.7 (CH₂), 25.0 (CH₂), 20.2 (CH₃), 14.4 (CH₂), 14.0 (CH₂). **LRMS** (m/z, EI): 373 (44), 240 (100). **HRMS** calculated for C₁₈H₂₂NO₂F₃S: 373.1323 found, 373.1322.

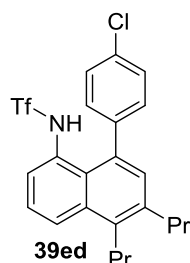
N-(5,6-diethyl-8-methylnaphthalen-1-yl)-1,1,1-trifluoromethanesulfonamide (39ae) major regioisomer

major regioisomer: 61% yield >12:1 inseparable regioisomers, brown solid. **¹H NMR** (300 MHz, CDCl₃) δ 7.95 (d, *J* = 8.3 Hz, 1H), 7.48 – 7.29 (m, 2H), 7.19 – 6.97 (m, 2H), 3.30 (q, *J* = 7.5 Hz, 2H), 2.75 (q, *J* = 7.5 Hz, 2H), 2.56 (s, 3H), 1.29 – 1.08 (m, 6H). **¹³C NMR** (75 MHz, CDCl₃) δ 142.4 (C), 134.5 (C), 133.3 (C), 133.2 (C), 130.6 (CH), 129.5 (C), 128.8 (C), 127.7 (CH), 127.0 (CH), 124.0 (CH), 119.9 (q, *J* = 323.4 Hz, C), 27.5 (CH₂), 22.4 (CH₂), 20.2 (CH₃), 16.5 (CH₃), 16.1 (CH₃). **LRMS** (m/z, EI): 345 (39), 212 (100). **HRMS** calculated for C₁₆H₁₈NO₂F₃S: 345.1010 found, 345.1013.

1,1,1-trifluoro-N-(8-phenyl-5,6-dipropylnaphthalen-1-yl)methanesulfonamide (39dd): 71%

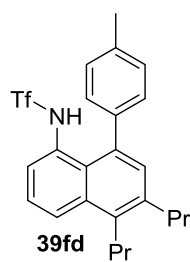
yield brown solid. **¹H NMR** (300 MHz, CDCl₃) δ 8.04 – 7.83 (m, 1H), 7.64 – 7.23 (m, 8H), 7.10 (brs, 1H), 3.40 (dd, *J* = 8.1, 5.8 Hz, 2H), 2.83 (dd, *J* = 11.2, 4.5 Hz, 2H), 1.93 – 1.47 (m, 4H), 1.31 – 0.89 (m, 6H). **¹³C NMR** (75 MHz, CDCl₃) δ 141.1 (C), 141 (C) 139.2 (C), 133.7 (C), 131.1 (CH), 130.4 (CH), 129.8 (C), 129.4 (CH), 128.6 (C), 128.5 (CH), 127.9 (CH), 127.6 (CH), 123.9 (CH), 119.9 (d, *J* = 324.0 Hz), 36.9 (CH₂), 32.0 (CH₂), 25.7 (CH₂), 25.0 (CH₂), 14.4 (CH₃), 14.1 (CH₃). **LRMS** (m/z, EI): 435 (50), 302 (100). **HRMS** calculated for C₂₃H₂₄NO₂F₃S: 435.1480 found, 435.1479.

N-(8-(4-chlorophenyl)-5,6-dipropynaphthalen-1-yl)-1,1,1-trifluoromethanesulfonamide



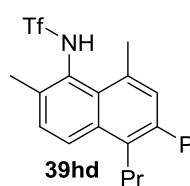
(39ed) major regioisomer: 90% yield 4:1 mixture of inseparable regioisomers, brown solid. **¹H NMR** (300 MHz, CDCl₃) δ 7.75 (dd, *J* = 8.5, 0.9 Hz, 1H), 7.44 – 7.01 (m, 9H), 3.38 – 3.23 (m, 2H), 2.82 – 2.64 (m, 2H), 1.62 (dd, *J* = 15.4, 7.6 Hz, 2H), 1.48 (dd, *J* = 16.3, 7.5 Hz, 2H), 1.07 – 0.91 (m, 6H). **¹³C NMR** (75 MHz, CDCl₃) δ 141.0 (C), 139.5 (C), 137.9 (C), 134.2 (C), 133.7 (C), 133.5 (C), 131.7 (CH), 131.1 (CH), 129.9 (C), 129.1 (CH), 128.7 (CH), 128.3 (CH), 128.2 (CH), 124.1 (CH), 119.9 (q, *J* = 323.6 Hz, C), 36.9 (CH₂), 31.8 (CH₂), 25.6 (CH₂), 25.0 (CH₂), 14.4 (CH₃), 14.1 (CH₃). **LRMS (EI)** (m/z, EI): 471 (19), 469 (50), 338 (34), 336 (100). **HRMS** calculated for C₂₃H₂₃NO₂F₃SCl: 469.1090 found, 469.1080.

N-(5,6-dipropyl-8-(p-tolyl)naphthalen-1-yl)-1,1,1-trifluoromethanesulfonamide (39fd): 90%



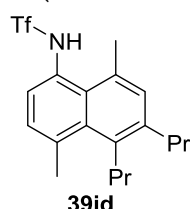
yield, brown solid. **¹H NMR** (300 MHz, CDCl₃) δ 7.88 (dd, *J* = 8.4, 1.3 Hz, 1H), 7.44 (d, *J* = 7.3 Hz, 1H), 7.30 – 7.19 (m, 6H), 7.08 (brs, 1H), 3.39 – 3.29 (m, 2H), 2.82 – 2.73 (m, 2H), 1.74 – 1.60 (m, 2H), 1.60 – 1.45 (m, 2H), 1.07 (t, *J* = 7.3 Hz, 3H), 0.99 (t, *J* = 7.3 Hz, 3H). **¹³C NMR** (75 MHz, CDCl₃) δ 141.04 (C), 139.2 (C), 138.1 (C), 137.3 (C), 133.8 (C), 133.5 (C), 131.1 (CH), 130.3 (CH), 129.8 (C), 129.5 (CH), 129.2 (CH), 128.6 (C), 127.9 (CH), 123.8 (CH), 119.9 (q, *J* = 323.7 Hz, C), 36.9 (CH₂), 31.8 (CH₂), 25.7 (CH₂), 25.0 (CH₂), 21.3 (CH₃), 14.4 (CH₃), 14.1 (CH₃). **LRMS (m/z, EI)**: 449 (53), 316 (100). **HRMS** calculated for C₂₄H₂₆NO₂F₃S: 449.1636 found, 449.1654.

N-(2,8-dimethyl-5,6-dipropynaphthalen-1-yl)-1,1,1-trifluoromethanesulfonamide (39hd)



major regioisomer: 60% yield <13:1 mixture of inseparable regioisomers, brown solid. **¹H NMR** (300 MHz, CDCl₃) δ 7.93 (d, *J* = 8.5 Hz, 1H), 7.32 (d, *J* = 8.5 Hz, 1H), 7.13 (s, 1H), 6.87 (brs, 1H), 3.35 (t, *J* = 7.5 Hz, 2H), 2.83 – 2.70 (m, 2H), 2.61 (s, 6H), 1.76 – 1.60 (m, 2H), 1.36 – 1.20 (m, 2H), 1.02 (t, *J* = 7.3 Hz, 3H), 0.87 (t, *J* = 7.3 Hz, 3H). **¹³C NMR** (75 MHz, CDCl₃) δ 140.8 (C), 137.5 (C), 132.8 (C), 132.7 (C), 131.7 (C), 131.2 (C), 130.4 (CH), 127.0 (CH), 126.8 (CH), 125.7 (C), 119.48 (q, *J* = 323.0 Hz, C), 37.3 (CH₂), 31.5 (CH₂), 24.9 (CH₂), 24.6 (CH₂), 19.8 (CH₂), 19.7 (CH₂), 14.3 (CH₃), 14.2 (CH₃). **LRMS (m/z, EI)**: 387 (23), 254 (100). **HRMS** calculated for C₁₉H₂₄NO₂F₃S: 387.1480 found, 387.1486.

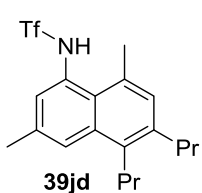
N-(4,8-dimethyl-5,6-dipropynaphthalen-1-yl)-1,1,1-trifluoromethanesulfonamide (39id)



major regioisomer: 72% yield >15:1 mixture of inseparable regioisomers, brown solid. **¹H NMR** (300 MHz, CDCl₃) δ 7.28 (d, *J* = 7.6 Hz, 1H), 7.15 (d, *J* = 8.3 Hz, 2H), 7.03 (brs, 1H), 3.36 – 3.23 (m, 2H), 2.86 (s, *J* = 7.6 Hz, 3H), 2.83 (s, 3H), 2.80 – 2.70 (m, 2H), 1.67 (dq, *J* = 14.9, 7.4 Hz, 2H), 1.44 (dq, *J* = 15.0, 7.4 Hz, 2H), 1.11 – 0.92 (m, 6H). **¹³C NMR** (75 MHz, CDCl₃) δ 140.5 (C), 138.4 (C), 135.3 (C), 133.7 (CH), 133.6 (C), 132.9 (C), 131.7 (C), 127.6 (CH), 127.1 (C),

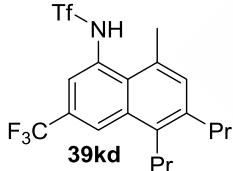
126.8 (CH), 119.8 (q, $J = 324.0$ Hz, C), 36.6 (CH), 32.2 (CH₂), 26.4 (CH₂), 26.1 (CH₃), 24.8 (CH₂), 24.8 (CH₂), 14.3 (CH₃), 14.1 (CH₃). **LRMS** (m/z, EI): 387 (34), 254 (100). **HRMS** calculated for C₁₉H₂₄NO₂F₃S: 387.1480 found, 387.1486 .

N-(3,8-dimethyl-5,6-dipropynaphthalen-1-yl)-1,1,1-trifluoromethanesulfonamide (39jd)



major regioisomer: 59% yield >10:1 mixture of inseparable regioisomers, brown solid. **¹H NMR** (300 MHz, CDCl₃) δ 7.79 (s, 1H), 7.35 (s, 1H), 7.17 (s, 1H), 7.03 (brs, 1H), 3.34 – 3.23 (m, 2H), 2.78 – 2.70 (m, 2H), 2.61 (s, 3H), 2.50 (s, 3H), 1.75 – 1.41 (m, 4H), 1.16 – 0.97 (m, 6H). **¹³C NMR** (75 MHz, CDCl₃) δ 140.1 (C), 134.5 (C), 133.6 (C), 132.1 (C), 132.0 (C), 131.1 (CH), 129.4 (CH), 128.7 (C), 127.6 (C), 126.2 (CH), 119.91 (q, $J = 323.7$ Hz, C), 36.7(CH₂), 31.6 (CH₂), 25.7(CH₂), 25.0 (CH₂), 21.2 (CH₂), 20.3 (CH₂), 14.4 (CH₃), 14.0 (CH₃). **LRMS** (m/z, EI): 387 (45), 254 (100). **HRMS** calculated for C₁₉H₂₄NO₂F₃S: 387.1480 found, 387.1478 .

N-(3,8-dimethyl-5,6-dipropynaphthalen-1-yl)-1,1,1-trifluoromethanesulfonamide (39kd)



major regioisomer: 61% yield 5:1 mixture of inseparable regioisomers, brown solid. **¹H NMR** (300 MHz, CDCl₃) δ 8.22 (s, $J = 0.8$ Hz, 1H), 7.59 (s, 1H), 7.24 (s, 1H), 7.13 (brs, 1H), 3.33 – 3.16 (m, 2H), 2.78 – 2.66 (m, 2H), 2.62 (d, $J = 9.6$ Hz, 3H), 1.70 – 1.51 (m, 2H), 1.49 – 1.34 (m, 2H), 1.08 – 0.90 (m, 6H). **¹³C NMR** (75 MHz, CDCl₃) δ 140.1 (C), 134.5 (C), 133.6 (C), 132.1 (C), 132.0 (C), 131.1 (CH), 129.4 (CH), 128.7 (C), 127.6 (C), 126.2 (CH), 119.91 (q, $J = 323.7$ Hz, C), 36.7(CH₂), 31.6 (CH₂), 25.7(CH₂), 25.0 (CH₂), 21.2 (CH₂), 20.3 (CH₂), 14.4 (CH₃), 14.0 (CH₃). **LRMS** (m/z, EI): 441 (43), 308 (100). **HRMS** calculated for C₁₉H₂₁NO₂F₆S: 441.1197 found, 442.1199

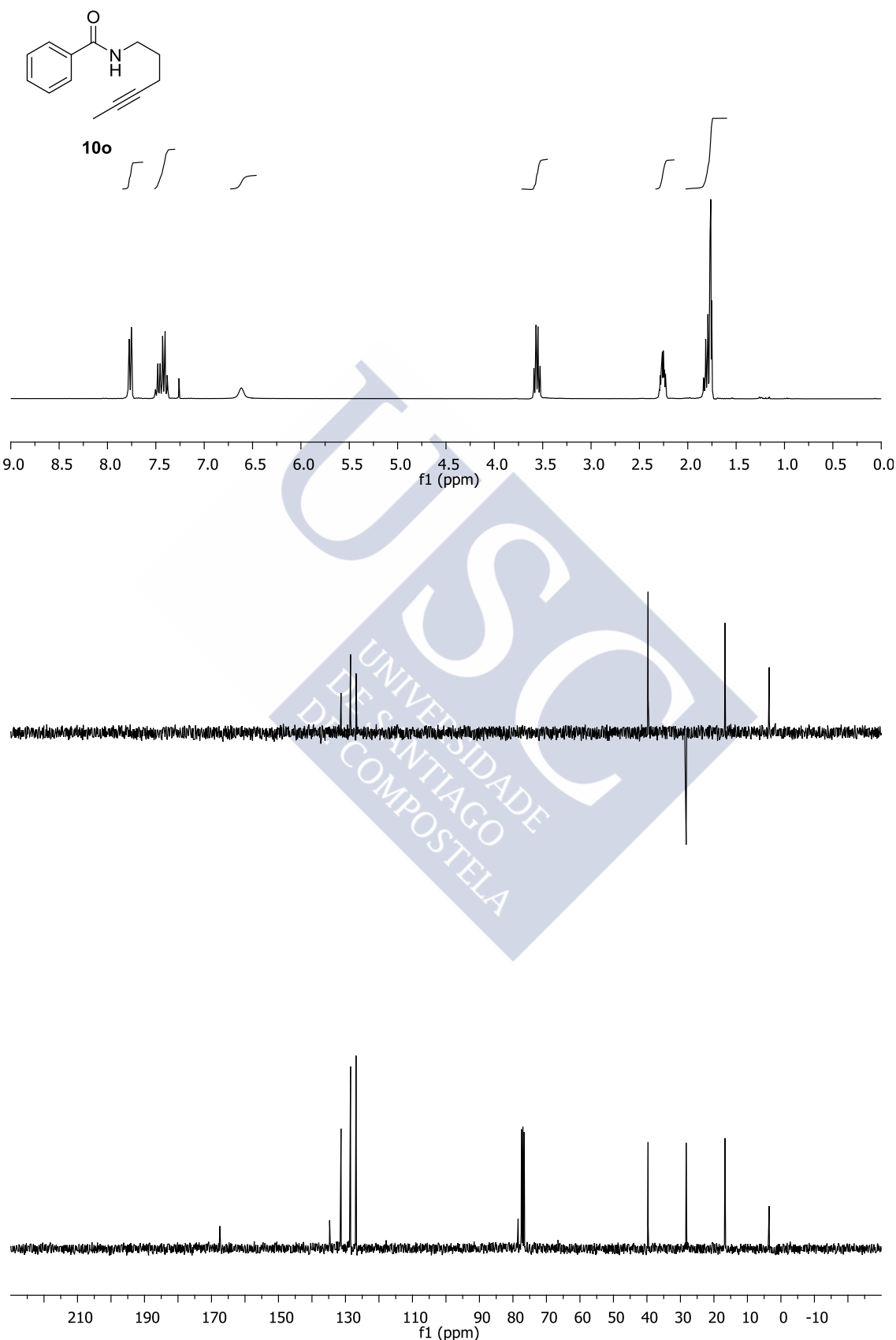


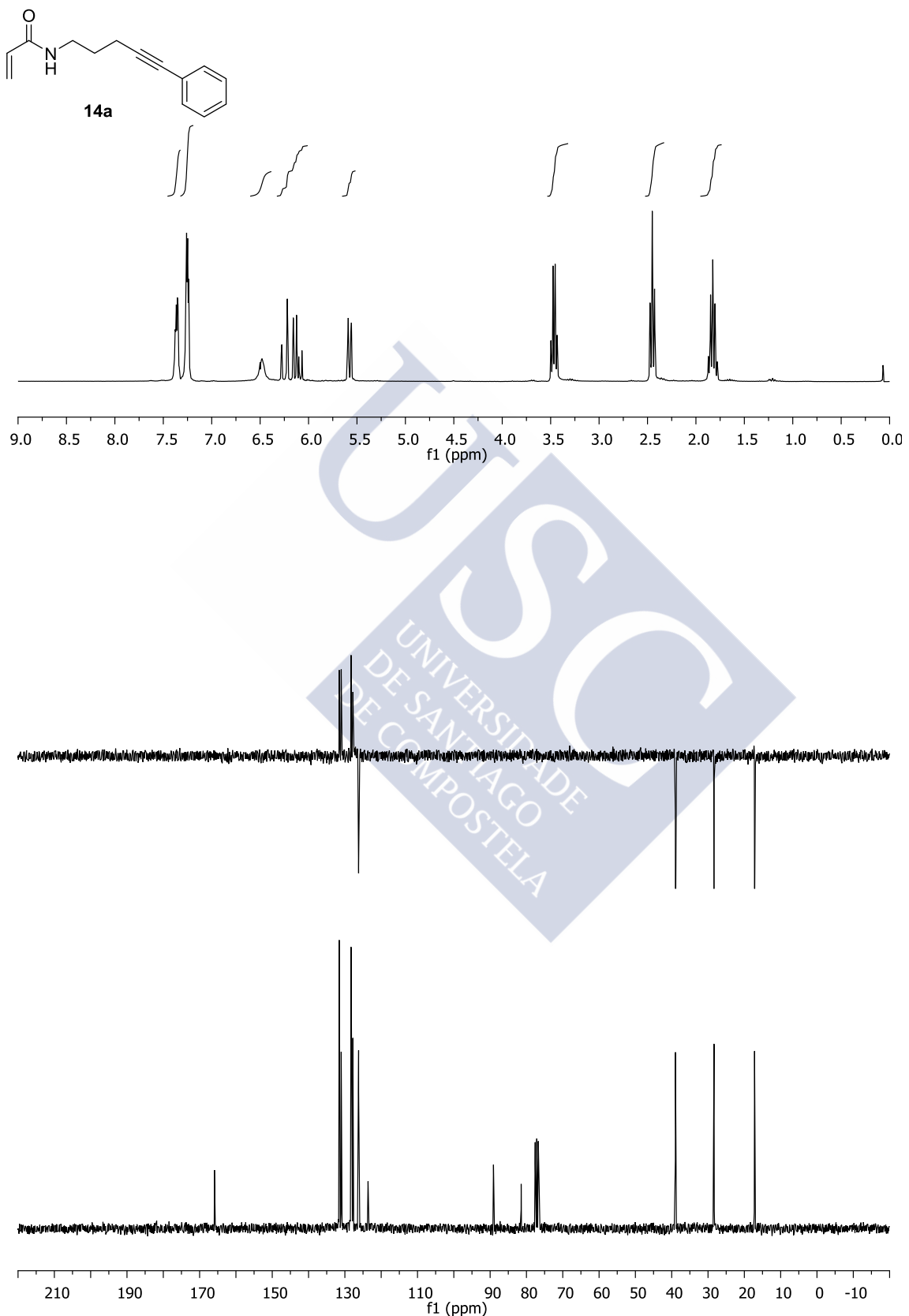


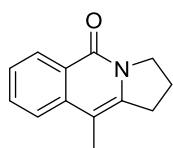
CHAPTER VII: Selected spectra



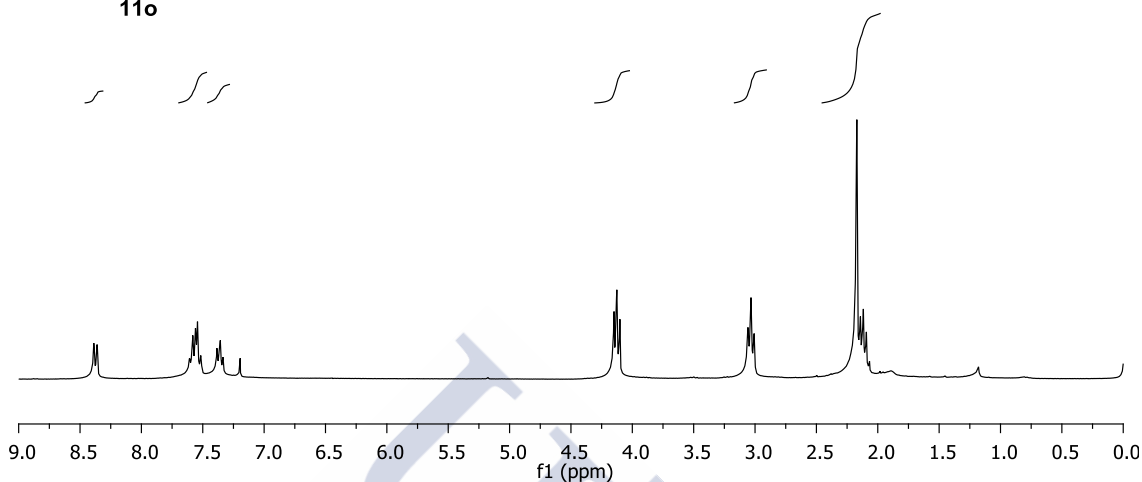
1. Selected spectra from chapter II.





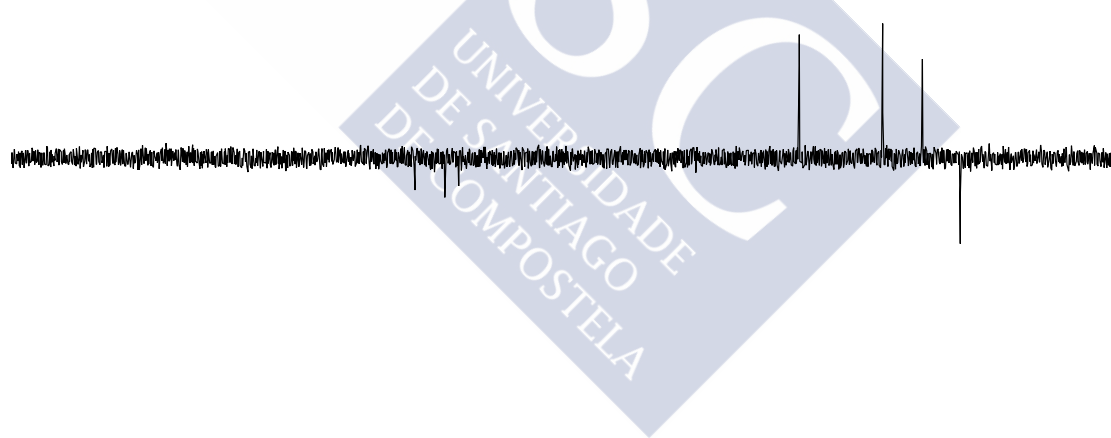


11o



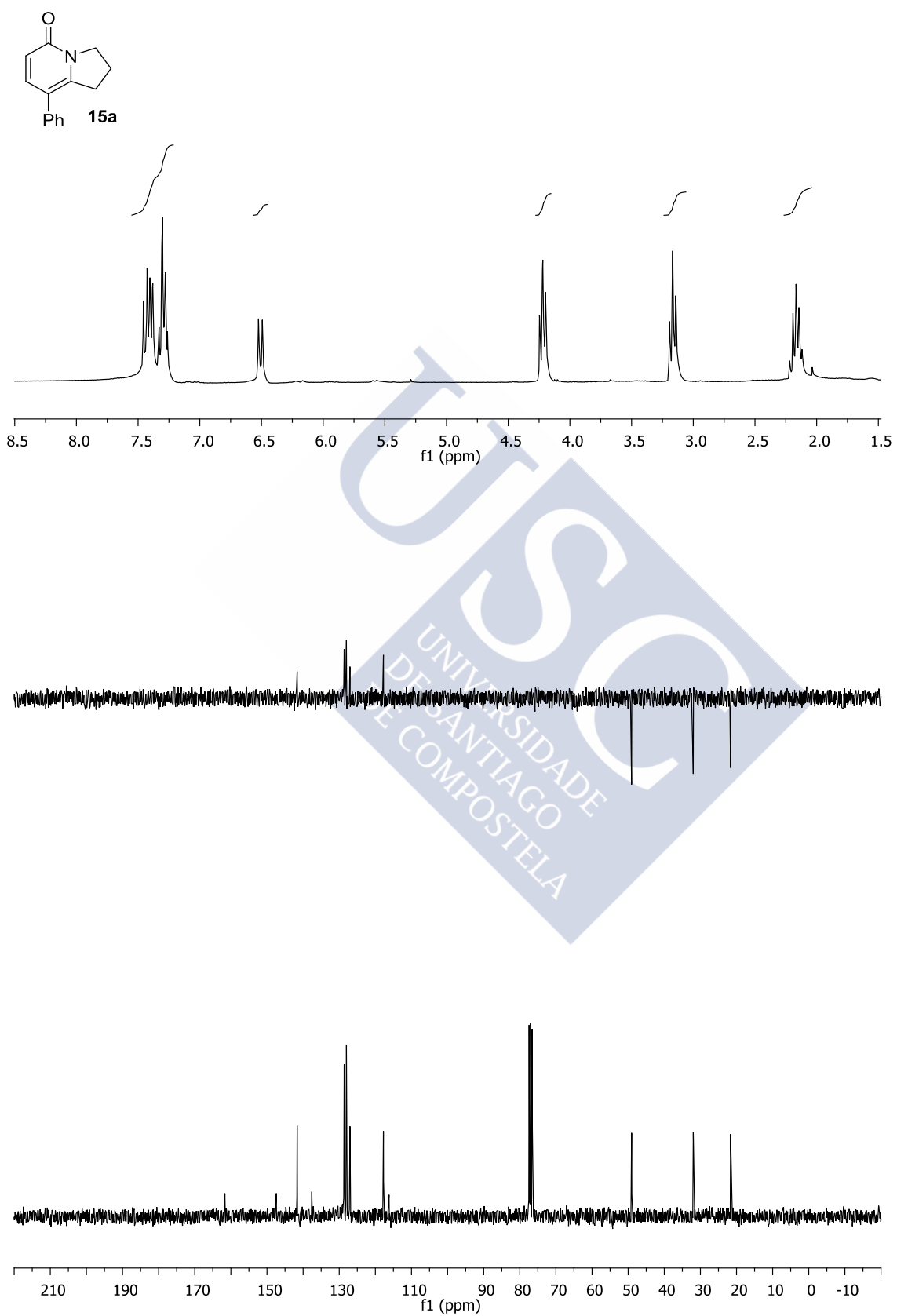
9.0 8.5 8.0 7.5 7.0 6.5 6.0 5.5 5.0 4.5 4.0 3.5 3.0 2.5 2.0 1.5 1.0 0.5 0.0

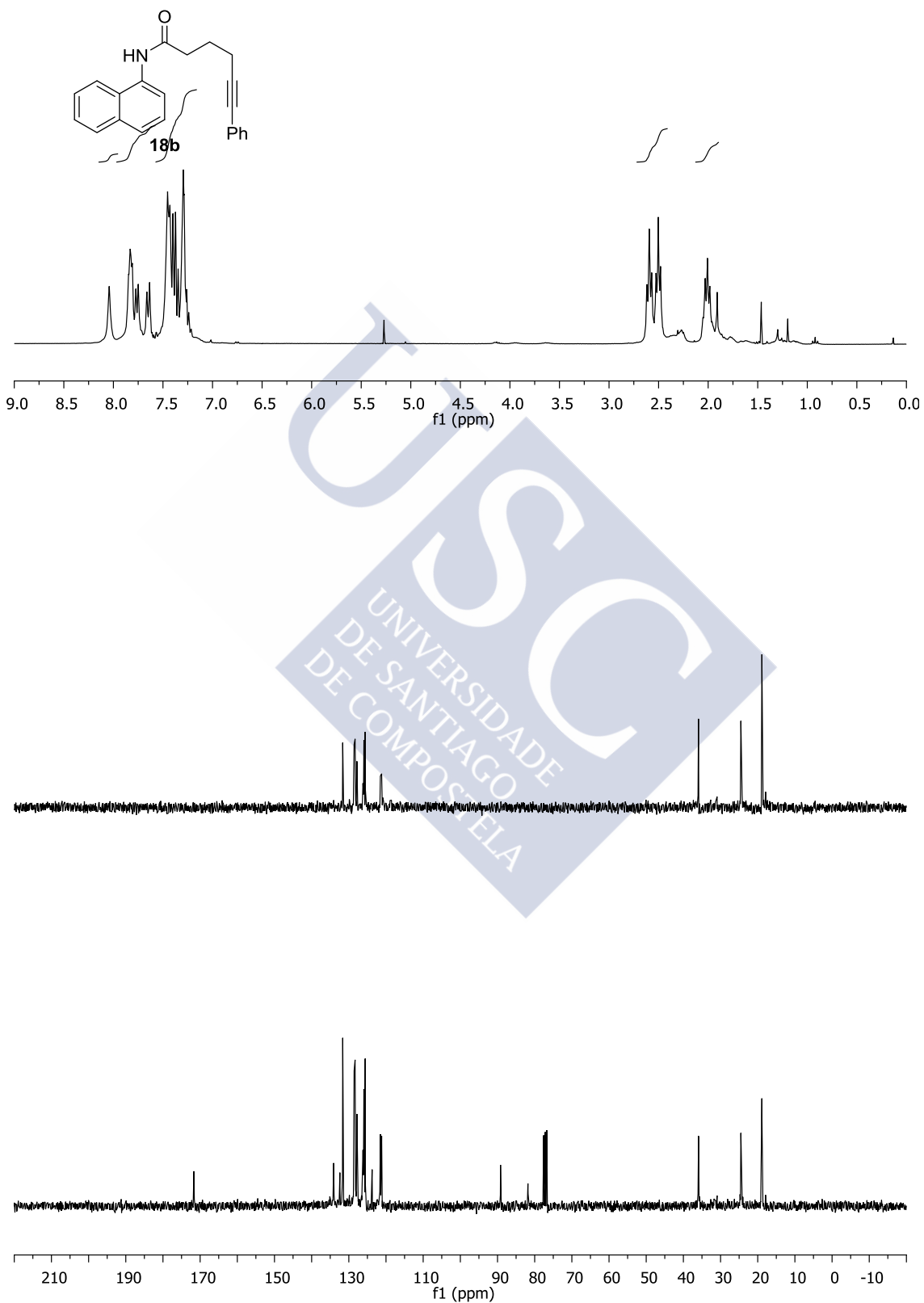
f_1 (ppm)

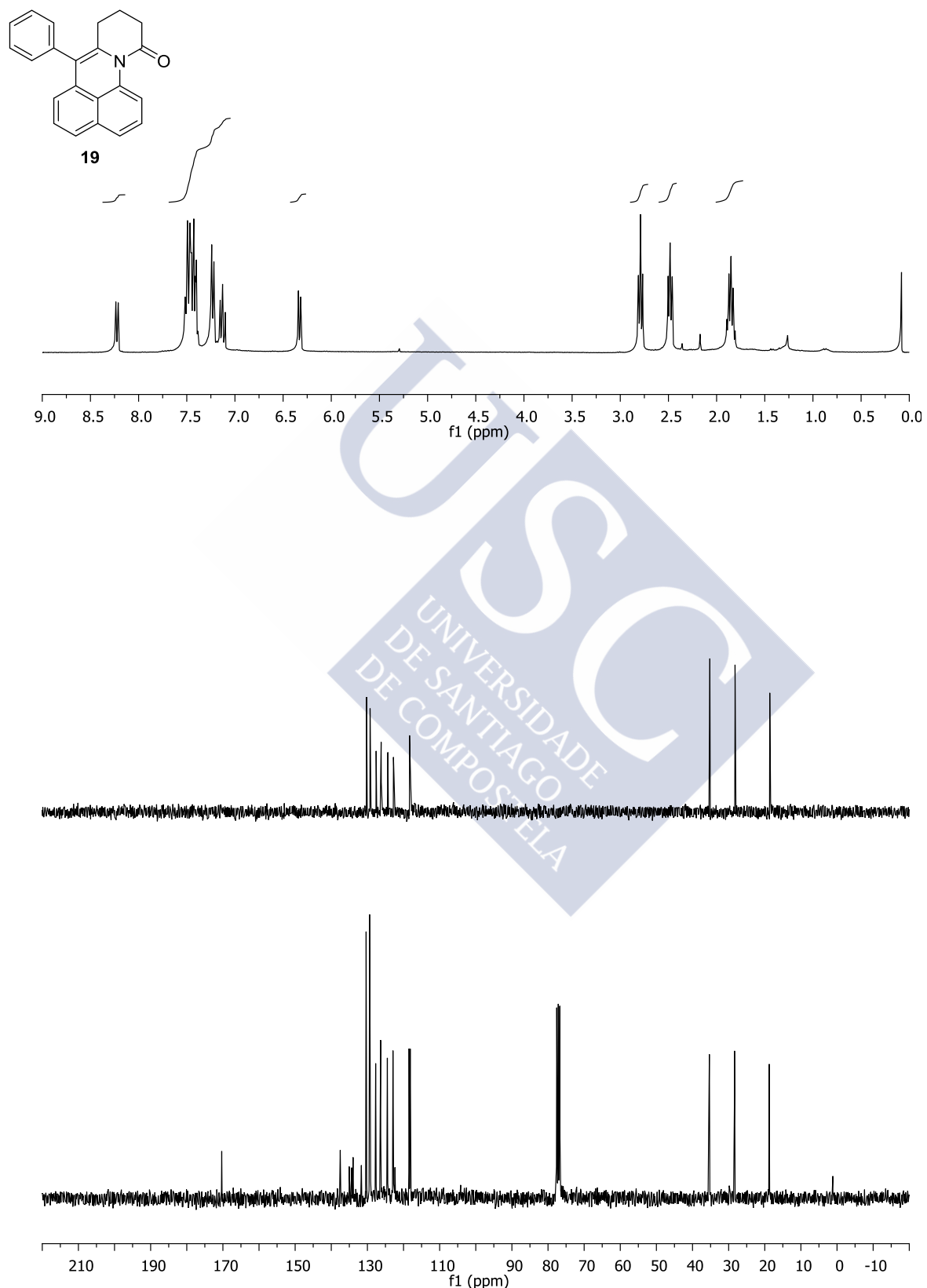


210 190 170 150 130 110 90 80 70 60 50 40 30 20 10 0 -10

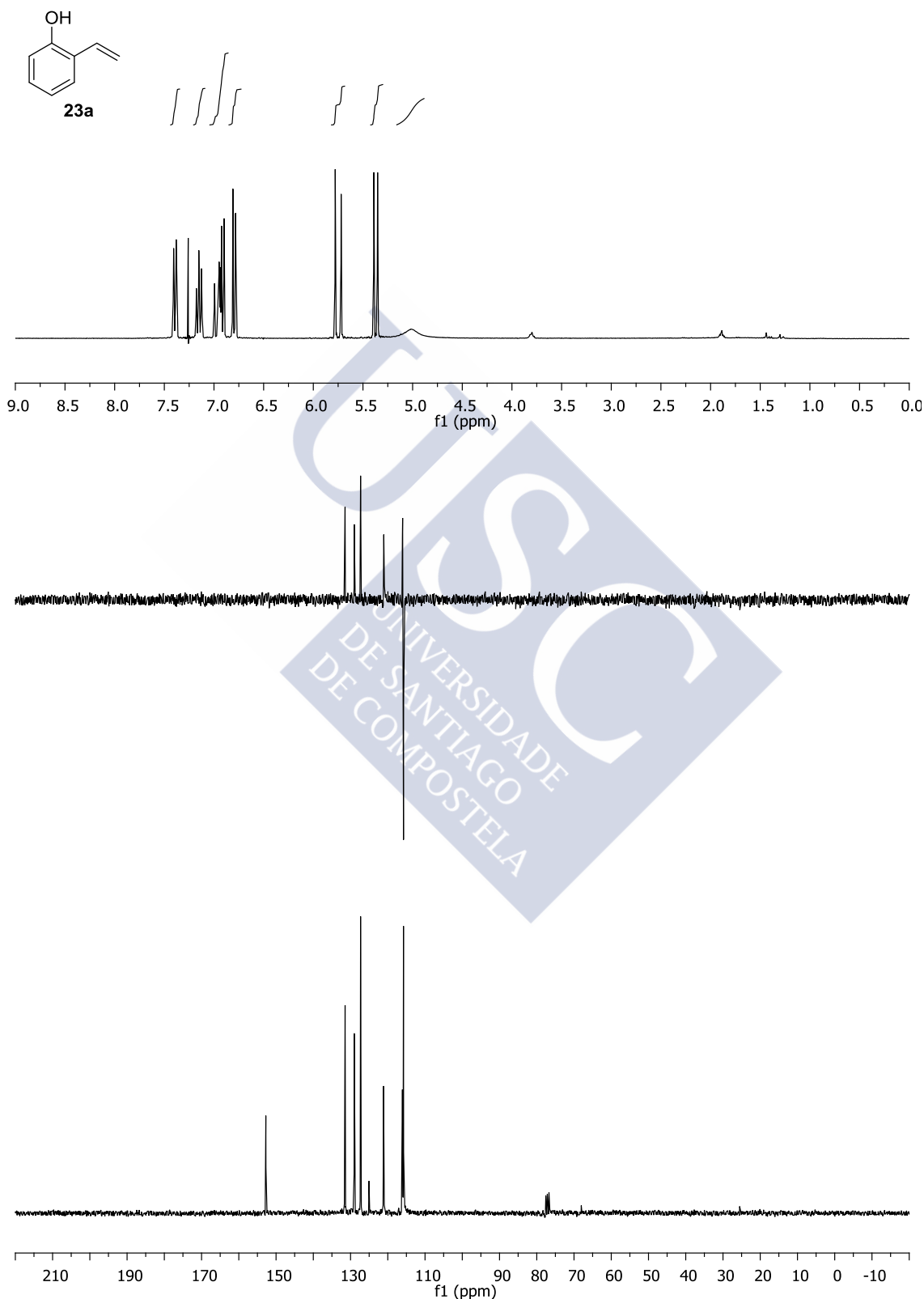
f_1 (ppm)

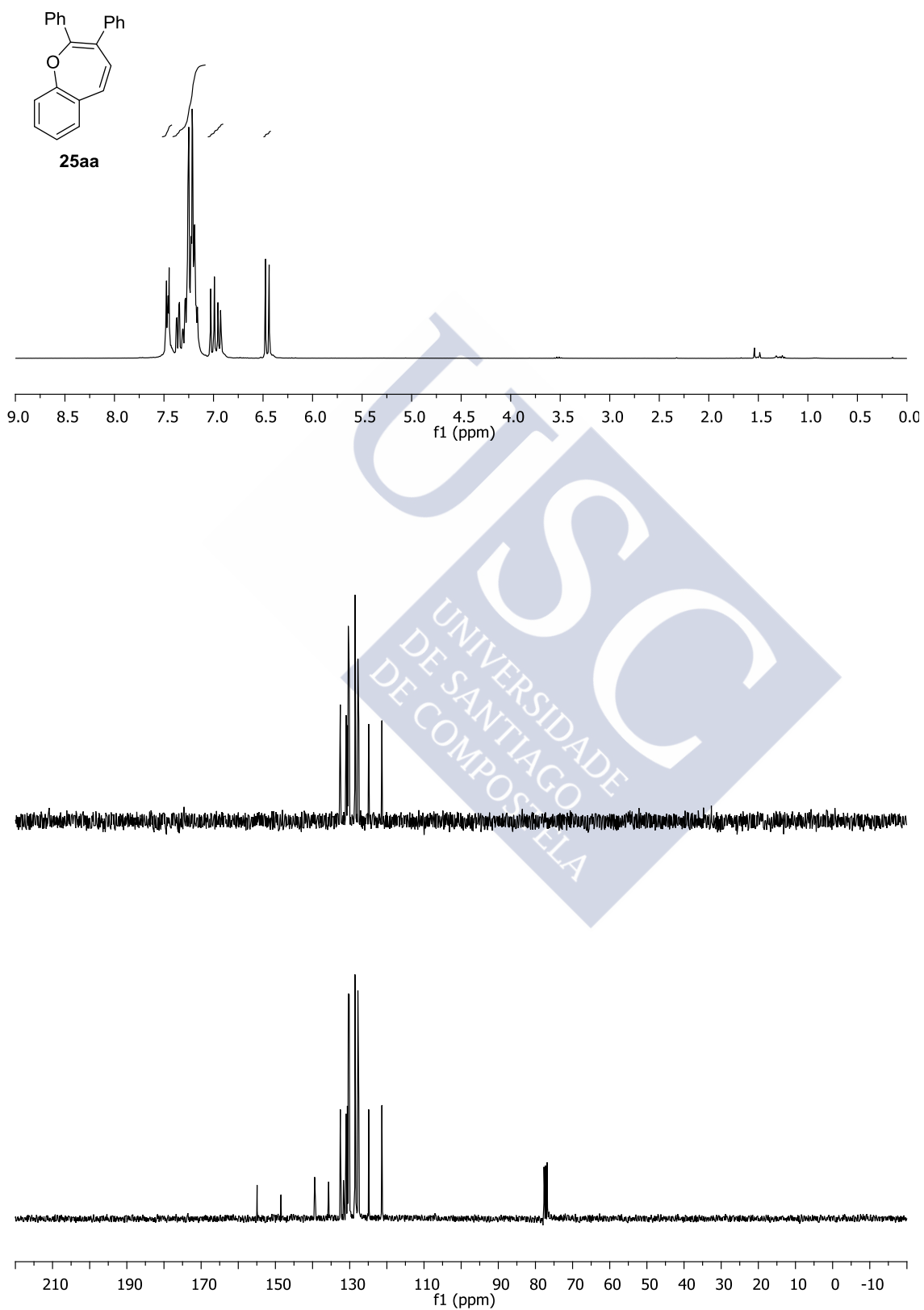


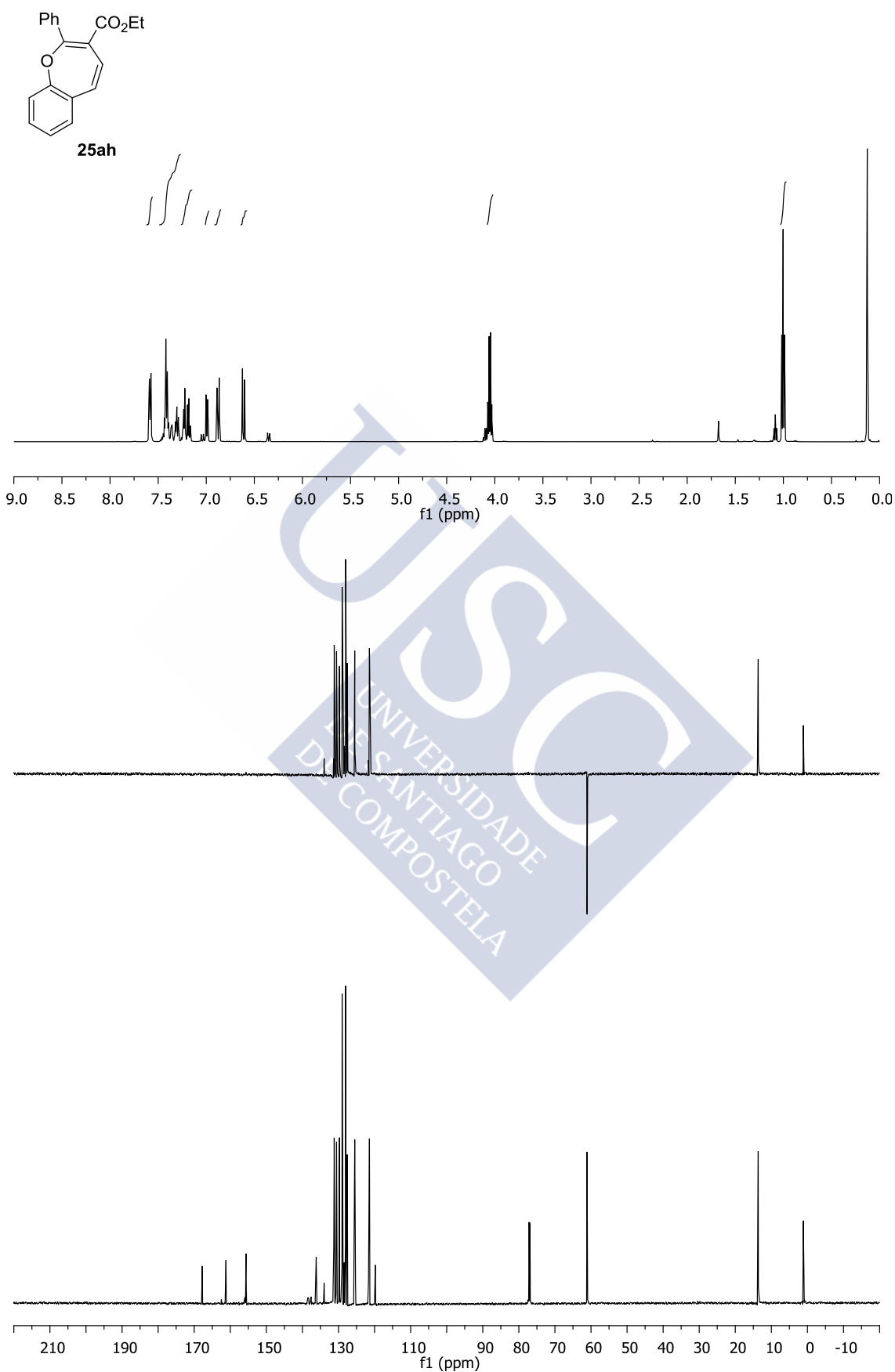




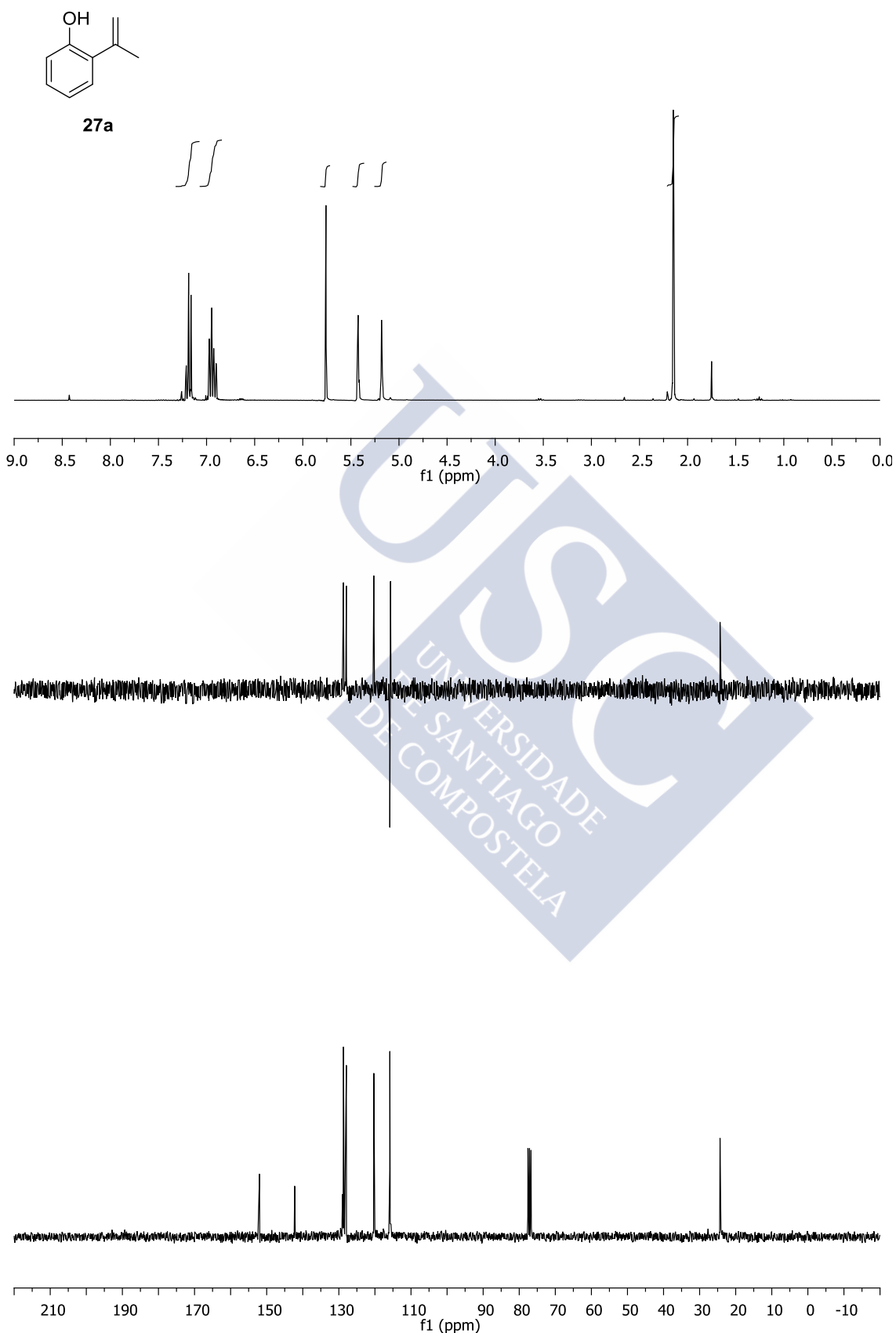
2. Selected spectra from chapter III.

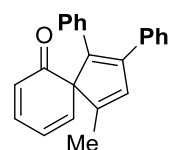




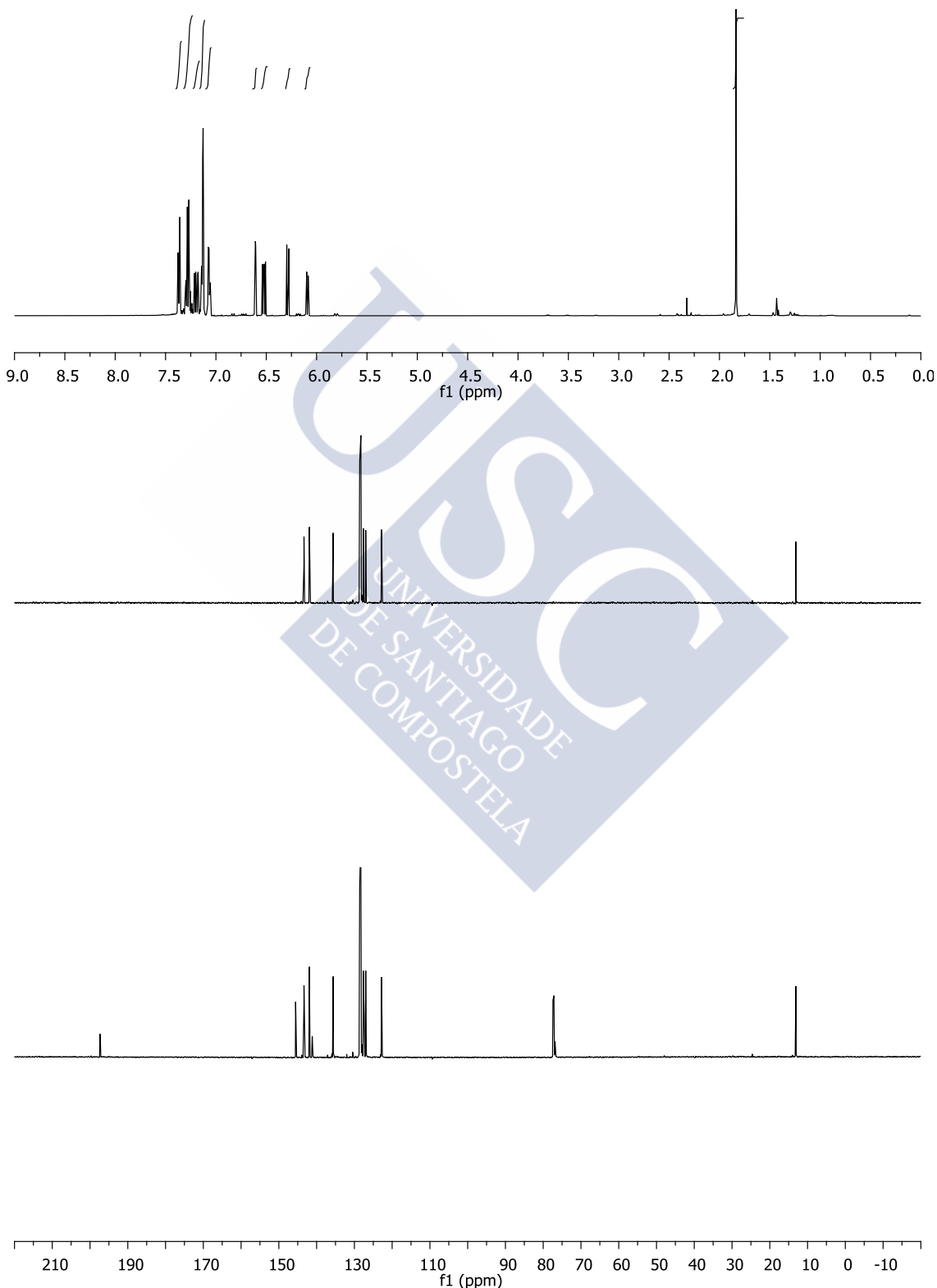


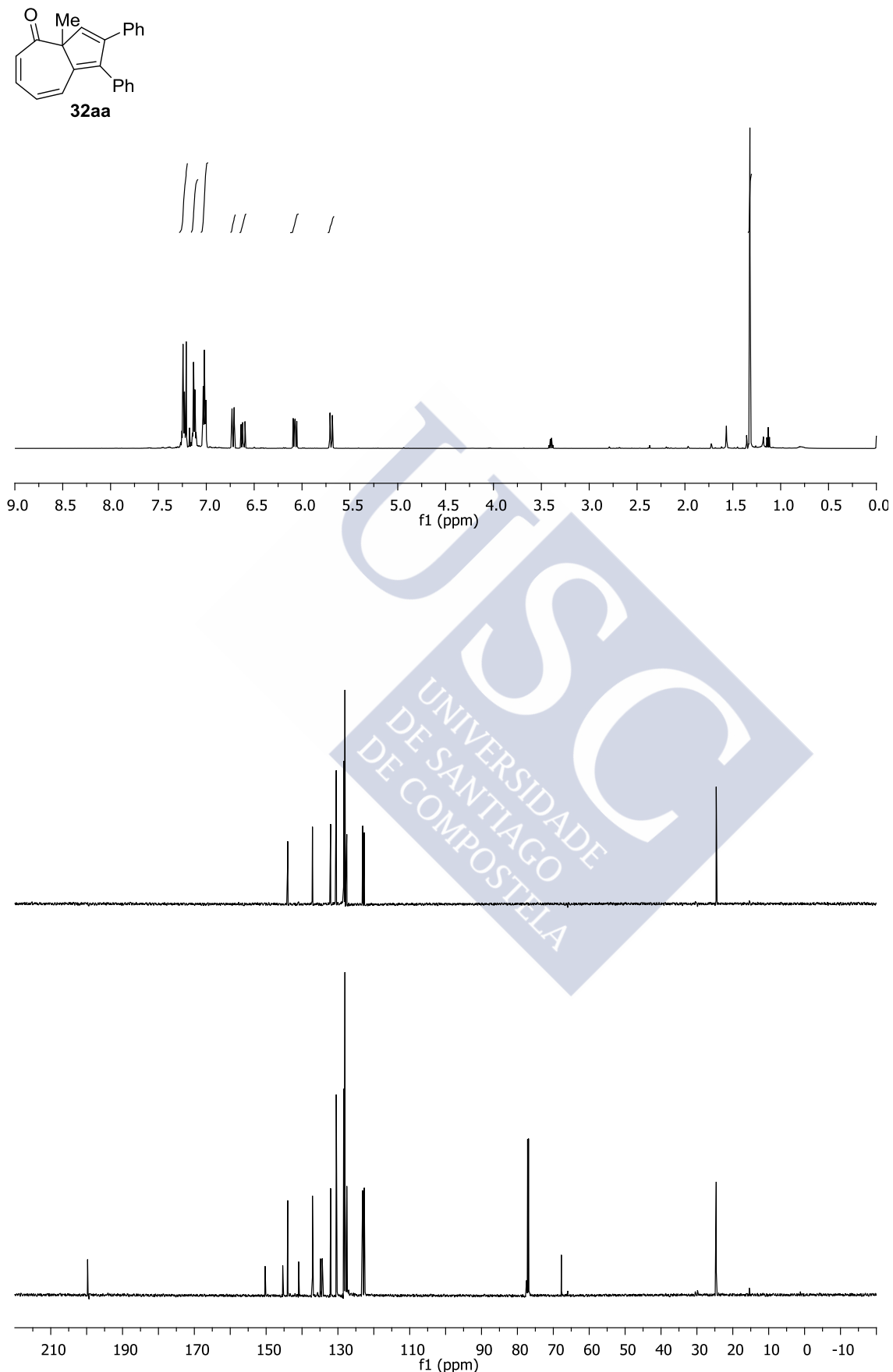
3. Selected spectra from chapter IV

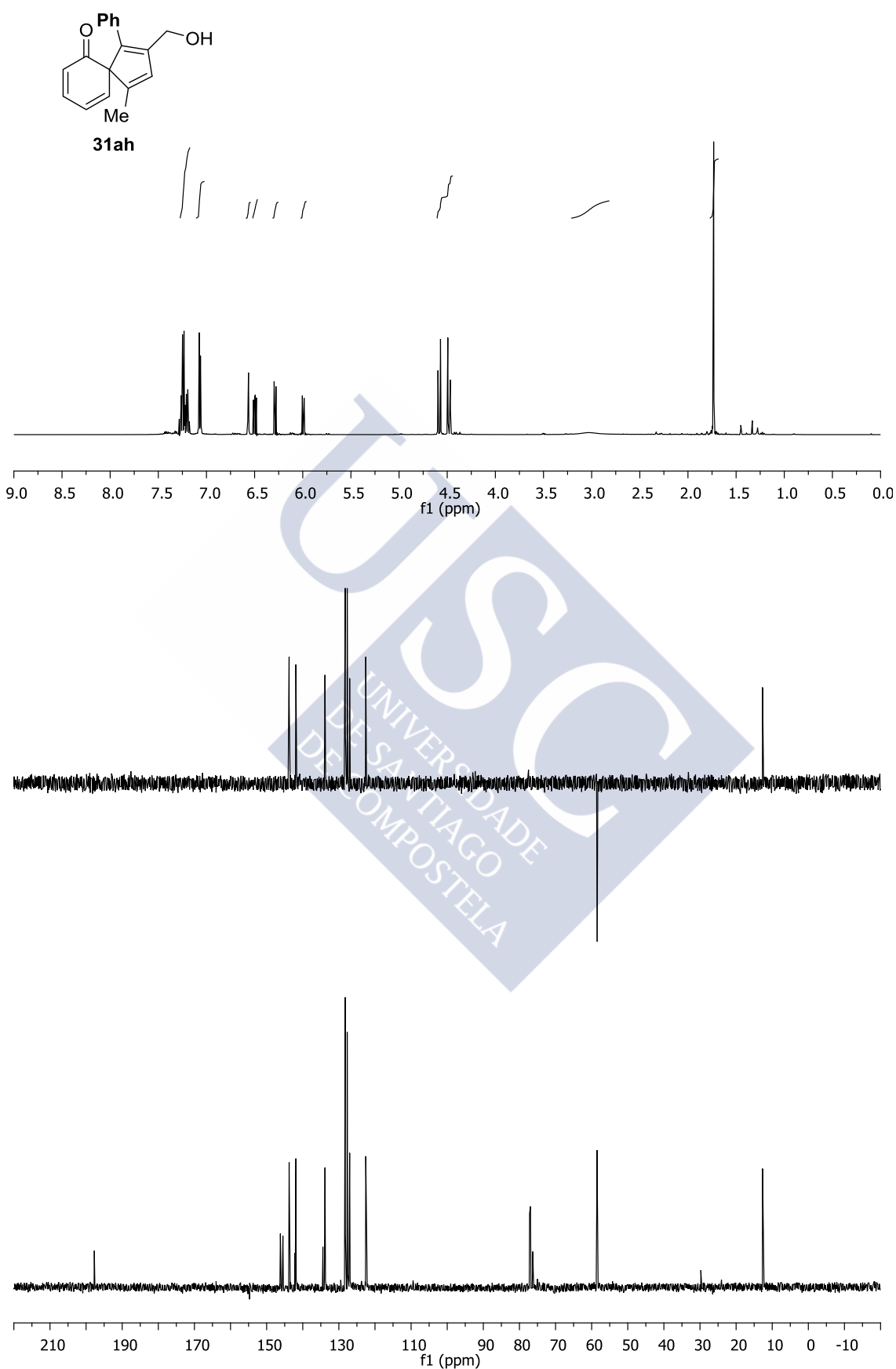


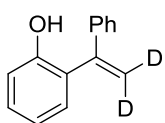


31aa

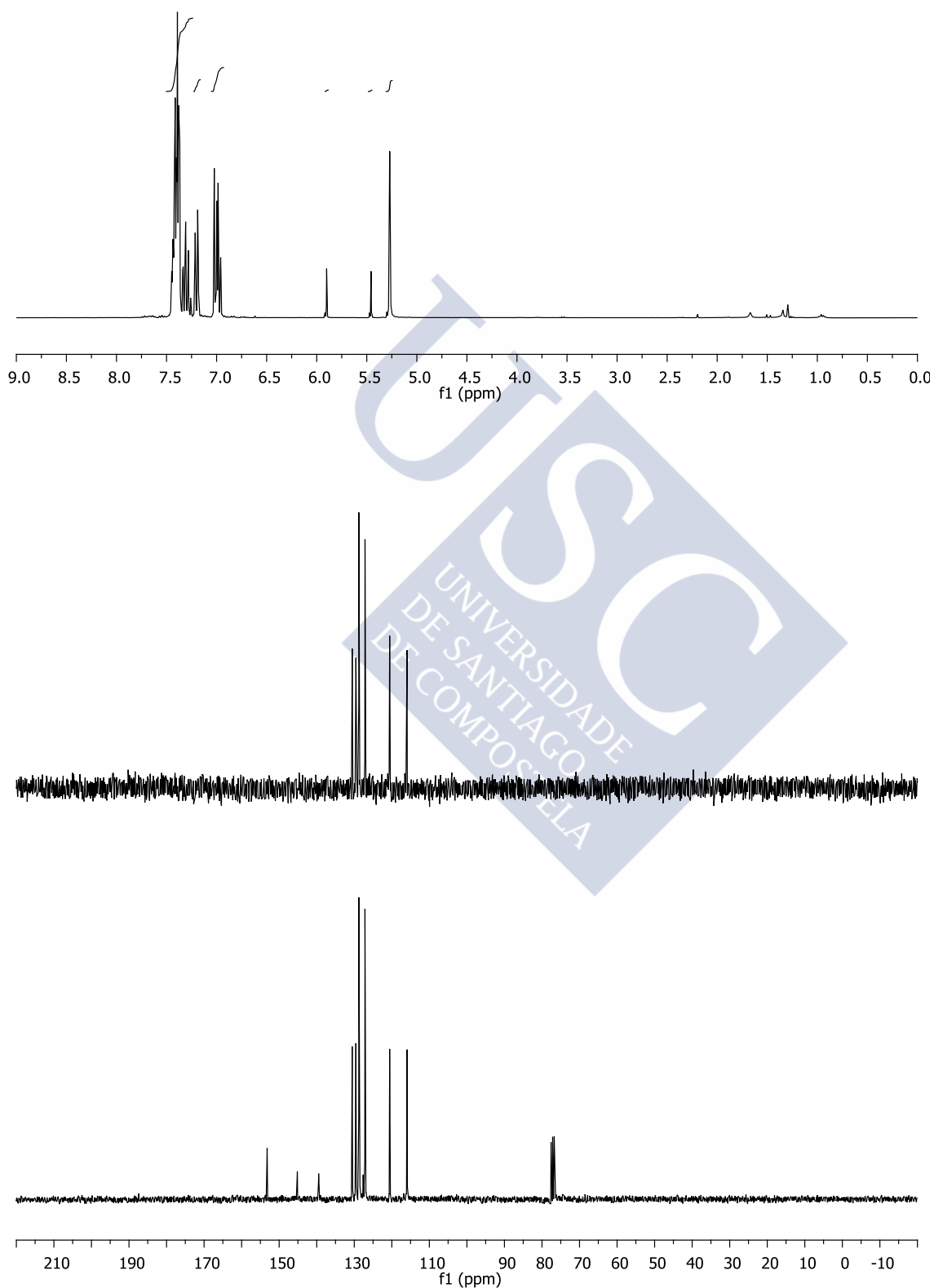




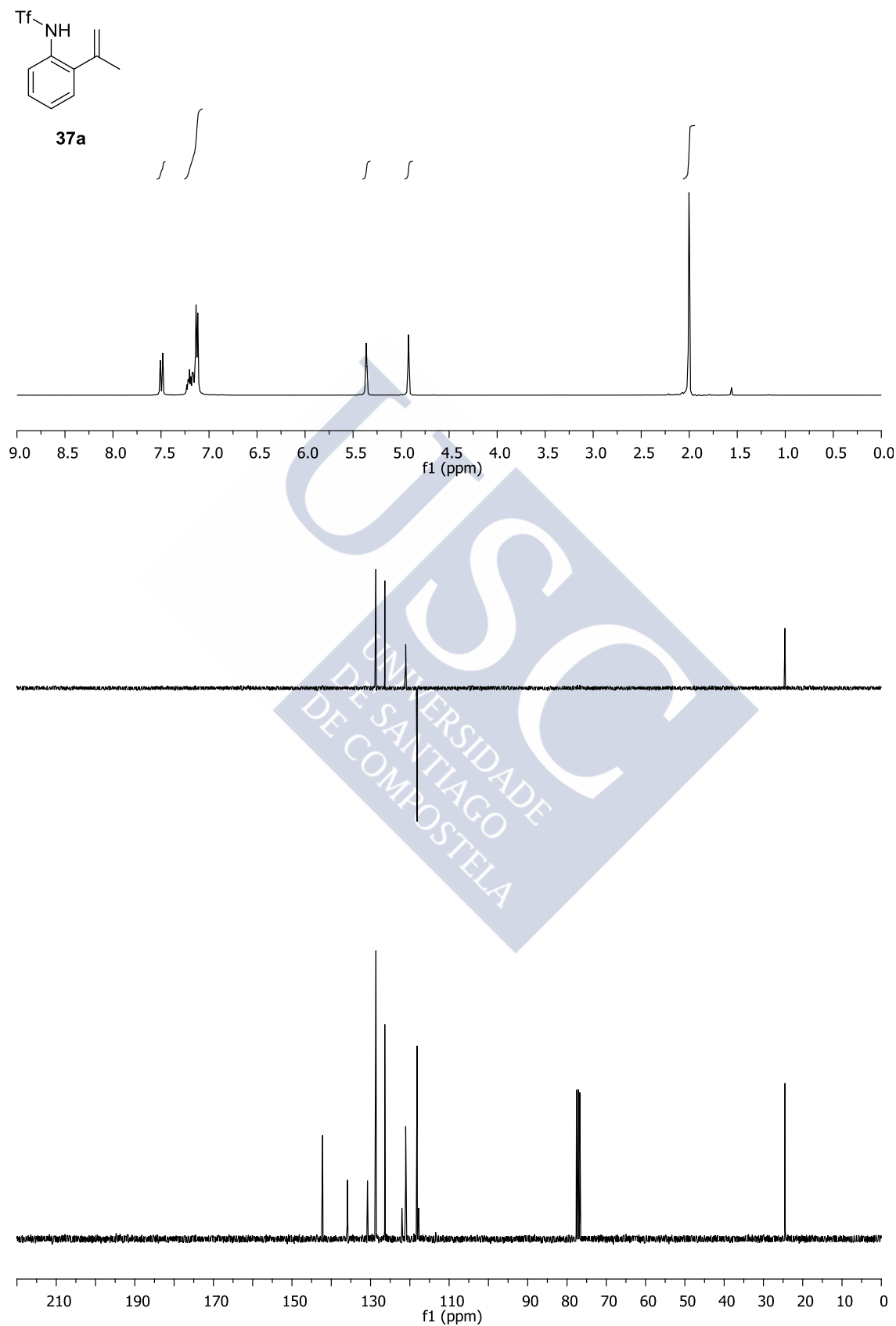


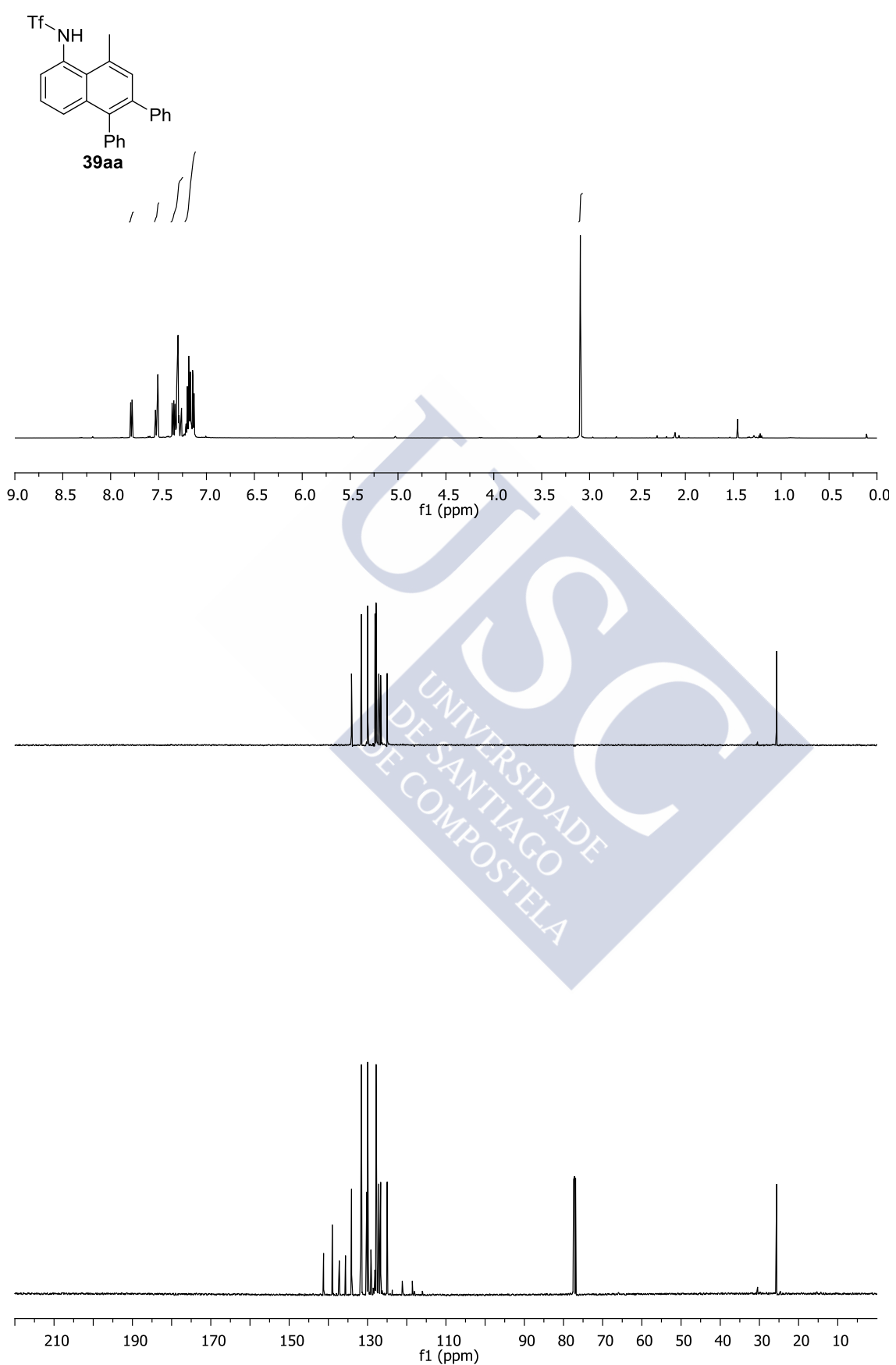


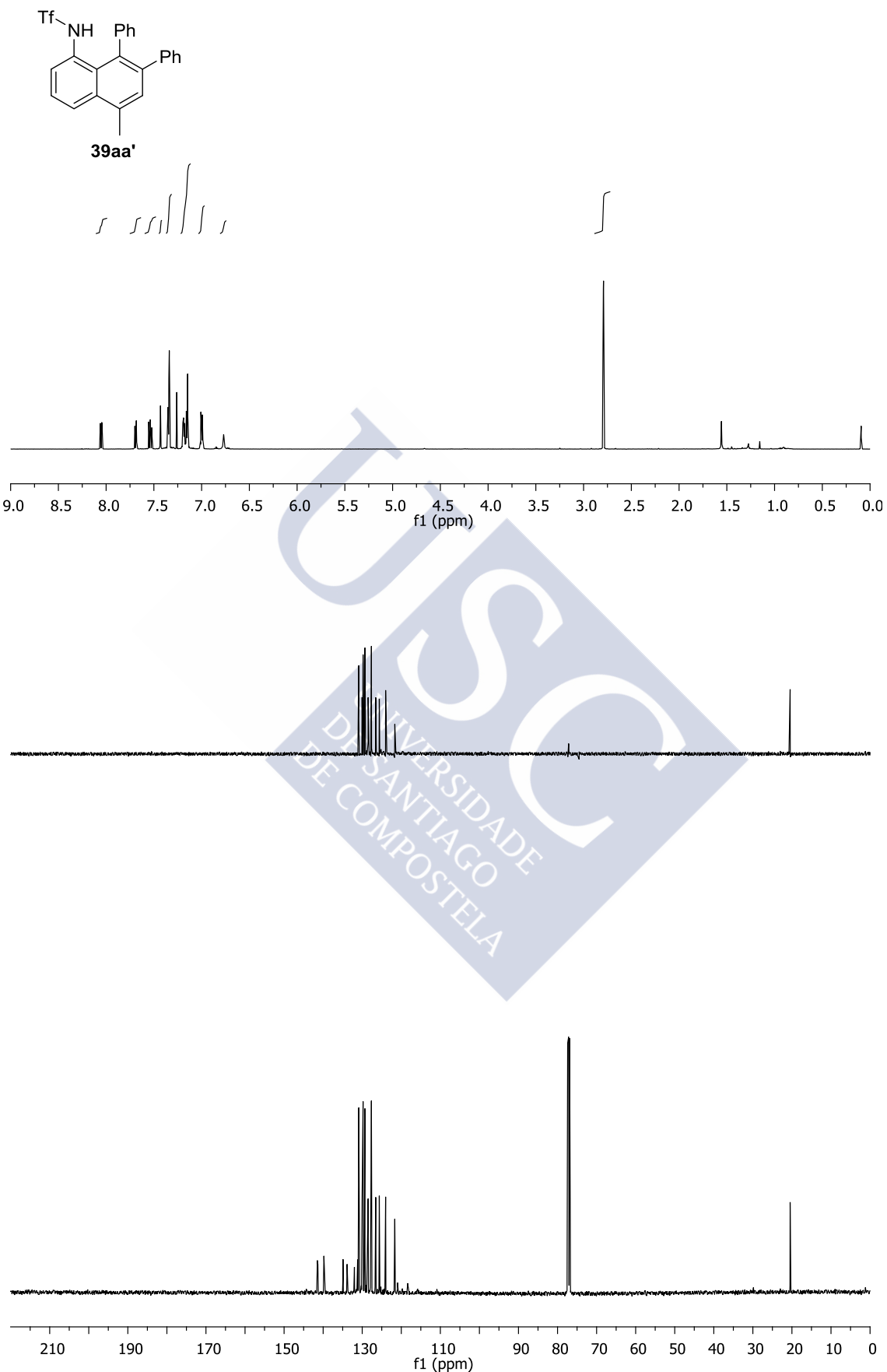
27c-d₂ (88% deuterated)

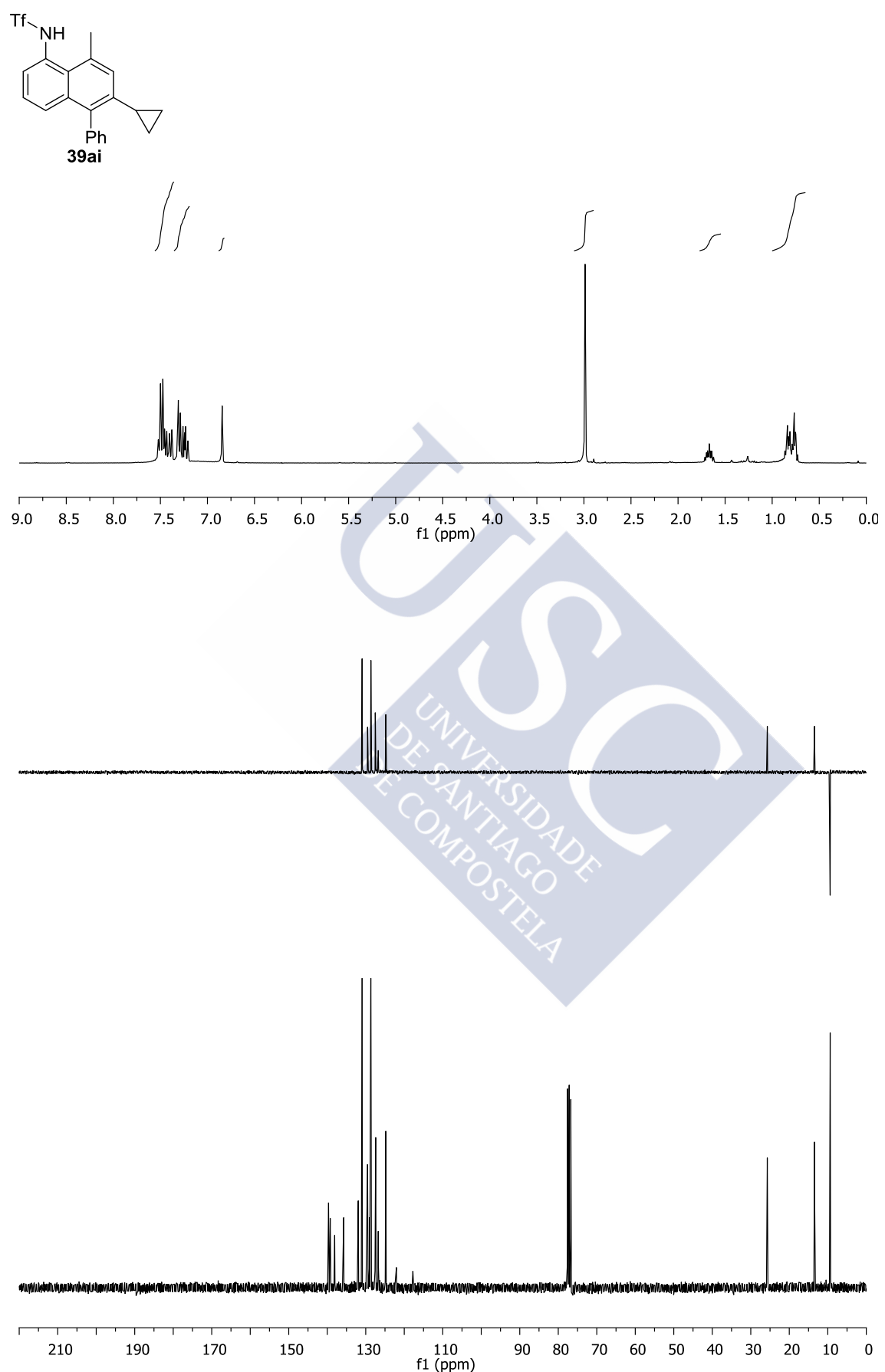


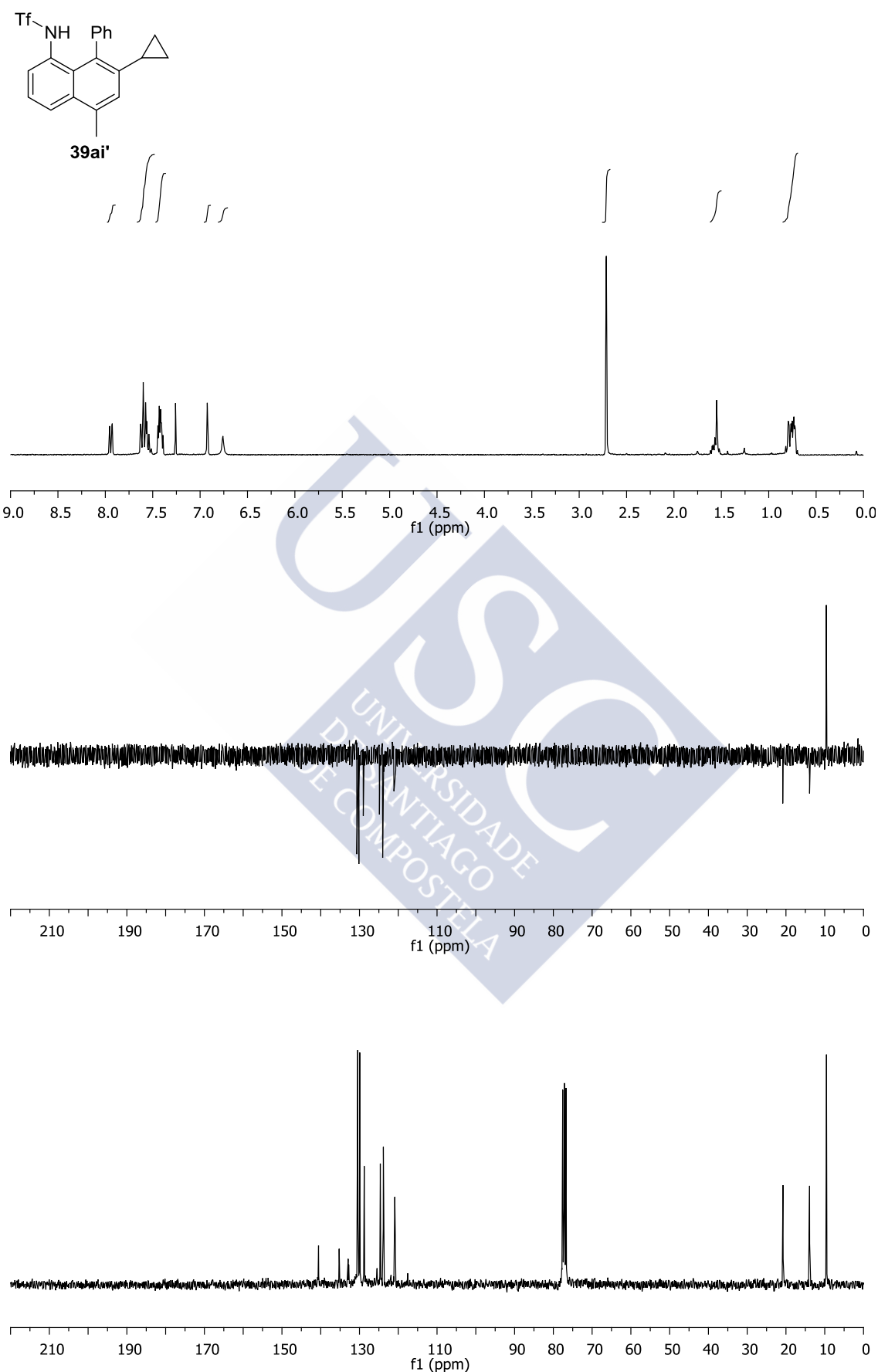
4. Selected spectra from chapter V.

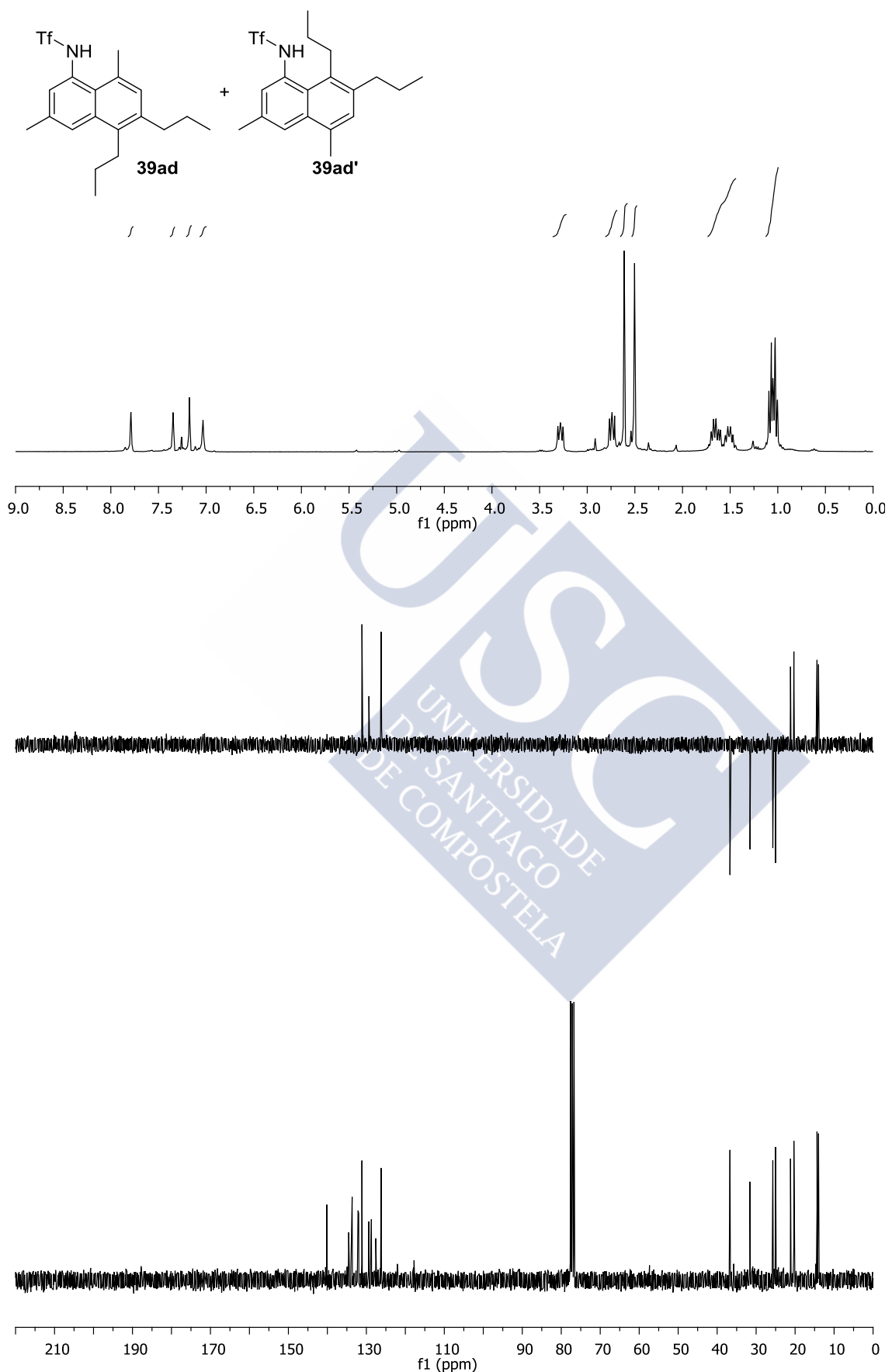












ANNEX I: Resumen





Resumen de la tesis doctoral.

En esta memoria de investigación se recogen los resultados obtenidos en los estudios sobre anelaciones basadas en activación de enlaces C-H y catalizadas por complejos de rodio (III). Concretamente, este sistema catalítico se ha utilizado en diversos sustratos para obtener moléculas cíclicas con distintas estructuras. Inicialmente se discute la importancia del desarrollo de nuevos procesos de activación de enlaces C-H debido a la baja generación de residuos y falta de necesidad de prefuncionalización de las sustancias de partida, lo que está acorde con los principios de la *química verde*. Se explica además, como el uso de grupos directores supone una ayuda inestimable en esta química ya que permite resolver problemas tanto de selectividad como de reactividad. También se hace hincapié en las ventajas de acoplar la activación de enlaces C-H con las cicloadiciones formales en procesos denominados “anelaciones oxidativas”. Se discuten además los mecanismos más representativos de la activación C-H mostrando ejemplos de su aplicación a diversos procesos. Una vez enmarcada la tesis doctoral dentro de los trabajos publicados en el campo, se procede a la exposición de los resultados obtenidos en la etapa de investigación.

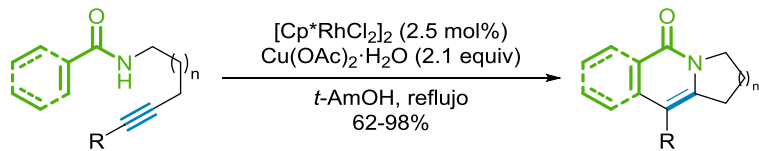
Anelaciones oxidativas intramoleculares de benzamidas y acrilamidas.

En el primer capítulo se describe la primera reacción de anelación totalmente intramolecular entre benzamidas y alquinos, que da lugar a isoquinolinas tricíclicas, un esqueleto de interés presente en diversos compuestos naturales. Además se exponen los diversos estudios mecanísticos dirigidos a averiguar le camino que sigue la reacción, enfocándose, particularmente, en la forma en la que sucede la etapa clave de inserción migratoria.

Tras una búsqueda de condiciones óptimas que permite detectar que el precatalizador $[\text{Cp}^*\text{RhCl}_2]_2$ en *t*-AmOH con acetato de cobre como oxidante, se logra la obtención de isoquinolinas tricíclicas en rendimientos superiores al noventa por ciento.

En esta parte también se describe cómo la reacción tolera diversas funcionalidades en distintas posiciones de la benzamida sin diminución importante de los rendimientos. Además se muestra como, cuando hay sustituyentes voluminosos y no coordinantes en *meta* a la amida, la reacción es selectiva hacia el enlace C-H más accesible estéricamente. Sin embargo, cuando en esa posición hay un metoxi, la relación de regiosómeros disminuye drásticamente, la explicación aportada es debida a la disminución de los efectos estéricos o a la actuación del oxígeno como ancla para el complejo de rodio en adición al efecto del grupo director de la amida.

También se demuestra cómo esta transformación es extensible a otros sustratos más exigentes como las acrilamidas aunque, para poder obtener buenos rendimientos, es necesario añadir acetato de cesio cuya función es desconocida pero se presume que facilita la C-H activación.



Además, se comenta cómo la bibliografía presentaba siempre la inserción del alquino a través de una carbometalación la cual, en el caso de las anelaciones intramoleculares entre benzamidas y alquinos, daría lugar a un intermedio altamente tensionado. Para poder averiguar si, en dicho caso, otras alternativas mecanísticas eran posibles, se realizan diversos cálculos DFT en la que se compara la carbometalación descrita para casos intermoleculares con una aminometalación que, en el caso de que suceda en casos intramoleculares, serviría para relajar la tensión de los intermedios. Dichos estudios demuestran que, para el caso de las anelaciones intramoleculares, la aminometalación es más probable, independientemente de la longitud de la cadena. Sin embargo, para los casos intermoleculares descritos, los cálculos realizados sugieren que la carbometalación previamente propuesta es el camino más favorable. En ambos casos las diferencias energéticas son relativamente pequeñas. Estos cálculos fueron validados mediante la realización de estudios experimentales cinéticos que, de acuerdo con los cálculos, indican que la etapa limitante de la reacción es la activación del enlace C-H. Con el objetivo de comprobar si el método de ciclación intramolecular de la reacción podría aplicarse a otros sistemas, se sintetizan anilinas unidas a alquinos mediante una cadena carbonada y se hacen reaccionar en condiciones análogas a las descritas para casos intermoleculares. En este caso no se obtiene la reactividad deseada lo que puede ser debido a la geometría de uno de los intermedios de reacción, que no permitiría la correcta aproximación del alquino. Para comprobar si la hipótesis propuesta es correcta, se sintetiza una naftilamina unida a un alquino. Este sustrato podría reaccionar a través de un intermedio diferente, con una geometría que permitiría la inserción migratoria del alquino. En este caso la reacción ocurrió dando lugar a un producto tricíclico fusionado. Para comprobar que la geometría del intermedio es clave en la formación de los dos productos, se añade un alquino externo y se obtiene la formación preferencial del indol tal y como estaba descrito. Este experimento sugiere que la hipótesis de que la geometría es la que afecta a la formación de los productos es correcta.

Construcción de benzoxepinas y cumarinas por anelación oxidativa de *o*-vinilfenoles.

En el segundo capítulo se expone el uso de 2-hidroxiestirenos como plataformas versátiles para llevar a cabo reacciones de anelación oxidativa. Asimismo se llevaron a cabo varios estudios con la finalidad de averiguar el mecanismo de la reacción y, concretamente, de la etapa clave de ruptura del enlace C-H.

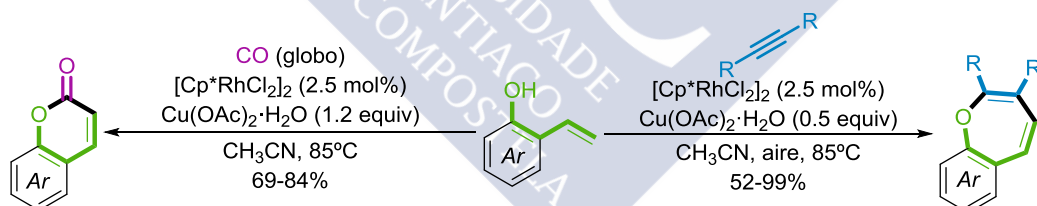
La bibliografía presentada en el capítulo muestra como los 2-fenilfenoles son sustancias capaces de participar en procesos de activación de enlaces C-H y cómo, en algunos casos, esta reactividad se puede extender a vinilfenoles. A pesar de que los precedentes, que usaban estos compuestos, estaban en su mayor parte realizados con complejos de Pd, trabajos de Miura sugerían que el complejo de rodio usado previamente podría ser activo para los

propósitos de la tesis. En el caso de los 2-hidroxiestirenos, la reacción se antojaba más problemática ya que existen varios enlaces C-H que podrían ser funcionalizados dando lugar a benzofuranos, benzoepinas y cromenos respectivamente. Se describe además, como la síntesis de los vinilfenoles se hace de forma sencilla por tratamiento de salicilaldehidos con iluros de fósforo mediante una reacción de Wittig.

Tras unas pruebas de optimización se encuentra que el precatalizador $[Cp^*\text{RhCl}_2]_2$ en MeCN a 85 °C, con acetato de cobre como oxidante (incluso cuando este último está presente a nivel subestequiométrico) permitía la obtención de benzoepinas por activación selectiva de la posición terminal del doble enlace del vinilfenol. Posteriormente, el metalacílico formado reacciona con un alquino dando lugar a los productos deseados en rendimientos casi cuantitativos.

Haciendo uso de las condiciones optimizadas, se demuestra que varios grupos funcionales, situados en diferentes posiciones del vinilfenol o en el alquino, son compatibles con la transformación otorgando eficientemente las benzoepinas descritas. Sin embargo, la reacción no es efectiva cuando el doble enlace está sustituido en alguna de las posiciones o el anillo aromático presenta alguna cadena en la posición *ortho* respecto del doble enlace.

Además de alquinos, la reacción también funciona con monóxido de carbono como reactivo dando lugar a cumarinas, estos productos son descritos como enormemente relevantes con usos en varios campos de la química y la medicina. En el caso de la síntesis de cumarinas, la sustitución de la posición interna del doble enlace del hidroxiestireno no afecta a la reacción, aislando el ciclo en rendimientos comparables. Se destaca que esta ciclocarbonilación sucede en condiciones relativamente suaves de presión y temperatura.



En un esfuerzo para entender la selectividad obtenida hacia el enlace C-H externo de la olefina y el mecanismo general de la reacción, se realizan diversas pruebas mecanísticas. Experimentos de competición por el mismo alquino entre vinilfenoles de electrónicas diferentes arrojan un resultado muy interesante. Cuando la competición se realiza en el mismo recipiente de reacción, se obtiene mayor proporción de la oxepina que proviene del anillo pobre en electrones. Sin embargo, la medición separada de las velocidades de ambos fenoles da lugar a un resultado opuesto, el vinilfenol electroquímicamente rico reacciona a más velocidad que el pobre (este experimento se hace con sustituyentes electroatractivantes de distinta naturaleza colocados en distintas posiciones del anillo aromático). La explicación que se propone es debida a la posible existencia una etapa irreversible de coordinación del fenóxido (cuya formación está favorecida por la presencia de grupos atractores) por lo que, cuando ambos fenoles compiten por el mismo alquino, el electroquímicamente pobre reacciona

preferencialmente. En el caso de los experimentos independientes, se propone que una, o varias, de las etapas posteriores a la coordinación del fenóxido al centro metálico se ven favorecidas cuando los anillos aromáticos son electrónicamente más ricos. De forma análoga al estudio de la influencia de la electrónica del anillo en la reactividad, se estudia la competición entre alquinos de sustitución diferente. Ésta muestra que los alquinos pobres en electrones reaccionan de forma preferente con respecto a los más ricos. Esta divergencia se explica en términos de una posible mejor coordinación del alquino pobre o a la disminución de la energía necesaria para llevar a cabo la inserción migratoria cuando el alquino dispone de sustituyentes electroatractores. Experimentos de efecto cinético isotópico arrojan resultados que pueden ser interpretados aduciendo que la etapa limitante de la reacción es la activación del enlace C-H. Una prueba, descrita como muy reveladora en términos mecanísticos, es la sustitución del vinilfenol por alilfenol en las condiciones habituales de reacción. Cuando se emplea el alilfenol como sustrato en la reacción, no se observa conversión, de lo que se puede deducir que la coordinación del doble enlace al anillo aromático es crucial para la reactividad.

A partir de los datos obtenidos, se propone un mecanismo de activación inusual. Éste comprende la coordinación del complejo de rodio monomérico al fenóxido seguido de una desaromatización del fenol que aumenta la acidez del protón a activar. Una posterior desprotonación genera un intermedio metalacíclico que recupera la aromaticidad. A partir de dicho radicílo se propone una inserción migratoria del alquino seguida de una eliminación reductora del intermedio de ocho miembros formado. Esta última daría lugar a la oxepina y al complejo de rodio reducido que podría ser reoxidado por el cobre con oxígeno como oxidante final.

Con todos los experimentos descritos, se concluye que los *o*-vinilfenoles son plataformas interesantes para la consecución de procesos de anelación oxidante y que, además, presentan una forma inusual de activación del enlace C-H lo que podría resultar en nuevas oportunidades en el campo.

Anelación oxidativa desaromatizante de *o*-alquenilfenoles y alquinos para la síntesis de espirociclos.

Esta parte de la tesis viene derivada del capítulo anterior en el que se describían los problemas de la anelación de vinilfenoles y alquinos cuando los primeros están sustituidos en la posición interna del doble enlace. Un análisis de los productos de reacción permitió caracterizar el resultado del proceso como una mezcla de benzoxepina, un espirociclo de anillos de seis y cinco miembros y una azulenona. Habiendo identificado esta mezcla se propone intentar dirigir la reacción a la formación selectiva del producto mayoritario, el espirociclo. Además, se plantea averiguar la razón de la aparición de diferentes productos en función de la sustitución en la olefina.

Para llevar a cabo el primer objetivo, se realiza un exhaustivo análisis de condiciones de reacción en el que se encuentra que, cuando ésta se lleva a cabo en condiciones análogas a las

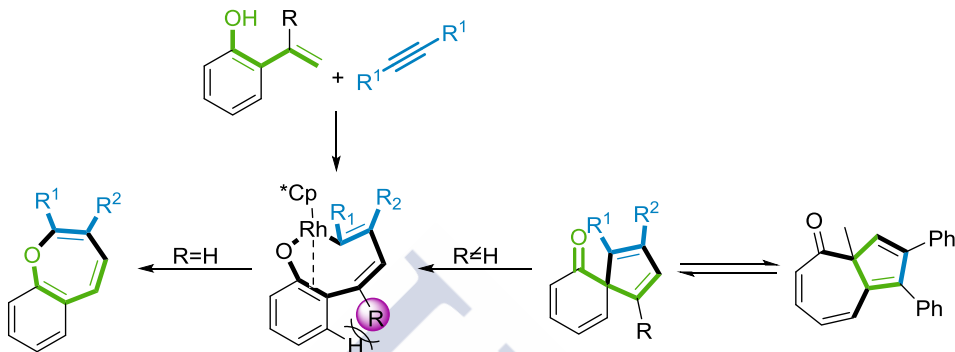
de la obtención de la oxepina pero a menor temperatura (40°C), se obtiene el espirociclo deseado en rendimientos excelentes y solo con trazas de la azulenona. Una vez llegado a ese resultado, se procede a estudiar el alcance de la reacción. Con dicho objetivo en mente, se sintetizan los alquenilfenoles de forma similar a la descrita en el capítulo anterior. Estos vinilfenoles poseen sustituyentes electrónicamente diversos en diferentes posiciones del anillo. Al igual que en el caso de las benzoxepinas, la reacción tolera sustitución en todas las posiciones del anillo aromático menos en *ortho* al alqueno lo que da lugar a la descomposición de las sustancias de partida. La metodología tampoco es efectiva cuando la olefina está sustituida en posición terminal. Cabe destacar que cuando la sustitución en la parte interna del alqueno es un anillo aromático, hay que calentar a 60°C para obtener buenos rendimientos. El mismo caso se daba para la sustitución en *para* al hidroxilo con un átomo de bromo lo que, en este caso, además conlleva la formación de un dieciocho por ciento de azulenona.

Una vez demostrada la robustez de esta metodología, se procede a investigar su mecanismo. En esa parte se describe que, como era esperable, el efecto cinético isotópico parece indicar que la activación del enlace C-H, al igual que en el caso anterior, está de alguna manera involucrado en etapa limitante de la reacción. Además, siguiendo con el esfuerzo por aportar pruebas al mecanismo de desaromatización y rearomatización, se realizan una serie de pruebas de deuteration que demuestran la reversibilidad de la activación del enlace C-H en ausencia de alquino mientras que en presencia del mismo, no se observa ninguna deuteration sugiriendo que la inserción migratoria del alquino es más rápida que la vuelta atrás del intermedio metalacíclico. Además, en ausencia del alquino se observado deuteration tanto en la posición *cis* como la *trans* del alqueno. Este hecho permite teorizar que puede existir un intermedio en el que ambos protones son indistinguibles, lo que coincide con la hipótesis propuesta de la desaromatización del fenol. Concretamente, la explicación aportada consiste en la formación exclusiva del producto *cis* deuterado que puede volver a sufrir un proceso de activación reversible del enlace C-H en el que protón in deutero serían indistinguibles. En este capítulo se muestra uno de los experimentos más indicativos de que esta transformación no ocurre vía un proceso de metalación desprotonación concertada (CMD). Éste consiste en el uso de una base monocoordinante, como la trietilamina, en ausencia de una fuente de acetatos externa y con una cantidad estequiométrica de catalizador de rodio. Bajo estas condiciones, la reacción sigue ocurriendo. Esto indica que la CMD clásica no puede estar formando parte del mecanismo propuesto ya que, la CMD necesita bases bidentadas, como los acetatos, para poder producirse.

Con las pruebas mecanísticas realizadas, se propone un mecanismo análogo al de la formación de oxepinas solo que, en uno de los intermedios propuestos, un anillo de ocho miembros, la repulsión estérica entre el sustituyente de la olefina y el anillo aromático es tal, que se produce un reordenamiento de tipo tautomérico que da lugar al espirociclo.

En este capítulo se comprueba además, que la azulenona observada en los experimentos iniciales, así como en el caso de la reacción del alquenilfenol bromado a 60°C , proviene de

una reorganización del espirociclo. De hecho, se propone que existe un equilibrio entre ambos productos en condiciones de reacción ya que, la disolución y calentamiento de cualquiera de los dos por separado, da lugar a una mezcla de espirociclo y azulenona. Para explicar dicho equilibrio se echa mano de la formación de un intermedio tricíclico zwitteriónico consistente en dos anillos de seis y cinco miembros fusionados formando un ciclopropano.



Anelación oxidativa de *o*-alquenylanilinas.

El último capítulo de la tesis se centra en trasladar la química de alquenilfenoles a alquenylanilinas ya que una gran parte de los productos farmacológicos de interés, poseen algún átomo de nitrógeno en su estructura.

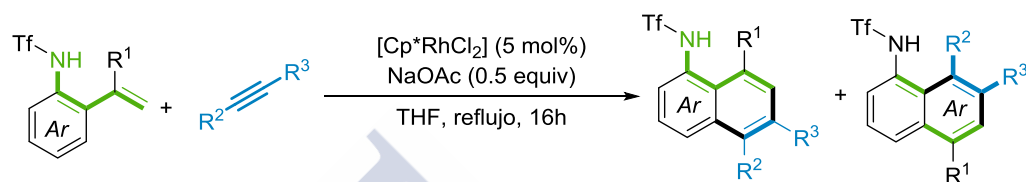
En primer lugar, se busca identificar un sustituyente apropiado para el átomo de nitrógeno que aporte los requerimientos estéricos y electrónicos necesarios para que la reacción tenga lugar. Entre los diversos grupos probados, se observa que los electroatractores son más propensos a reaccionar de forma productiva. Sin embargo, en lugar de las benzazepinas o espirominas esperados, se obtiene una mezcla de naftilaminas regiosoméricas. Estos dos isómeros provienen de una cicloadición formal (4+2) entre el aminoestireno y el alquino y otra cicloadición formal (4+2) entre ambos sustratos pero con una migración formal 1,2 del alqueno previa a la anelación.

Una posterior optimización de las condiciones permite llegar a rendimientos globales superiores al ochenta por ciento. Concretamente, cuando se usan 5 mol% de precatalizador de rodio en dioxano a reflujo con un equivalente de cobre como oxidante. Sorpresivamente, se demuestra que aunque el catalizador es, previsiblemente, imprescindible para que la reacción ocurra, no lo es así el oxidante de cobre ya que, su sustitución por acetato de sodio sigue dando lugar a una mezcla similar de naftilaminas en rendimientos comparables.

Se demuestra, además, que la transformación también puede ser llevada a cabo en condiciones más suaves como THF a reflujo sin disminución apreciable del rendimiento global.

Al igual que en capítulos anteriores, se estudia el efecto de la sustitución en la reactividad obteniéndose que, con respecto al anillo, tanto sustituyentes dadores como atractores son

aceptados. En el caso de los alquinos empleados se encuentran diferencias significativas entre los sustituidos con grupos arilo o alquilo ya que estos últimos, generalmente, dan lugar a mezclas de regiosómeros más favorables hacia la anelación sin migración formal. También se describe cómo la reacción es incapaz de producirse cuando no hay sustitución en la posición interna del doble enlace o cuando la hay en la externa. Asimismo se comenta que la reacción falla cuando se usan 2-fenilanilinas en lugar de 2-alquenylanilinas. Por último describen un resultado interesante cuando se usan olefinas sustituidas con un grupo isopropilo, que es la isomerización del doble enlace hacia el isopropilo generando la olefina trisustituida.



En este caso no se han realizado estudios mecanísticos pero sí se proponen varias hipótesis capaces de explicar cómo se producen ambos isómeros (para lo cual se postula la formación de una espiroimina intermedia) y cómo la reacción puede suceder en ausencia de un oxidante “clásico” como el aire o el cobre:

- La primera explicación consiste en la hidroarilación del alquino catalizada por rodio (III) y la posterior formación del espirociclo mediada por el mismo complejo de rodio y completada con una β -eliminación de hidruro. La protonación del hidruro de rodio generado daría lugar a hidrógeno gas y a la recuperación del complejo catalíticamente activo.
- En segundo lugar se propone la formación de las dihidronaftilaminas a partir del dihidroespirociclo las cuales, al entrar en contacto con el oxígeno en la elaboración, se oxidan dando lugar a las naftilaminas correspondientes.
- Por último se postula que la reacción sigue un ciclo análogo a los propuestos para los alquenilfenoles y la oxidación del complejo de rodio (I), formado en la etapa de eliminación reductora, por adición oxidante al ácido acético, formado en el paso de activación C-H, y protonación del hidruro de rodio generado como en el caso anterior.

Conclusión general.

Como conclusión general, en esta tesis se describen varios procesos de anelación oxidativa catalizados por rodio (III) dando lugar a diferentes productos y realizando experimentos mecanísticos para elucidar los caminos que siguen las reacciones.

